STUDIES OF DROPLET BEHAVIOUR IN SPRAY DRYING TOWERS

BY

KOLAWOLE RASHEED ONIFADE, B.Sc., M.Sc.

A thesis submitted to
The University of Aston in Birmingham
for the degree of
Doctor of Philosophy

Department of Chemical Engineering
University of Aston in Birmingham, England.

May 1983

STUDIES OF DROPLET BEHAVIOUR IN SPRAY DRYING TOWERS

BY

Kolawole Rasheed Onifade, B.Sc., M.Sc.

A thesis submitted to
The University of Aston in Birmingham
for the degree of
Doctor of Philosophy 1983

Summary

Aspect of spray drying concerning the flow patters of air and feed, atomization and drying of sprays of droplets and the design and performance of spray driers have been extensively reviewed.

The experimental programme consists of:
(1) Droplet residence time distribution experiments.
(2) Droplet trajectories experiments
(3) Drop size distribution experiments.

Swirl nozzles were mainly used in droplet residence time distribution experiments. The distribution was established by tracer analysis. The experimental response data were simulated by a model. The model response which were returned by a program that analysed the model were found to be in very good agreement with the experimental response data.

The trajectories of droplets of cement slurries were calculated using a model based on force balance and equations of motion. A program was developed for the model.

Drop size distributions were estimated by both a Particle size analyser incorporating a laser beam and high speed flash photography. The sauter mean diameters calculated using both techniques of measurement were in good agreement.

Key Words

DROPLET RESIDENCE TIME DISTRIBUTION
TRACER ANALYSIS
DROPLET TRAJECTORY
DROP SIZE DISTRIBUTION

DEDICATION

This work is dedicated to my wife, children, parents and friends who have supported me financially and morally during those periods when the goal seemed unattainable.

ACKNOWLEDGEMENTS

The author is indebted to and wishes to record his gratitude to the following:

Professor G. V. Jeffreys, Head of Department of Chemical Engineering, Aston University, for his invaluable guidance, encouragement and personal supervision of this work.

Dr. C. J. Mumford, for his helpful technical and scientific suggestions from time to time.

Dr. B. Gay for his helpful advice on computer programs.

The entire staff of the Workshop, Analytical Lab., Photographic section, Stores and general office for their prompt attention to my needs.

The Director and Board of Management of Cocoa Research Institute of Nigeria for their financial support.

My wife for her patience and skill in typing the manuscript.

Almighty Allah for imbuing me with sustained health throughout the course of my studies.

CONTENTS

	PAGE
SUMMARY	
CHAPTER 1 INTRODUCTION	1
INTRODUCTION	2
CHAPTER 2 LITERATURE REVIEW	3
2.1 PROCESS STAGES OF SPRAY DRYING	6
2.1.1 Atomization and Mechanism	7
2.1.1.1 Centrifugal Energy Atomization	10
2.1.1.2 Pressure Energy Atomization	14
2.1.1.3 Kinetic Energy Atomization	18
2.1.1.4 Sonic Energy Atomization	19
2.1.2 Spray Air Contact	21
2.1.2.1 Flow patterns and residence time distribution of spray droplets	22
2.1.2.2 Flow patterns and residence time distribution of air	24
2.1.3 Drying of Spray droplets	26
2.1.3.1 Pure Single drops	27
2.1.3.2 Single droplets containing dissolved solids	28
2.1.3.3 Spray of drops	31
2.1.4 Separation of dried products	34
2.2 DROP SIZE DISTRIBUTION	36
2.3 DESIGN AND PREDICTION PERFORMANCE OF SPRAY DRIERS	45
CHAPTER 3 MATHEMATICAL MODELS	55
3.1 DROPLETS RESIDENCE TIME DISTRIBUTION MODEL	57

PAGE

3.2 CALCULATION OF PARTICLE TRAJECTORIES 65

CHAPTER 4 EXPERIMENTAL WORK AND EQUIPMENT 71

4.1 SPRAY TOWERS 73

4.2 SPRAY ATOMIZERS 83

4.3 CONDUCTIVITY TRANSMITTER AND CELLS 87

4.4 POTENTIOMETRIC RECORDER 88

4.5 PARTICLE SIZE ANALYSER 89

4.6 EXPERIMENTAL PROCEDURE 99

4.6.1 Droplet residence time distribution analysis for pure water 99

4.6.2 Drop size distribution analysis 100

4.6.3 Droplet trajectories 105

CHAPTER 5 RESULTS 107

5.1 DROPLETS RESIDENCE TIME DISTRIBUTION 109

5.2 DROPLETS TRAJECTORIES 159

5.3 DROP SIZE DISTRIBUTION 170

CHAPTER 6 DISCUSSION 174

6.1 DROPLETS RESIDENCE TIME DISTRIBUTION 176

6.2 DROPLETS TRAJECTORIES 177

6.3 DROP SIZE DISTRIBUTION 180

CHAPTER 7 CONCLUSION 182

7.1 DROPLETS RESIDENCE TIME DISTRIBUTION 184

7.2 DROPLETS TRAJECTORIES 184

7.3 DROP SIZE DISTRIBUTION 185

CHAPTER 8 RECOMMENDATION FOR FURTHER WORK 186

APPENDICES

APPENDIX A 189

APPENDIX B 240

APPENDIX C 275

APPENDIX D 280

PAGE

NOMENCLATURE 285

Greek Letters 286

Subscripts 287

REFERENCES 288

INDEX OF TABLES

TABLE		PAGE
2.1	Classification of Atomizers	11
2.2	Kinds of mean diameters	41
2.3	Size distribution functions	43
4.1	Dimensions of counter-current spray driers	74
4.2	Residence time distribution experimental operating variables - Feed.	101
4.3	Residence time distribution experimental operating variables - Air.	102
4.4	Droplet trajectory experimental operating variable.	106
5.1-5.9	Droplets residence time distribution results	110-118
5.10-5.19	Droplets trajectories results	160-164
5.20-5.22	Drop size distribution results	171-173

INDEX OF PLATES

PLATE		PAGE
4.1	Counter-current spray drier	75
4.2	Co-current spray drier	79
4.3	Spray tower	82
4.4	Pressure Nozzles	84
4.5	Rotary Atomizer	86
4.6	Particle size analyser -Optical processing unit	93
4.7	Particle size analyser - Electronic processing unit	94

INDEX OF FIGURES

FIGURE		PAGE
2.1	Mechanism of atomization for rotary atomizer.	13
3.1	Residence time distribution model for the droplets.	58
3.2	Force diagram for droplet trajectory.	67
4.1	Schematic diagram for counter-current spray drier.	76
4.2	Schematic diagram for co-current spray drier.	80
4.3	Principle of operation of the Particle size analyser.	90
4.4	Schematic diagram for particle size analyser.	95
5.1 - 5.40	Droplets residence time distribution results	119-158
5.41- 5.44	Droplets trajectories results	165-169

CHAPTER ONE

INTRODUCTION

INTRODUCTION

The list of the processing and other industries which use spray drying as a unit operation is extensive. It ranges from the foodstuffs industries in the application of the drying of milk, baby foods, powdered cheese and fruits to heavy industries using spray drying of dyestuffs and pigments (for furnishing and clothing), plastics, detergents, fertilizers and antibiotics to mention a few. Spray drying converts a feed in the form of a slurry, solution or paste into a dry powder, granules or agglomerates. This is achieved by atomizing the feed into a hot drying medium usually air which rapidly evaporates the moisture in the feed.

Unlike many other unit operations such as distillation and extraction in which the design of equipments have trascended empiricism stage, spray drier design is still to a large extent based upon the experience of the manufacturer. This is largely due to the fact that many factors have to be considered. Research work hitherto have concentrated on various aspects of the process such as atomization, spray-air contact, and drying of individual droplets etc. It is after considerable data have been acquired that it is hoped that correlations of important parameters which are pertinent to the design of spray drier would result. The experiments carried out here is an attempt to contribute to the elucidation of the mechanism taking place in spray

drying. The experimental programme is divided into the following phases:

(1) Residence time analysis of sprayed droplets.

(2) Particle trajectories of sprayed droplets.

(3) Testing of a new equipment - particle size analyser incorporating a laser beam - for the measurement of drop size distribution of sprayed droplets.

(4) Development of appropriate models to simulate the experimental data obtained in (1) and (2).

(5) Development of computer programs to carry out the simulation exercise.

CHAPTER TWO

LITERATURE REVIEW

2.1 PROCESS STAGES OF SPRAY DRYING

2.1.1 Atomization and Mechanism

2.1.1.1 Centrifugal Energy Atomization

2.1.1.2 Pressure Energy Atomization

2.1.1.3 Kinetic Energy Atomization

2.1.1.4 Sonic Energy Atomization

2.1.2 Spray Air Contact

2.1.2.1 Flow Patterns and Residence Time Distribution of Spray Droplets

2.1.2.2 Flow Patterns and Residence Time Distribution of Air

2.1.3 Drying of Spray Droplets

2.1.3.1 Pure Single Drops

2.1.3.2 Single Droplets Containing Dissolved Solids

2.1.3.3 Spray of Drops

2.1.4 Separation of Dried Products

2.2 DROP SIZE DISTRIBUTION

2.3 DESIGN AND PREDICTION PERFORMANCE OF SPRAY DRIERS.

2.1 PROCESS STAGES OF SPRAY DRYING

Many parameters are important in a spray drier design (1 - 4) and to appreciate them, one needs to consider the basic process stages of spray drying. These are:

(1) Atomization of feed into spray

(2) Spray air contact

(3) Drying of spray

(4) Separation of dried product from the gas (or drying) medium.

Intensive research studies have been undertaken in the first three stages with a view to gaining a fundamental understanding that could serve as a base for proper engineering design of spray driers. The design and operation of equipments in each stage coupled with physical and chemical properties of the feed materials are also essential in determining the characteristics of the dried products.

2.1.1 ATOMIZATION AND MECHANISM

Atomization ensures the production of droplets having a high surface to mass ratio from slurry, solutions or pure liquid feed. Control of the atomization variables to produce an ideal spray composed of droplets of equal size coupled with a right drying chamber design will result in the droplets having the same sufficient residence time for moisture removal. Besides, equal residence time for all the droplets implies that the heat and mass transfer rates will be the same ensuring that there is no product deterioration due to heat and that uniformly dried product characteristics are achieved. Although many commercial atomizers are available that could produce sprays which closely approach uniformity for certain liquids and at certain feed rates (usually low), the achievement of an ideal spray is still illusory.

Many workers have investigated the mechanism of atomization with a view to obtaining information that could be applied to the design of commercial atomizers. The various mechanisms proposed are based on the pioneering work on the stability and collapse of simple liquid jet systems. The liquid break up results from the destruction of the jet's initial stability by the forces acting on and within the jet such as the gravity. This simple explanation was extended by various workers to deduce the mechanism of atomization of a spray.

However in the case of a spray, the work of obtaining theoretical relationship to explain the mechanism of atomization is made arduous by the interplay of factors such as friction and drag from interaction between the droplets and the drying medium, irregular break up due to non-ideal liquid distribution and influence of droplets on one another.

Lord Rayleigh (5) obtained a mathematical equation for the break up of non-viscous liquid jets under laminar flow conditions. He postulated that a jet became unstable and ready to disrupt if its length was greater than its circumference. Tyler (6) arrived at more or less the same conclusion. Haenlin (7), Castleman (8) and Weber (9) extended the conclusion of Rayleigh and Tyler to include the effects of viscosity, surface tension, liquid density and air resistance on the jet break up. Ohnesorge (10) related jet stability to the magnitude of Reynolds Number and obtained the dimensional number Z', where

$$Z' = \frac{\text{Weber Number}}{\text{Reynolds Number}}$$

$$= \frac{\mu}{(\rho_1 \sigma d_n)^{\frac{1}{2}}}$$

$$= \frac{V_j \left(\rho_1 d_n\right)^{\frac{1}{2}}}{\sigma} \cdot \left(\frac{V_j d_n \rho_1}{\mu}\right)^{-1} \qquad (2.1)$$

Based on Z', he concluded that the mechanism of liquid break up could be elucidated by three zones:

Zone 1 Low Reynolds Number ($<10^4$) where Rayleigh mathematical prediction prevailed through the creation of oscillation at the liquid jet surface.

Zone 2 Intermediate Re ($>10^4 <10^5$) where the degree of atomization was governed by wave motion set up in the jet.

Zone 3 High Re ($>10^8$) characterised by complete disintegration.

Studies with results similar to the above findings were carried out by other workers (11 - 14).

Many of the above mechanisms and theories based on them are oversimplified because in commercial atomizers all the mechanisms act simultaneously to influence spray characteristics. Therefore to get a comprehensive idea of the interplay of the mechanisms, it would be essential to consider the different classes of atomizers available. Atomizers employing centrifugal, pressure and kinetic energy for atomization are the types most commonly used in industrial applications, while those employing sonic and vibrational energy are less commonly used. Atomizers are selected according to the nature of the feed and the desired characteristics of the dried product. The degree of atomization depends upon the fluid properties of the feed. For instance, the size of droplets increase with increase in viscosity and surface tension for the same energy of atomization.

A complete classification of the atomizers according to the source of energy employed is shown in Table 2.1.

2.1.1.1 CENTRIFUGAL ENERGY ATOMIZATION

This class employs nozzles in which liquid feed introduced under gravity or at low pressure is accelerated centrifugally to a high velocity across a rotating surface. From the edge of this surface, a ligand is discharged into individual droplets or as ligaments or films that subsequently disintegrate into droplets. The degree of atomization depends upon peripheral speed, feed rate, liquid properties and atomizer design.

Wheel and Disc rotary atomizers are the atomizers mostly employed in this class. Wheel atomizers have either vanes or bushings design. Vaned wheel atomizers are high, wide, straight or curved. They are used to produced sprays in the medium-coarse size range. The wheel atomizers with bushings are circular or square and are mostly used for handling abrasive feeds and products with high bulk density. Droplet size distribution produced by wheel atomizers is controlled by change in wheel speed which should be within the permissible limit to prevent distortion and fracture of the wheel especially at high drying temperatures.

Disc atomizers include vaneless plates (discs), cups and inverted bowls. Sprays from disc atomizers are coarser than those from wheel atomizers for a

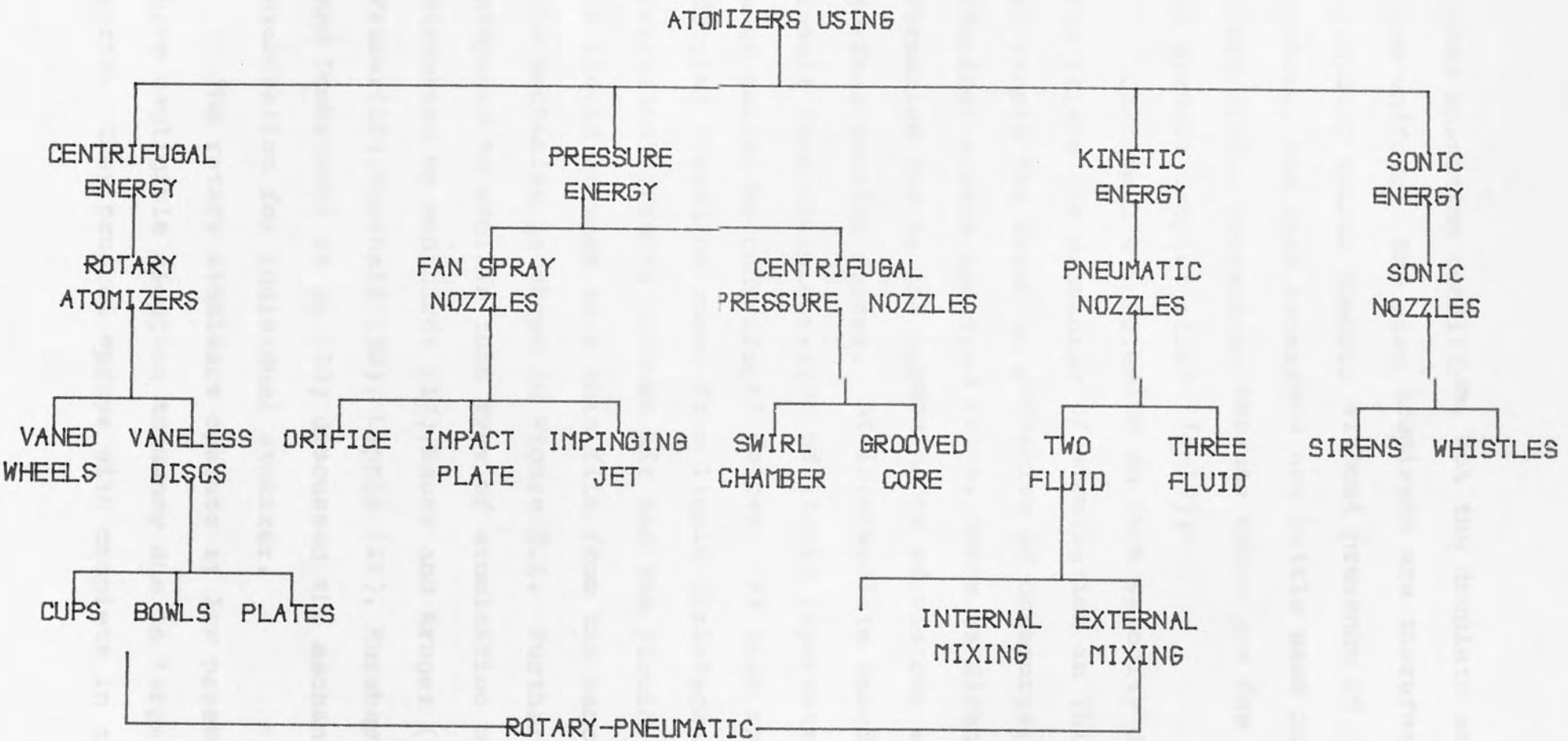

TABLE 2.1: CLASSIFICATION OF ATOMIZERS

given operating condition, but the droplets are much more uniform. The disc atomizers are therefore used in producing coarse powders without presence of fines. However, the disc atomizers are little used in commercial spray drying operations because there are few correlations to predict droplet sizes (15-16).

Castleman's conclusion on high velocity disturbance can relate the mechanism of atomization in this class to simple jet break up mechanism of Ohnesorge. At low atomizer speeds and feed rates, there is direct droplet formation due to the predominance of viscous and surface tension forces. At intermediate speeds, droplets result from disintegration of liquid ligaments from the edge mainly by centrifugal forces. At high speeds, droplet formation comes from liquid disintegration by frictional effects between air and the liquid surface as liquid emerges as a thin film from the vance or disc. The mechanism is shown in Figure 2.1. Further mechanisms proposed to explain this type of atomization were discussed by Mehrhardt (17),Bauer and Kruger (18). Fraser(19),Marshall (20), Lapple (21), Kurabayasi (22) and Dombrowski et al (23) discussed the mechanism of atomization for individual atomizer.

The rotary atomizers operate at low pressure and have negligible clogging tendency due to large flow ports. They produce sprays with droplets in the size

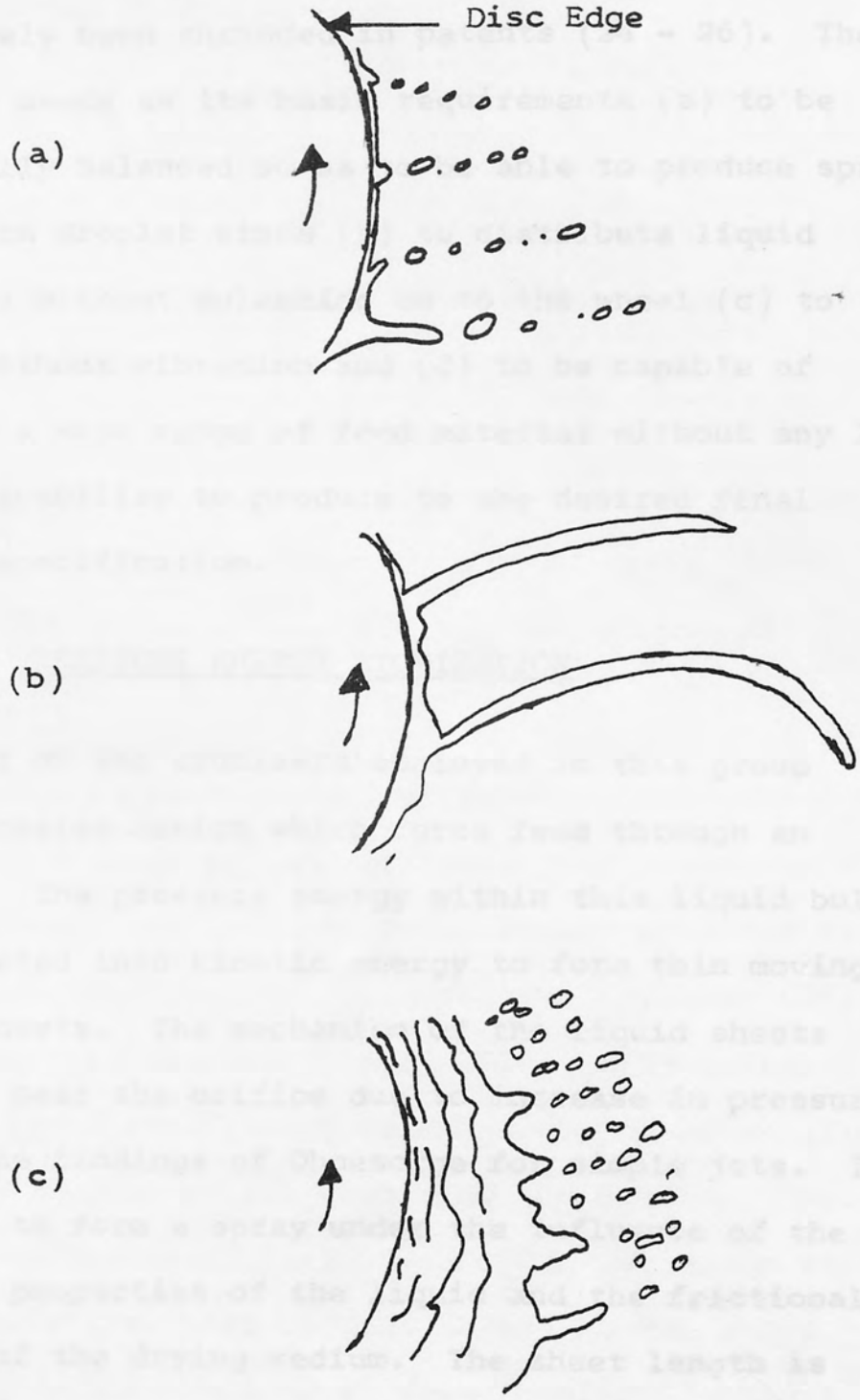

FIGURE 2.1 MECHANISM OF ATOMIZATION

(a) Direct Droplet Formation

(b) Ligament Formation

(c) Sheet Formation

range 30 - 120 microns. The design of the atomizers has largely been shrouded in patents (24 - 26). The atomizer needs as its basic requirements (a) to be dynamically balanced so as to be able to produce sprays of uniform droplet sizes (b) to distribute liquid uniformly without splashing on to the wheel (c) to rotate without vibration and (d) to be capable of handling a wide range of feed material without any loss in the capability to produce to the desired final product specification.

2.1.1.2 PRESSURE ENERGY ATOMIZATION

Most of the atomizers employed in this group employ nozzles design which force feed through an orifice. The pressure energy within this liquid bulk is converted into kinetic energy to form thin moving liquid sheets. The mechanism of the liquid sheets break up near the orifice due to increase in pressure follow the findings of Ohnesorge for simple jets. They break up to form a spray under the influence of the physical properties of the liquid and the frictional effects of the drying medium. The sheet length is directly proportional to viscosity and inversely proportional to surface tension, pressure, sheet velocity and frictional effects which increase turbulence. Two types of sheets are formed, the conical and fan sheets. Conical sheets give rise to conical spray patterns while fan sheets produce fan spray patterns.

CONICAL SPRAY PATTERN

Conical spray patterns are mostly produced by centrifugal pressure nozzles. The conical sheet which results in the spray is produced where the liquid is flowing in radial lines when caused to flow through a narrow divergent annular orifice. In commercial atomizers, the conical sheet lengths are very short and can hardly be seen. Also the process of liquid disintegration proceeds very fast. So it is difficult to distinguish individual phases of liquid break up experimentally.

Two types of conical spray patterns are obtained, the hollow cone spray and the solid cone spray. The former is produced by centrifugal pressure nozzle with tangential liquid entry (27), with swirl insert (28) or with inclined slotted inserts (29). The hollow cone spray has an air core formed from liquid rotating within the nozzle at the centre of the orifice. Angle of spray increases with air core which increases with greater rotation. Air core is absent in the solid cone spray because the spray cone consist of almost evenly distributed mass of spray drops. It can be obtained from hollow cone by balancing the rotational motion with an axial liquid velocity component.

The hollow cone nozzles are mostly employed in co-current spray driers because the majority of the droplets lie on the extreme edge of the cone where

the contact with the drying air can initiate rapid evaporation. Solid cone nozzles are best suited to counter-current systems as the solid centre is fully met by the drying air. The use of hollow or solid cone nozzles in a 'mixed' system depends upon whether the first phase of the droplet air flow is co-current or counter-current. Hollow cone nozzles are used for the former and the solid cone nozzles for the latter.

Centrifugal pressure nozzles produce coarser sprays than rotary atomizers hence their use in forming coarse particle powder having good free flowability with mean size in the range of 120 - 250 microns. The mean size is directly proportional to feed rate and viscosity and inversely proportional to pressure. The nozzles are also used where feeds are of low viscosity and contain no large solid particles in suspension. They are easy to replace and maintain and have low cost. However they require high pressure pumps, good filtering to prevent clogging, are prone to wear at high feed solid content and velocity and not very flexible. The feature often considered in the selection of the atomizers include

(1) Uniformity of feed distribution

(2) Possibility of observing nozzle in operation or of isolating nozzles where multiple nozzles are used

(3) Easy access to nozzle

(4) Ease of removal.

Complete theoretical and mathematical treatment of centrifugal pressure nozzles is given by Green (30).

FAN SPRAY PATTERN

Fan spray patterns are produced by deflector atomizers, impinging jet nozzle and fan spray nozzles. The deflector atomizer has a circular orifice. Liquid discharged from this orifice is deflected from the nozzle axis by a curved deflector plate. The impinging jet nozzle incorporate a design in which two or more jets are caused to impinge outside the nozzle. In fan spray nozzle with a single orifice design, two streams of liquid are made to impinge behind the orifice to produce sheet in a plane perpendicular to the plane of the streams.

The mechanism of flow through fan spray nozzles had been investigated by Dorman (31), Fraser (32) and Hargerty and Shea (33). Dombrowski et al (34) in investigating the principal flow characteristics of fan spray nozzles concluded among other things that the thickness of the sheet was a function of injection pressure, surface tension, density, viscosity and the sheet distance from the orifice while the trajectory was a function of sheet thickness, injection pressure and surface tension.

Rectangular or oval orifices are usually employed. The spray angle depends upon the orifice configuration.

2.1.1.3 KINETIC ENERGY ATOMIZATION

In this kind of atomization high velocity gas (usually air) jets are directed at a liquid bulk. The kinetic energy of the gas creates frictional forces over the liquid surface thus causing it to become unstable and then disintegrate into droplets. The liquid disintegration follows two phases. The first involves the tearing of liquid into filaments and large droplets while the second breaks the products of the first phase into smaller droplets. These two phases are influenced by the fluid properties such as surface tension, density, viscosity and the gaseous properties of velocity and density. At low liquid flow rates the above condition can be brought about by impacting the solid liquid jet by high velocity gas. When the flow rates are high, a prefilming stage is required to create instability by transforming the bulk liquid into thin sheets. This is achieved by rotation of the liquid within the nozzle. Many workers (34 - 37) have discussed the general mechanism of drop formation for individual atomizer under this type of atomization.

Designs arrived at producing optimum condition for optimization comprise of contacting of air and liquid:

(a) Within the nozzle (internal moving head)

(b) Outside the nozzle (external mixing)

(c) Combination of (a) and (b) by using two

air flows (three fluid nozzles).

(d) At the rim of a rotating nozzle head (pneumatic cup atomizers).

Convergent nozzle head are the most widely employed in spray drying. The nozzles have great flexibility in that they can be used for highly viscous Newtonian or non-Newtonian feeds (such as slurries, pastes and glues) or to obtain fine sprays of low viscous Newtonian liquids. However fine sprays demand the liquid orifice being circular and air annulus being concentric. Three fluid nozzles produce sprays of mean sizes lower than the two fluid nozzle under 100 microns. When compared with other alternative atomizers, both nozzles produce sprays of high uniformity and smaller droplet sizes. They have less tendency towards clogging and do not require high pressure pump. The disadvantage lies in the fact that they are best suited to moderate flow rates, require high cost of compressed air and have very low nozzle efficiency. The spray characteristics of some of the nozzles have been reported (38 - 40).

2.1.1.4 SONIC ENERGY ATOMIZATION

Development of atomizers using sonic energy are still in the early stages and like the design of many of the other kinds of conventional atomizers, results from work on design have been largely if not wholly patented. Four main types of nozzles are known - the vortex whistle nozzle, the mechanical vibratory nozzle,

the stem jet nozzle and the Hartmann mono whistle nozzle. Discussion about them were given by Kaltenbach (41), Popov et al (42), Litsios (43) and Wilcox et al (44). Antonevich (45) discussed the theory of sonic atomization. Some of the above workers also discussed the spray characteristics of the nozzles.

Once successfully developed sonic energy atomizers may be suitable in dealing with abrasive and corrosive materials, non-Newtonian and highly viscous liquids that cannot be adequately or profitably catered for by other atomizers. A spring off from this advantage is that ultrasonic could then be employed to increase the drying rates (46, 47).

2.1.2 SPRAY AIR CONTACT

A sound knowledge of the manner in which air and spray are contacted and about the flow patterns of both the air (or the drying medium) and the droplets is essential for spray drier design and performance. Parameters of design such as the rate and extent of drying, residence time of droplets; and the avoidance of pitfalls like atomizer deposits and the deposition of partially dried products on the walls of the driers depend very much on the type of flow patterns created by air disperser. An accurate prediction of droplet trajectories will also enhance a good estimation of spray drier capacity and efficiency.

Spray air contact is determined by the position of the atomizer relative to the drying air inlet. There are three principal arrangements (48, 49). The 'co-current flow' where both air and feed enter the spray tower from the same end, the 'counter-current flow', where they enter from opposite ends and the 'mixed flow' which is a mixture of the first two. The product to be dried determines how best to contact the spray with the drying medium. Of the three arrangements, counter-current flow has been claimed to give the best performance in most spray drying processes because:

(1) It enhances greater mixing of spray and air enabling coarser sprays to be dried per given chamber size.

(2) It increases droplets residence times due to the drag on the droplets by the upflowing air.

(3) It reduces radial trajectory of the spray so that the wall impingement of the dried product is decreased.

However the arrangement has tendency for deposit formation on the surface of the atomizer.

In spite of numerous attempts to obtain the air and droplet flow patterns the amount of information available in the literature is too few and is applicable to small driers. Data are treated with caution because in obtaining them, there is often interference with the normal flow such as in the use of probing devices. Also visual observations such as the use of light powder or smoke suspended in air streams are often employed. General reviews (50,51) have shown that the droplets attain the velocity of the surrounding in the proximity of the atomizer as soon as they are released. The distance they travel before being finally influenced by air flow depends upon the droplet size, shape and density.

2.1.2.1 FLOW PATTERNS AND RESIDENCE TIME DISTRIBUTION OF SPRAY DROPLETS

A common approach used in determining droplets flow pattern is to calculate the droplet trajectory from the atomizer to the chamber wall using stepwise methods.

Most of the studies on the flow patterns of spray droplets seem to have come out with the conclusion that the droplets movement can be identified by two zones, "the jet or nozzle zone" and the "free entrainment zone" (52). Using this conclusion, Gauvin et al (53) predicted the droplet trajectory for water spray and found this to be in good agreement with experimental results. Their findings were extended by Katta et al (54) in predicting the three dimensional motion of droplets of calcium lignosulfonate in a spray drier.

The droplet movement in the nozzle zone depends largely on the characteristics of the atomizer employed to obtain the spray (55 - 56). For a rotary atomizer in a small spray drier, the droplet trajectory is governed initially by the air swirl around the wheel caused by rotation and finally by the drying air. For large industrial driers the influence of wheel rotation is negligible. In the free entrainment zone, there is a considerable amount of spray-droplet mixing and the trajectory mostly depends on the drying air. Friedman et al (57) proposed a relation to assess the variations in trajectories for changes in atomization condition for drops produced by low speed disc atomizer.

Residence Time distribution (RTD) analysis for droplets has not received the same attention as that of RTD for air or drying medium. This is because most workers believed that droplets will have the

same RTD as air or in the extreme display plug flow characteristics (58). Pham and Keey (59) used carbon-14 in the form of sodium carbonate as a tracer. They concluded that in a turbulent stream, the relative motion and degree of entrainment of droplets were affected by the inertia of the particle and the magnitude of the drag. These findings were incorporated in a parameter which they claimed was useful for measuring the turbulence effect.

In their studies on flow visualization and residence time in a spray drier, Ade-John and Jeffreys (60) used iodine solution in pottasium iodide as tracer to obtain the RTD of water and slurry. Their results showed that the drop phase residence time increased with higher air flow rates. But much more detailed analysis of the results was hindered because they were unable to eliminate the delay imposed by the accumulation of the tracer on the wall of the drier.

2.1.2.2 FLOW PATTERNS AND RESIDENCE TIME DISTRIBUTION OF AIR

The flow patterns of air have received much more direct investigation than that of the droplets (61 - 63). The use of dispersion models to elucidate the flows in reactors such as packed beds and packed columns (64,65) was extended to characterise the air flow patterns in terms of a mixture of 'plug flow' zone, 'well-stirred tank' zone and 'air inert' zone

called the by-pass stream.

Paris et al (66) proposed a flow model consisting of two stirred tanks in parallel with a plug by-pass in thier studies of spray in a counter current arrangement. The model mirrored a rapidly ascending central core surrounded by annular zone of intense turbulence. This observation was also reported by Chaloud et al (67) in studying the air flow characteristics in a co-current drying chamber with no spray.

Ade-John and Jeffreys in the same type of studies as mentioned above proposed a model consisting of two well stirred tanks separated by a plug flow zone, the three in parallel with a by-pass stream to describe the flow characteristics of air in a counter-current spray drier.

2.1.3 DRYING OF SPRAY DROPLETS

Drying of spray or moisture evaporation involves simultaneous heat and mass transfer. Heat is transferred by convection from the hot gass (air) to the droplet surface and by conduction into the droplet. The vaporised liquid passes first by diffusion through pores in the crust formed on the drop and finally by convection into the gas stream (68 - 70). The drying follows two stages - the first and second periods of drying.

In the first period, the majority of moisture droplet is removed and the rate of evaporation is virtually constant because moisture migration from the droplet interior is sufficient to maintain surface saturation. The droplet temperature is represented by the wet-bulb temperature. The second period consists of one or two falling rate periods. In this period, the moisture level within the droplet has decreased to a point (critical moisture content) whereby surface saturation cannot be maintained by moisture migration. The evaporation rate thus decreases until drying is complete. Evaporation at this stage is predominantly through diffusion and capillarity mechanism. Findings from the studies into evaporation of pure liquid droplets and liquid droplets containing solids to a large extent form the basis of mechanism used to explain spray evaporation.

2.1.3.1 PURE SINGLE DROPS

Majority of the equations used to explain the evaporation of droplets are based on the premise that the mechanism of evaporation for still air, explained by boundary layer theory, can be justifiably applied to many spray drying conditions. Thus by taking into consideration the flow conditions and the properties of the droplets, dimensionless groups Nu, Re, Sc are combined in deriving two principal equations:

$$Sh = 2.0 + \Psi Re^{0.5} Sc^{0.33} \quad (2.2)$$

and $$Nu = 2.0 + \Psi Re^{0.5} Pr^{0.33} \quad (2.3)$$

where 2.2 and 2.3 correlate the mass transfer and heat transfer rates respectively.

The constant 2.0 arises from the condition Re = 0, where the relative velocity between the droplet and the drying medium is zero. Froesling (71) from studies into evaporation from spherical drops reported a value of Ψ=0.552 for Re values of 2-1300. This value of Ψ was also reported by Maxwell and Storrow (72). Miura (73) gave Ψ value of 0.6 for Re = 1-1000 while Tsubouchi and Sato (74) gave Ψ value of 0.5. But the most widely quoted value is that of Ranz and Marshall given as

Ψ = 0.6 for re = 2-220.

There are some limitations in the use of the above equations. There is an inherent supposition that the boundary layer thickness will remain constant.

This is based on the assumption that the droplet internal structure is stable and that droplets are also stable in air flow. Hence any deviation from the sphericity of the droplets and any swirling of the droplets in the air flow are bound to change the thickness of the boundary layer and therefore change the mass and heat transfer rates. Also drag coefficient is assumed at steady state while the heat transfer to evaporated moisture is neglected. Both assumptions are not true in reality.

Further investigations were carried out due to the above limitations. These took into consideration other effects such as bouyancy, free and forced convections, partial pressure and temperature (75-78). A relatively recent work by Jeffreys and Audu (79) resulted in a correlation of the form:

$$Sh = 2.0 + 0.44\left(\frac{T_a - T_p}{293}\right)^{0.008} Re^{0.5} Sc^{0.33} \qquad (2.4)$$

Their correlation was temperature dependent and closely simulated the operations in a spray drier.

2.1.3.2 SINGLE DROPLETS CONTAINING DISSOLVED SOLIDS

The evaporation from droplets containing dissolved solids differs completely from that of pure droplets because of the formation of solid material at the droplet surface. The initial evaporation rate is

virtually the same as for pure free liquid droplets of equal size due to a free liquid interface between the gas stream and the solution being dried. However as drying proceeds, a crust is formed when the solution becomes concentrated beyond saturation. At this point a particle with a core of saturated solution is formed due to the separation of liquid and gas interface by the crust. Heat and mass transport paths then took forms different from Colburn analogy. So drying takes place by heat conduction through the crust and by evaporation through the pores in the crust. If the crust remains intact, the drying rate falls and the water vapour passes through the pore by diffusion and then by convection back into the gas stream.

Most of the earlier works on crust formation during the drying of drops containing dissolved solids used models based upon transient mass and heat balances and mass transfer by molecular diffusion. The model was initiated by Ranz and Marshall. Their studies were carried out on solutions of Ammonium Nitrate and Sodium Chloride. They concluded that when the drop formed a solid structure and the diameter became constant, the falling rate period ensued during which the temperature rise continually due to sensible heat transfer in the case of solution and to both heat of crystallization and sensible heat transfer in that of

$$\frac{\partial C}{\partial \theta} = D\left(\frac{\partial^2 C}{\partial r^2} + \frac{2}{r}\frac{\partial C}{\partial r}\right) \qquad (2.5)$$

Charlesworth and Marshall (80) studied the evaporation from single drops containing dissolved solids such as sodium sulphate and Ammonium Chloride. By extending the above model they obtained a correlation which related time required for the completion of the solid crust to solute weight fraction and density. Their findings were later extended by Duffie and Marshall (81).

In extending their studies to the drying of drops of particulate slurries, Audu and Jeffreys estimated crust thickness from stereoscan micrographs and the crust porosity from Kozeny's equation. They then correlated the coefficient of mass transfer through the crust in terms of diffusion coefficient, crust porosity and thickness. They proposed the equation:

$$K_c = \frac{D_v \epsilon^{1.5}}{C_T} \qquad (2.6)$$

where K_c is the coefficient of mass transfer of the crust, P_o is porosity and C_T is the crust thickness.

They further observed that K_c decreased with increase in drop size and drying and concluded that

equation 2.6 could be used to estimate the overall mass transfer coefficient for use in the design and analysis of spray drying equipment.

2.1.3.3 SPRAY OF DROPS

Although the same basic theory applies to simple droplets as well as droplets in a spray, there is a great difference between the evaporation characteristics of the two. Unlike single droplets, the analysis of drying characteristics of spray of droplets present enormous difficulties experimentally. The difficulties arise mainly in determining the factors of analysis such as mean diameter and size distribution of spray, droplet trajectory and the number of droplets present at any given time per volume of drying air.

SPRAY OF PURE LIQUIDS DROPS

For spray of pure liquid droplets, many attempts have been made to analyse the spray evaporation. These attempts could be grouped into theoretical, practical, mathematical and computational analysis. Theoretical approach was used by Probert (82) who considered the droplets to have no relative velocity and the temperature driving forces to be negligible. He observed that the rate at which evaporation proceeded to completion was a function of the spray homogeneity. These findings were extended to spray evaporation under relative velocity by Fledderman and Hanson (83).

A practical method in which the size distribution is divided into small size groups was used by Marshall (84). Evaporation for each group was then considered individually for selected time interval until evaporation was complete.

Mathematical approach was used by Shapiro and Erikson (85) for one dimensional spray motion. This approach was similarly used by Bose and Pei (86) who studied evaporation of water sprays in a co-current flow nozzle dryer. They concluded that a substantial part of the evaporation took place during spray deceleration and that the relative velocity between spray and air contributed greatly to heat and mass transfer rates. In addition, they claimed that the relative velocity could not be replaced by terminal velocity in an equation involving evaporation analysis.

Computational methods were used by Dickinson and Marshall (87) to determine the evaporation history of water sprays. They obtained equation for spray evaporation of non-uniform distribution in terms of mean diameter, size distribution, droplet population, drying air and droplet temperature and air velocity.

SPRAY OF DROPLETS CONTAINING SOLIDS

The analysis of evaporation of spray of droplets containing solids is very complex. Apart from the assumption made in the analysis for single

droplets containing dissolved solids, consideration also has to be given to the following:

(a) Crust are not formed simultaneously by all the droplets within the size distribution.

(b) Vapour pressure lowering depends upon droplets size.

The evaporation history of sodium nitrate was studied by Baltas and Gauvin (88) using computer programming for stepwise techniques. Even though simple system of spray movement at terminal velocity in the free fall zone of a single nozzle dryer was chosen, the computations were complex. The results obtained could still not give accurate prediction of spray evaporation due to the difficulty in obtaining representative data for spray drying parameters. Stepwise method of calculation was also used by Dlouchy and Gauvin (89) to predict total evaporation time.

Other workers also investigated either the factors influencing the properties of spray dried materials (90) or the effects of drying conditions on the properties of spray dried particles (91). However many of the data reported in literature are incomplete and were obtained in different type of driers with different atomizers and collecting systems. Hence only the trends of the data need be taken seriously.

2.1.4 SEPARATION OF DRIED PRODUCTS

This is the final stage of spray drying operation and involves the separation of dried product from air followed by the removal of dried product from the dryer. Two types of design are usually incorporated - one point and two point discharges.

In one point discharge the dried product and air are both conveyed to the collecting equipment for separation. This type is employed mostly in the co-current spray dryers. For two point discharge, there is a primary product discharge, usually from the base of the dryer followed by recovery of fines from the collecting equipment. Counter-current and mixed flow spray dryers favour this type.

Equipments for separation range from conventional types such as cyclones, bag filters, scrubbers, electrostatic precipitators (92) to recent ones such as intensive filter fabric filler, differential bag shelving equipment and the ultrajet air pulsed fabric filler (93).

Klein (94) described the use of ultra-high efficient mechanical powder separator, termed the "tornado dust collector" while Alonso (95) described the modern trends in separation. Stairmand (96) gave guidance on the selection of powder-air separating equipments.

Factors usually considered before final selection is made include:

(1) Space area requirement of the equipment. This has to fit well with the overall plant layout of the spray dryer.

(2) Product handling suitability. This means that the equipment chosen must be one that can cope with the characteristics of the product such as the powder properties. It must also be able to withstand the operating conditions of the drying process such as temperature and air flow rates.

(3) Operational procedure - The equipment must be able to operate continuously or batchwise according to the demands of the spray drier operation.

(4) Collection efficiency - This factor is crucial where consideration has to be given to environmental pollution.

(5) Cost - The investment and operational cost of the equipment must fit in well with the total operational cost of the spray drier plant to ensure the profitable running of the whole plant.

2.2 DROP SIZE DISTRIBUTION

This refers to the range of sizes of droplets which form the spray from an atomizer or of dried products resulting from the drying of such spray. Many methods are available for measuring the size distribution of droplets and dried particles.

(A) METHODS FOR DROPLET SIZE DISTRIBUTION

These fall into the following groups:

(i) The Droplet Collection Method in which part or all of the spray is collected in sampling cells (97, 98). The accuracy of this method has always been in doubt due to the interference of sampling device with the spray.

(ii) Droplet freezing or solidification - This method is used to prevent the droplets from coalescing (99 - 100). Many of the experimental set-ups in this method are expensive and some suffer from the fact that due to the unknown behaviour of a liquid droplet, the droplets may shrink or expand on freezing (101).

(iii) Photographic Method - This involves high speed double exposure photography which freezes the droplets motion so that their images are recorded for subsequent analysis (102,-103). Problems confronting this

method include illumination, depth of field and the selection of the right distance from the nozzle at which the photograph should be taken.

(iv) Optical Methods - These range from methods based upon light absorption, diffraction or scattering by the droplet (104, 105); to the more recent ones based upon laser holography (106) and low powered laser diffraction (107). The low powered particle sizer is used in the course of the present studies and is fully described in chapter four.

(v) Methods based on inertia or velocity differences - The impaction coated slides are the most significant in this group (108, 109). The impactor act as a separating device in that drops impacting on the plate are run off, collected and their volume is measured while those which escape impaction are subsequently separated from air stream, run off, collected and their volume also measured.

Some of the above methods are extensively reviewed by Ashton (110).

(B) METHODS FOR PARTICLE SIZE DISTRIBUTION OF DRIED PRODUCT

Several methods for measuring the size distribution of particles have been reviewed (111). These fall into six broad groups namely:

(i) The microscopic technique - This involves the individual examination of a large number of particles by an operator (112). It is direct and therefore often used to standardise other methods. However because the operator has to use his initiative as to what particles to examine and include it is tedious and often not as reliable as expected.

(ii) Sedimentation methods - These measure Stoke's diameter of the particles, hence are very good for particles in suspension of low concentration (113). These methods are either cumulative or differential(114). For cumulative methods (such as sedimentation balances) all the samples are collected and quantitative assessments of the weight of particles of a particular size on a greater amount of powder are made. In the differential methods (such as photo sedimentometers) a small proportion of the suspension is measured. Practical

problems with these methods occur in wetting and dispersing the sample. And because of Stoke's principle they cannot ideally be used for particles with flat platelets or long thin-shred configuration.

(iii) Sieving Method - It is the most popular because compared with others it is easy. Sizes of the particles are the sizes of the holes of the sieve mesh through which the particles pass. Elongated particles use square and rectangular meshes. Mesh binding is one of the practical problems encountered in sieving(115).

(iv) Coulter Counter - This examines each particle individually and measures the volume of the particles against the number of particles (116). It can be used for determining sizes in the range 0.3 to 300 microns. For successful application it needs careful and accurate standardisation.

(v) Particle Size Analyser - This is the low powered laser particle sizer referred to above in A (iv).

(vi) Others - These include air elutriation (117), sampling methods such as scoop sampling and quatering (118) and surface

area measurement such as gas absorption techniques (119).

Size distribution may be defined by number, area, weight and volume depending upon the method of measurement used to obtain the distribution. Mean diameters are often used as size characteristics to represent the whole size distribution. They all arise from the basic equation given by:

$$(\bar{D}_{qp})^{q-p} = \frac{\Sigma ND^{q}}{\Sigma ND^{p}} \qquad (2.7)$$

The values of p and q and the particular field of application in which the resulting diameters can be used are shown in Table 2.2. In addition to these mean diameters, the following are also used:

(a) Geometric Mean Diameter (D_{gm})

$$D_{gm} = (D_i^{Ni})^{1/\Sigma Ni}$$

or
$$\log D_{gm} = \frac{1}{\Sigma N_i} N_i \log D_i \qquad (2.8)$$

(b) Most Frequent Diameter (D_f)

This corresponds to the diameter having the highest value on the frequency curve.

(c) Harmonic Mean Diameter (D_{HM})

$$D_{HM} = \frac{100}{\Sigma f_N(D)/(D)} \qquad (2.9)$$

TABLE 2.2

MEAN DIAMETERS, $\bar{D}$ USING EQUATION (2.7)

p	q	Name of mean diameter	Field of Application
0	1	Linear	Comparisons, evaporation
0	2	Surface	Absorption
0	3	Volume	Hydrology
1	2	Surface diameter	Adsorption
1	3	Volume diameter	Molecular diffusion and evaporation
2	3	Sauter or volume surface	Mass transfer reaction and efficiency studies.
3	4	De Brouckere	Combustion equillibrium.

(d) Median Diameter (D_M). This is the diameter above or below which 50% of the number of droplets or particles lie. It is represented by the 50% line on the cumulative curve.

Of all these mean diameters, the Sauter mean diameter and the median diameter are the most commonly used in spray drying operations.

Single parameter does not adequately define the complete size distribution. Therefore for design purposes the size distribution is often represented by distribution function. The mathematical equations defining these functions and their sources of reference are shown in Table 2.3

The Normal distribution is rarely used in spray drying. Log normal is applicable to sprays from rotary (vane wheel) atomizers. The square-root normal is claimed to be good for centrifugal pressure nozzle while the Nukiyama Tanasawa distribution is credited for representing spray from pneumatic nozzles. Rosin - Rammler distribution which is a special case of Nukiyama - Tanasawa is widely quoted to represent size distribution from nozzle sprays. The major problem with these distribution functions is that taken individually they are only good for calculating one or two kinds of mean diameters and not the others (120). This has led to Mugele and Evans

TABLE 2.3

SIZE DISTRIBUTION FUNCTIONS

Normal

$$\frac{d(N)}{d(D)} = \frac{1}{S_N\sqrt{2\pi}} \exp -\left[\frac{(D-\bar{D})^2}{2S_N^2}\right] \qquad (2.10)$$

Log Normal

$$\frac{d(N)}{d(D)} = \frac{1}{D.S_G\sqrt{2\pi}} \exp -\left[\frac{(\log D - \log D_{GM})^2}{2S_G^2}\right] \quad (122) \qquad (2.11)$$

Square-root Normal

$$\frac{d(N)}{d(D)} = \frac{1}{2\ (2\ DS_G)^{0.5}} \exp -\left[\frac{(\sqrt{D}-\sqrt{D_{GM}})^2}{2S_G}\right] \quad (123) \qquad (2.12)$$

Rosin Rammler

$$\bar{V}_D = 100^{-\left[(D/\bar{D}_R)^q\right]} \qquad (124) \qquad (2.13)$$

Nukiyama-Tanasawa

$$\frac{d(N)}{d(D)} = B.D^2.\exp -(C.D^q) \qquad (125) \qquad (2.14)$$

Mugele and Evans Upper Limit law

$$\frac{d(N)}{d(D)} = \frac{1}{D.S_G\sqrt{2\pi}}.\exp -\left[\frac{\log((D_{max} - D)/D_{GM})^2}{2.S_G^2}\right] \qquad (2.15)$$

(126)

to propose the Upper-limit function which is an extension of the log-normal distribution. Their function include a third parameter, the maximum stable droplet size which ensures greater flexibility in fitting experimental data. The distribution also places practical limits on the minimum and maximum droplet sizes. This function was compared with log-normal and square-root normal functions in fitting data from centrifugal pressure nozzles by Nelson and Stevenson (121). They found the upper-limit function and the square-root normal function to approximate the drop size distribution of the data.

Size distribution of dried particles are mostly narrower than size distribution of droplets from which the dried particles are obtained. And unless for low solid feed and low drying temperature conditions, when the size distribution of wet spray follows a known distribution function, that of its dried products follows a different one. The difference between the mean sizes of wet spray and dried product depends upon the nature of the dried products. For crystalline products the difference decreases for increasing feed concentration. This difference is negligible for products characterised by their film forming properties.

2.3 DESIGN AND PREDICTION PERFORMANCE OF SPRAY DRIERS

Although spray drying process has been successfully applied to many industrial processes (1) and is still being tried as possible alternatives to many other existing drying operations, the design and performance prediction of spray driers are based to a very large extent upon empiricism and manufacturer's long experience. As outlined in the process stages of drying, there are many factors involved. These range from droplet or particles sizes and shapes, flows, atomizer types and arrangements to the large variety of products being handled. Hence rather than a unified approach, many design methods have evolved over the years. These methods have been grouped into three types (126), the empirical or semi-empirical, the analytical and the numerical or stepwise method.

EMPIRICAL AND SEMI-EMPIRICAL METHODS

Many attempts had been made using this approach to propose designs. However equations derived had been of limited use practically due mainly to the numerous simplifying assumptions made in arriving at the equations. Turba and Nemeth (127) designed a small spray drying unit for treating pastes containing 40 percent solids and investigated the effect which changes in the two fluid nozzle geometry had upon the drier performance. They then calculated from their

data the drier volume using Luikov's semi-empirical equation (128). This equation which is of the form:

$$\alpha = 1.58 \times 10^{-3} \frac{kW_s}{\rho_s F} \left(\frac{1}{\delta}\right)^{1.6} \left(\frac{1}{u + u_1}\right)^{0.8} \qquad (2.16)$$

gives the volumetric heat transfer coefficient (α) in terms of droplet mean diameter, droplet velocity and other parameters. For both 40 percent chalk slurry and dihydrochlorurite pastes, the values obtained using the equation were bigger by a factor of 10 than the actual size. So they concluded that the equation probably did not take thick paste or slurries into consideration but could predict the trend of volumetric heat transfer coefficients. Froesling's equation:

$$N_A = 2\pi D_v \frac{\Delta P}{RT} \quad 1 + 0.276 Re^{0.5} Sc^{0.33} \qquad (2.17)$$

for evaluating the rate of mass transfer (N_A) from drops of pure liquids also fall into this category.

Longwell and Weiss (120) predicted the size distributions of liquids sprayed into high velocity air streams in terms of the air velocity, diffusivity, liquid concentration and other physical properties and the system geometrical data. Their empirical data were used as the basis of a graphical method that was employed by Feder (130) in predicting the rate of

evaporation of any fluid in a moving air stream. He had to extrapolate to obtain his charts because experimental data exist over a limited range.

Finally dimensional analysis were used by Borde (131) and Dolinsky (132) to predict spray drier performance.

From the above brief resume it could be concluded that the only good point about these methods of approach is that they can be used to give qualitative idea about the effects which some of the operating variables have on the design and prediction performance of spray driers.

ANALYTICAL METHODS

Analytical methods fall into two main categories. One uses a single droplet to characterise the behaviour and drying of spray while the other uses a size distribution.

Methods which consider a single drop

Under these methods, a single drop usually the largest droplet produced from the atomizer is used to represent the entire spray. Equations of motion and evaporation for this drop are then developed and solved.

Johnstone and Eads (133) derived an equation based on Froessling's correlation of mass transfer data from evaporating drops. Their equation:

$$\Theta=(2/3)Z^{1.5}-\left(\frac{2}{\epsilon^2}\right)Z+\frac{8Z^{\frac{1}{2}}}{\epsilon^3}-\frac{16}{\epsilon^4}\ln\left(1+\frac{\epsilon}{2}Z^{\frac{1}{2}}\right) \qquad (2.18)$$

which can be written in form of

$$\Theta = \frac{f(z,\epsilon)}{\gamma}$$

was used in predicting the time required for complete evaporation of liquid drop. By means of the equation they were also able to determine the diffusivities of di-n-butyl phthalate and sulphur vapours.

Miesse (134) solved the equation of motion and evaporation for a pure liquid drop in constant accelerating and decelerating gas streams. He assumed a Stokesian regime and Nu = 2 (that is as for droplets in a quiescent fluid). Specifically for spray drying with counter-current air flow he developed an equation of the initial diameter of the droplet as a function of the governing variables. The equation is:

$$D_o = \frac{\lambda L}{U_o}\left(\frac{1+q}{2}\right)(0.6)^q \qquad (2.19)$$

where Do is the initial drop size.

Glukert (135) developed correlation for predicting the performance of spray driers with disc, twin fluid and pressure atomizers. He based his design on the

maximum droplet diameter, D_m which he took to be equal to D_{vs} (the volume surface mean diameter). Due to large sizes (30-200 microns) encountered in spray drying, his correlation need to be treated with caution because of the underlying assumption that droplets have the same velocity as that of the drying gas. Using data obtained from the effect of atomizing conditions on the initial droplet sizes and velocities, he arrived at these equations:

$$q = \frac{4.19K_f(R_c - r/2)^2}{(D_m^2)} \frac{\Delta T_t}{\rho_s} \sqrt{\frac{W_s \rho_t}{rN}} \qquad (2.20)$$

for Centrifugal disc atomizer.

$$q = \frac{10.98K_f v^{0.667}}{D_m^2} \Delta T_t \cdot D_s \sqrt{\frac{\rho_t}{\rho_s}} \qquad (2.21)$$

for Pressure nozzle atomizer.

$$q = \frac{6.38K_f v^{0.667}}{D_m^2} \Delta T_t \cdot \frac{W_s}{\rho_s} \sqrt{\frac{\rho_s}{W_a V_a} \frac{W_A + W_s}{W_A}}$$

for two-fluid atomizer.

By using Ranz and Marshall equation for heat and mass transfer to spherical particles, and assuming constant air conditions and pure liquid

droplets, Sjenitzer developed charts in form of humidity and thermal efficiency to predict the performance of spray driers (136). He also introduced equations for determining the height of transfer units. This graphical approach was also adopted by Greene et al (137) to propose humidity chart for powdered egg.

In summary, because the largest drops are by and large the determining factor for the design and operation of spray driers, the analytical methods offer a better approach to empirical methods. However, most of the equations apply only to pure liquids. In addition, for accurate work the mechanism of drying needs to be taken into consideration.

Methods based on Size Distributions

These methods consider a size distribution of the spray. The total evaporation of the spray is obtained from this distribution by integrating the evaporation in each size range over the whole size spectrum.

Many of the methods resolved around solving differential equations for a cloud of particles or drops undergoing evaporation and acceleration. Such equations usually involve inter-relating the number or size distribution G and rate of growth of particle

or droplet diameter R to other parameters such as distance of spray from nozzle, velocity and position of droplets. Shapiro and Erikson obtained the following equation:

$$\frac{\partial G}{\partial t} + U_p \frac{\partial G}{\partial x} + R \frac{\partial G}{\partial D} = -G \frac{\partial U_p}{\partial x} + U_p \frac{dA}{dx} + A \frac{\partial R}{\partial D_p} \qquad (2.23)$$

This equation was solved by assuming some forms of $A(x), R(D_p), U_p(D_p)$ and $G(D_p)$. Further assumptions involve taking $\frac{dA}{dx}$ as zero and $\frac{\partial U_p}{\partial D_p}$ being negligibly small (uniform cloud motion). Hence only $G(D_p)$ and $R(D_p)$ need be determined.

Marone (138) and Yaron and Gal-or (139) used similar approach as above. Schlunder (140) obtained a complex analytical expression for the evaporation history by trying normal distribution for $G(D_p)$ and a power law for $R(D_p)$. McIlvried and Massoth (141) applied similar reasoning to obtain mathematical evaluation of gas-solid kinetics for spherical particles. The results obtained by them may perhaps be useful for spray drying cases where the falling rate period has been reached.

To avoid the complex equations typified by equation (2.3), many workers resorted to choosing

expressions for R(Dp) and G(Dp) by assuming solutions in form of first order reactions or constant mean evaporative diameter (MED), De. This approach was sought because smaller droplets evaporate quickly and migrate from the evaporation process for the larger droplets. Thus, although all the droplets are shrinking, their MED remain constant. This also implies that their specific evaporation (ie evaporation per unit remaining mass) also remain approximately constant.

De is given in terms of K, the evaporation rate by:

$$k = \frac{(\pi/2)D_e^2 R(D_e)}{(\pi/6)D_e^2}$$

$$= \frac{\int_0^\infty (\pi/2)D_p^2 R(D_p)G(D_p)dD_p}{\int_0^\infty (\pi/6)D_p^3 G(D_p)dD_p} \qquad (2.24)$$

K and De were said to remain constant as evaporation proceeded by Hopkin and Eisenklam (145) and Shapiro and Erikson provided

$$G \propto D_p^{n-1} \exp(-kD_p^n)$$

and $$R \propto -D_p^{1-n}$$

Assuming Nu=2 and using polynomial form for the size distribution, Dombrowski also showed that De remained roughly constant up to 90% evaporation in pure liquid sprays and for much longer for slurries and pastes.

The most widely quoted equations for the size distribution assumed by the MED methods are:

(1) The Nukiyama-Tanasawa (NT) distribution

$$\frac{dv}{dD_p} = KD^5 \exp(-aD_p^{\delta}) \qquad (2.25)$$

(2) The Rosin-Rammler distribution (RR)

$$\frac{dv}{dD_p} = KD_p^{\delta-1} \exp(-aD_p^{\delta}) \qquad (2.26)$$

(3) The root-normal distribution (RN)

$$d(\sqrt{D}_p) = \frac{1}{\sqrt{2\pi}\sigma_{RN}} \cdot \exp\left[-\frac{(\sqrt{D}_p - \mu_{RN})^2}{2\sigma_{RN}^2}\right] \qquad (2.27)$$

(4) The Log-Normal distribution (LN)

$$\frac{dv}{d(\ln D_p)} = \frac{1}{\sqrt{2\pi}\sigma_{LN}} \qquad (2.28)$$

Pham and Keey examined the MED methods critically. They found out that the assumption of MED being constant held only for a limited range of σ_{LN}, σ_{RN} and up to a certain value of the fraction evaporated. Also depending on the drying behaviour of the sprayed feed, the results may or may not be affected by the presence of solids. And because of the limit imposed by other underlying assumptions such as constant Nu, infinite droplet size, constant drying conditions and

uniform particle movement, they concluded that constant MED methods could be used only for the early stages of evaporation.

NUMERICAL METHODS

In this approach, size ranges based on the initial sizes of groups of droplets are used, making it possible to follow each group throughout its history. The evaporation of each size range in the spray for a given increment of time and space is calculated. The values for all the size ranges are then summed up to get the total evaporation for that increment. This process is repeated for the next increment until the total time or space is covered. First proposed by Marshall, the method had been modified and used by other workers (143-144).

Provided the basic assumption are sound, the methods are flexible, fairly accurate and can take into consideration a great number of operating factors such as turbulence effect, sensible heat, absolute and relative velocity of droplets, temperature, mass flux on heat transfer and initial evaporation due to atomizing.

CHAPTER THREE

MATHEMATICAL MODELS

3.1 Droplets Residence Time Distribution Model

3.2 Calculation of Particle Trajectories

3.1 DROPLETS RESIDENCE TIME DISTRIBUTION MODEL

INTRODUCTION

The model proposed here is an extension of that used by Ade-John and Jeffreys (60) for predicting the residence time distribution of air in a counter current spray drier. They based their model on a visual observation of the flow patterns of smoke injected into the air stream when they identified zones. Therefore the present model is made up of three sections. The first consists of two well stirred tanks separated by a plug flow. The second consists of a plug flow and a stirred tank while the third section is just a plug flow. This model is shown in Figure 3.1 .

A shot of tracer was injected into the water flow rate and exit concentration profile of the tracer was monitored at the bottom of the tower.

DEVELOPMENT OF EQUATIONS

A variety of methods have appeared in literature for the analysis of residence time distribution (RTD) data (145-146). Gamma function is particularly useful if the volume of the zones can be determined accurately by other means such as the smoke experiment used by Ade-John and Jeffreys. In the absence of such a determination, the overall equation that will evolve

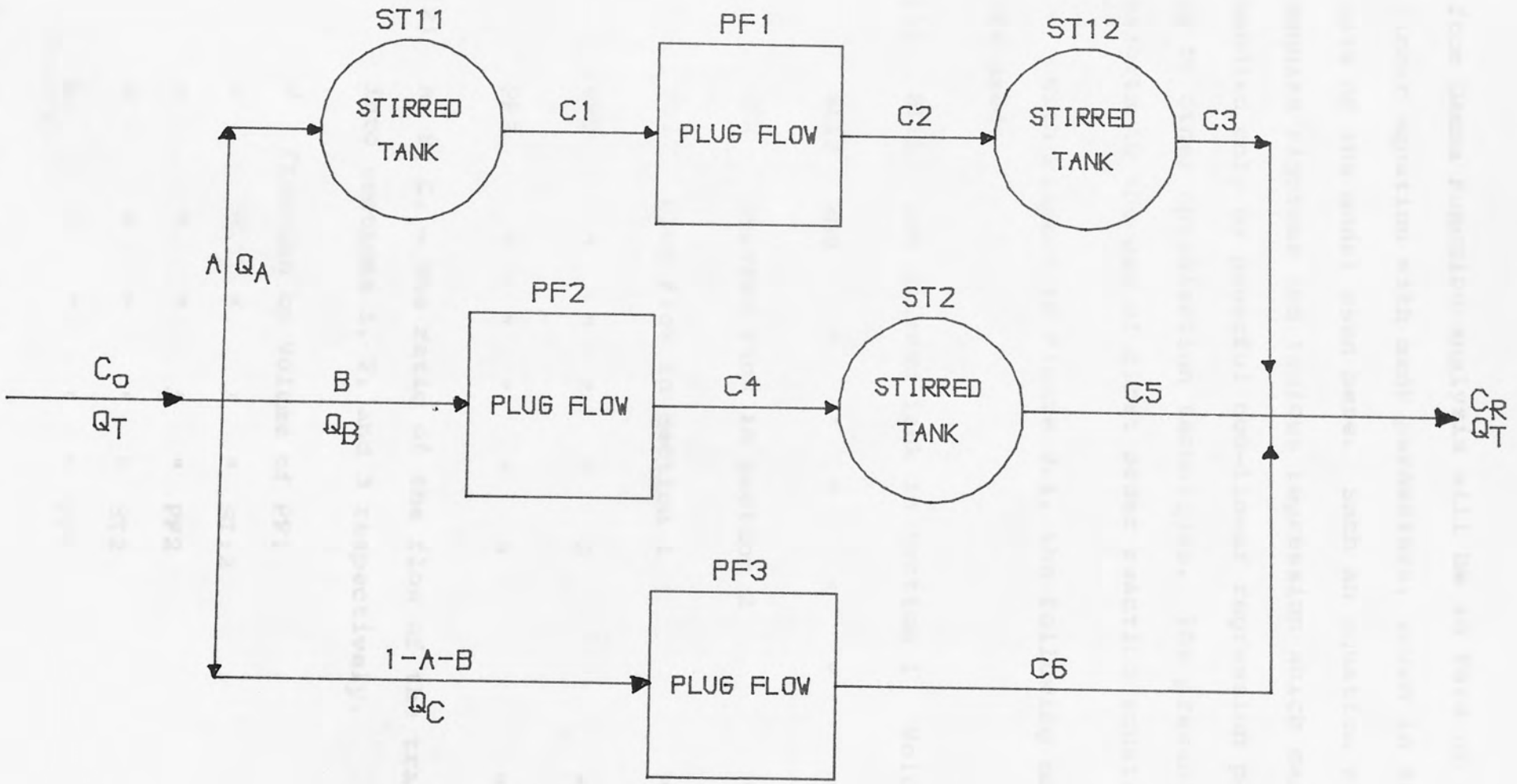

FIGURE 3.1: MODEL FOR DROPLETS RESIDENCE TIME DISTRIBUTION

from Gamma Function analysis will be in form of non-linear equation with many parameters, seven in the case of the model used here. Such an equation will require rigorous and tedious regression which can be handled only by powerful non-linear regression packages or by other optimization techniques. The present work resorts to the use of first order reaction equations.

With respect to Figure 3.1, the following notations are used:

(1) ST11 1st Stirred Tank in Section 1 Volume V_1

ST12 2nd " " " " " " V_K

ST2 Stirred Tank in Section 2 " V_N

PF1 Plug Flow in Section 1 " V_J

PF2 " " " " 2 " V_M

PF3 " " " " " " V_L

(2) A, B, C, - the ratio of the flow of the tracer into sections 1, 2, and 3 respectively.

(3) J fraction by Volume of PF1

K " " " " ST12

M " " " " PF2

N " " " " ST2

L " " " " PF3

(4) Q_A, Q_B, Q_C, - the flow rates into Section 1, 2, and 3 respectively.

From (2), (4) and (5)

$$A = \frac{Q_A}{Q_T} \tag{3.1}$$

$$B = \frac{Q_B}{Q_T} \tag{3.2}$$

$$C = \frac{Q_C}{Q_T} = 1-A-B \tag{3.3}$$

From (1), (3) and (5)

$$J = \frac{V_J}{V_T} \tag{3.4}$$

$$K = \frac{V_K}{V_T} \tag{3.5}$$

$$M = \frac{V_M}{V_T} \tag{3.6}$$

$$N = \frac{V_N}{V_T} \tag{3.7}$$

$$L = \frac{V_L}{V_T} \tag{3.8}$$

. the fraction by volume in ST11

$$= I-J-K-M-N-L$$

Hence $$\frac{V_1}{V_T} = I-J-K-M-N-L \tag{3.9}$$

ST11 REGION

$$V_1 \frac{dC_1}{dt} = Q_A(Co-C_1)$$

$$\therefore \quad \frac{dC_1}{dt} = \frac{Q_A}{V_1}(C_o - C_1) \tag{3.10}$$

From 3.9 and 3.1

$$\frac{Q_A}{V_1} = \frac{A.Q_T}{1-J-K-M-N-L} \tag{3.11}$$

But $\frac{V_T}{Q_T} = \bar{t}$

therefore 3.11 becomes

$$\frac{Q_A}{V_1} = \frac{A}{\bar{t}(1-J-K-M-N-L)} \tag{3.12}$$

3.12 into 3.10 gives

$$\frac{dC_1}{dt} = \frac{A.(C_o - C_1)}{\bar{t}(1-J-K-M-N-L)} \tag{3.13}$$

In dimensionless form

$$\theta = \frac{t}{\bar{t}}$$

therefore $dt = \bar{t}d\theta$ (3.14)

3.14 into 3.13 gives

$$\frac{dC_1}{d\theta} = \frac{A.(C_o - C_1)}{1-J-K-M-N-L} \tag{3.15}$$

PF1 REGION

This region constitutes a time delay and the only requirement for simulation exercise is to calculate the

delay time Θ_j

T_j is the real time delay

$$T_j = \frac{V_j}{Q_A} \tag{3.16}$$

3.1 and 3.4 in 3.16 gives

$$T_j = \frac{J.V_T}{A.Q_T} = \frac{\bar{t}J}{A} \tag{3.17}$$

$$\therefore \quad \Theta_J = \frac{T_j}{\bar{t}} = \frac{J}{A} \tag{3.18}$$

ST12 REGION

$$\frac{dC_3}{dt} = \frac{Q_A}{V_K} (C_2 - C_3) \tag{3.19}$$

Using 3.1 and 3.5 and performing the same substitution as for ST11 gives

$$\frac{dC_3}{dt} = \frac{A}{K} (C_2 - C_3) \tag{3.20}$$

PF REGION

This is also a time delay

$$T_M = \frac{V_M}{Q_B} \tag{3.21}$$

3.2 and 3.6 in 3.21 and using the same procedure as for PF1 gives:

$$\Theta_M = \frac{M}{B} \qquad (3.22)$$

ST2 REGION

$$\frac{dC_5}{dt} = \frac{Q_B}{V_N} (C_4 - C_5) \qquad (3.23)$$

3.2 and 3.7 in 3.23 and following the same procedure for ST11 gives

$$\frac{dC_5}{d\Theta} = \frac{B}{N} (C_4 - C_5) \qquad (3.24)$$

PF3 REGION

This is also a time delay

$$T_L = \frac{V_L}{Q_L} \qquad (3.25)$$

3.3 and 3.8 in 3.25 and using the same substitution as in PF1 gives

$$\Theta_L = \frac{L}{1-A-B} \qquad (3.26)$$

The total response from the simulation is the sum total of the concentration from the three sections and is given by:

$$C_R = C_3 + C_5 + C_6 \qquad (3.27)$$

SIMULATION PROGRAM

The exit concentration profile of the tracer for

a particular water flowrate was used as the inlet experimental data (pulse) and constitutes the C_o while the exit concentration profiles of the tracer in that water flowrate with various air flowrates constitute the experimental response data. Unlike the usual analysis where $\bar{t}$ is calculated from the reactor or equipment parameter, V_T and Q_T, the alternative way suggested by Levenspiel and Bischoff was used. This involves determining the $\bar{t}$ values from the exit concentration profiles.

Runge Kutta-Merson routine was used to solve all the first order equations (3.15),(3.20) and (3.23). The whole simulation exercise was carried out using a fortran program run on Aston University Harris 500 computer system. A full listing of the program is shown in Appendix C. Values of A,B,J,K,M,N,L were varied until a close fitting occurs between the overall exit response C_R obtained from simulation and experimental response data.

3.2 CALCULATION OF PARTICLE TRAJECTORIES

INTRODUCTION

A knowledge of the paths taken by particulate systems such as solid particles or liquid drops can be of significant contribution to the design or improved performance of the equipments for handling the particles such as spray coolers, spray absorbers and other forms of classification equipments. For instance in spray drying the tower dimensions must be such that the largest droplets are maintained in the drying air long enough to dry to the required specification before striking the walls of the chamber.

When a particle moves in a fluid with an initial velocity, it will be decelerated by frictional forces and accelerated or decelerated by external forces such as gravity so that the net force acting on such a particle will be the vectorial sum of the frictional force and the external forces. The frictional drag depends upon the instantaneous velocity of the particle and therefore on the Reynolds Number, Re. This relationship is always expressed in terms of drag coefficient (C) versus Re plot. Such curves have been determined for spheres, disks and other shapes by many workers (147 - 148). In determining the trajectories, the velocity-time relations for the particle in component directions are determined and the distance

travelled in those component directions are calculated using graphical integration of velocity-time curves.

DEVELOPMENT OF EQUATIONS

The following model has been derived for a special case of a spray of droplets from a centrifugal pressure nozzle, though it can be modified for any other nozzle or atomizer.

Consider that the spray issues from the nozzle at a cone angle Θ and representative velocity U - Figure 3.2. If m is the mass of a droplet, from force balance

$$\frac{mdU_h}{dt} = -F.\text{Sin}\ \frac{\Theta}{2} \qquad (3.28)$$

$$\text{and } \frac{mdU_v}{dt} = mg.\left(\frac{\rho_s - \rho_a}{\rho_s}\right) - F.\text{Cos}\ \frac{\Theta}{2} \qquad (3.29)$$

where U_h and U_v are the components of U in the horizontal and vertical directions respectively.

$$\text{But } F = \tfrac{1}{2}\rho_a U^2 C.A \qquad (3.30)$$

$$\text{and } C = f(R_e) = f\left(\frac{DU\rho_a}{\mu_a}\right)$$

Also

$$\text{Sin}\ \frac{\Theta}{2} = \frac{U_h}{U} \qquad (3.31)$$

$$\text{Cos}\ \frac{\Theta}{2} = \frac{U_v}{U} \qquad (3.32)$$

$$\therefore\ U_h^2 + U_v^2 = U^2(\text{Sin}^2\frac{\Theta}{2} + \text{Cos}^2\frac{\Theta}{2}) = U^2 \qquad (3.33)$$

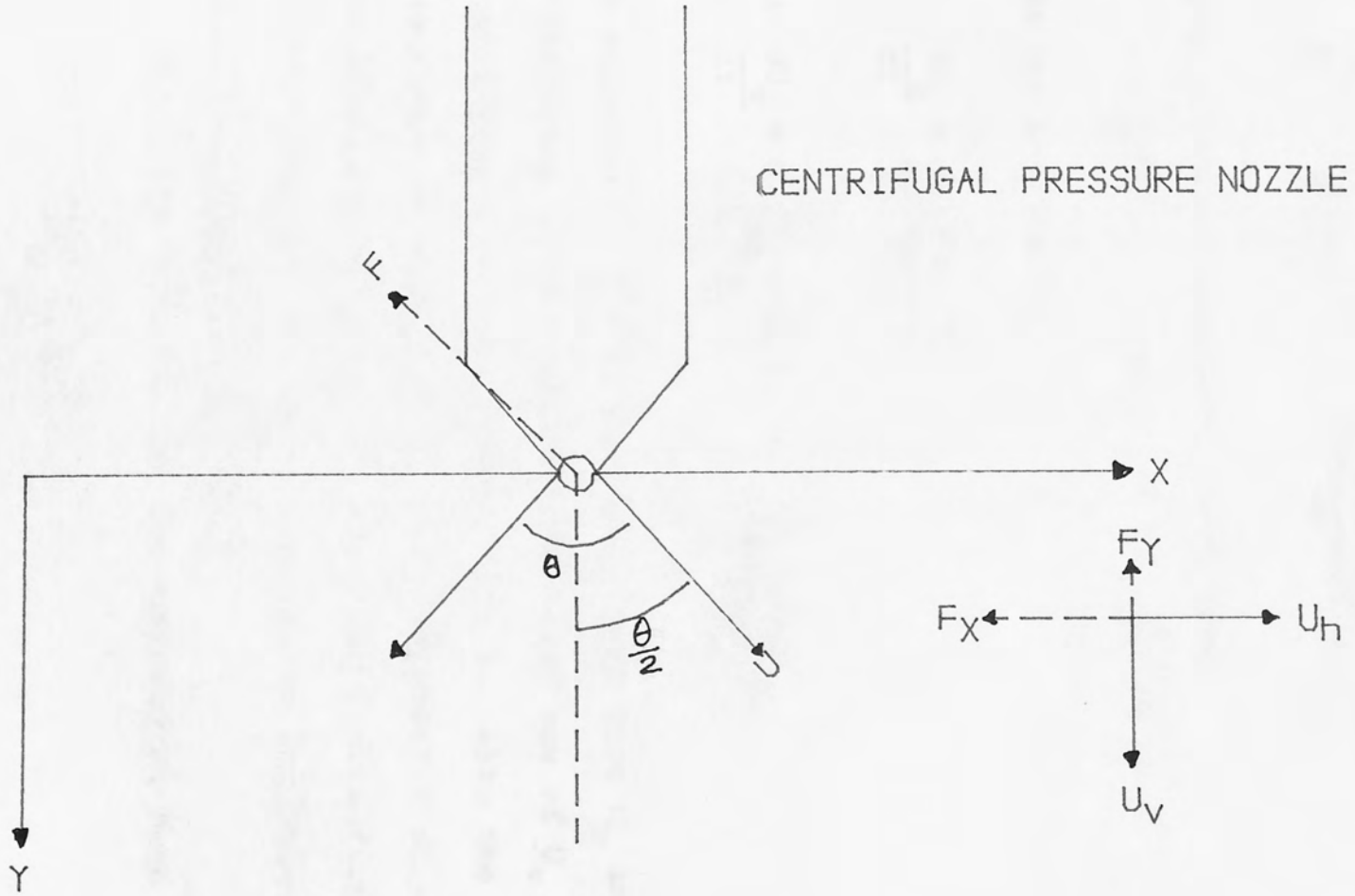

FIGURE 3.2: FORCE DIAGRAM FOR DROPLET TRAJECTORY

Substituting 3.30, 3.31 and 3.32 into 3.28 and 3.29 give

$$\frac{dU_h}{dt} = \frac{\rho_a C.A.U.U_h}{2m} \qquad (3.34)$$

and $$\frac{dU_v}{dt} = g\left(\frac{\rho_s - \rho_a}{\rho_s}\right) - \frac{\rho_a C.A.U.U_v}{2m} \qquad (3.35)$$

The droplets are spherical, therefore

$$m = \frac{1}{6}\pi D^3{}_s \quad \text{and since} \quad A = \pi D^2/4$$

3.34 and 3.35 become

$$\frac{dU_h}{dt} = \frac{-3\rho_a C.U.U_h}{4D_s} \qquad (3.36)$$

and $$\frac{dU_v}{dt} = g\left(\frac{\rho_s - \rho_a}{\rho_s}\right) - \frac{3\rho_a.C.U.U_v}{4D\rho_s} \qquad (3.37)$$

The solution of (3.36) and (3.37) will give U_h and U_v at different times t and the vectorial sum of U_v and U_h will give U at a particular time t. Also the integration of values of U_h and U_v against t will give distances S_h and S_v in the x and y directions and therefore map out the trajectory of the particle.

SOLUTION OF EQUATIONS OF MOTION

Rewriting 3.36 and 3.37 in incremental form give

$$\Delta U_h = \frac{-3\rho_a C.U.U_h \Delta t}{4\ {}_sD} \qquad (3.38)$$

and $$\Delta U_v = g\left(\frac{\rho_s - \rho_a}{\rho_s}\right) - \frac{3\rho_a C.U.U_v \Delta t}{4\rho_s D} \qquad (3.39)$$

The third equation required in the program for solving the equations of motion is:

$$U = (U_h^2 + U_v^2)^{0.5} \qquad (3.40)$$

Starting from initial velocity U_o and t=0, U_{ho}, U_{vo} and Re are calculated and C is determined from the Table of Re against CRe^2 (Appendix D) by interpolation method. A certain time increment Δt is then assumed. ΔU_{ho} and ΔU_{vo} are then computed from (3.38) and (3.39). U_{h1} and U_{v1} are calculated from the addition of ΔU_{ho} and ΔU_{vo} to U_{ho} and U_{vo} respectively. U_{h1} and U_{v1} are now used to compute the second set, ΔU_{h1} and ΔU_{v1}. The first average of ΔU_h and ΔU_v are calculated from ΔU_{ho} and ΔU_{h1}; and ΔU_{vo} and ΔU_{v1}.

The first approximation of the velocities at the end of the interval Δt, V_{h1} and V_{h2} are calculated from addition of the first average of ΔU_h and ΔU_v to U_{ho} and U_{vo}. ΔU_{h3} and ΔU_{v3} are then calculated from V_{h1} and V_{h2} and the second average of ΔU_h and ΔU_v are calculated from ΔU_{ho} and ΔU_{h3}; and ΔU_{vo} and ΔU_{v3}. The first and second average are compared. If they agree to within a reasonable tolerance, V_{h1} and V_{v1} are taken as velocities at the end of t and U for the next increment is calculated using (3.40). If they do not, V_{h2} and V_{v2} are calculated from addition of second average of U_h and U_v to U_{ho} and U_{vo}. They are

used to generate ΔU_{h4} and ΔU_{v4}. The third average of ΔU_h and ΔU_v are calculated from ΔU_{ho} and ΔU_{h4}; and ΔU_{vo} and ΔU_{v4}. This third average and any subsequent average is compared with the one before it until the tolerance is acceptable. V_h and V_v used to generate the last set of U_h and U_v are taken as the velocities at the end of the time increment. The distance 'x' and 'y' at the end of an interval are then calculated. The whole process is repeated for the next time increment Δt until 'x' and 'y' or either of them exceeds the value of the width and axial length of the spray column respectively.

A fortran program was developed to carry out this calculation and run on Aston University Harris 500 computer. Complete listing of the program appears in Appendix D.

CHAPTER FOUR

EXPERIMENTAL WORK AND EQUIPMENT

4.1 Spray Towers

4.2 Spray Atomizers

4.3 Conductivity Transmitter and Cells

4.4 Potentiometric Recorder

4.5 Particle Size Analyser

4.6 Experimental Procedure

4.6.1 Droplet Residence Time Distribution Analysis For Pure Water

4.6.2 Drop size Distribution Analysis

4.6.3 Droplet Trajectories

4.1 SPRAY TOWERS

Three spray driers, two counter-current, one co-current, and one spray tower were used in the course of these studies.

COUNTER CURRENT SPRAY DRIERS

The two counter-current spray driers were similar in shape and dimension. They differed only in the material of construction. One was made of transparent 4.8 mm thick P.V.C. and the other of stainless steel. They both consisted of a cylindrical section and a conical base. The photograph of the stainless steel spray drier is shown on Plate 4.1 while the Schematic diagram for both driers is shown in Figure 4.1. The dimensions of the spray driers are shown in Table 4.1. The feed was introduced from two stainless steel tanks, 0.61 m x 0.61 m x 0.91 m, fitted with stirrers, heaters and Ether temperature controllers. The feed was fed through a 0.038 m diameter piping to the spray nozzle by Beresford Single Stage Self priming pump (for water and solutions) or by Marshall Mono pump (for slurries). The feed flow was controlled by three gate valves, two on the feed line and one on the by-pass to the pump. Delavan hollow cone spray nozzles were used to atomize the feed into spray at the top of the drier. A recovery tank and a recirculation pump were located at the bottom of the tower.

Atmospheric air with which the spray was contacted

TABLE 4.1

DIMENSION OF COUNTER CURRENT SPRAY DRIERS

	PVC (m)	STAINLESS STEEL (m)
CYLINDRICAL SECTION		
Height	2.74	2.44
Diameter	1.22	1.22
CONICAL SECTION		
Base	1.22	1.22
Height	1.22	1.22

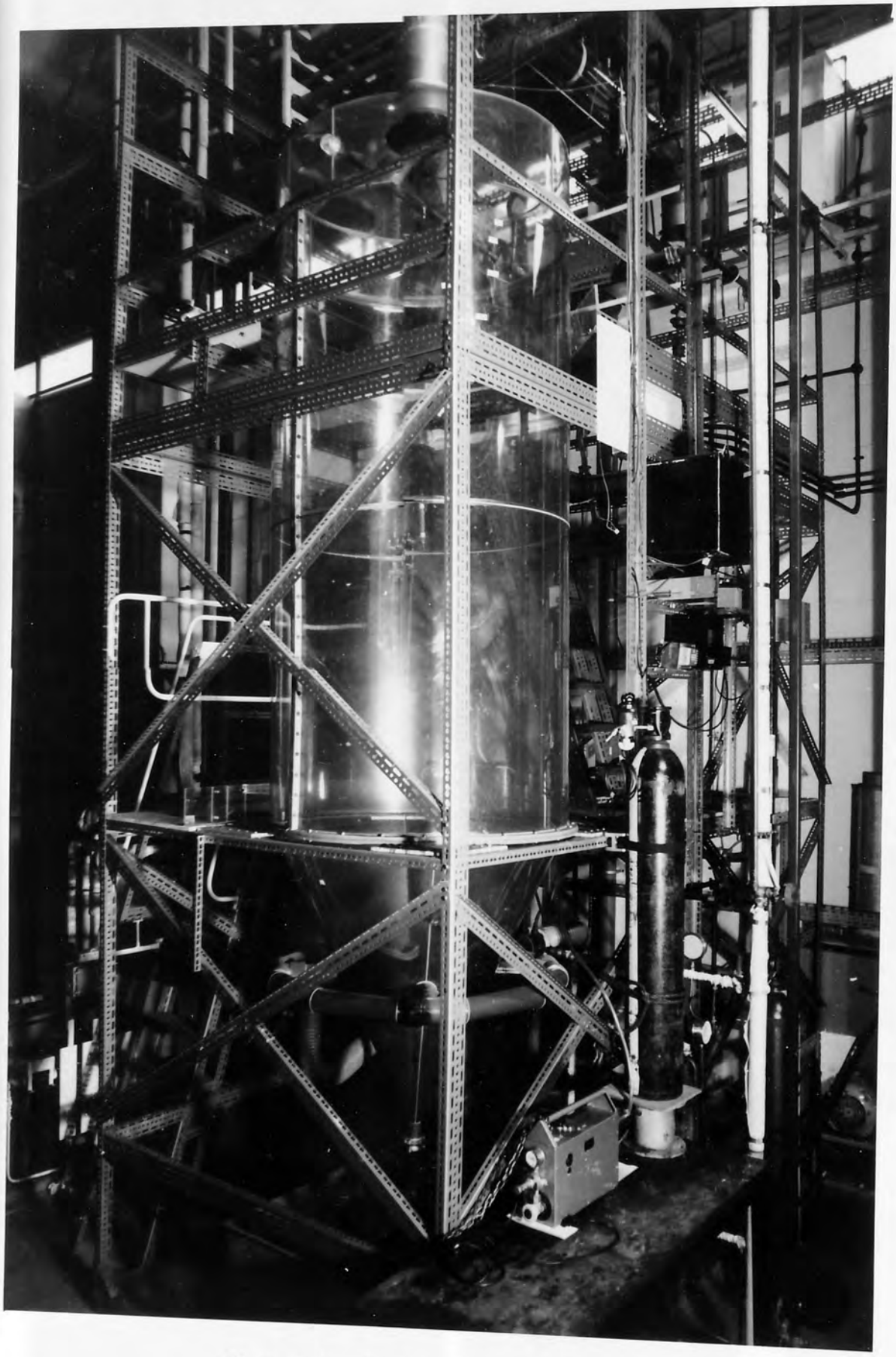

Plate 4.1 Counter-Current Spray Drier

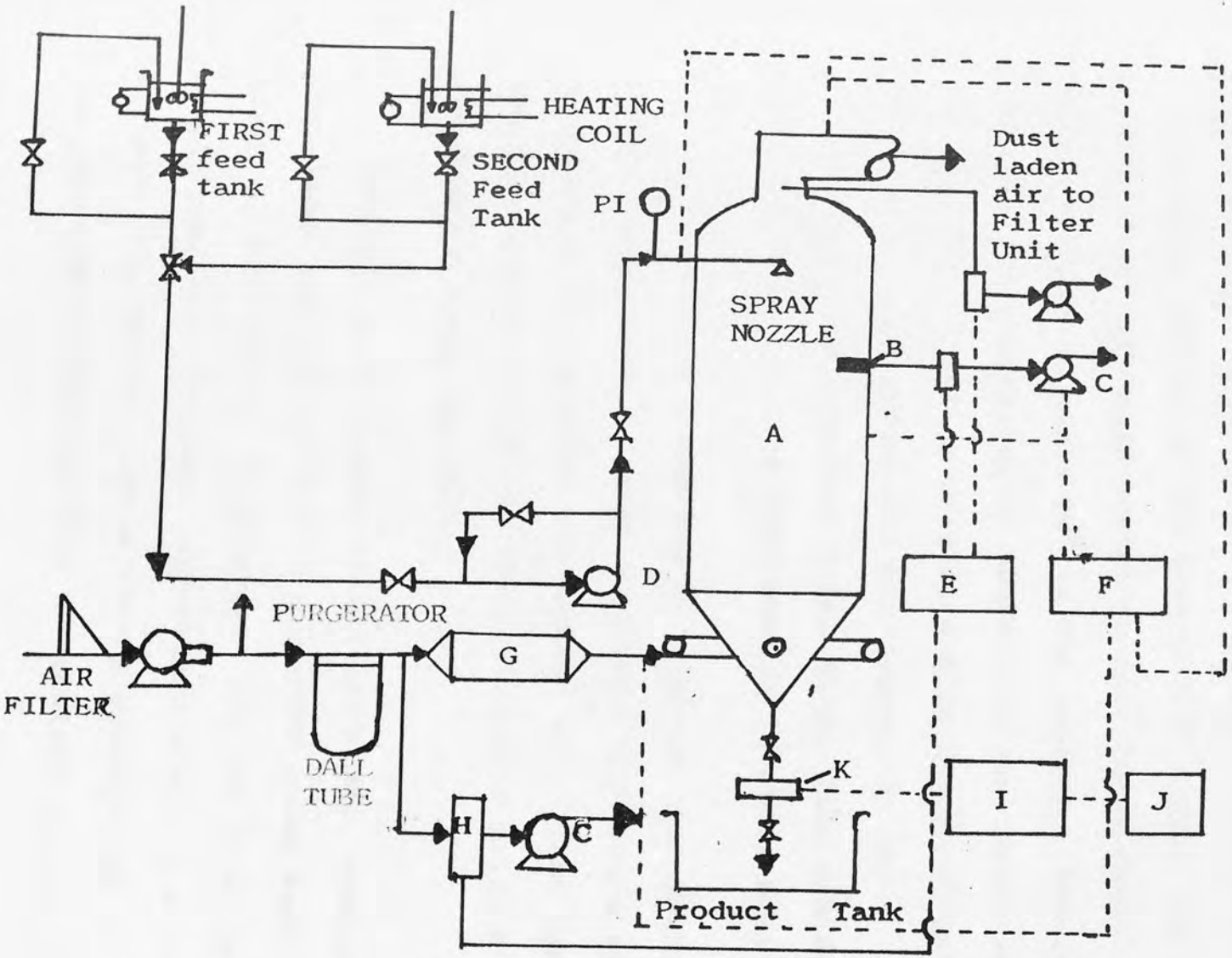

A Spray Tower
B Filter
C Sampling pump
D Feed pump
E Multiple point Hygrometer
F Temperature recorder
G Air Heater
H Constant temp. unit
I Conductivity transmitter
J Pen recorder
K Conductivity cell

FIGURE 4.1 SCHEMATIC DRAWING OF CO-CURRENT SPRAY DRIER

was drawn from the atmosphere by a 20 H.P., 3 phase Parkinson air supply fan into a 0.1016 m diameter mild steel piping. It flowed through two models 15/2 Secomak Industrial Heater, each 0.47 m in length, flanged at each end, both capable of heating the air to 300°C. It finally passed through a 0.127 m piping, and a reducer, into a 0.076 m ring main placed around the conical section of the tower, 0.61 m from the top of the base. The main contained four inlet ducts equally spaced at angle 90° to one another. The air flowrate was controlled by Audco Slim Seal Valve and measured by a 10.16 cm Dall Tube with a bore throat of 4.64 cm. Any excess air was removed by Air purgerator. The stainless steel spray drier was fully lagged with fibre glass insulator to minimize heat loss.

Thermocouples connected to a George Kent Multiple Points Temperature Recorder were used to measure the temperature of the inlet and exhaust air, inlet feed and temperature inside the tower at height 0.121 m and 0.182 m above the cone.

Humidity measurements of the inlet air, exhaust dust-laden air and air within the spray tower were taken by Shaw six-way Hygrometer. Air was drawn by a sample pump into constant temperature unit. The sensor screwed into the unit converted the dewpoint of the air into capacitance and this information was relayed

to the dewpoint meter. Direct reading from the meter was converted to relative humidity numbers from the calibration chart supplied with each sensor.

CO-CURRENT SPRAY DRIER

The co-current spray drier used was a mini industrial type supplied by Niro Atomizer. The photograph and schematic diagram of this drier are shown in Plate 4.2 and Figure 4.2 respectively. It consisted essentially of a drying chamber, 0.6 m (high) x 0.8 m (diameter) in its cylindrical section and a conical base with a cone angle of 60^{o}. Its internal surfaces were made of stainless steel and was fully insulated to minimize heat loss. Windows were installed in the cylindrical section for observation of atomization and drying process in the chamber. The chamber was rigidly mounted within a framework that supported the auxilliary equipments such as the control panel, the product recovery cyclone, air heater and suction fan.

The feed was introduced to the vaned wheel rotary atomizer under gravity or by using a small capacity Stuart Turner pump. The atomizer sat on a supporting ring in a cylindrical recess within the chamber roof and was driven by a compressed air turbine. The resulting spray from the atomizer was contacted with hot air drawn by a suction fan installed on the exit side of the cyclone. The air passed through a air

Plate 4.2 Co-Current Spray Drier

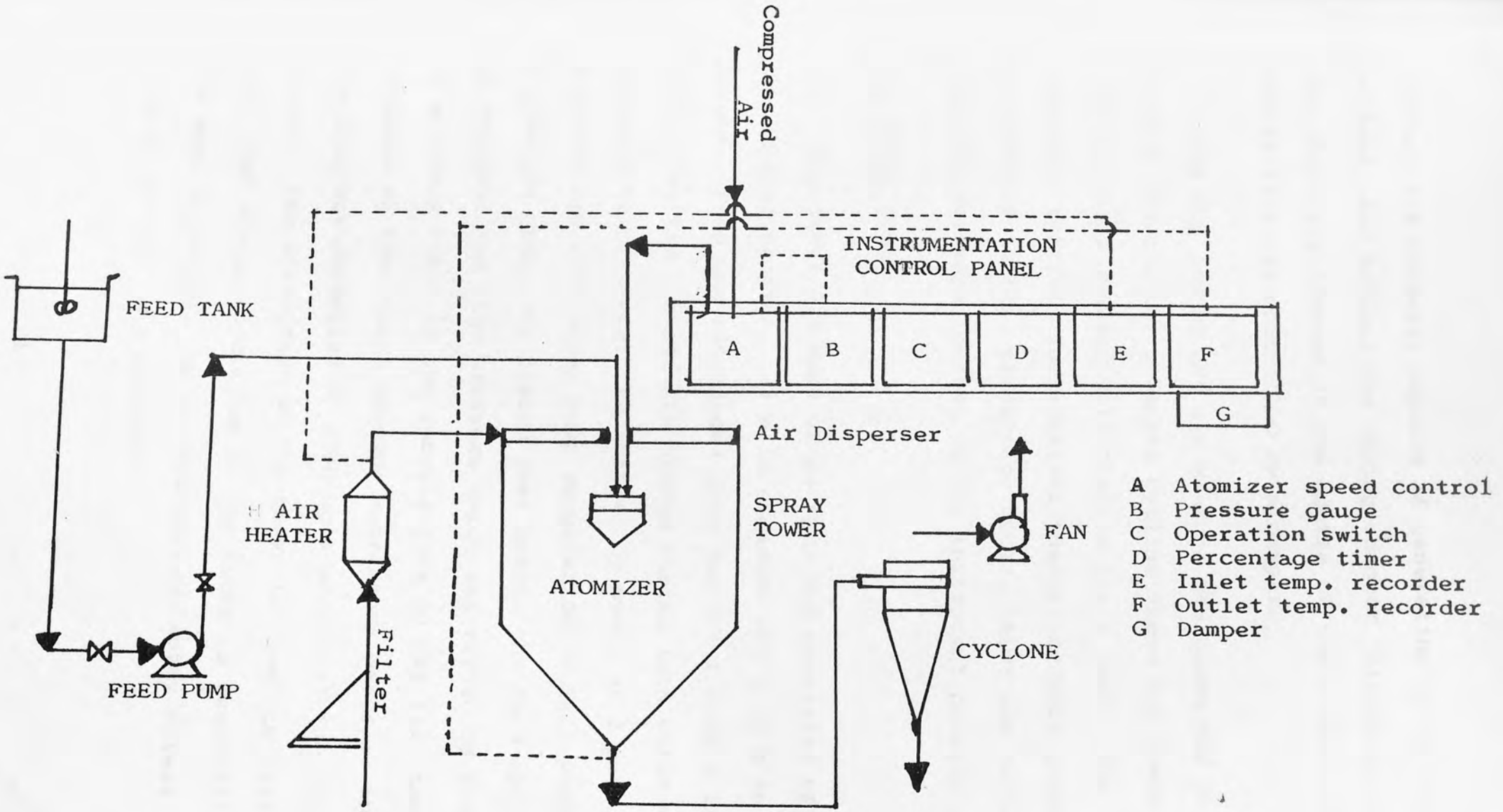

FIGURE 4.2 SCHEMATIC DRAWING OF CO-CURRENT SPRAY DRIER

filter, air heaters, capable of generating up to 7.5 KW of heat, and entered the drying chamber through a ceiling air disperser located at the centre of the chamber roof. The airflow was controlled by a damper.

The dry powder and air mixture was drawn off at the base of the chamber into the cyclone where dry powder was separated out and collected in glass jars. The necessary controls for atomizer speed, pressure gauge, operational switch, percentage timer, inlet and outlet temperatures were located on the instrument control panel.

THE SPRAY TOWER

This tower was made of perspex and consisted of a cylindrical section, 1.5 m in diameter and 1.22 m in height. Feed was introduced into the tower from a large glass tank via a centrally placed piping into which the pressure nozzles could be screwed by means of 3 phase, 3 piston Neo Cold Water pump supplied by Neolith Pump. A pressure gauge was placed just before the feed entry to register the line pressure which was varied by means of a needle valve in the recycle line to the feed tank. Blockage of the nozzle through extraneous material in the feed was minimized by placing a screen at the pump outlet. The photograph of the tower is shown in Plate 4.3. The schematic diagram of the tower is essentially the same as that of the counter-current spray driers without the air line included.

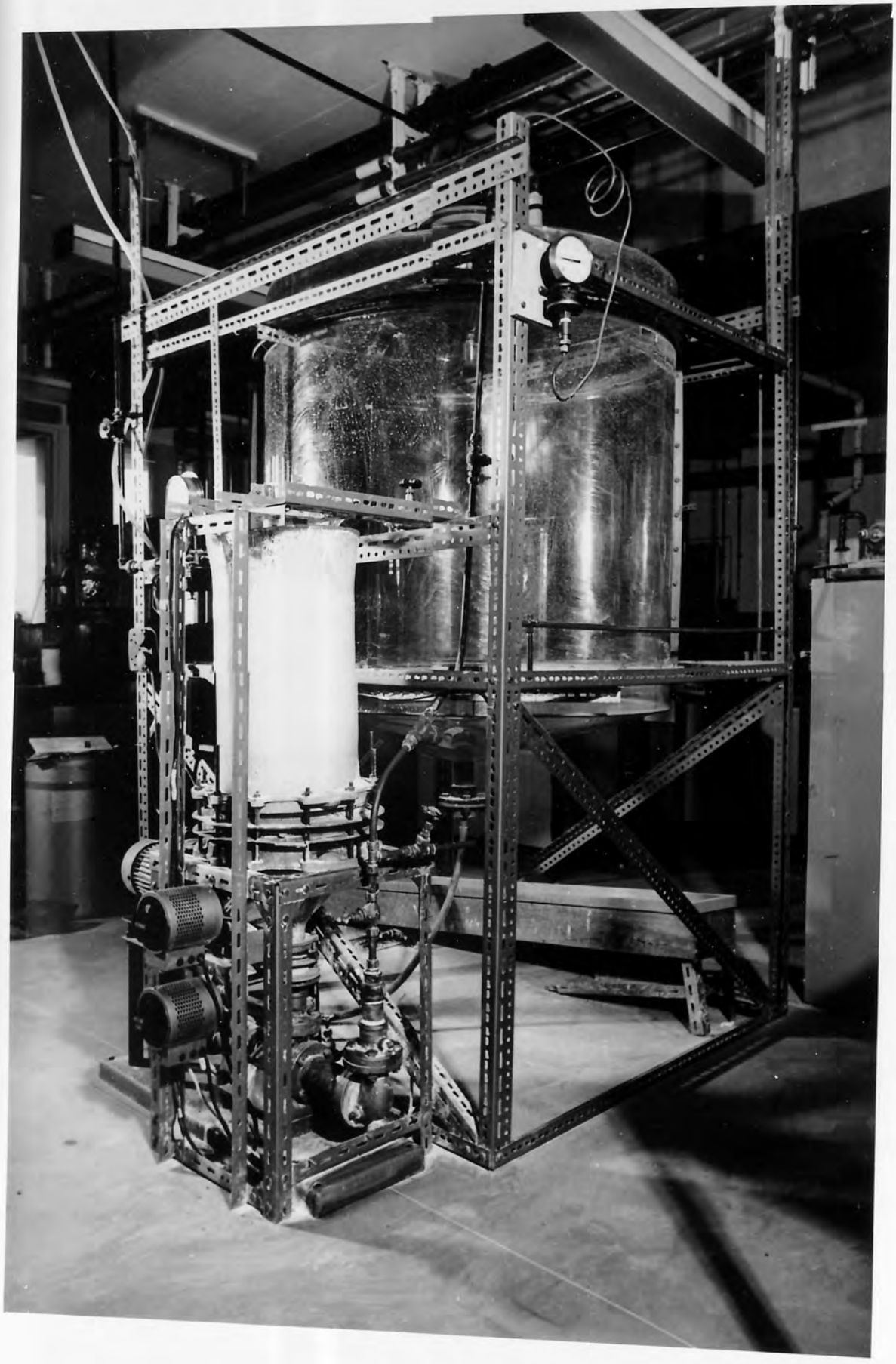

Plate 4.3 Spray Tower

4.2 THE SPRAY ATOMIZERS

Two types of spray atomizers - the Pressure nozzles and Rotary atomizers - were studied.

THE PRESSURE NOZZLES

For experiments in the counter-current spray driers, Delavan hollow cone spray Pressure nozzles were employed. These are shown on Plate 4.4. Nozzle A was type 'WM' with a 1.67 cm cylindrical strainer attached to the feed inlet to prevent blockage of the nozzle by unwanted solid material. It had a ¼ in B.S.P. male thread and was made of 18-8-3 stainless steel. It was mostly used for spray drying water.

Nozzle B was type "Mini SDX". It consisted a recessed orifice disc of Tungsten carbide, a body, a stem adapter fitted with a ¼ in B.S.P., a ceramic swirl chamber and a viton O-ring seal. Both the body and adapter were made of 303 stainless steel. The chamber is the unique aspect of the nozzle design as it is claimed to be capable of minimizing plugging and friction to produce drops of uniform size distribution.

Nozzle C was type 'SDX'. It consisted of a body, orifice seal, orifice disc, swirl chamber, chamber end plate, screw pin, body seal and a female. The body screw pin and female were made of 316 stainless steel.

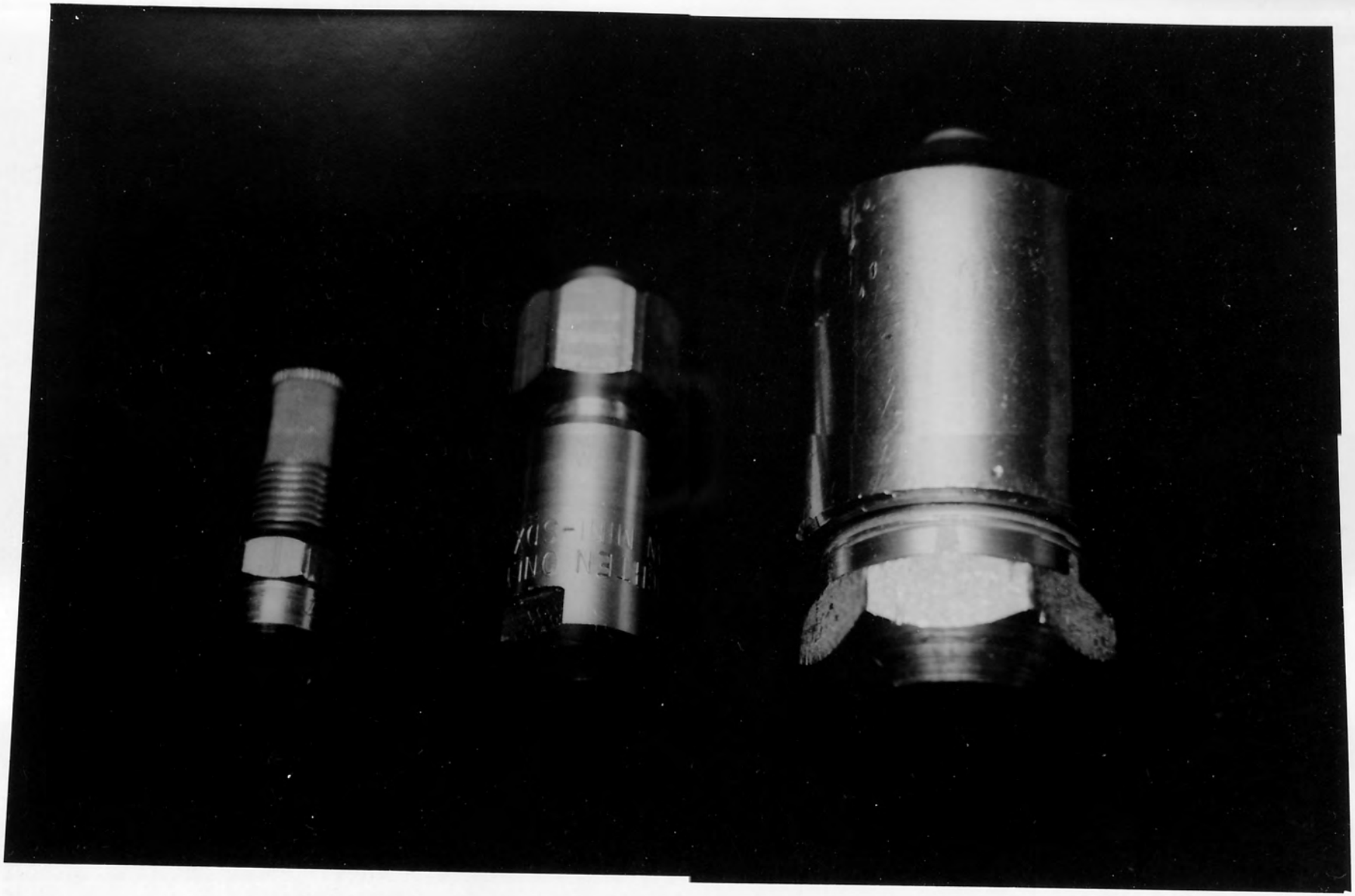

Plate 4.4 Pressure Nozzles (Left to Right, A, B, C).

THE ROTARY ATOMIZER

This was solely used in the mini industrial co-current spray drier. It was also supplied by Niro Atomizer and is shown in Plate 4.5. It consisted of a vaned atomizer wheel mounted on a high speed spindle, a liquid distributor, atomizer drive (turbine) and inlet pipes for the feed and compressed air to drive the turbine. The vaned wheel was capable of rotating within the range 25,000 to 35,000 r.p.m.

Plate 4.5 Rotary Atomizer

4.3 CONDUCTIVITY TRANSMITTER AND CELLS

A tracer of Pottasium Iodide injected at the feed inlet was monitored at the tower exit by using a conductivity transmitter type TX2/P and tubular epoxy flowline conductivity cells supplied by Electrical Instruments Ltd. The transmitter continuously measured the electrolytic conductivity of the sprayed droplets at the outlet of the drier. Two types of cells were used. One with a cell constant of 0.1 detected conductivity in the range of 0 - 100 micromhos/cm (10^{-6}ohm^{-1}cm^{-1}) while the other with a cell constant of 1.0 detected in the range 0 - 1000 micromhos/cm.

4.4 POTENTIOMETRIC RECORDER

This received 0 - 1 mA direct current signal proportional to the conductivity measured by the conductivity transmitter to produce a graph of the continuous measurement of conductivity against time.

4.5 PARTICLE SIZE ANALYSER

THEORY

If a parallel beam of monochromatic, coherent beam such as that of a laser falls onto a spherical or non-circular particle, a diffraction pattern is formed provided the wavelength of the beam is smaller than that of the particle diameter. The amount of light deflected is dependent upon the size of the particle (Figure 4.3) The diffraction pattern is superimposed on the geometrical image of the particle and is larger compared with the image. If a lens is placed in the light path behind the particle and a screen or detector placed at the focal plane, the undiffracted light is brought to a point of focus on the axis and the deflected light produces a pattern of concentric ring at a distance from the axis proportional to the diameter of the particle. This pattern is called Fraunhofer diffraction pattern because it is a far field pattern produced by parallel rays of light. A sample consisting of particles of different size will create a series of concentric rings of various radii, each radius being inversely proportional to the diameter of particle giving rise to it. The radial displacement in the focal plane remains constant irrespective of the particle position in the light path (149).

The droplet size distribution can be determined by

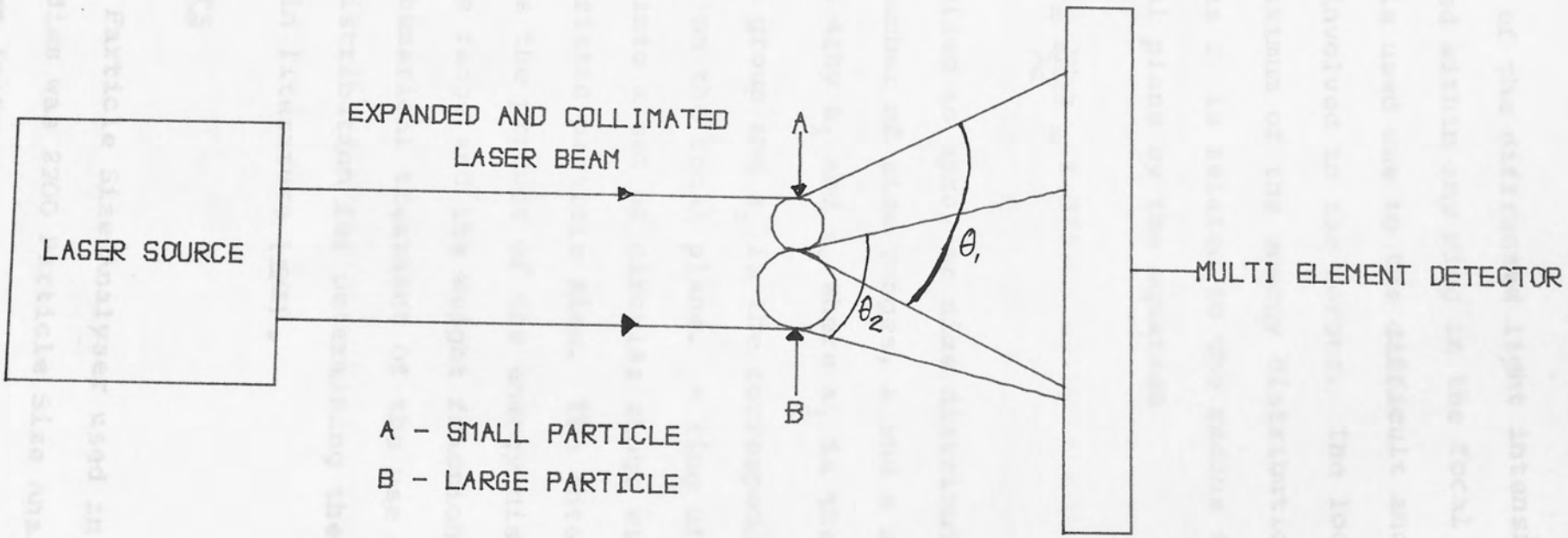

FIGURE 4.3: PARTICLE SIZE ANALYSER - PRINCIPLE OF OPERATION

the use of the diffracted light intensity or the energy contained within any ring in the focal plane. The latter method is used due to the difficult and tedious calculation involved in the former. The location of the first maximum of the energy distribution for a particle of radius r is related to the radius s of the ring on the focal plane by the equation

$$X_m = \frac{2\pi as}{\lambda f} = 1.375 \qquad (4.1)$$

When applied to spray or size distribution classified into a number of size ranges, a and s are replaced in equation 4.1 by a_i and s_i where a_i is the mean size of i^{th} size group and s_i is the corresponding radius of the ring on the focal plane. A ring of a detector divided into a set of circular rings will define a characteristic particle size. The total energy distribution is the product of the energy distribution from each size range and the weight fraction in the range. Full mathematical treatment of the use of the light energy distribution for determining the size distribution appears in literature (150).

COMPONENTS

The Particle Size Analyser used in the course of this studies was 2200 Particle Size Analyser supplied by Malvern Instruments. It is a versatile equipment capable of determining particle sizes in the range

1 to 1800 microns. It consists of two main units, the optical precessing unit shown in Plate 4.6 and the electronic processing unit shown in Plate 4.7. The schematic diagram of the instrument is shown in Figure 4.4.

The optical processing unit is made up of a low power He/Ne laser (λ= 0.6328 microns) Transmitter and a Receiver. The transmitter produces a parallel monochromatic beam of light to illuminate the particles. The diffracted light gives rise to a stationary diffraction pattern corresponding to the instantaneous size distribution of the particles entering and leaving an illuminated area. A representative bulk sample of the particles is obtained from the final measured diffraction pattern by integration over a suitable period of time. The receiver consists of a Fourier transform lens which focusses the diffraction pattern onto a multi-element photo-electric detector consisting of thirty concentric, semi circular photo-sensitive rings. The detector produces an analogue signal proportional to the received light intensity.

The electronic processing unit consists of a desk top computer system, high speed line printer and application software packages. The computer is interfaced to the detector so that it can read the diffraction pattern and perform the necessary integration digitally.

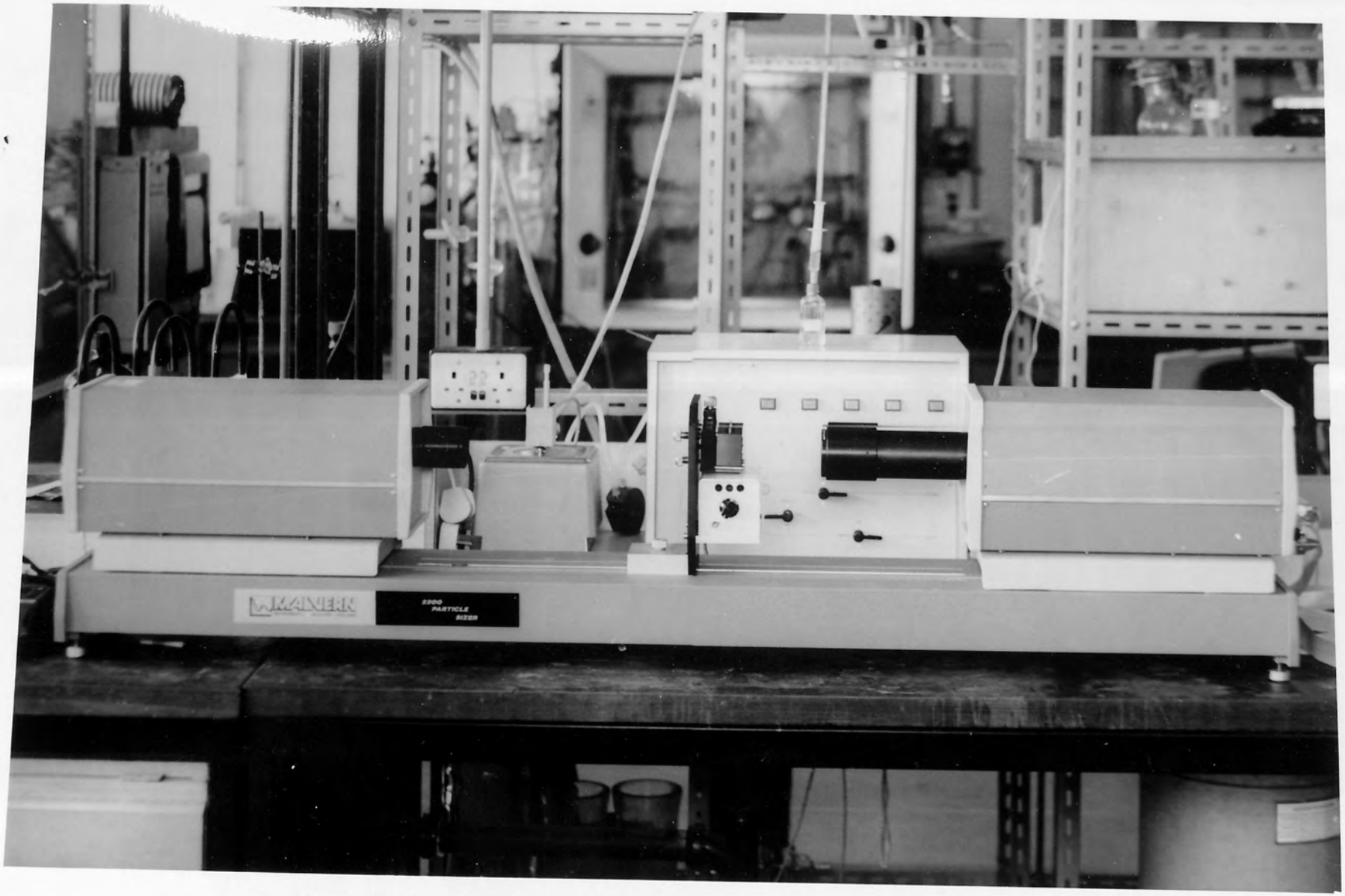

Plate 4.6 Particle Sizer - Optical Processing Unit

Plate 4.7 Particle Sizer - Electronic Processing Unit

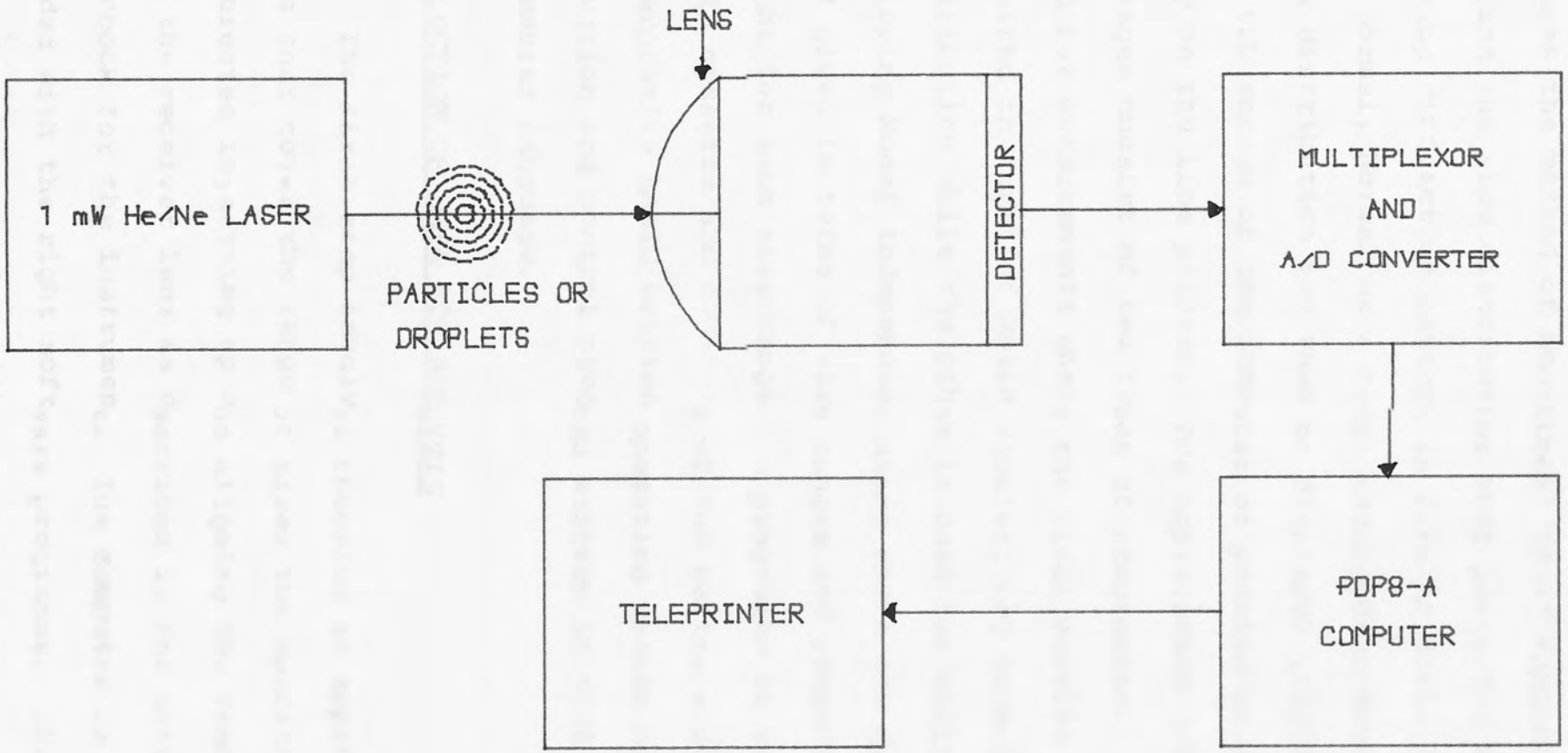

FIGURE 4.4: SCHEMATIC DIAGRAM OF PARTICLE SIZE ANALYSER

It uses the method of non-linear least squares analysis to find the size distribution that gives the best fitting diffraction pattern in form of Rosin Rammler, Log Normal, Normal or a model independent means. This size distribution may then be displayed graphically on the VDU screen of the computer or printed as a hard copy on the line printer. The Application software packages consist of two types of programmes. One is used for measurements where the final results are required in terms of Rosin Rammler, Log Normal or Normal distribution while the other is used for analysis employing Model Independent means where the results are just given in terms of size ranges and proportion in weight for each size range. A programme is recorded on a C15 cassette and consists of two parts, a line interpretive BASIC written operating system and a Data reduction and control program written in 6502 Assembler Language.

COLLECTION OF DATA FOR ANALYSIS

The first step involves choosing an appropriate lens that cover the range of sizes the operator is interested in, setting up and aligning the transmitter and the receiver lens as described in the accompanying handbook for the instrument. The computer is then loaded with the right software programme. The next step involves obtaining the background data using BL command with the requisite parameters. The background

data represents the residual light diffracted with no particles present in the beam. The data is listed on the printer and carefully examined to ensure that no single detector reading exceeds 30. If any reading exceeds 30 or there is tendency towards peaking in the readings, reallignment is done or the controls are adjusted until all readings are below 30. Unless there is any major disturbance to the set up of the instrument, this background data would suffice for a set of experimental runs performed over a stretch of continuous period of time e.g. a day. However a new background data will be required when the instrument is switched off. The final step is concerned with obtaining the signal data by issuing the command EL or variation of it. The signal data represents the diffracted light energy when sample has been introduced into the beam.

The background and the signal data are combined to give a derived data which is automatically placed into a Block Memory of the computer. The computer has 32 block memories thereby permitting 32 experimental runs to be done consecutively, while their derived data are saved for later analysis.

PROCESSING THE RESULT

Three things may be done to the derived data. It may be processed immediately after it is obtained by

following the EL command by the appropriate result processing command. A set of derived data may be recalled from the block memories and processed after the experiment is completed. Finally the derived data may be stored on magnetic tape and processed later by re-reading them into block memories and processing them. The results obtained would correspond to the size distribution of the models present in the software programme loaded into the computer when the data were collected. Care should therefore be taken to match the derived data to the programme used in obtaining them.

4.6 EXPERIMENTAL PROCEDURE

4.6.1 DROPLET RESIDENCE TIME DISTRIBUTION ANALYSIS FOR PURE WATER

WATER FLOWRATES

Because of the problems enumerated by Ashton (110) the flow measurements were done manually, a method that involved collecting the water for a known interval of time and weighing it to obtain the mass flowrate. This process was repeated several times to guarantee accurate measurement. The mass flowrates obtained were celibrated against the feed line pressures.

AIR FLOWRATES

For each setting of Audco Valve which controlled the air flowrate, the pressure drop across the Dall tube was measured by a mercury manometer connected to the tappings on the tube and its throat bore. The air mass flowrate was then calculated from this pressure drop using the equation supplied by the manufacturer.

PROCEDURE

Pure water was sprayed, the temperatures being kept constant by an Ether Temperature controller. Both the Conductivity Transmitter and the Potentiometric Recorder were switched on. After a stable operating condition had prevailed and a conductivity baseline has been established for the spray by the recorder, 5 ml of

Pottasium Iodide of known concentration was injected at the point of feed entry into the drier. Using a digital stop watch, the time taken to introduce the tracer was noted. The pen recorder then produced on a chart moving at a selected speed a graph which represented the exit concentration profile of the tracer against time. Several minutes after the recorder pen has returned to the baseline, air of known flowrate was introduced into the drier and the tracer concentration profile was also obtained. Five different air flowrates against four different water flowrates were used for WM nozzle and five different water flowrates against five different air flowrates were used for SDX nozzle.

Table 4.2 and 4.3 show the list of the operating variables used in these sets of experiments.

4.6.2 DROP SIZE DISTRIBUTION ANALYSIS

The bulk of work for this investigation were carried out in the spray tower, the mini-industrial spray drier and the stainless steel spray drier.

EXPERIMENT IN SPRAY TOWER

Both photograph method and Particle Sizer were used to obtain the size distributions of the droplets. The set up for the photographic method involved draping the tower with a black cloth to prevent over exposure of the film and providing a high intensity short duration flash triggered automatically when the camera shutter release

TABLE 4.2

PRESSURE ($KN.M^{-2}$)	WATER FLOWRATE ($X10^{-3}$ $KG.S^{-1}$)	CODE
68.95	.33	W1
88.25	.37	W2
154.44	.48	W3
413.61	3.60	W4
482.63	4.20	W5
551.58	4.60	W6
620.53	5.10	W7
689.48	5.50	W8

TABLE 4.3

PRESSURE (MM.HG)	AIR FLOWRATE ($X10^{-3}$ $KG.S^{-1}$)	CODE
60.0	.1802	A1
70.0	.1946	A2
80.0	.2080	A3
90.0	.2206	A4
100.0	.2326	A5

was actuated to illuminate the droplets. The flash came from argon jet unit supplied by Pulse Instrument and Controllers Ltd. Photographs were taken using 35 mm Chinon CM-3 camera with 100 mm Macro, Takumar 135 mm Galaxy telephoto to give short depth of field. For particle sizer operation windows were cut on the opposite sides of the tower for the passage of the laser beam and the sizer receiver and transmitter were placed on either side of the window. The computer was loaded at the commencement of each day's experiment.

Flow measurements of the water sprayed were determined as in the previous experiment. The particle sizer was aligned and the optical units adjusted until a reasonable set of background data was obtained. Water of known flowrate was sprayed and after a stable condition had prevailed, command was typed into the computer for signal data to be obtained. This was followed immediately by taking the photograph of the droplets. The next higher flowrate was chosen and both the signal data and photograph of the droplets were obtained. The process was repeated for all the chosen flowrates. The derived data in the computer block memories were saved on magnetic tape for later processing, care being taken to ensure that the data were accurately saved. This involved listing out the first and last derived data on the printer, rereading the saved data into empty block memories and comparing the first and last data

in the new memories with the first and last data earlier listed.

EXPERIMENTS IN MINI INDUSTRIAL SPRAY DRIER

The taking of background and signal data and the saving of the derived data followed the same procedure as for those in the spray tower. The derived data were first obtained for a water spray without air flow. Then another derived data was obtained for the same flowrate with air flow. Rotary atomizer was solely employed here.

EXPERIMENTS IN STAINLESS STEEL SPRAY DRIER

The derived data were obtained as above. Different water and slurry flowrates were sprayed and the derived data were obtained and saved. SDX nozzle was used in spraying.

PROCESSING OF THE DERIVED DATA

This followed the procedure outlined in Section 4.5.

PROCESSING OF THE PHOTOGRAPH

Zeiss automatic counter was used to measure the droplets sizes. The droplet on the print was matched to a circle of light from an adjusted iris while a foot pedal was actuated to record the count of that size range within a particular size range. This was done for all droplets which were in focus on the photograph prints. The number counts for the various size ranges were then recorded on a page.

4.6.3 DROPLET TRAJECTORIES

Experiments for droplet trajectories were carried out in the stainless steel spray drier. They were of two kinds. One was to determine the velocity and the other to determine the drop size distribution of the droplets. Both were determined at particular levels from the atomizer. Double exposure high speed photography was used to obtain the velocity of the droplets of the sprayed slurry. A delay time of 1 millisecond was used. The velocity was calculated from the distance travelled by a drop divided by the time delay. The size distribution of the sprayed droplets was determined in the same way as outlined in Section 4.6.2. The range of variables employed are shown in Table 4.4.

TABLE 4.4

SLURRY	-	CEMENT (MASON)
DENSITY	-	1040.0 ($KG.M^{-3}$)
SURFACE TENSION	-	0.0715 (N/M)
AIR DENSITY	-	1.2 ($KG.M^{-3}$)
AIR VISCOSITY	-	1.76×10^{-5} $KG.M.S^{-1}$)
SPRAY ANGLE	-	60.0^{0}
SPRAY NOZZLE	-	SDX (SE-703-056)

PRESSURE ($KN.M^{-2}$)	FLOWRATE ($X10^{-3}$ $KG.S^{-1}$)	VELOCITY ($M.S^{-1}$)	CODE
68.95	7.72	3.656	P1
103.42	8.64	4.478	P2
137.90	9.78	5.171	P3
172.37	10.81	5.781	P4
206.84	11.74	6.333	P5

CHAPTER FIVE

RESULTS

5.1 Droplets residence time distribution

5.2 Droplets trajectories

5.3 Drop size distribution

5.1 DROPLETS RESIDENCE TIME DISTRIBUTION

The residence time distribution experiments were carried out in the P.V.C. pilot plant spray drier using water as the liquid feed and pottasium iodide as the tracer. The experimental data obtained were in the form of pulse and experimental response data. The real time components of the data were converted into dimensionless form. The various pulse data were used in the program written to simulate the response from the model for droplets residence time distribution in Chapter 3.1.

The parameters obtained for the various zones and streams of the model, the variance between the experimental and model response data are summarised in Tables 5.1 to 5.8. The pulse data used to generate the model 1 results are shown in Table 5.9 while the actual tabulation of the pulse data is done in Appendix A.

The code of the air and water flowrates (as shown in Tables 4.2 and 4.3) used for the various experimental response data and the full tabulation of the experimental and model response data are also shown in Appendix A. Graphs of the model and experimental response data are shown in Figures 5.1 to 5.40.

EXPERIMENTAL DATA	A	B	J	K	M	N	L	STANDARD DEVIATION
WMF2	.750	.250	.850	.020	.120	.005	0	4.8294
WMF3	.500	.500	.620	.080	.210	.050	0	2.3945
WMF4	.750	.250	.820	.080	.025	.025	0	3.3297
WMF5	.900	.100	.820	.030	.050	.010	0	4.5798
WMF6	.900	.100	.800	.060	.020	.020	0	4.0608

TABLE 5.1 : MODEL1 RESULTS - CODE RESIDENT1

EXPERIMENTAL DATA	A	B	J	K	M	N	L	STANDARD DEVIATION
WMF8	.750	.250	.600	.080	.210	.025	0	1.6395
WMF9	.500	.500	.450	.111	.225	.046	0	1.3855
WMF10	.750	.250	.470	.060	.270	.010	0	2.0554
WMF11	.900	.100	.490	.201	.131	.072	0	2.7250
WMF12	.900	.100	.695	.200	.020	.052	0	3.0831

TABLE 5.2 : MODEL1 RESULTS - CODE RESIDENT2

EXPERIMENTAL DATA	A	B	J	K	M	N	L	STANDARD DEVIATION
WMF14	.750	.250	.420	.100	.220	.090	0	2.4064
WMF15	.500	.500	.440	.000	.220	.010	0	1.3241
WMF16	.750	.250	.445	.000	.220	.015	0	1.2146
WMF17	.900	.100	.630	.021	.045	.036	0	1.5786
WMF18	.900	.100	.610	.160	.000	.050	0	2.2400

TABLE 5.3 : MODEL1 RESULTS -- CODE RESIDENT3

EXPERIMENTAL DATA	A	B	J	K	M	N	L	STANDARD DEVIATION
SDX20	.774	.226	.630	.070	.190	.030	0	4.5579
SDX21	.770	.230	.610	.110	.200	.060	0	2.1002
SDX22	.730	.270	.650	.070	.150	.040	0	3.3198
SDX23	.751	.249	.630	.120	.190	.040	0	3.9103
SDX24	.734	.266	.650	.090	.210	.040	0	3.7462

TABLE 5.4 : MODEL1 RESULTS - CODE RESIDENT4

EXPERIMENTAL DATA	A	B	J	K	M	N	L	STANDARD DEVIATION
SDX26	.772	.228	.710	.120	.100	.060	0	2.1974
SDX27	.768	.232	.670	.281	.000	.049	0	3.4845
SDX28	.730	.270	.650	.270	.010	.065	0	2.6748
SDX29	.751	.249	.650	.265	.000	.085	0	2.8151
SDX30	.734	.266	.643	.242	.000	.115	0	2.9784

TABLE 5.5 : MODEL1 RESULTS - CODE RESIDENT5

EXPERIMENTAL DATA	A	B	J	K	M	N	L	STANDARD DEVIATION
SDX32	.772	.228	.750	.176	.004	.060	0	2.3197
SDX33	.768	.232	.697	.243	.000	.060	0	4.6157
SDX34	.730	.270	.680	.156	.003	.055	0	2.9543
SDX35	.751	.249	.730	.170	.010	.082	0	1.7484
SDX36	.734	.266	.700	.246	.004	.048	0	2.2263

TABLE 5.6 : MODEL1 RESULTS - CODE RESIDENT6

EXPERIMENTAL DATA	A	B	J	K	M	N	L	STANDARD DEVIATION
SDX38	.772	.228	.720	.176	.005	.061	0	1.4656
SDX39	.768	.232	.741	.151	.092	.003	0	2.9183
SDX40	.730	.270	.700	.220	.007	.050	0	2.4786
SDX41	.751	.249	.721	.151	.030	.082	0	2.9276
SDX42	.734	.266	.690	.245	.004	.046	0	1.3505

TABLE 5.7 : MODEL1 RESULTS - CODE RESIDENT7

EXPERIMENTAL DATA	A	B	J	K	M	N	L	STANDARD DEVIATION
SDX44	.772	.228	.710	.175	.001	.058	0	2.2210
SDX45	.768	.232	.710	.250	.000	.040	0	2.5954
SDX46	.730	.270	.698	.118	.001	.045	0	1.4992
SDX47	.751	.249	.690	.148	.001	.081	0	2.1848
SDX48	.734	.266	.680	.242	.001	.046	0	2.1625

TABLE 5.8 : MODEL1 RESULTS - CODE RESIDENT8

MODEL1 RESULTS CODE	PULSE DATA
RESIDENT1	WMF1
RESIDENT2	WMF7
RESIDENT3	WMF13
RESIDENT4	SDX19
RESIDENT5	SDX25
RESIDENT6	SDX31
RESIDENT7	SDX37
RESIDENT8	SDX43

TABLE 5.9 : PULSE DATA FOR MODEL1 RESULTS

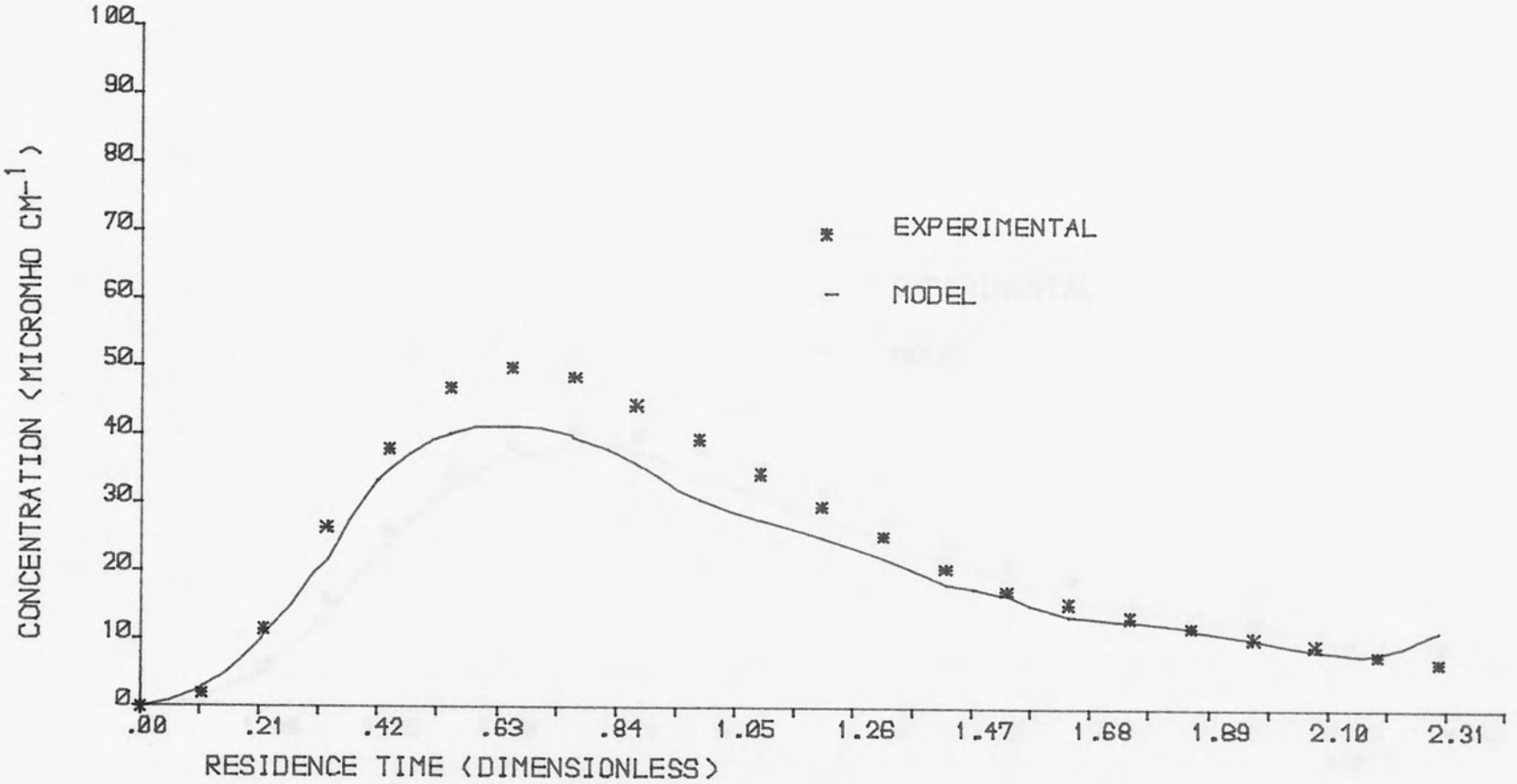

FIGURE 5.1 :RESIDENCE TIME DISTRIBUTION - RUN CODE WMF2

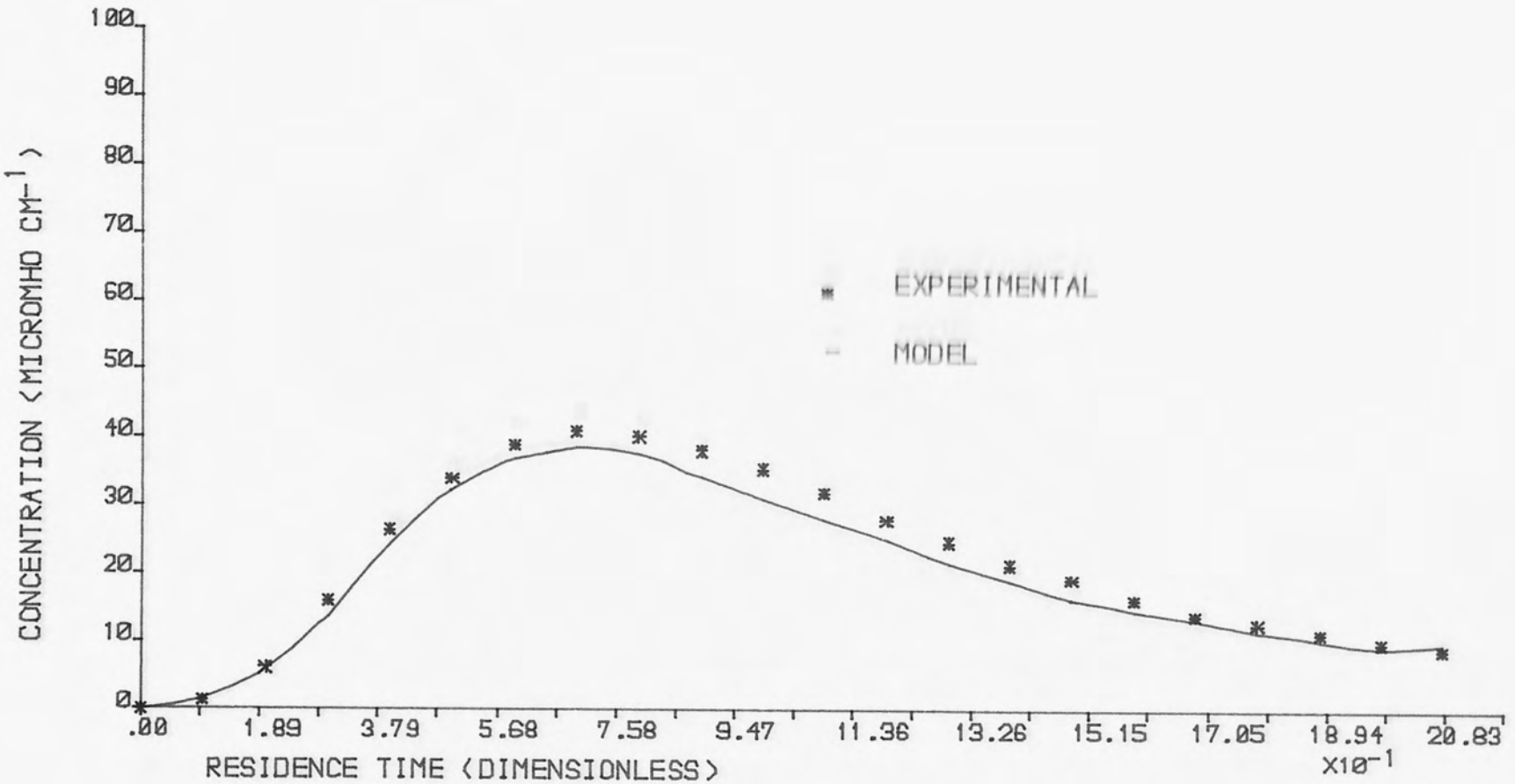

FIGURE 5.2 :RESIDENCE TIME DISTRIBUTION - RUN CODE WMF3

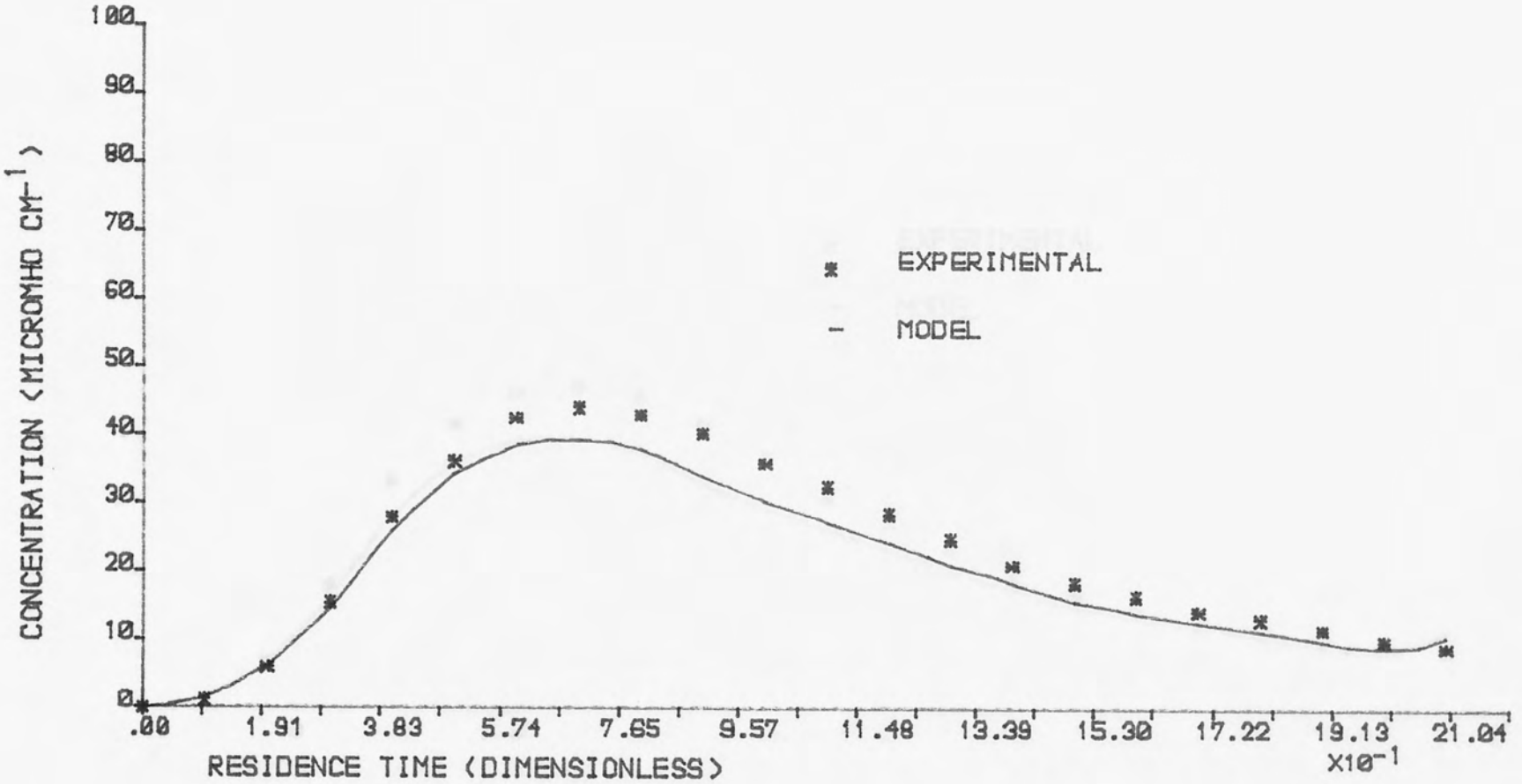

FIGURE 5.3 :RESIDENCE TIME DISTRIBUTION - RUN CODE WMF4

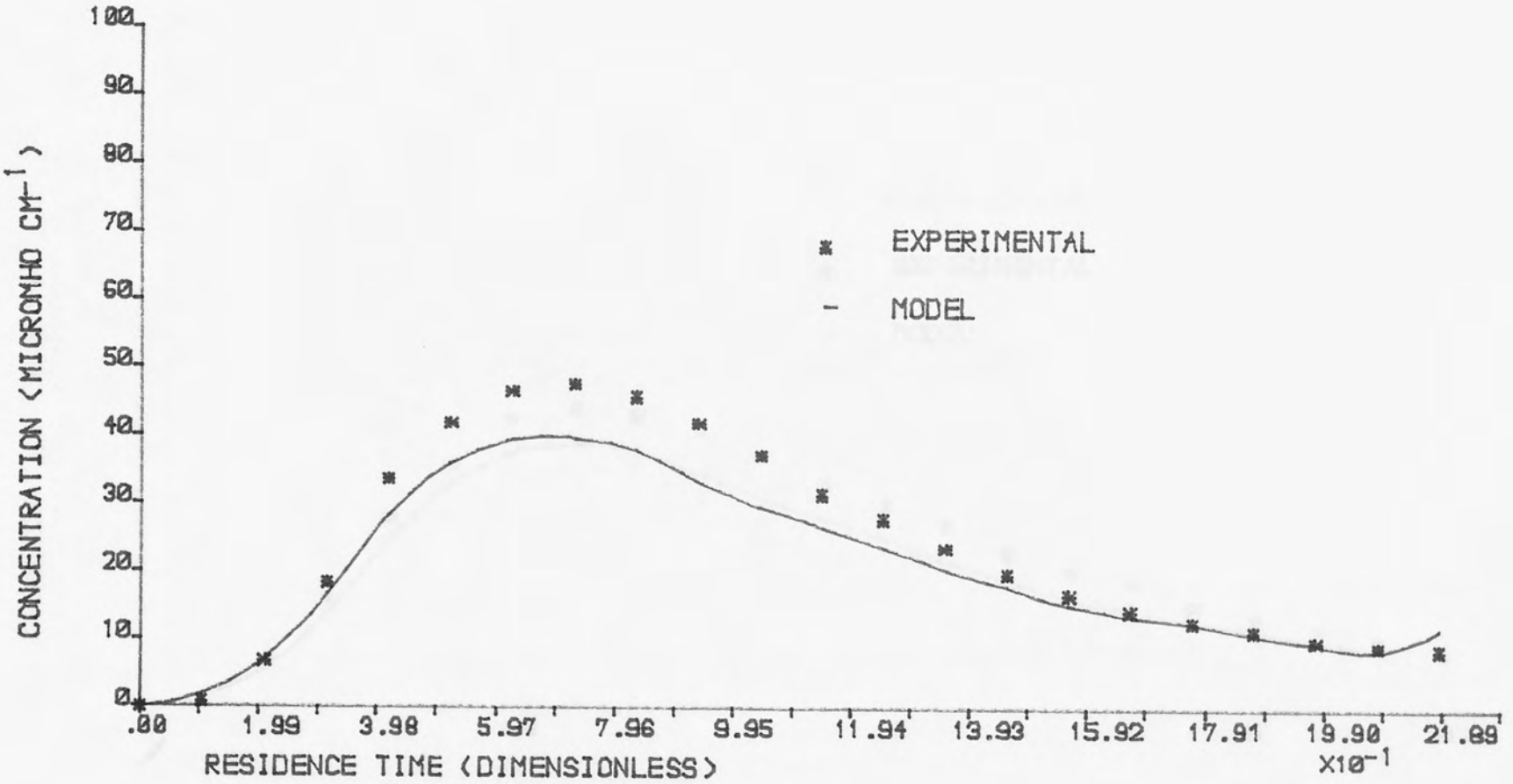

FIGURE 5.4 :RESIDENCE TIME DISTRIBUTION - RUN CODE WMF5

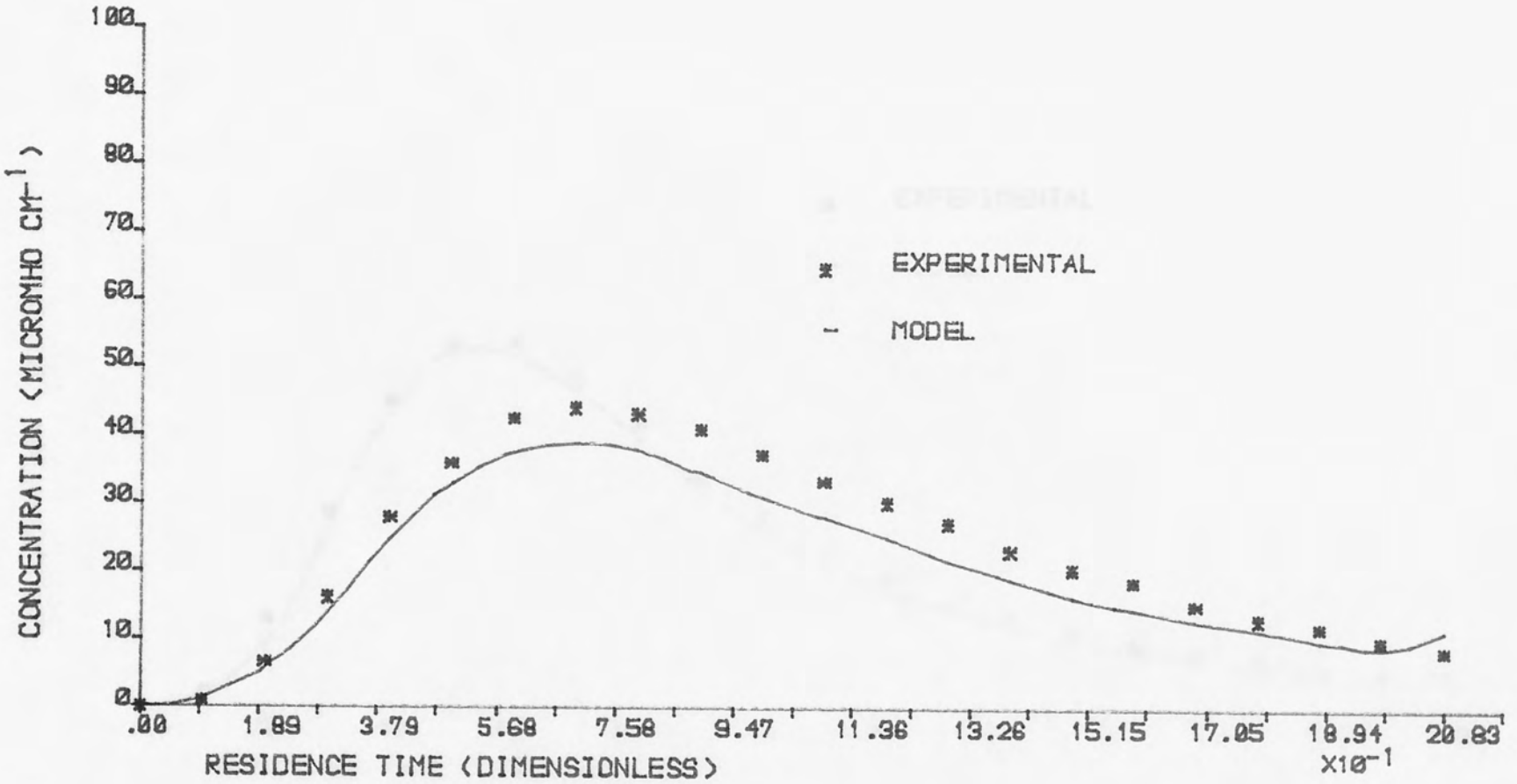

FIGURE 5.5 :RESIDENCE TIME DISTRIBUTION - RUN CODE WMF6

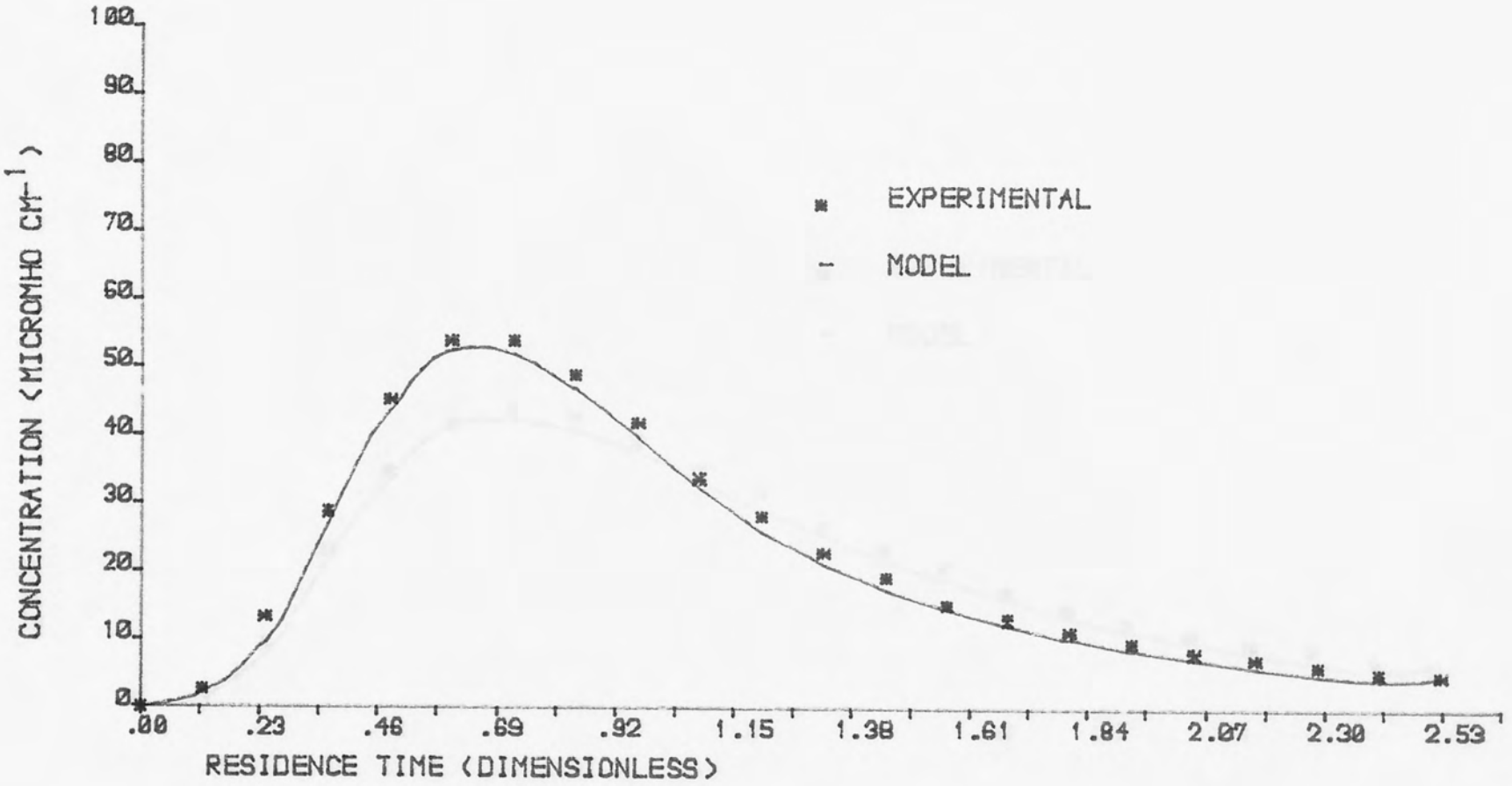

FIGURE 5.6 :RESIDENCE TIME DISTRIBUTION - RUN CODE WMF8

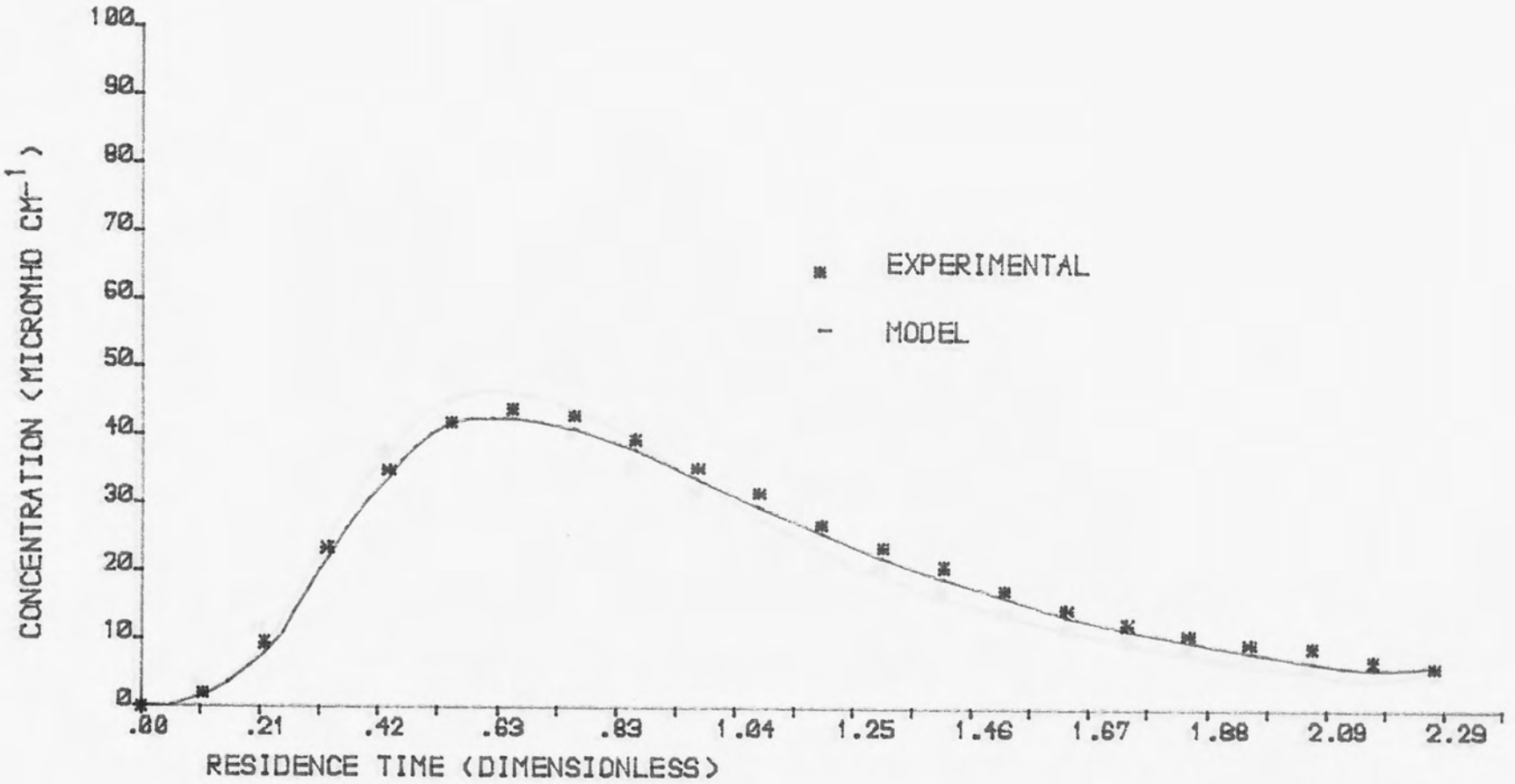

FIGURE 5.7 :RESIDENCE TIME DISTRIBUTION - RUN CODE WMF9

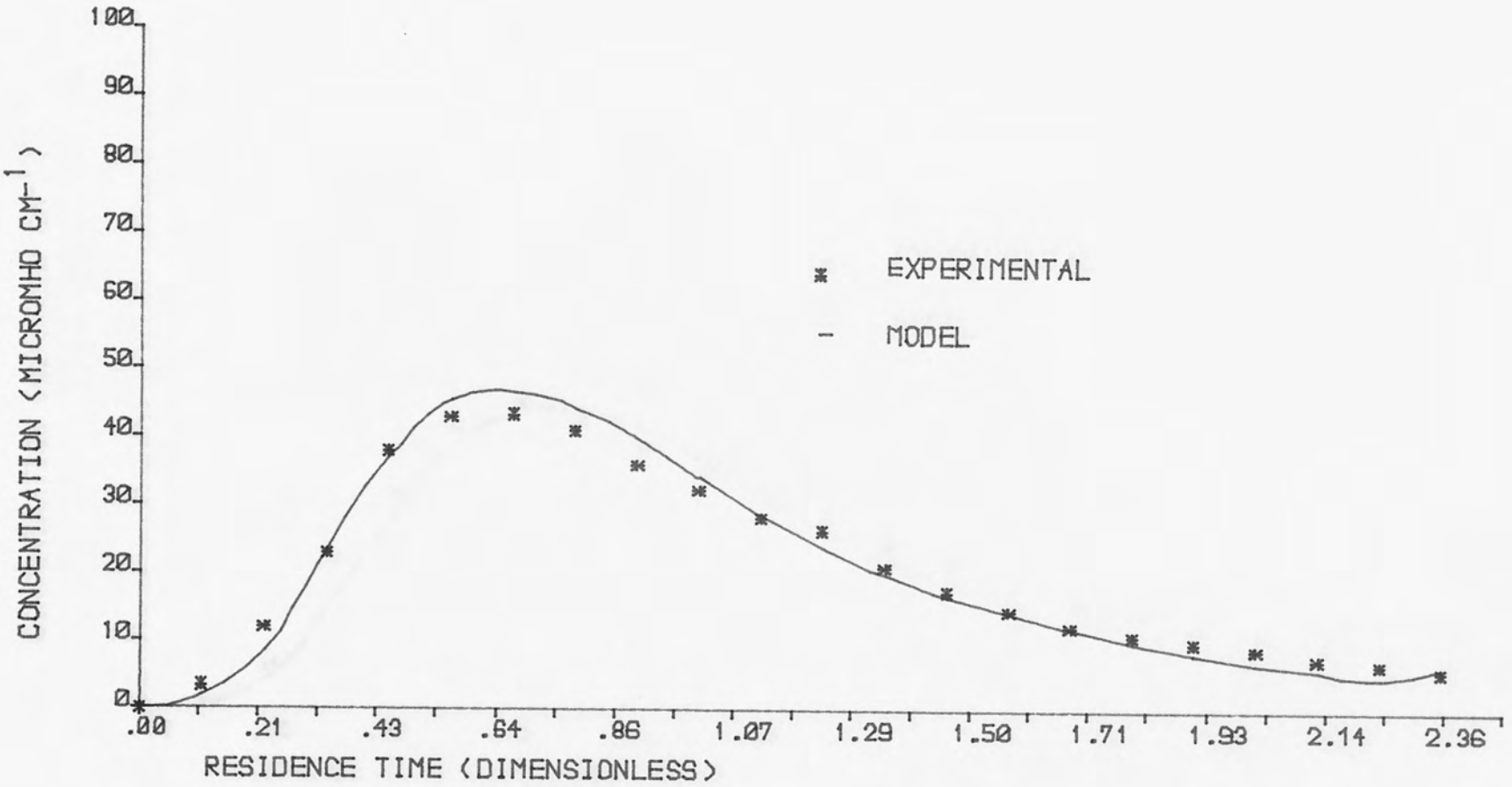

FIGURE 5.8 :RESIDENCE TIME DISTRIBUTION - RUN CODE WMF10

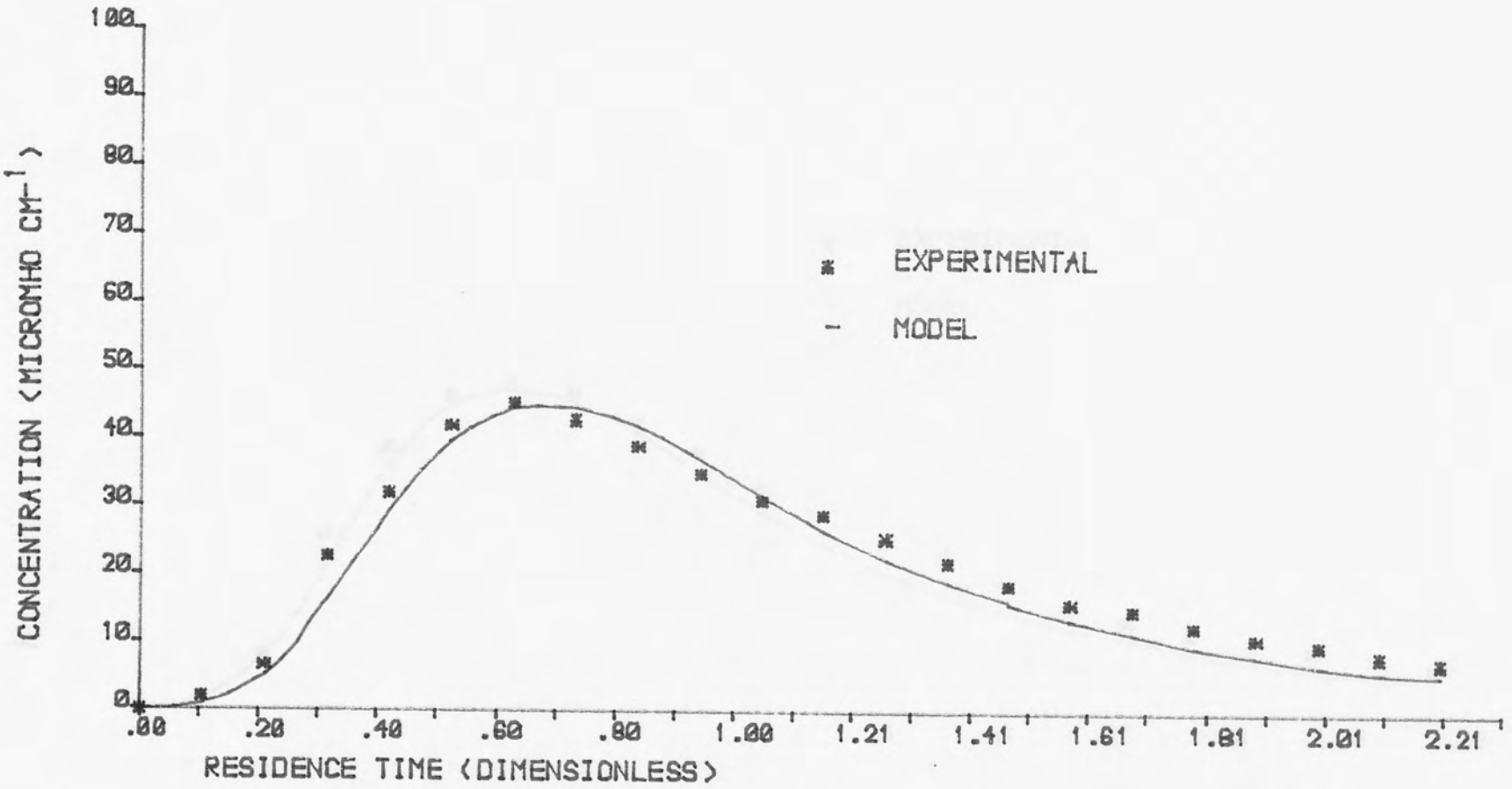

FIGURE 5.9 :RESIDENCE TIME DISTRIBUTION - RUN CODE WMF11

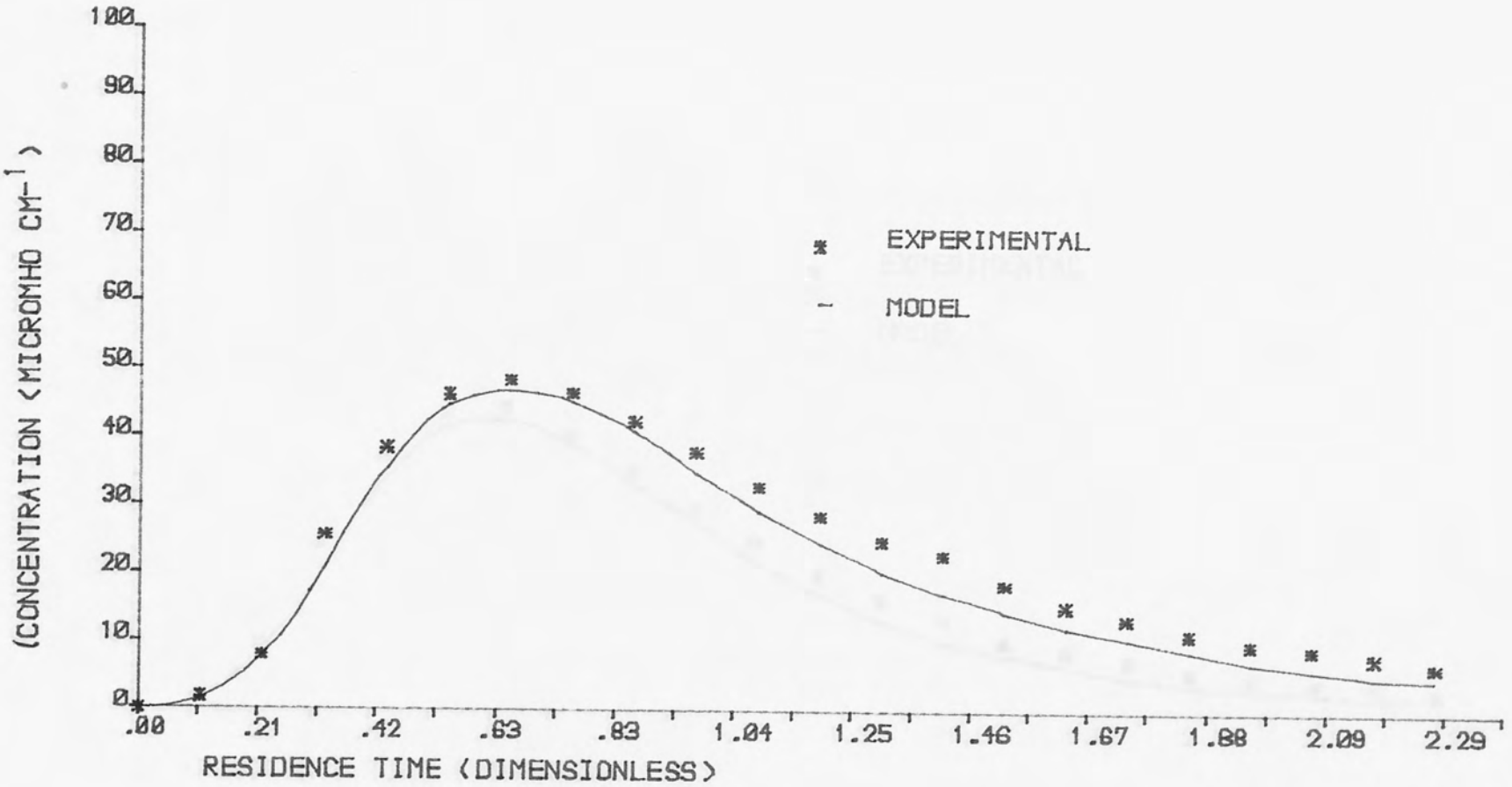

FIGURE 5.10 :RESIDENCE TIME DISTRIBUTION - RUN CODE WMF12

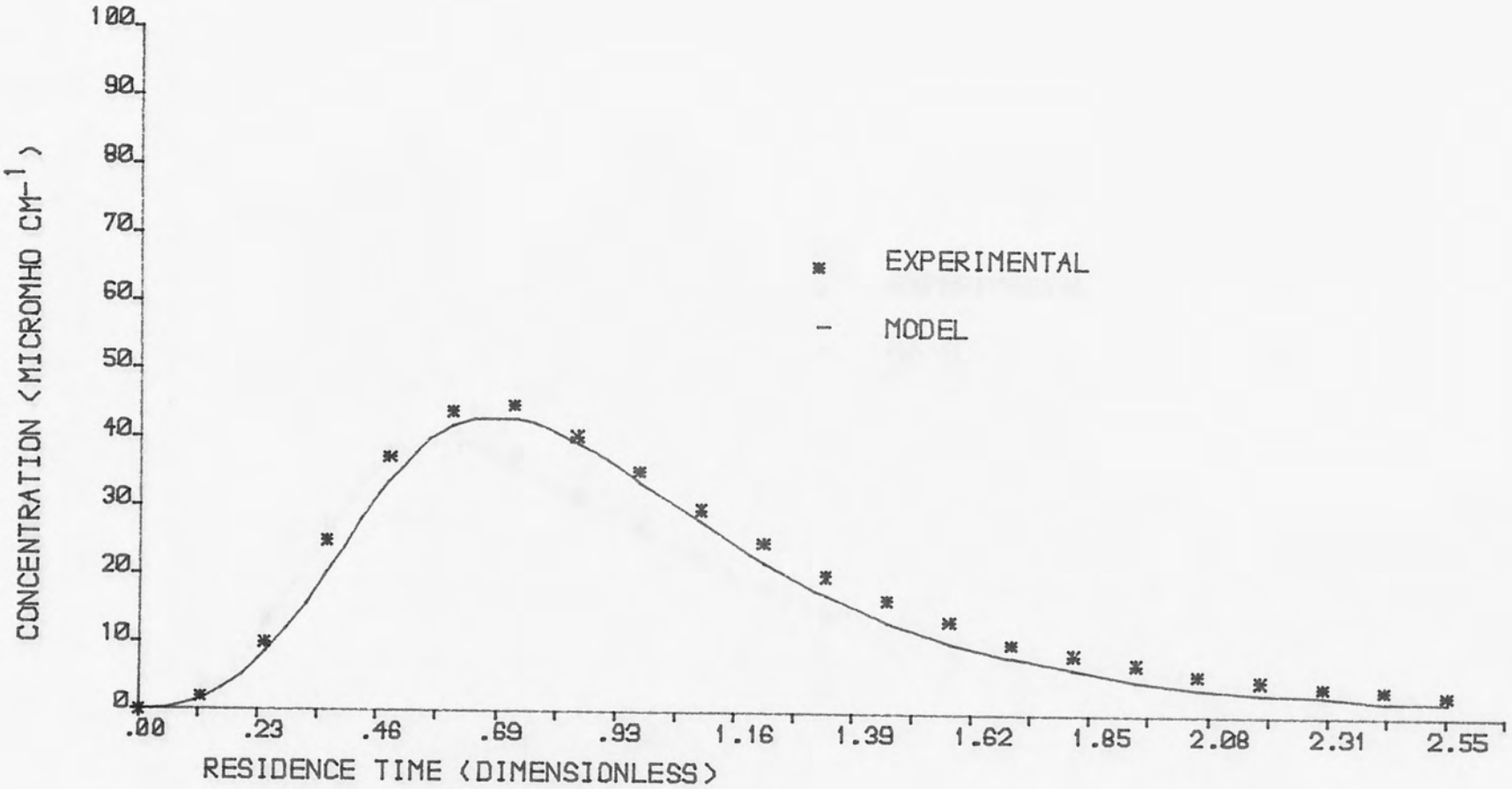

FIGURE 5.11 :RESIDENCE TIME DISTRIBUTION - RUN CODE WMF14

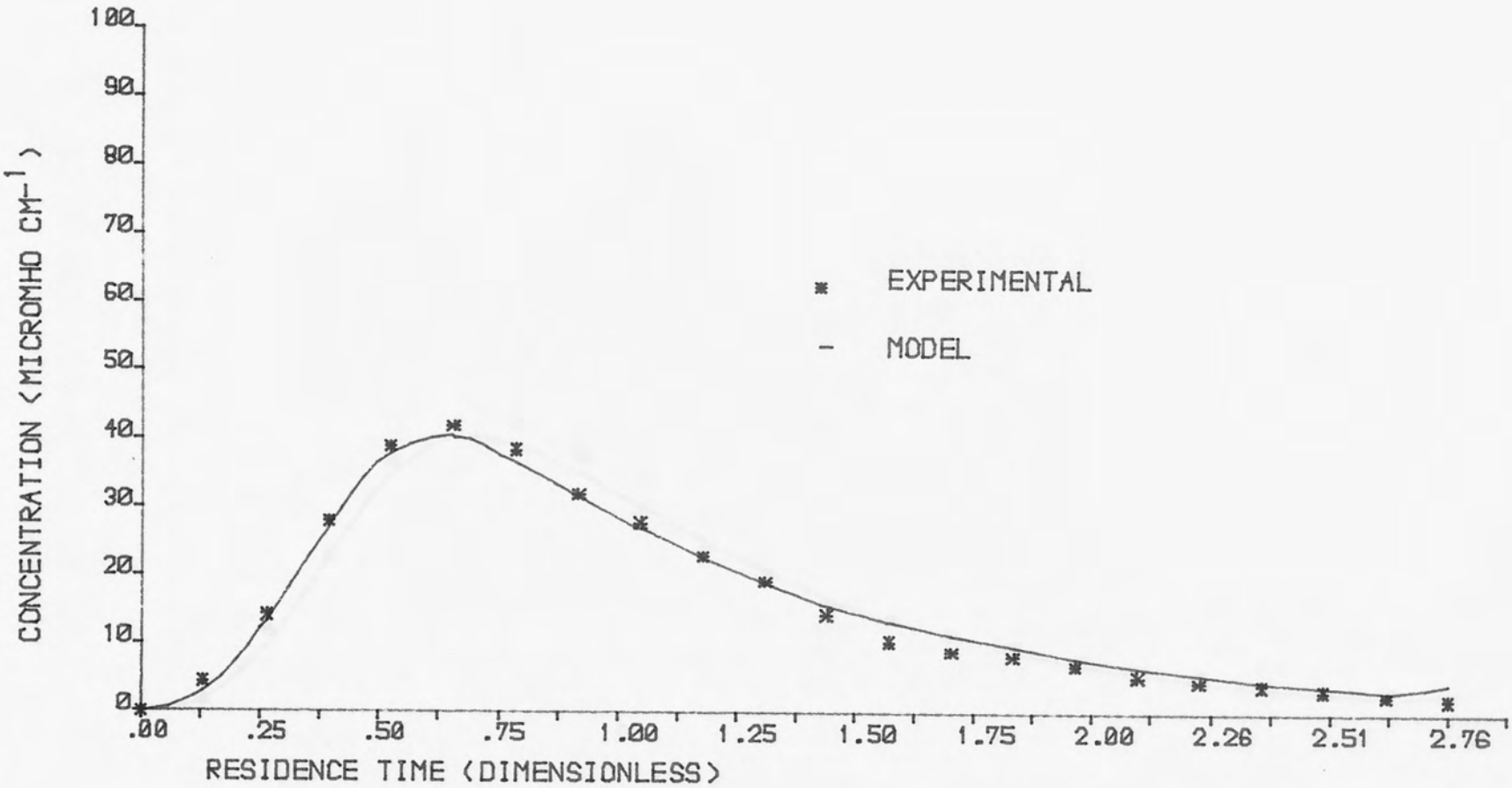

FIGURE 5.12 :RESIDENCE TIME DISTRIBUTION - RUN CODE WMF15

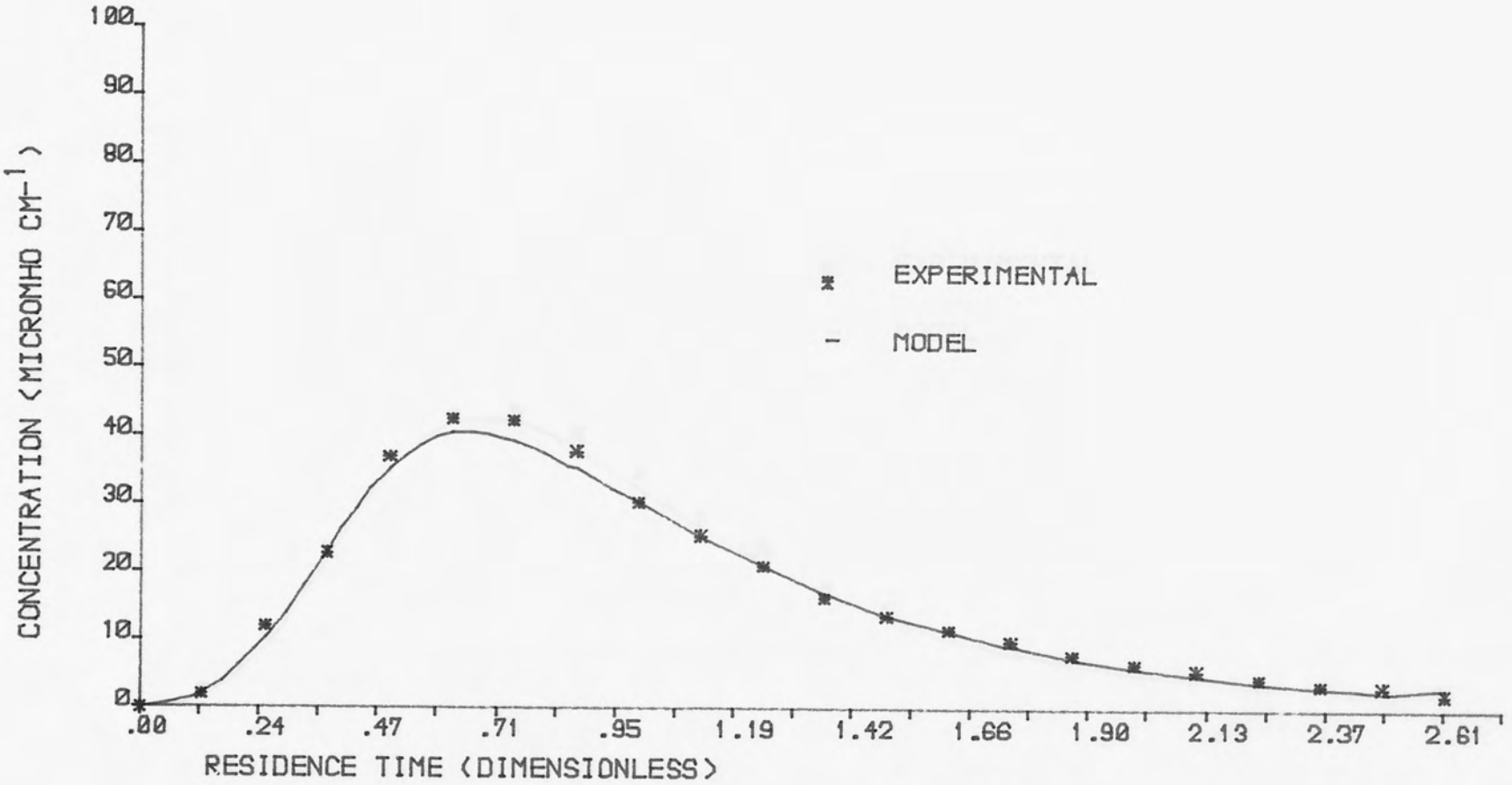

FIGURE 5.13 :RESIDENCE TIME DISTRIBUTION - RUN CODE WMF16

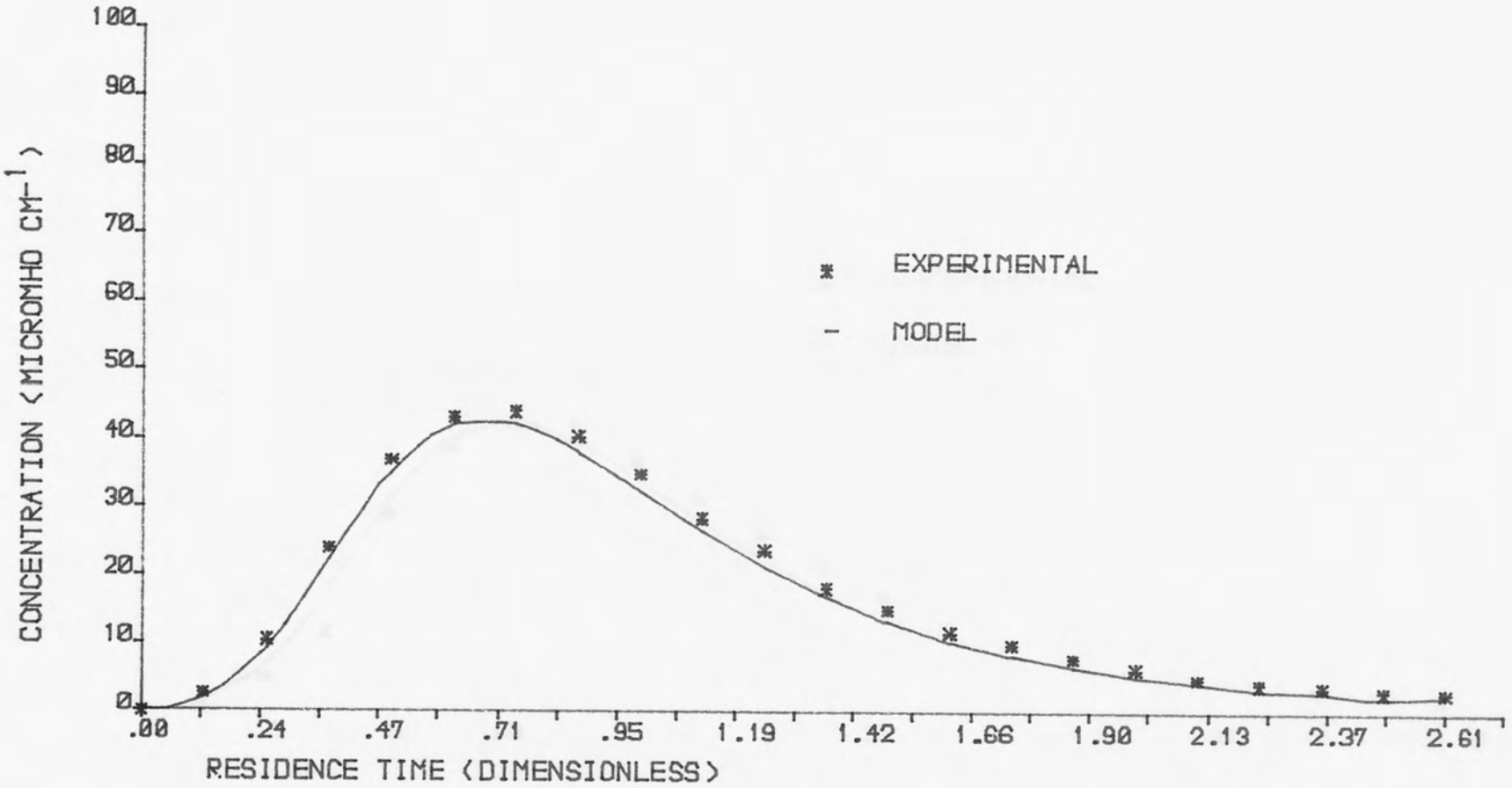

FIGURE 5.14 :RESIDENCE TIME DISTRIBUTION - RUN CODE WMF17

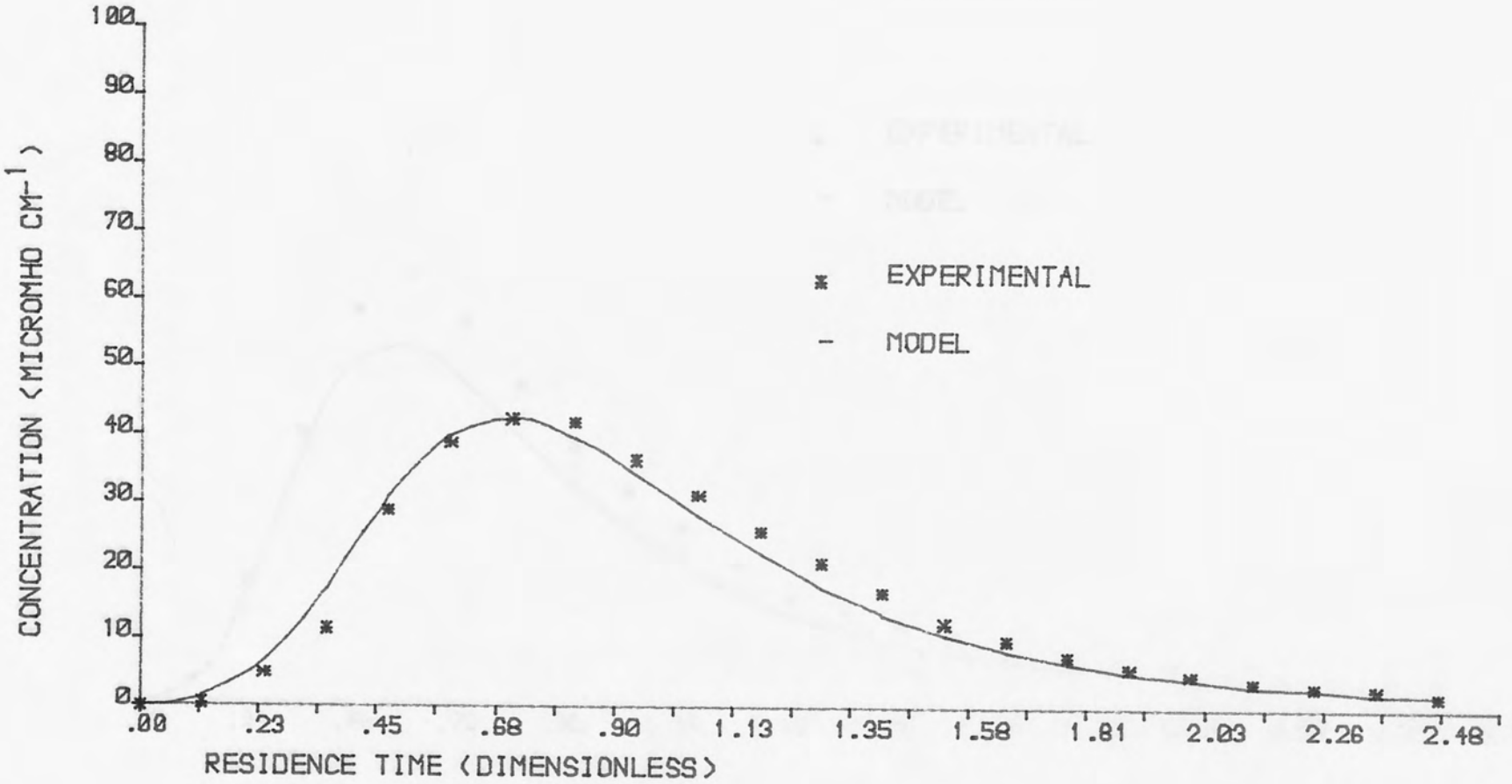

FIGURE 5.15 :RESIDENCE TIME DISTRIBUTION - RUN CODE WMF18

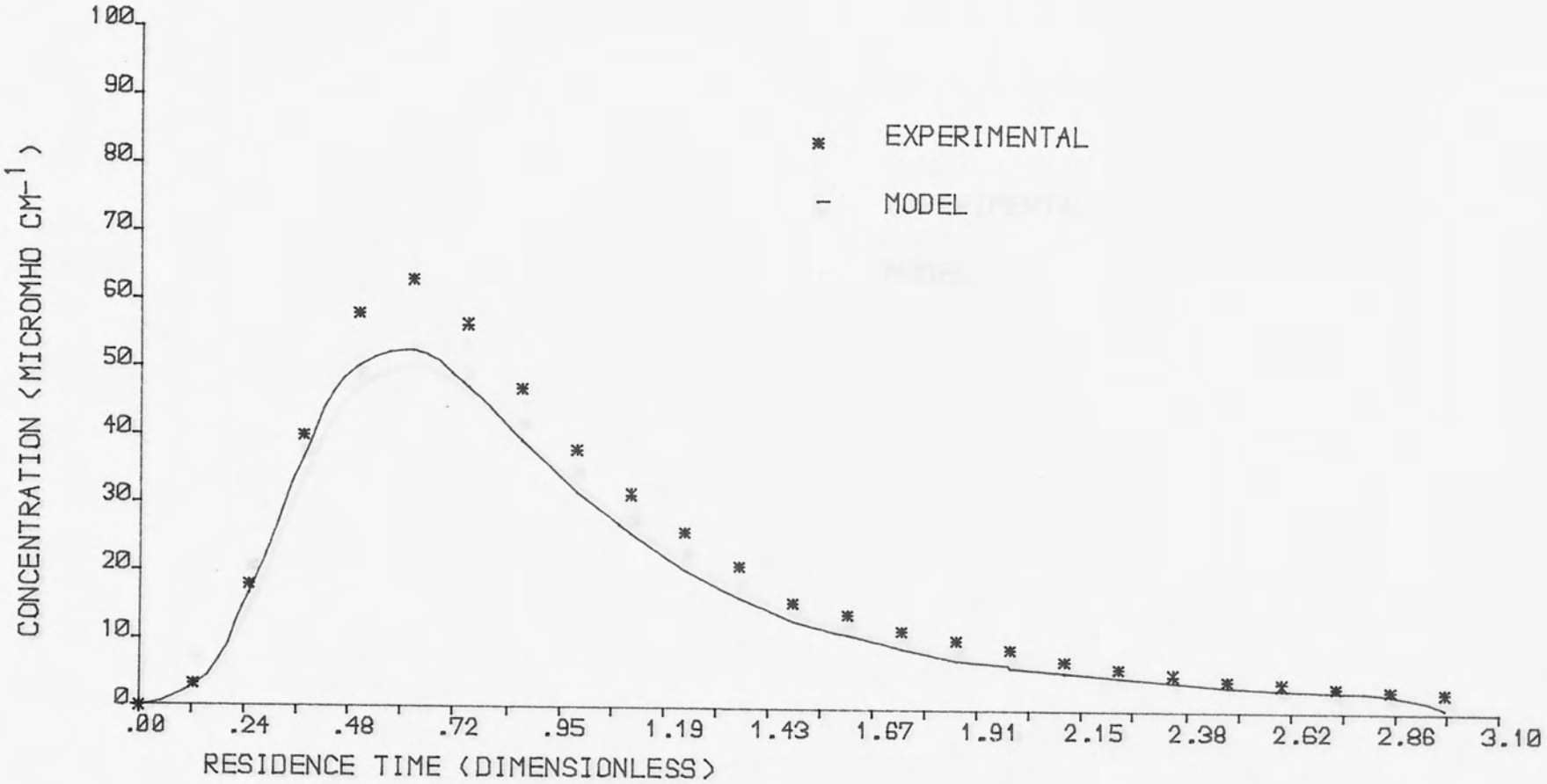

FIGURE 5.16 :RESIDENCE TIME DISTRIBUTION - RUN CODE SDX20

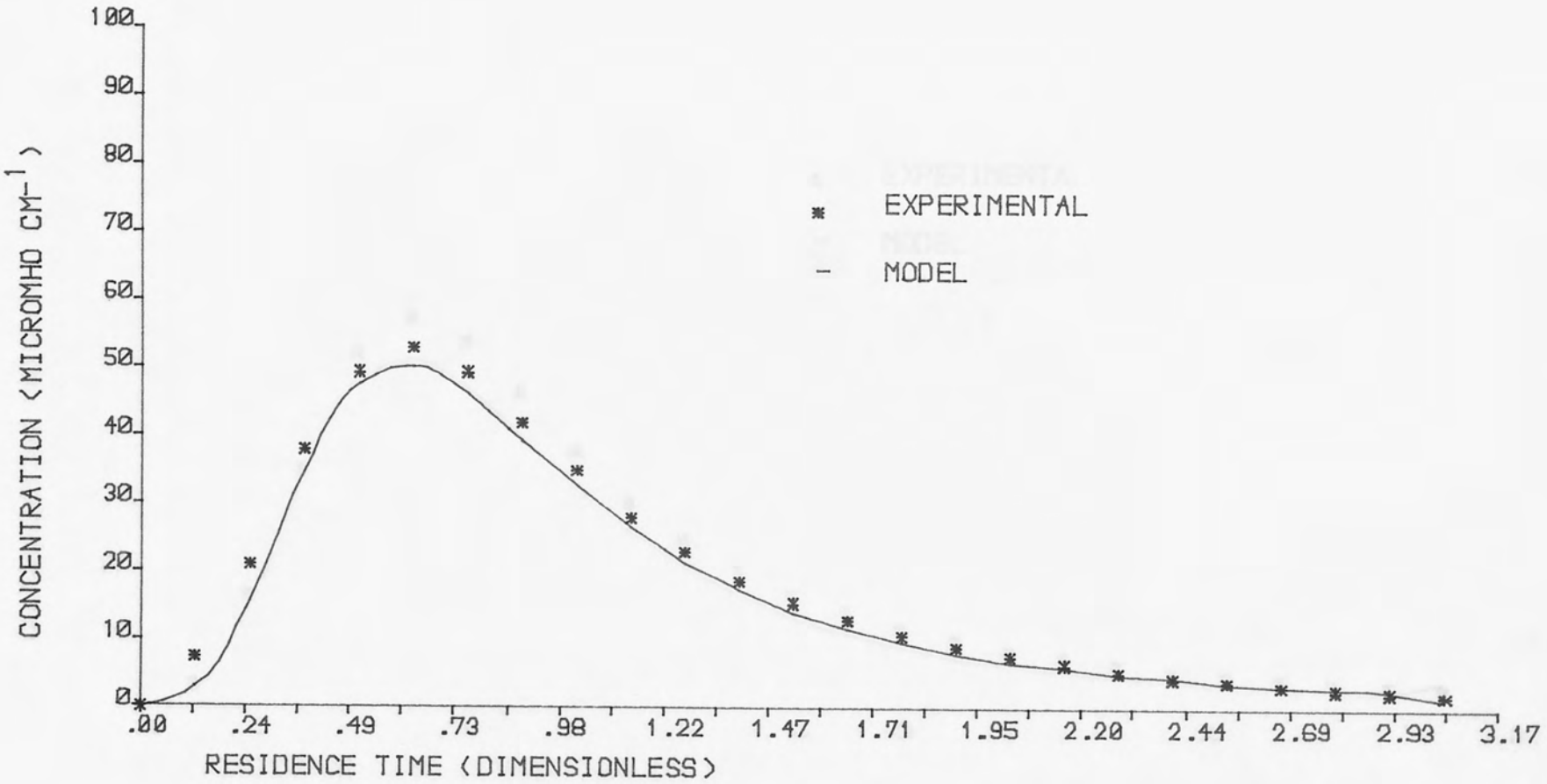

FIGURE 5.17 :RESIDENCE TIME DISTRIBUTION - RUN CODE SDX21

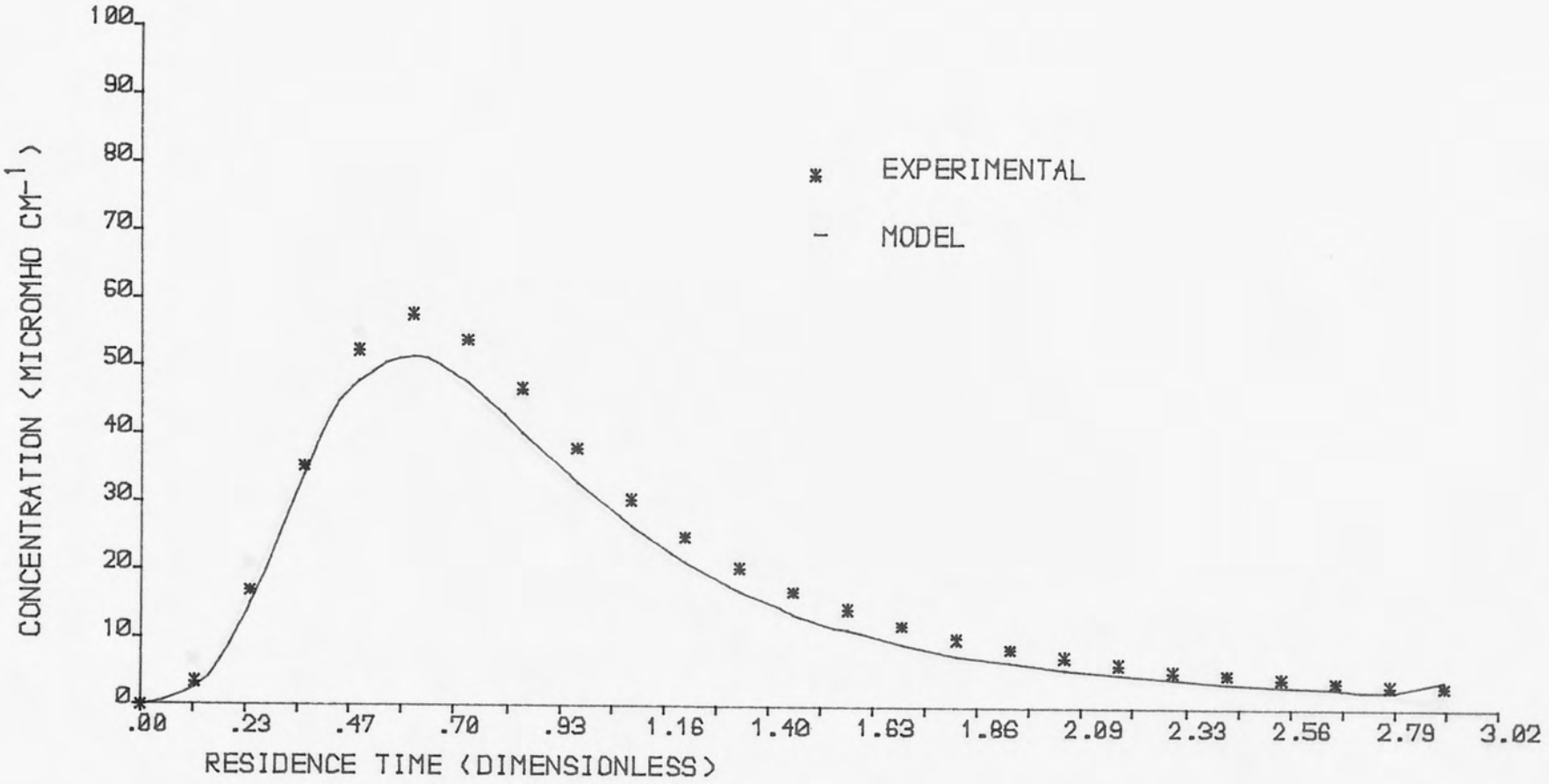

FIGURE 5.18 :RESIDENCE TIME DISTRIBUTION - RUN CODE SDX22

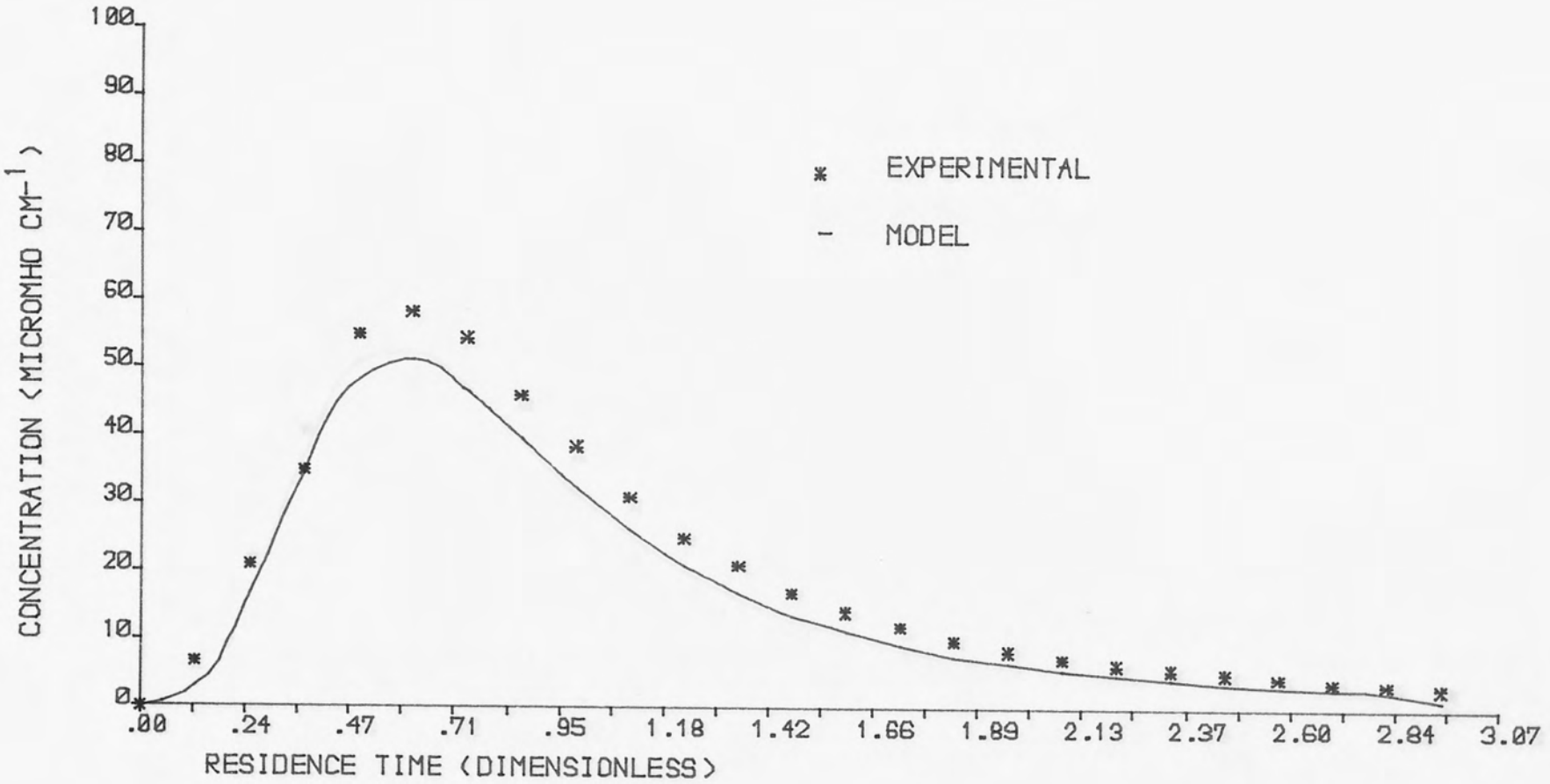

FIGURE 5.19 :RESIDENCE TIME DISTRIBUTION - RUN CODE SDX23

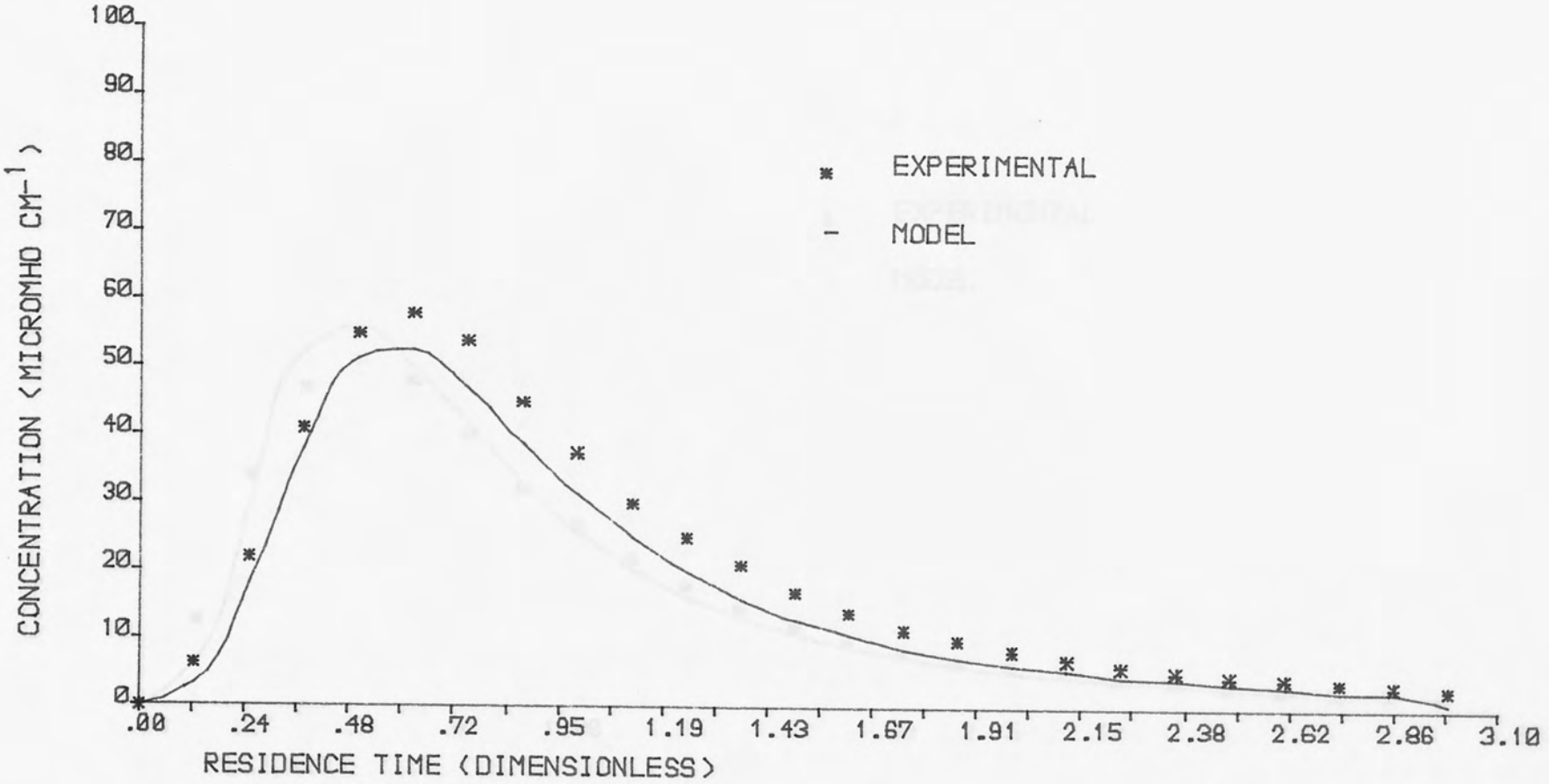

FIGURE 5.20 :RESIDENCE TIME DISTRIBUTION - RUN CODE SDX24

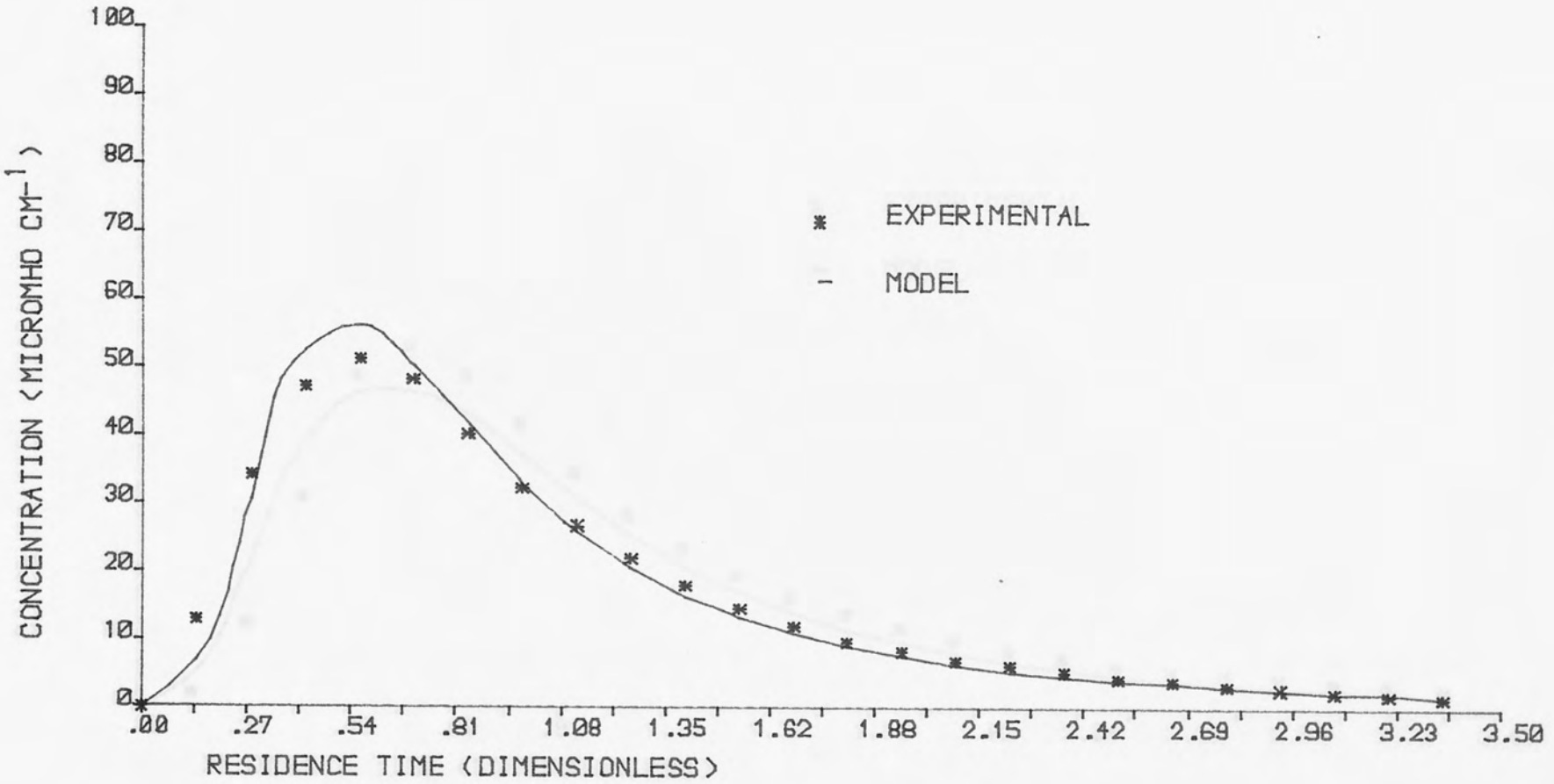

FIGURE 5.21 :RESIDENCE TIME DISTRIBUTION - RUN CODE SDX26

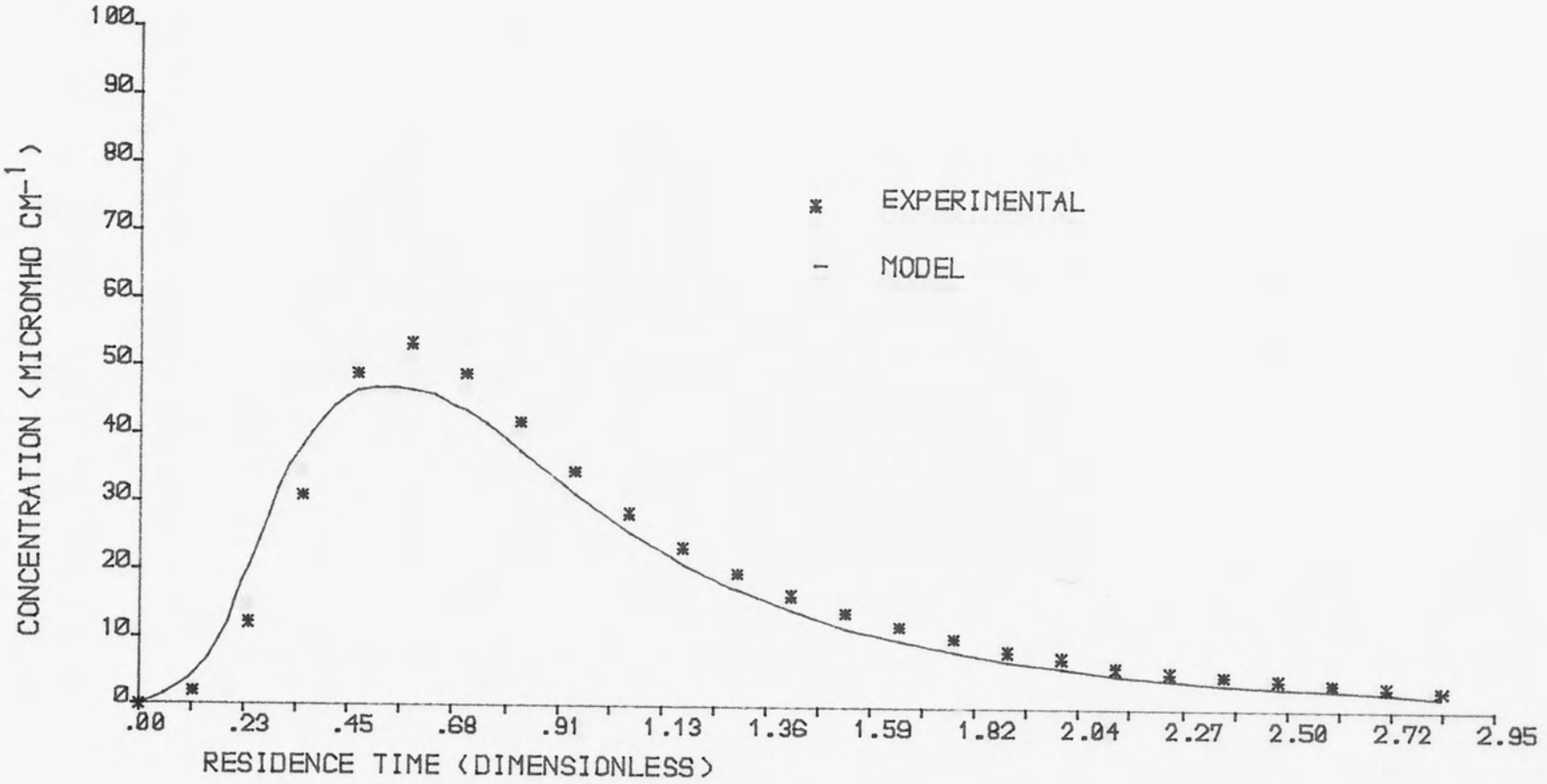

FIGURE 5.22 :RESIDENCE TIME DISTRIBUTION - RUN CODE SDX27

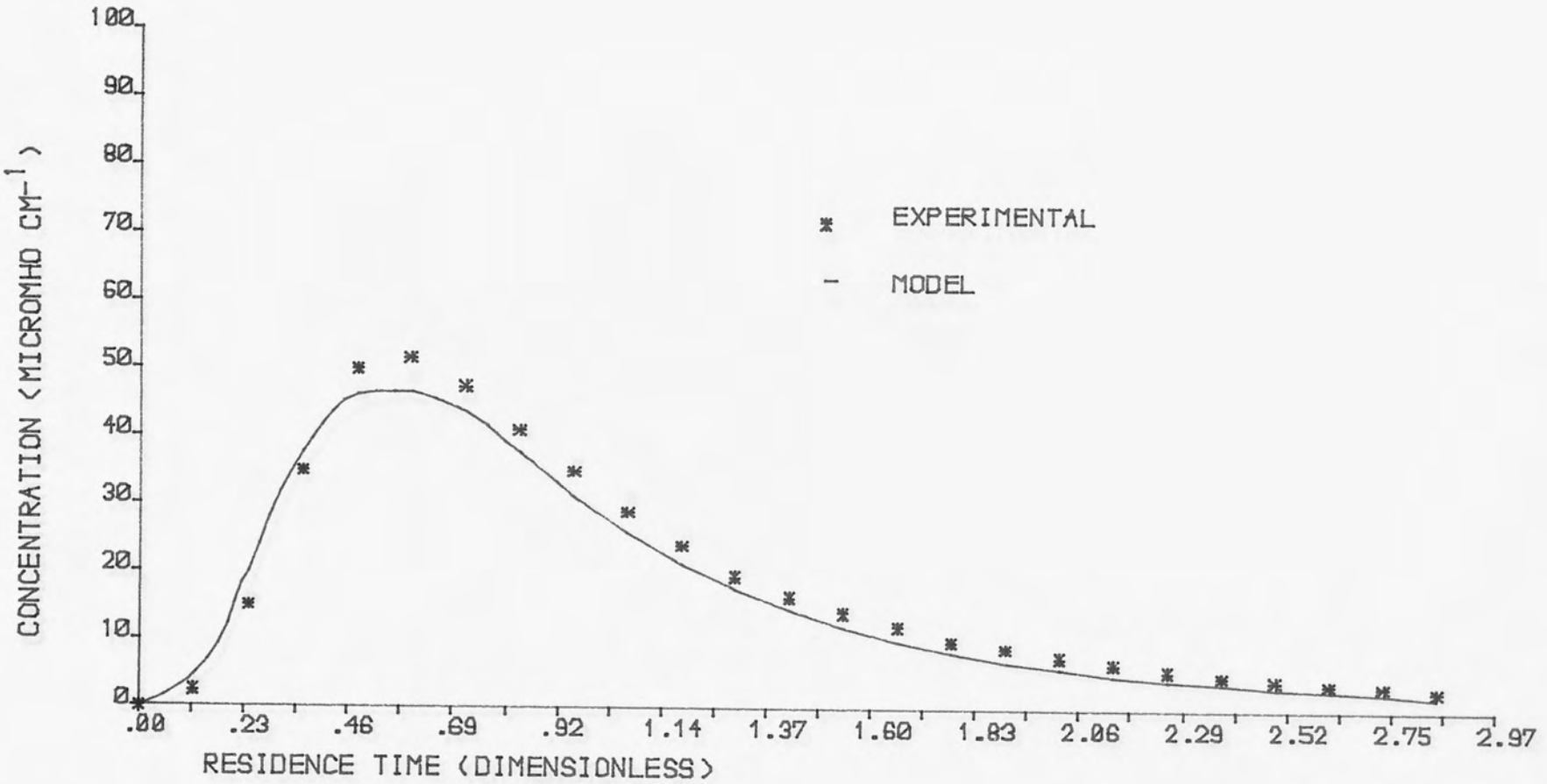

FIGURE 5.23 :RESIDENCE TIME DISTRIBUTION - RUN CODE SDX28

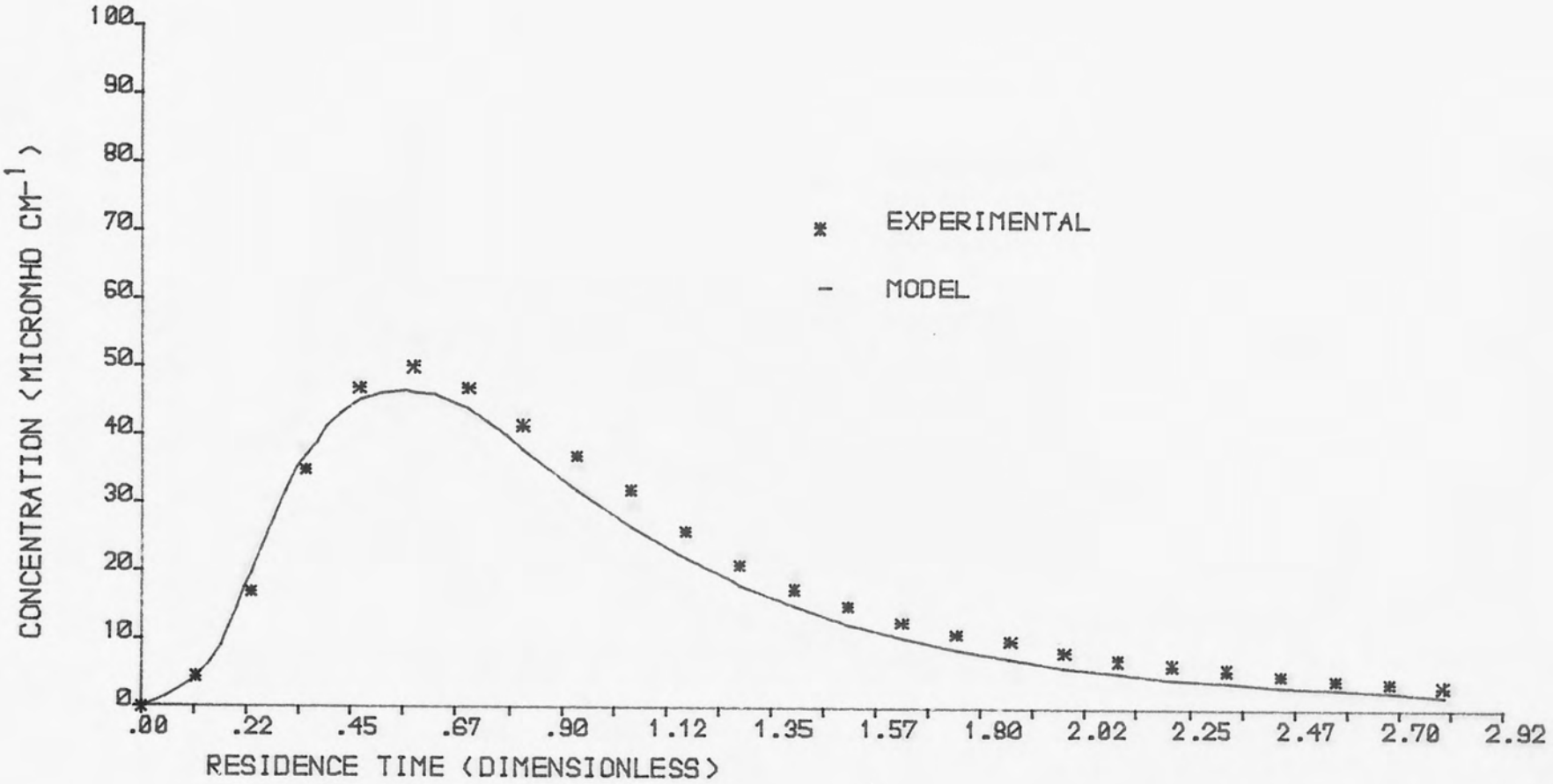

FIGURE 5.24 :RESIDENCE TIME DISTRIBUTION - RUN CODE SDX29

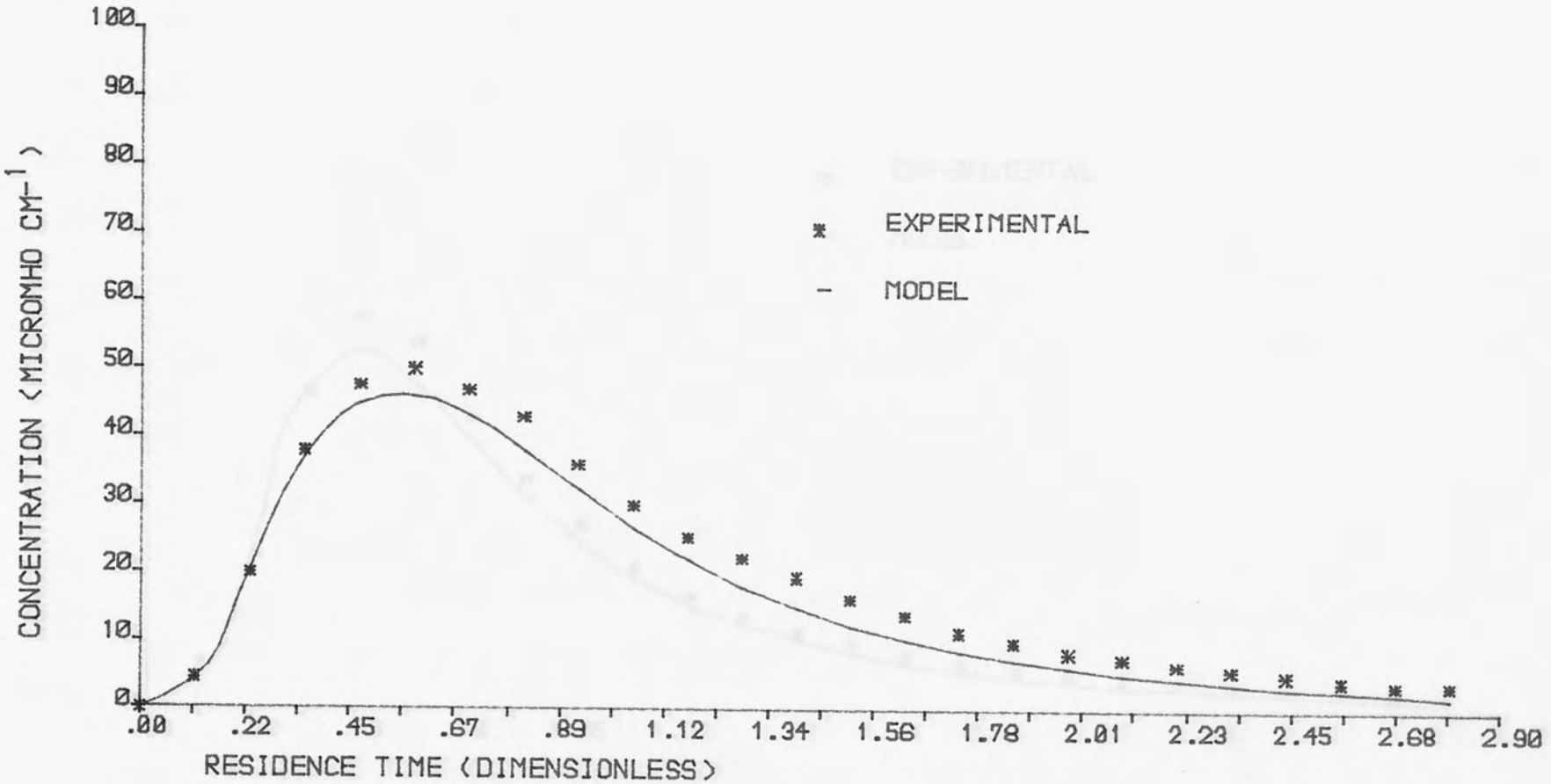

FIGURE 5.25 :RESIDENCE TIME DISTRIBUTION - RUN CODE SDX30

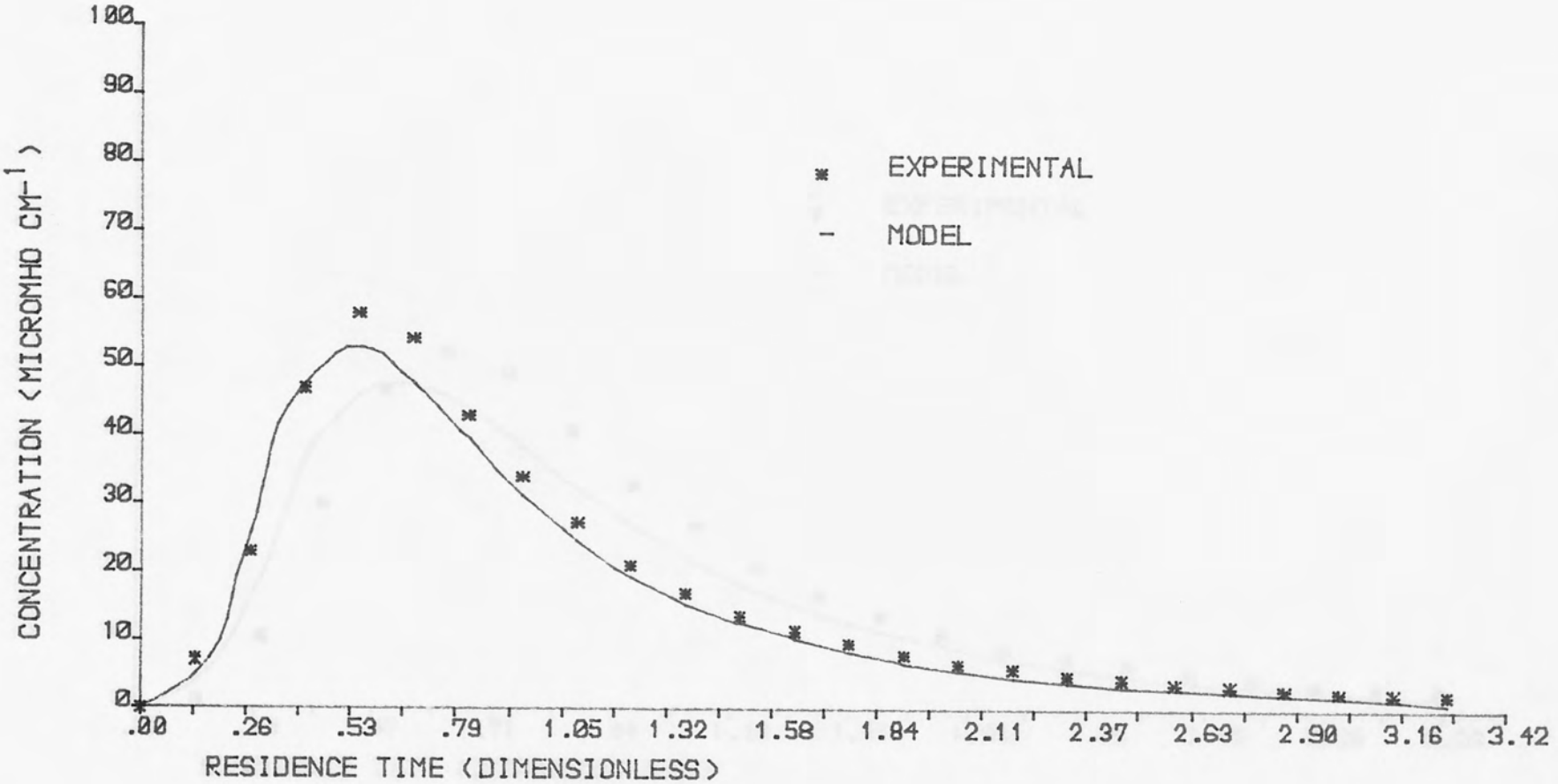

FIGURE 5.26 :RESIDENCE TIME DISTRIBUTION - RUN CODE SDX32

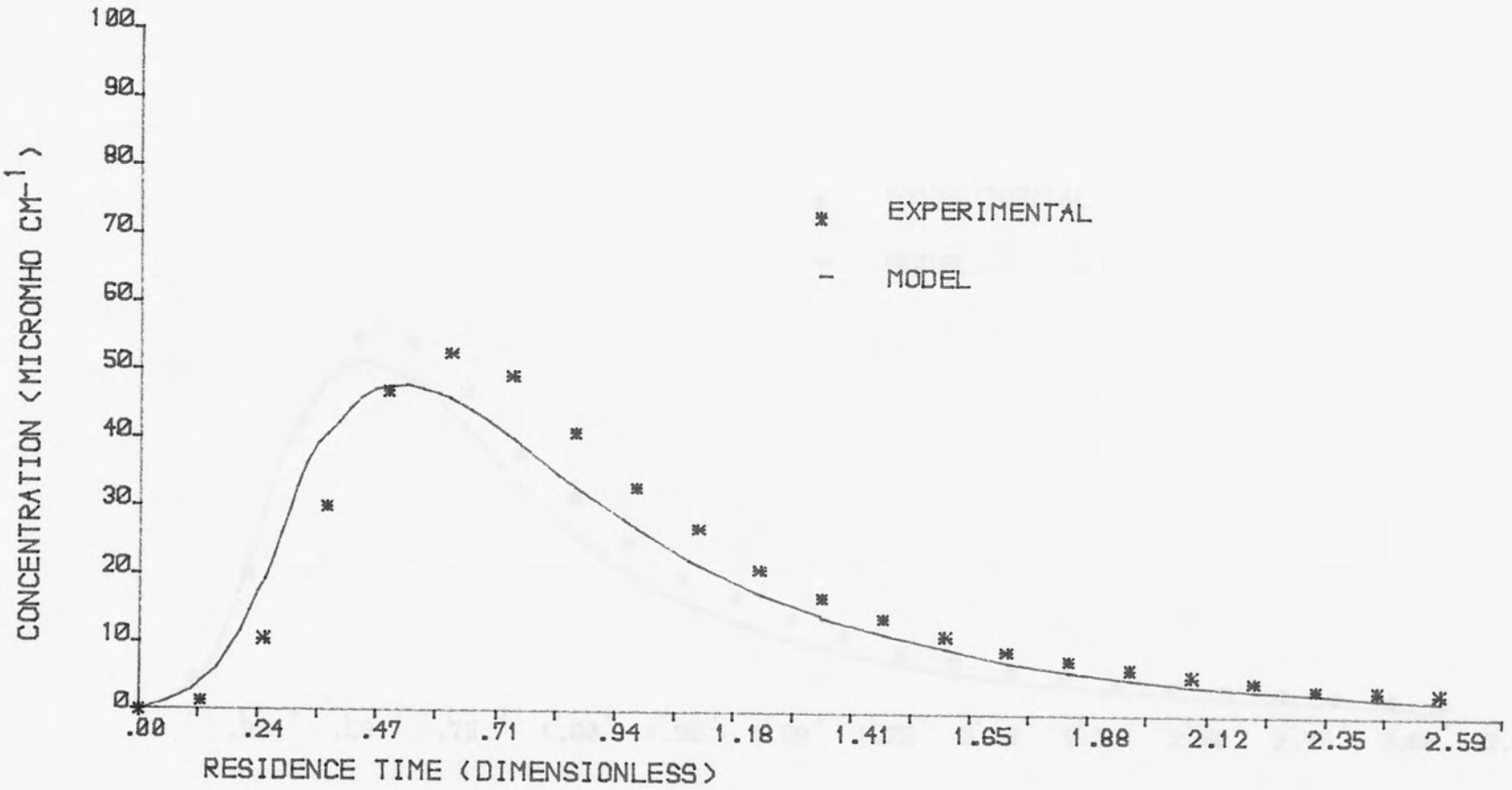

FIGURE 5.27 :RESIDENCE TIME DISTRIBUTION - RUN CODE SDX33

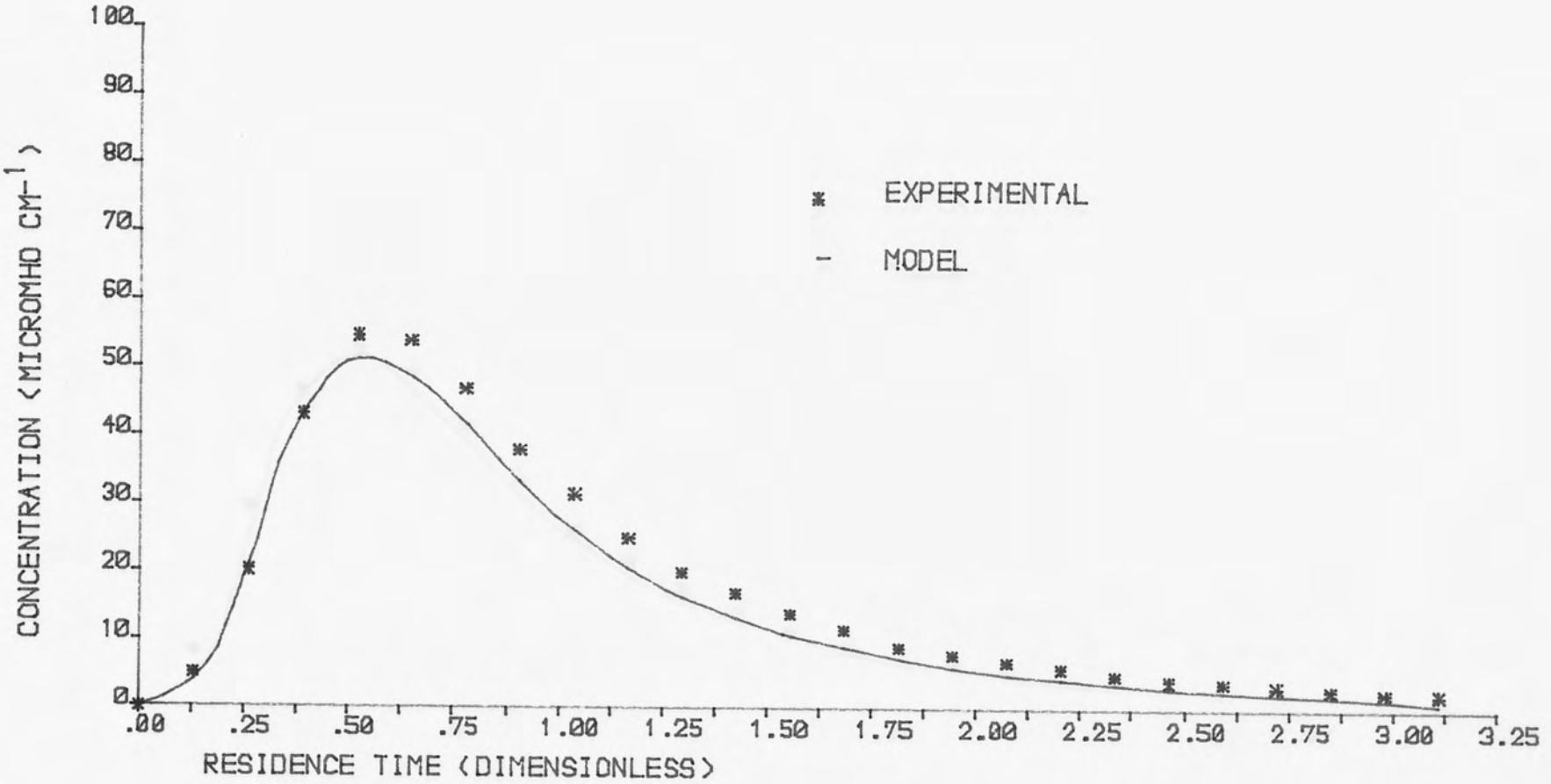

FIGURE 5.28 :RESIDENCE TIME DISTRIBUTION - RUN CODE SDX34

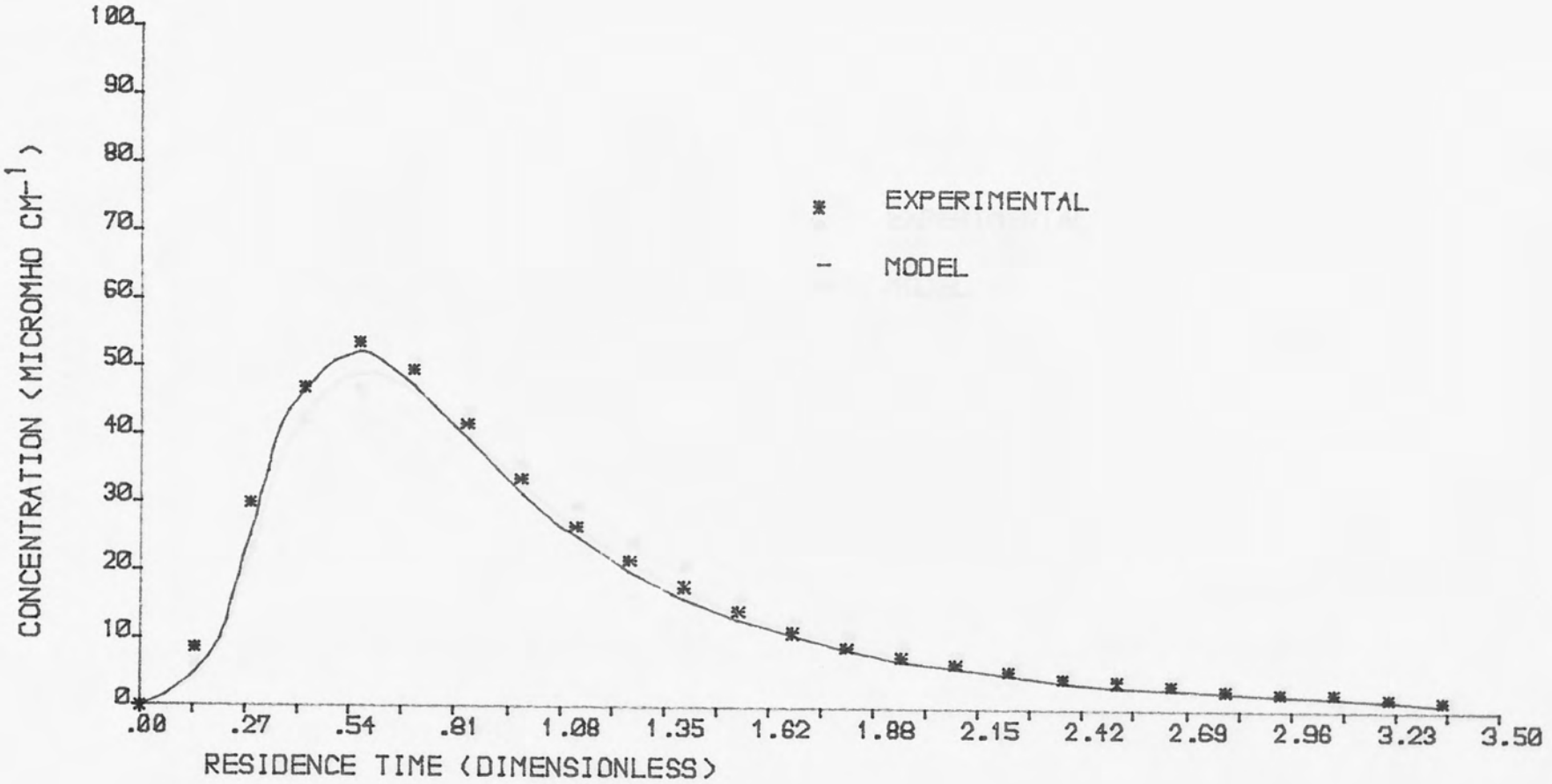

FIGURE 5.29 :RESIDENCE TIME DISTRIBUTION - RUN CODE SDX35

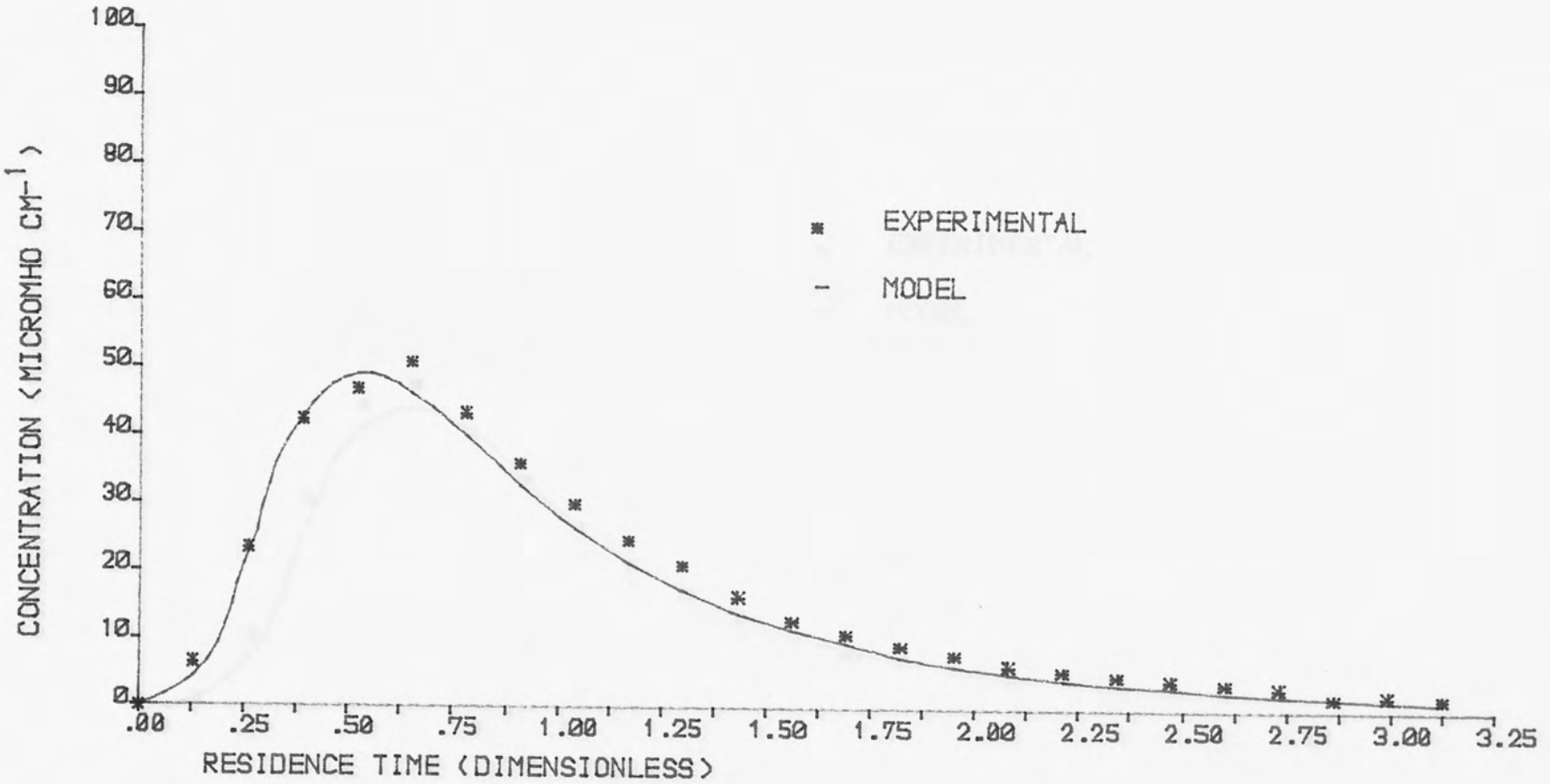

FIGURE 5.30 :RESIDENCE TIME DISTRIBUTION - RUN CODE SDX36

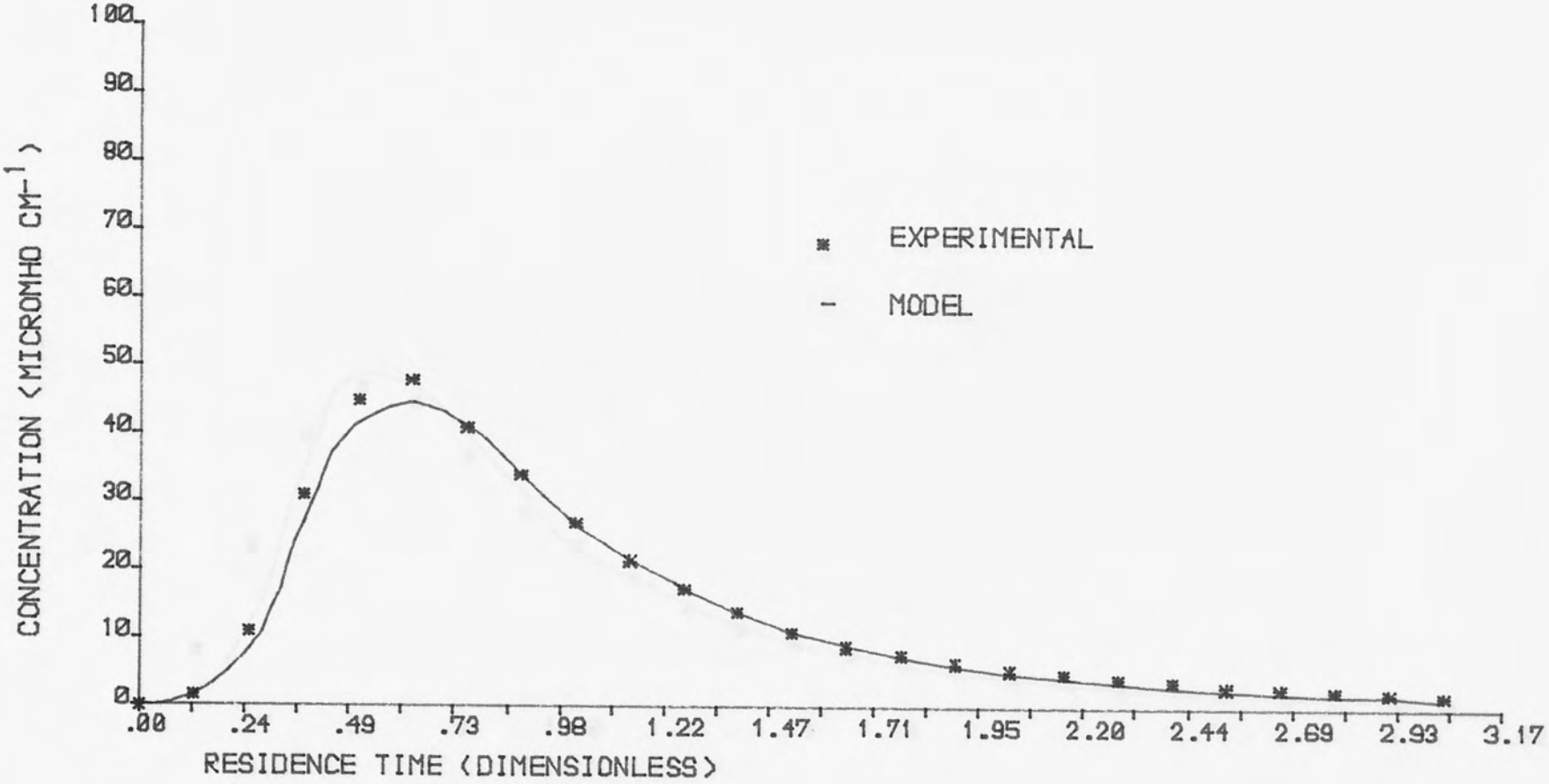

FIGURE 5.31 :RESIDENCE TIME DISTRIBUTION - RUN CODE SDX38

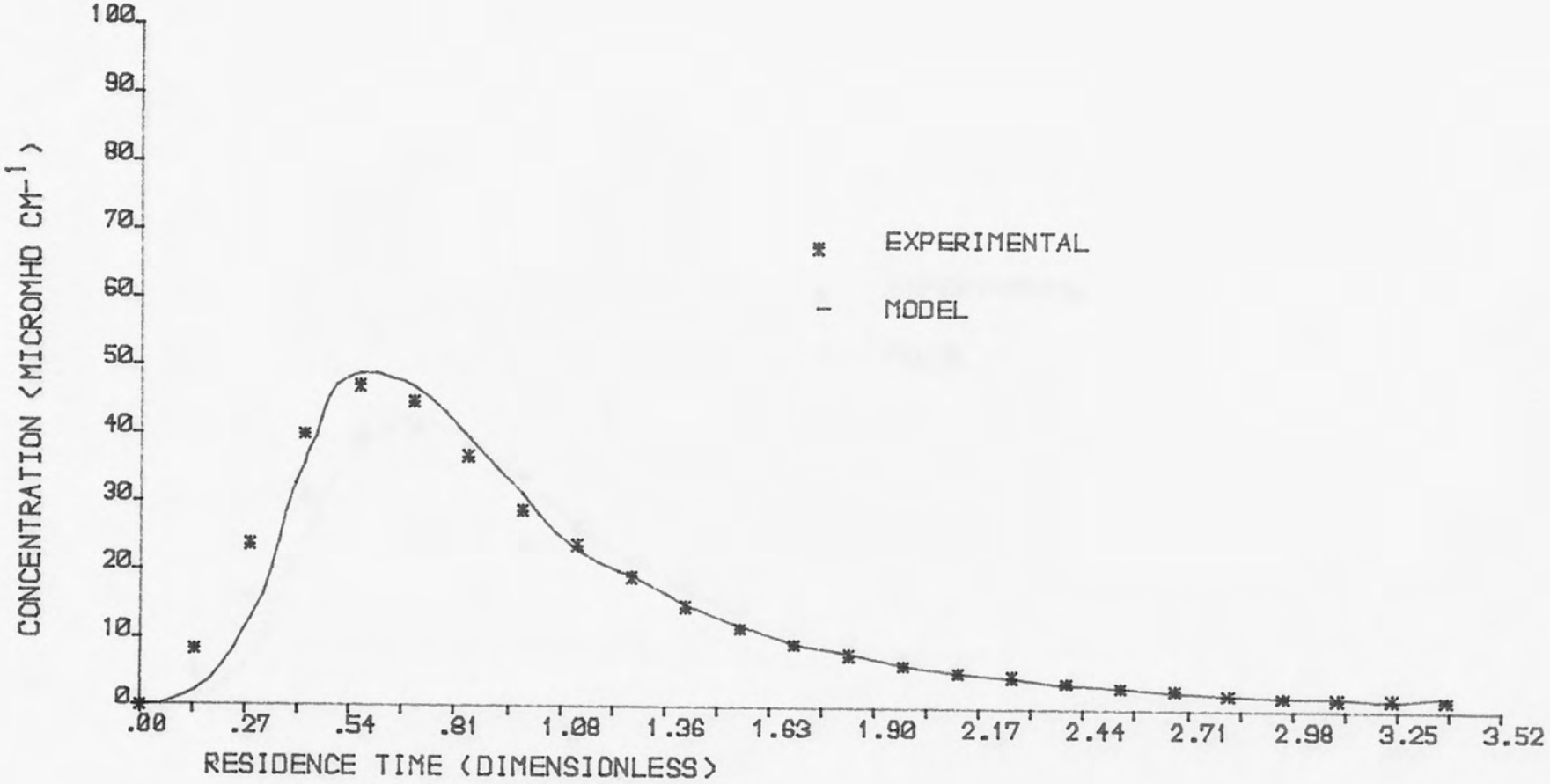

FIGURE 5.32 :RESIDENCE TIME DISTRIBUTION - RUN CODE SDX39

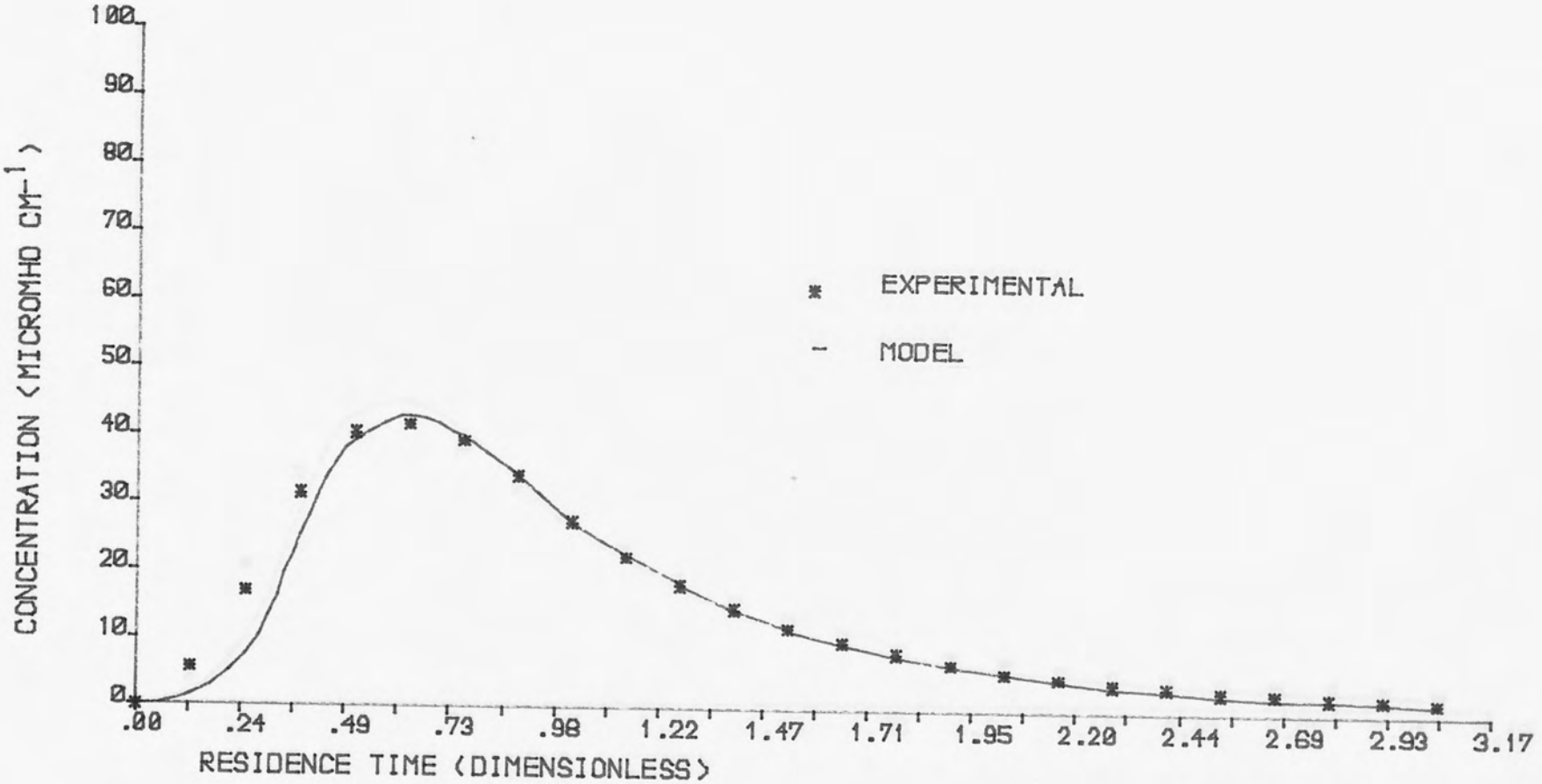

FIGURE 5.33 :RESIDENCE TIME DISTRIBUTION - RUN CODE SDX40

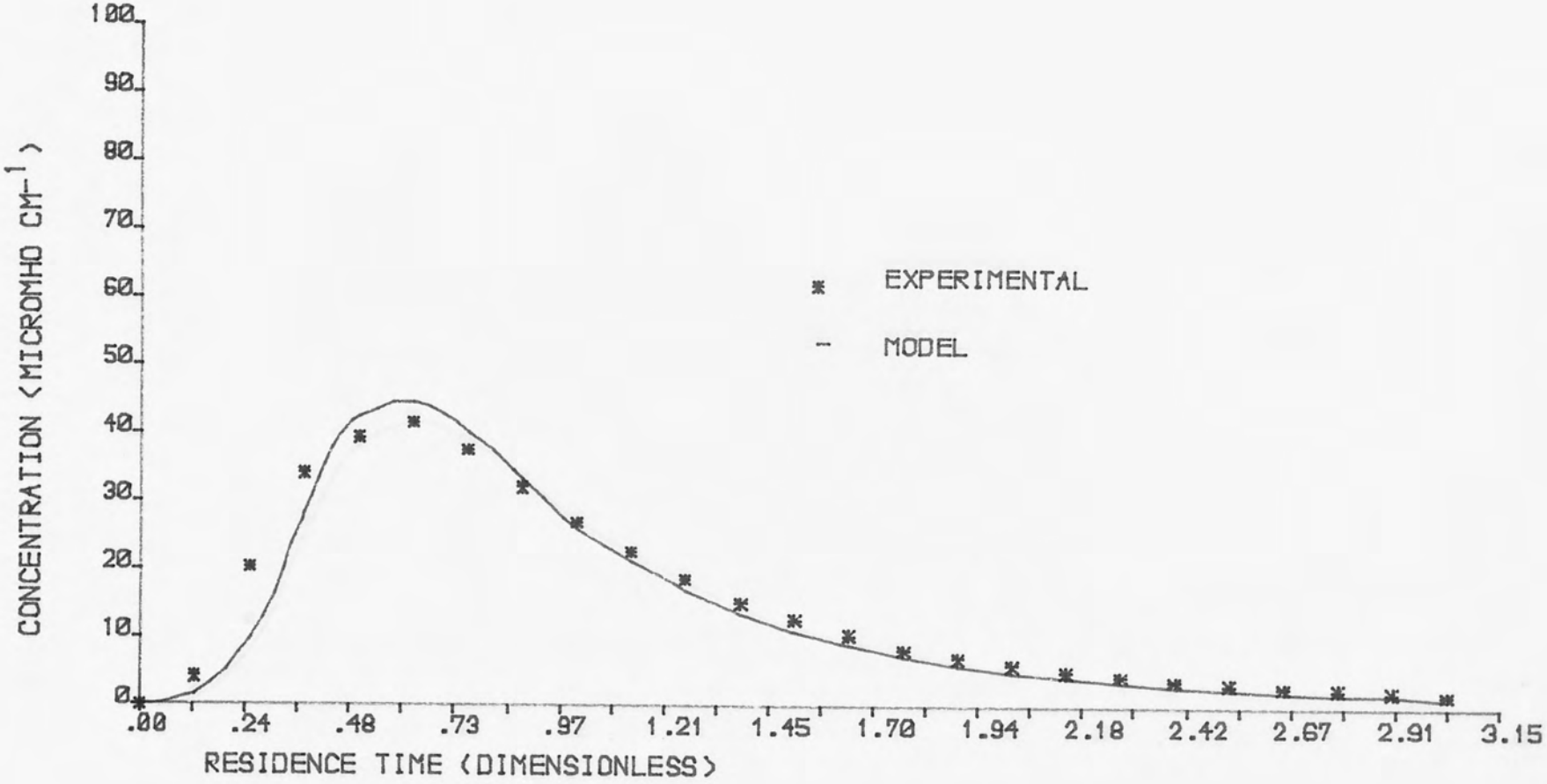

FIGURE 5.34 :RESIDENCE TIME DISTRIBUTION - RUN CODE SDX41

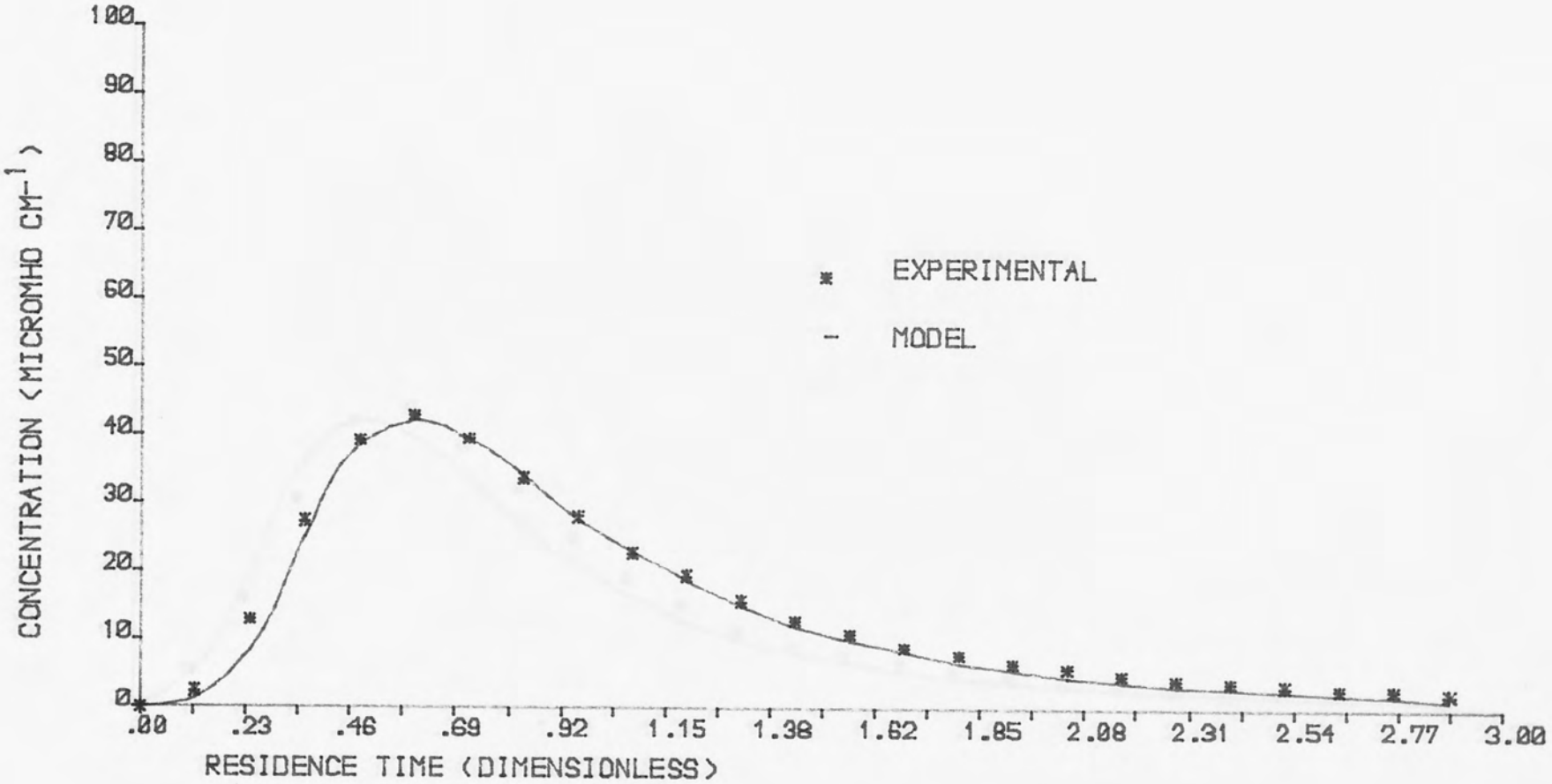

FIGURE 5.35 :RESIDENCE TIME DISTRIBUTION - RUN CODE SDX42

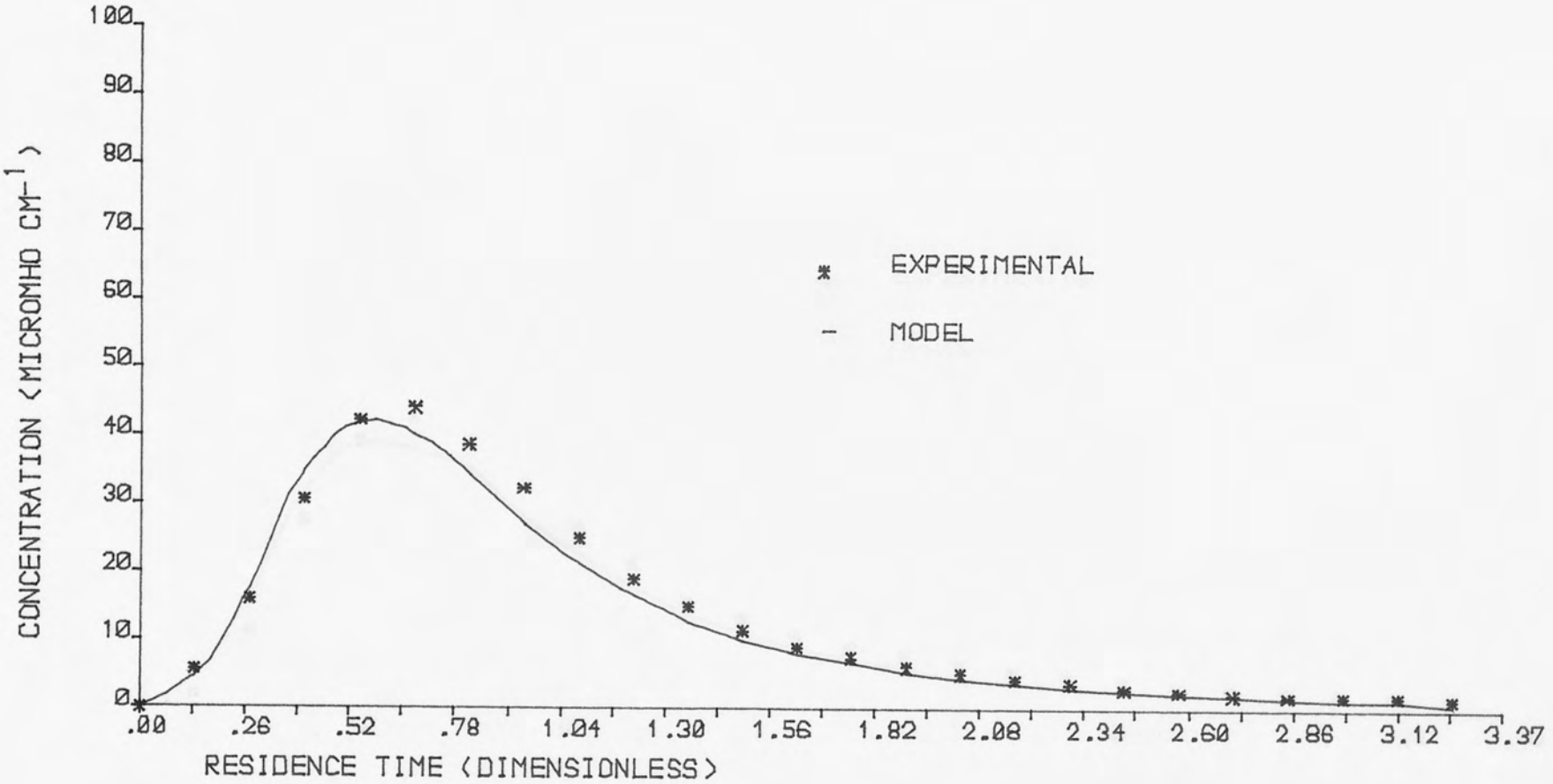

FIGURE 5.36 :RESIDENCE TIME DISTRIBUTION - RUN CODE SDX44

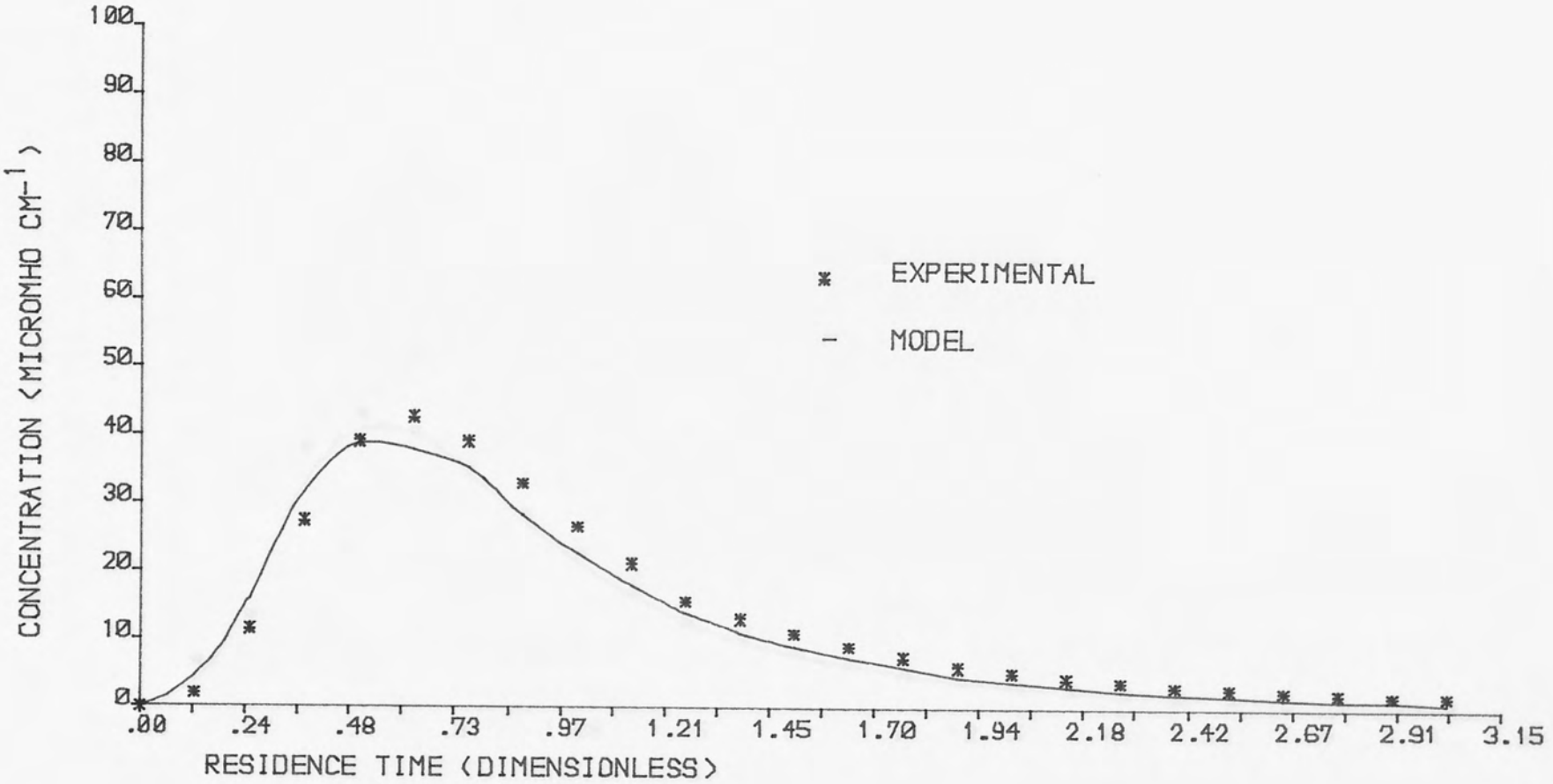

FIGURE 5.37 :RESIDENCE TIME DISTRIBUTION - RUN CODE SDX45

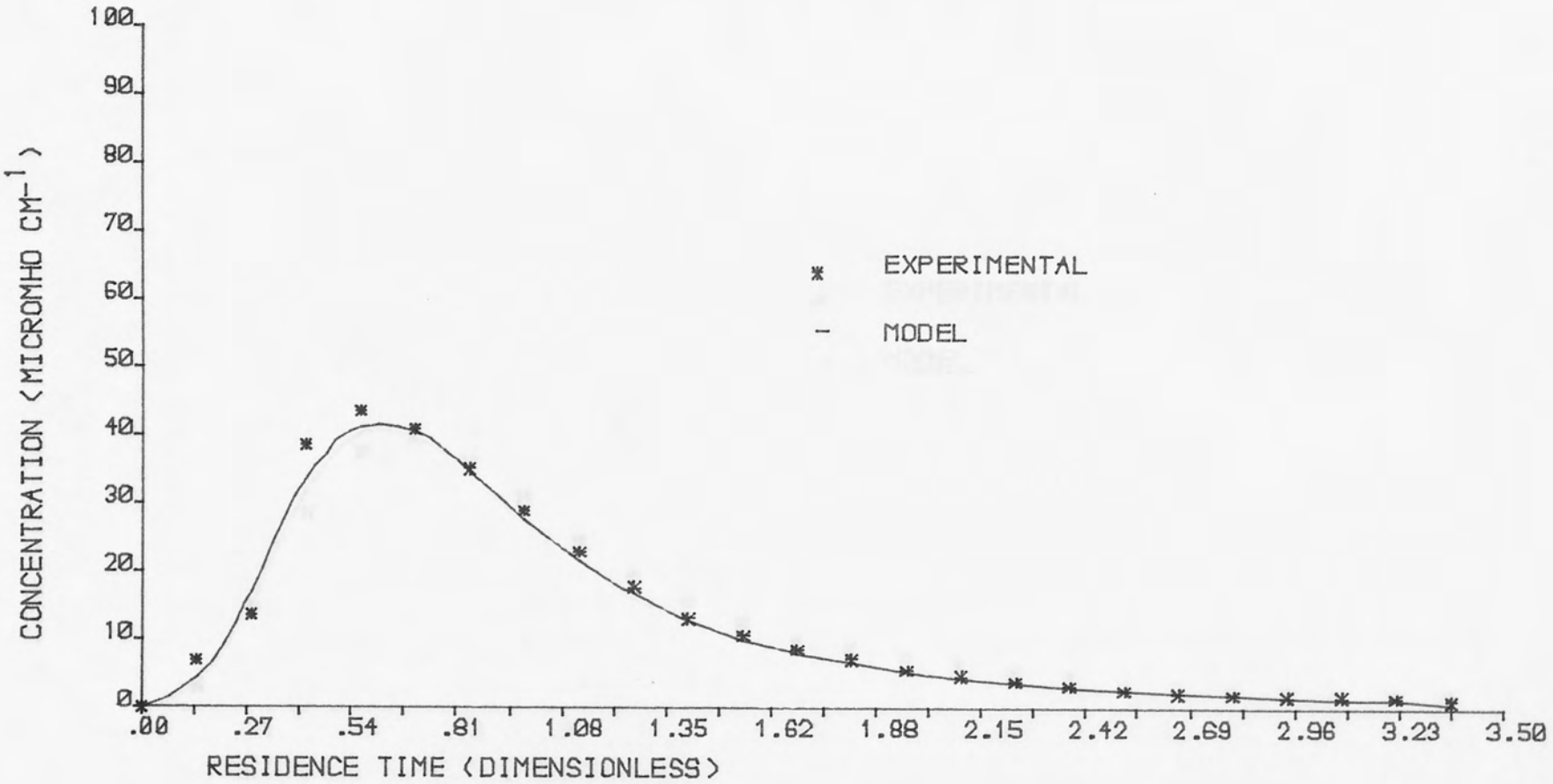

FIGURE 5.38 :RESIDENCE TIME DISTRIBUTION - RUN CODE SDX46

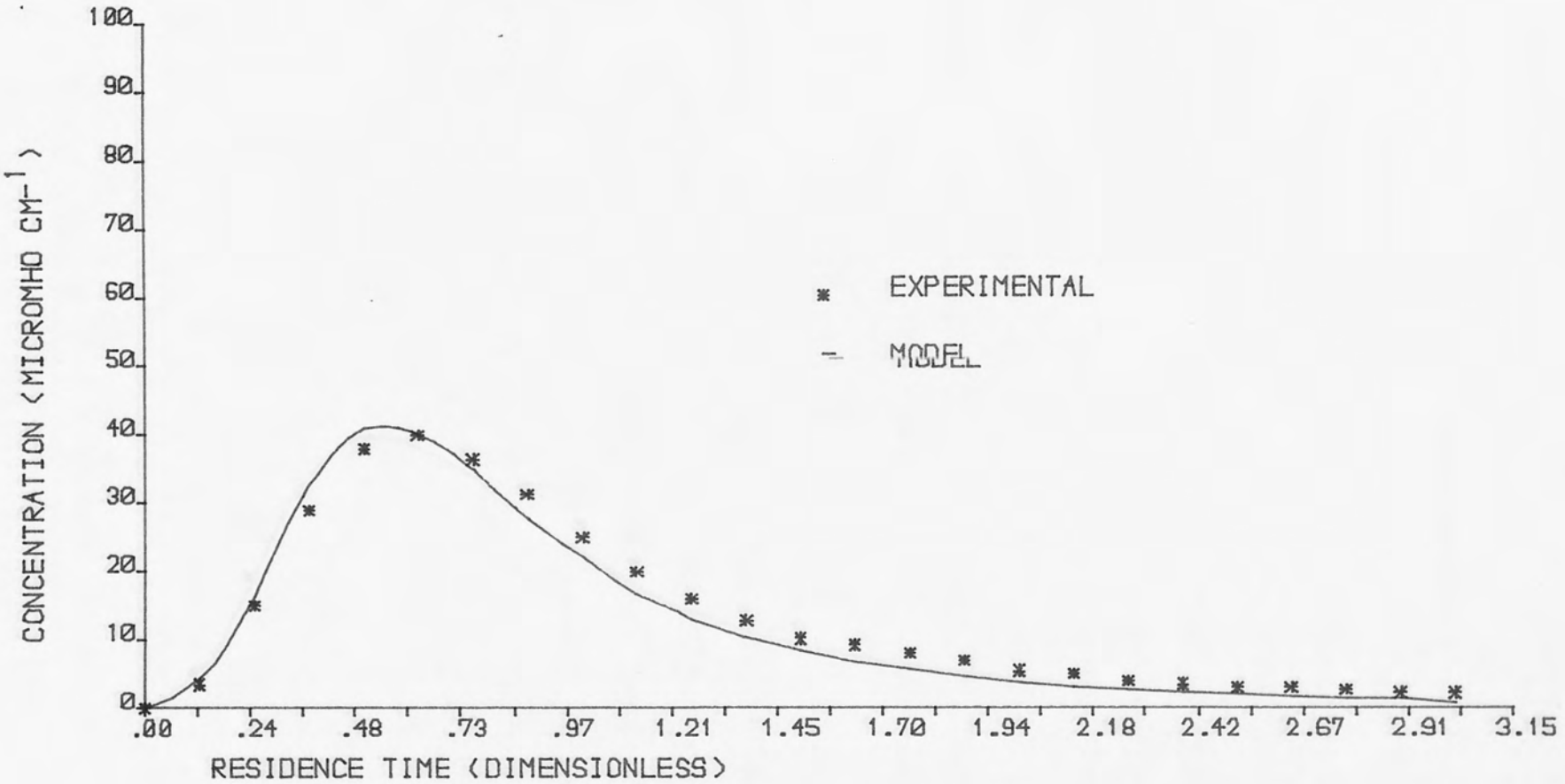

FIGURE 5.39 :RESIDENCE TIME DISTRIBUTION - RUN CODE SDX47

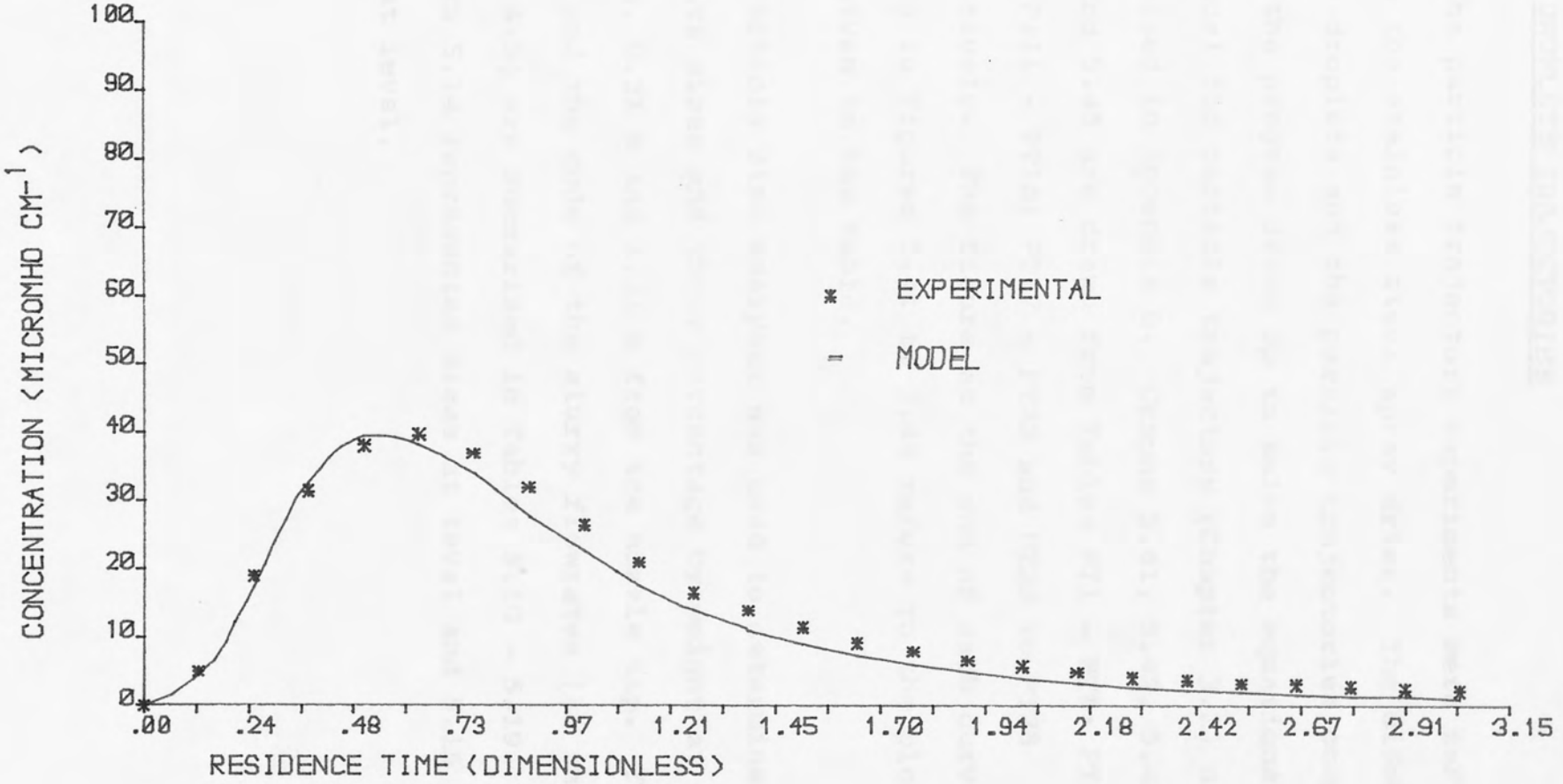

FIGURE 5.40 :RESIDENCE TIME DISTRIBUTION - RUN CODE SDX48

5.2 DROPLETS TRAJECTORIES

The particle trajectory experiments were carried out in the stainless steel spray drier. The diameters of the droplets and the particle trajectories computed using the program drawn up to solve the equations in the model for particle trajectory (Chapter 3.2) are summarised in Appendix B. Graphs 5.41, 5.42, 5.43, 5.44 and 5.45 are drawn from Tables PT1 - PT6; PT7 - PT10; PT11 - PT16; PT17 - PT22 and PT23 to PT28 respectively. The figure at the end of each curve (1 - 6) in Figures 5.41 to 5.45 refers to the plot code given in the table.

Particle size analyser was used to determine the droplets sizes and their percentage by weight at two levels, 0.31 m and 1.31 m from the nozzle tip. The sizes and the code of the slurry flowrates (as shown in Table 4.5) are summarised in Tables 5.10 - 5.19. Tables 5.10 to 5.14 represented sizes at level and 5.15 to 5.19 at level.

TABLE 5.10

SLURRY FLOWRATE: P1

DIAMETER (MICRONS)	WEIGHT PERCENTAGE
74.45	1.9
98.55	7.8
136.55	15.3
210.95	37.7
412.80	37.2

TABLE 5.11

SLURRY FLOWRATE: P2

DIAMETER (MICRONS)	WEIGHT PERCENTAGE
74.45	4.0
98.55	8.4
136.55	19.4
210.95	38.7
412.80	29.5

TABLE 5.12

SLURRY FLOWRATE: P3

DIAMETER (MICRONS)	WEIGHT PERCENTAGE
57.40	1.7
74.45	3.4
98.55	9.2
136.55	25.4
210.95	40.9
412.80	19.4

TABLE 5.13

SLURRY FLOWRATE: P4

DIAMETER (MICRONS)	WEIGHT PERCENTAGE
57.40	2.0
74.45	4.9
98.55	14.1
136.55	25.9
210.95	37.2
412.80	15.9

TABLE 5.14

SLURRY FLOWRATE: P5

DIAMETER (MICRONS)	WEIGHT PERCENTAGE
57.40	2.3
74.45	7.2
98.55	16.2
136.55	28.2
210.95	32.9
412.80	13.2

TABLE 5.15

SLURRY FLOWRATE: P1

DIAMETER (MICRONS)	WEIGHT PERCENTAGE
34.65	.1
44.60	.2
57.40	.5
74.45	1.2
98.55	3.5
136.55	11.0
210.95	34.2
412.80	49.3

TABLE 5.16

SLURRY FLOWRATE: P2

DIAMETER (MICRONS)	WEIGHT PERCENTAGE
27.00	.1
34.65	.1
44.60	.0
57.40	3.4
74.45	.0
98.55	7.1
136.55	6.6
210.95	42.4
412.80	40.3

TABLE 5.17

SLURRY FLOWRATE: P3

DIAMETER (MICRONS)	WEIGHT PERCENTAGE
27.00	.1
34.65	.3
44.60	2.6
57.40	2.1
74.45	3.1
98.55	7.2
136.55	10.5
210.95	42.9
412.80	31.0

TABLE 5.18

SLURRY FLOWRATE: P4

DIAMETER (MICRONS)	WEIGHT PERCENTAGE
21.10	.1
27.00	.2
34.65	.0
44.60	3.0
57.40	2.4
74.45	3.7
98.55	8.0
136.55	8.1
210.95	46.6
412.80	28.0

TABLE 5.19

SLURRY FLOWRATE: P5

DIAMETER (MICRONS)	WEIGHT PERCENTAGE
21.10	.1
27.00	.2
34.65	.4
44.60	3.0
57.40	2.4
74.45	3.9
98.55	8.7
136.55	7.2
210.95	46.6
412.80	27.5

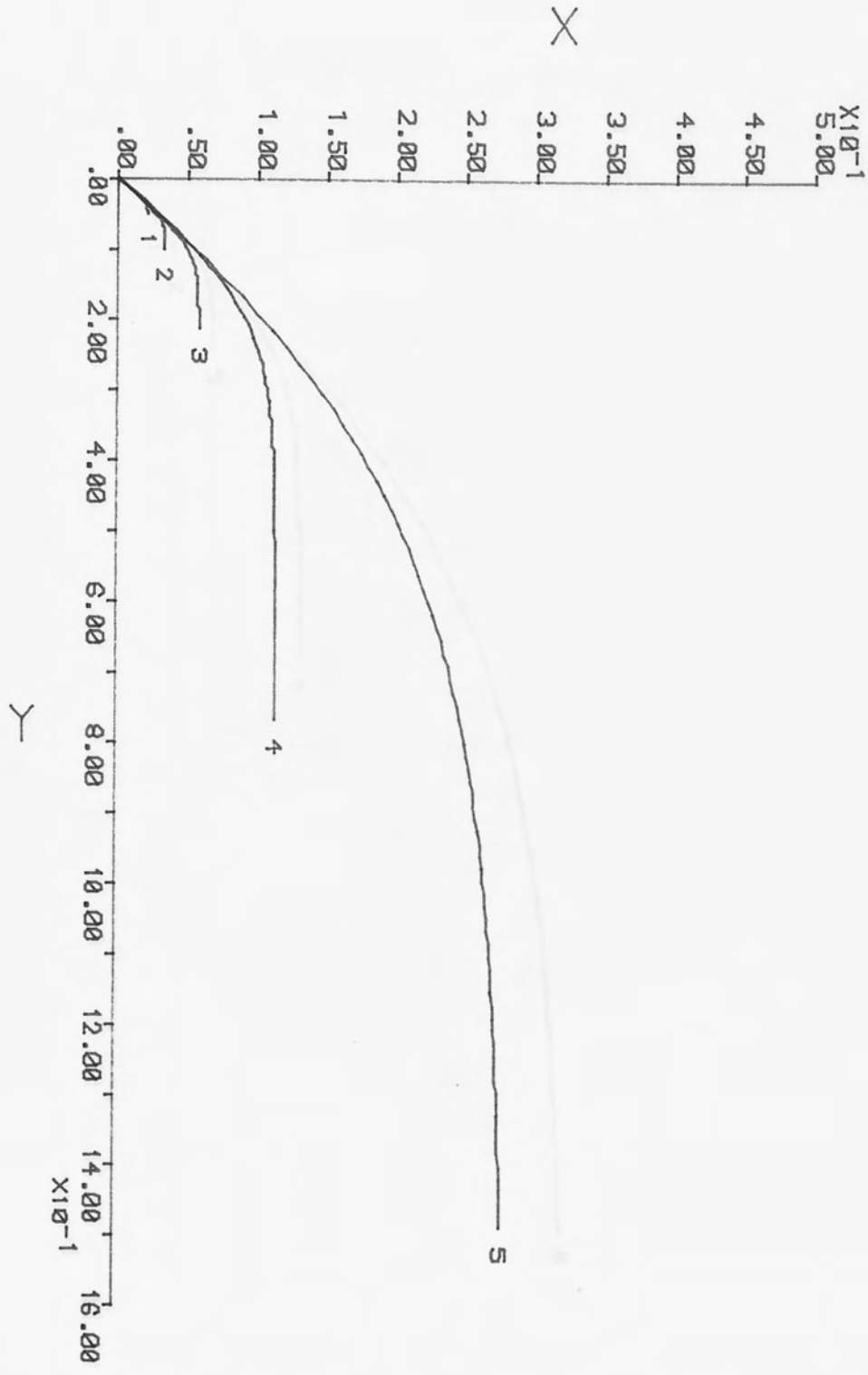

FIGURE 5.41 :PARTICILE TRAJECTORY - RUN CODE PARTICLE1

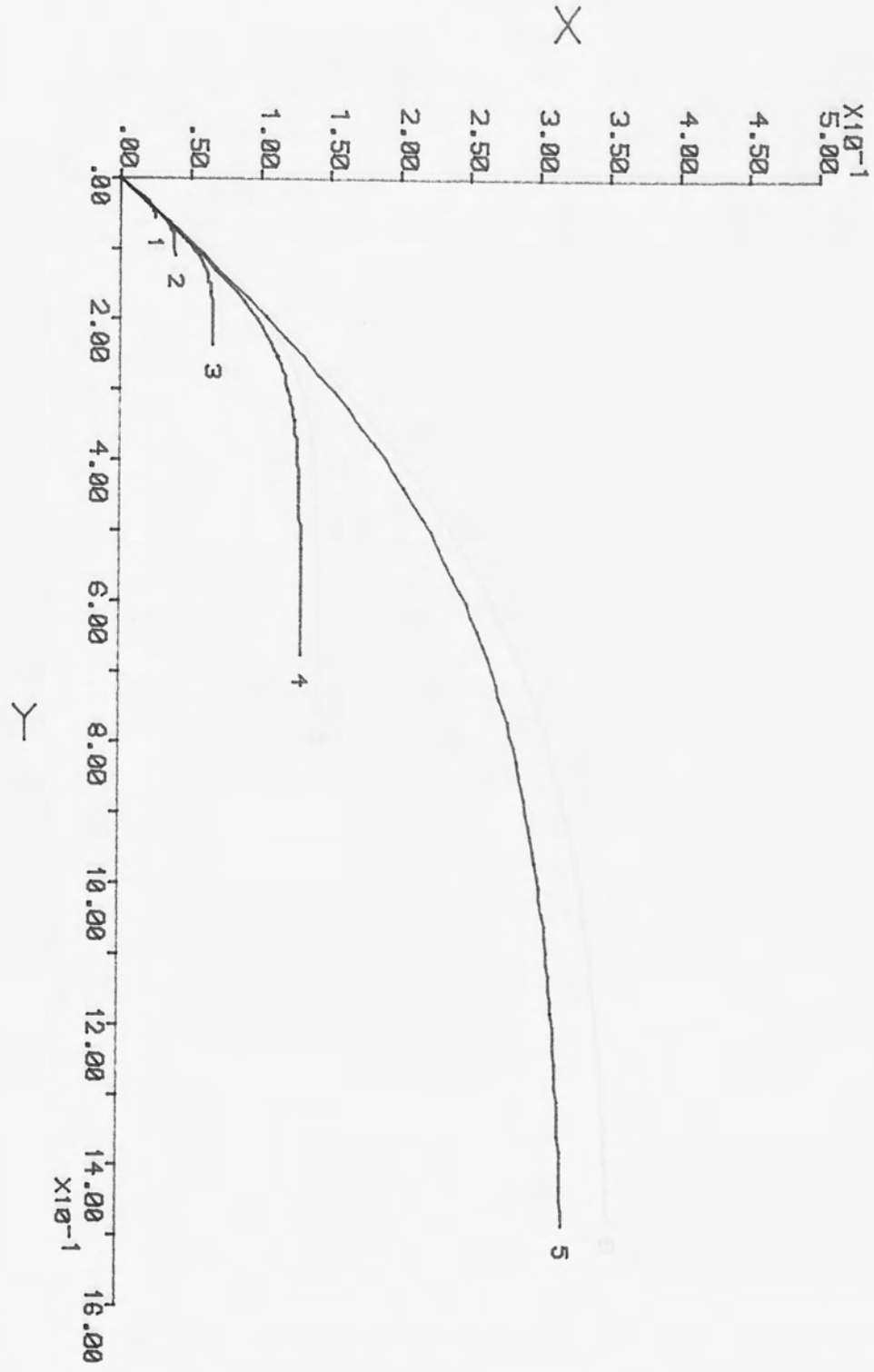

FIGURE 5.42 :PARTICILE TRAJECTORY - RUN CODE PARTICLE2

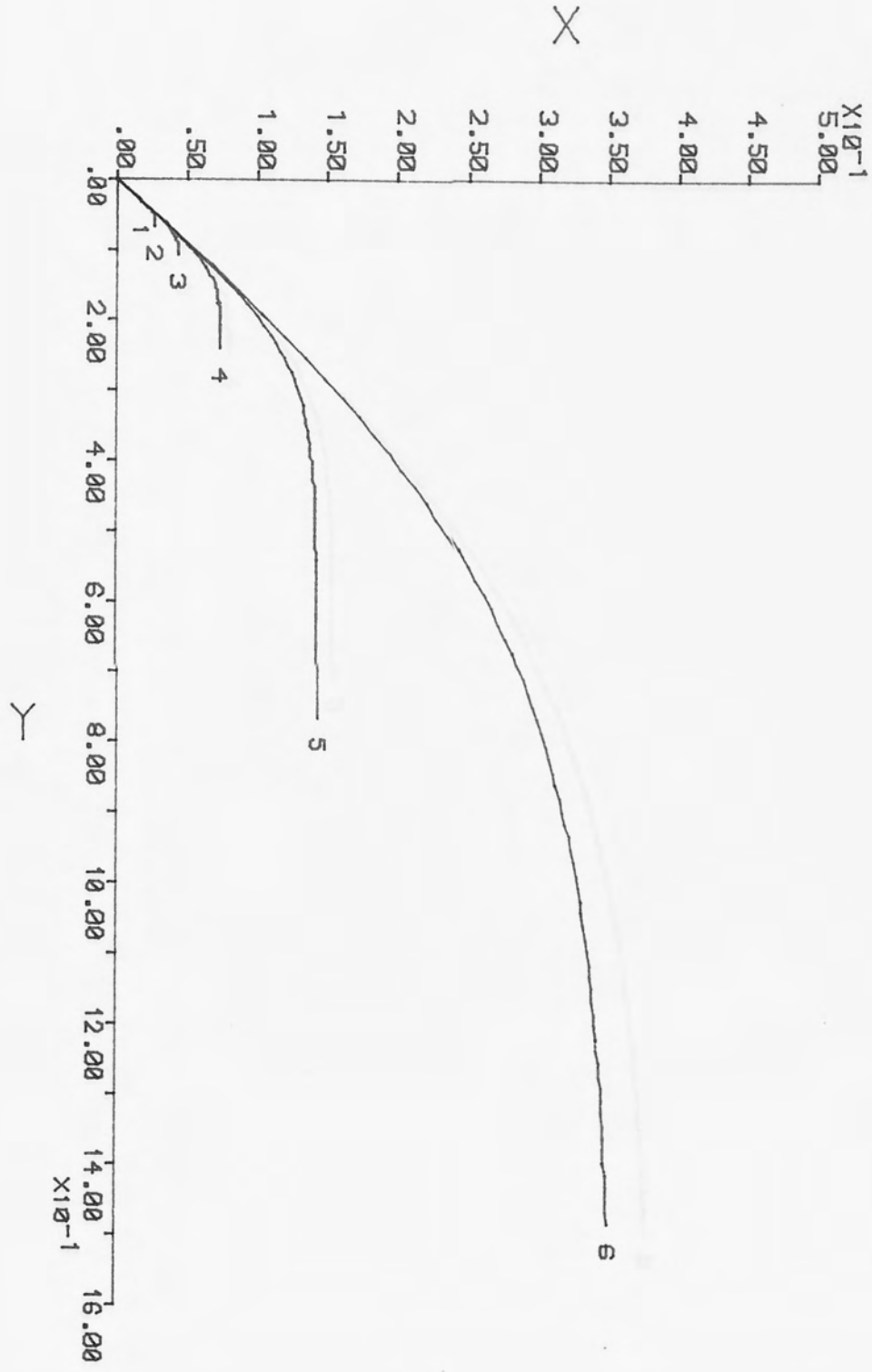

FIGURE 5.43 :PARTICILE TRAJECTORY - RUN CODE PARTICLE3

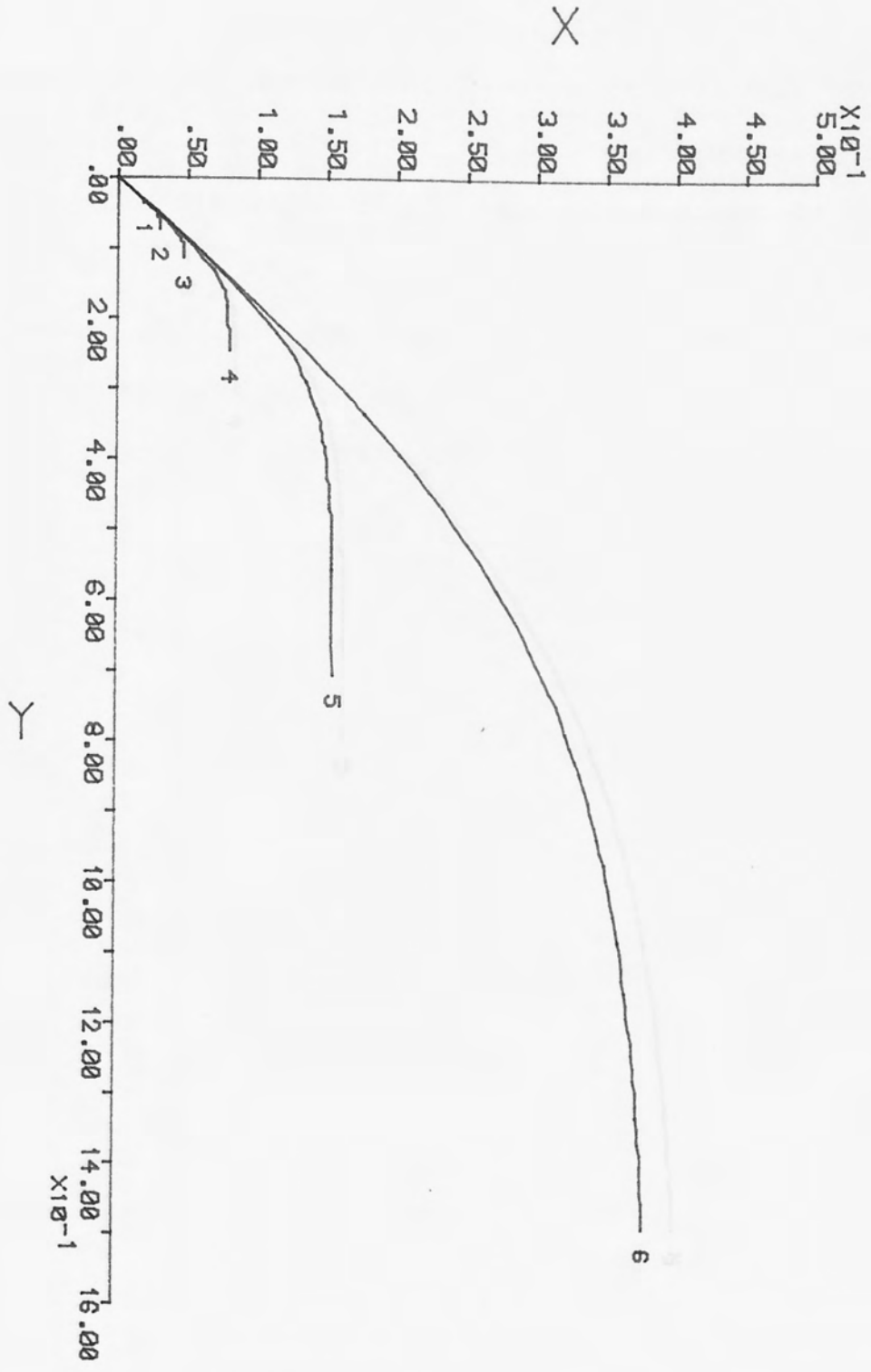

FIGURE 5.44 :PARTICILE TRAJECTORY - RUN CODE PARTICLE4

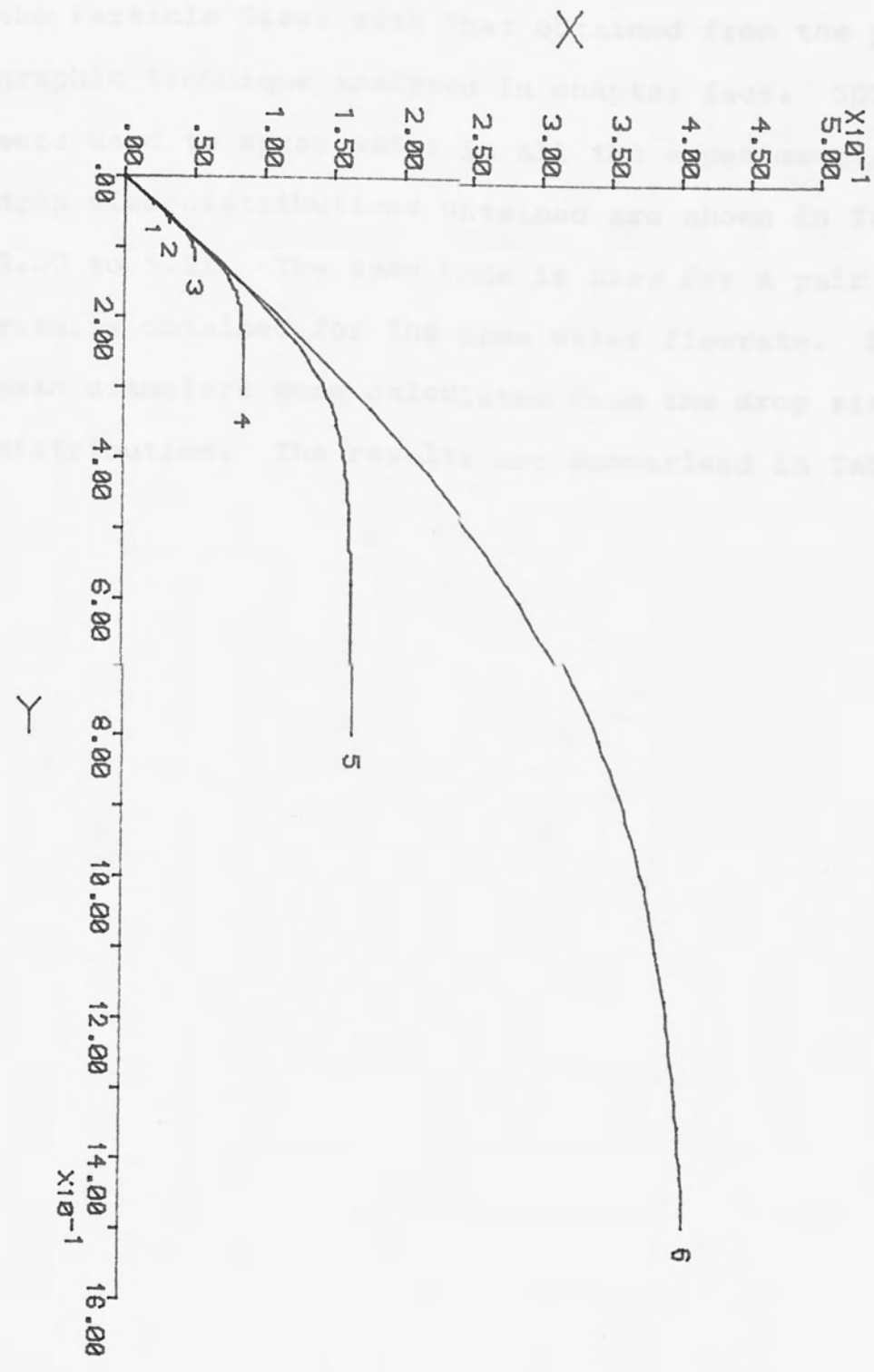

FIGURE 5.45 :PARTICILE TRAJECTORY - RUN CODE PARTICLE5

5.3 DROP SIZE DISTRIBUTION

The experiments carried out here were solely meant for comparing the drop size distribution obtained using the Particle Sizer with that obtained from the photographic technique analysed in chapter four. SDX nozzles were used to spray water in all the experiments. The drop size distributions obtained are shown in Table 5.20 to 5.21. The same code is used for a pair of results obtained for the same water flowrate. Sauter mean diameters were calculated from the drop size distribution. The results are summarised in Table 5.22.

DROP SIZE DISTRIBUTION RESULTS

PHOTOGRAPHIC METHOD

WEIGHT FREQUENCY	SIZE (MICRONS)																				
	40.0	54.4	68.8	84.0	98.4	113.6	128.0	142.4	157.6	172.0	187.2	201.6	216.0	231.2	245.6	260.8	275.2	289.6	304.8	319.2	334.4	348.8
D/2/3/2	.00	.93	10.05	14.86	11.02	14.13	16.17	.00	7.55	.00	25.30											
D/2/3/3	.31	6.56	31.17	16.81	7.60	7.60	6.56	23.03														
E/2/3/1	.48	.57	2.51	1.83	1.05	.97	.92	5.73	5.18	.00	4.34	8.03	22.21	8.17	9.88	.00	13.78	.00	6.24	7.17		
E/2/3/2	3.23	6.13	1.35	4.91	3.94	13.35	1.74	9.56	3.24	4.21	10.86	6.78	.00	30.69								
E/2/3/3	3.56	5.96	10.72	14.63	5.88	12.07	12.94	23.77	.00	10.47												
E/8/3/1	1.77	.59	1.18	1.73	1.39	2.13	1.53	.00	8.55	7.41	.00	29.81	7.33	.00	10.78	25.82						
E/9/3/2	7.49	4.06	5.13	3.11	4.50	8.46	9.90	9.09	16.43	8.01	3.44	8.60	5.29	6.49								
D/9/3/1/1	.65	2.39	3.50	3.67	1.71	1.91	4.45	5.18	3.83	4.98	4.28	12.02	6.57	6.04	2.42	.00	3.40	3.96	4.62	5.30	12.20	6.92
D/9/3/1/2	4.42	3.56	8.40	6.00	8.77	4.85	9.68	5.32	.00	4.69	6.04	.00	.00	22.76	.00	16.34						

TABLE 5.20

DROP SIZE DISTRIBUTION RESULTS

PARTICLE SIZE ANALYSER

SIZE	WEIGHT PERCENTAGE								
(MICRONS)	D/2/3/2	D/2/3/3	E/2/3/1	E/2/3/2	E/2/3/3	E/9/3/1	E/9/3/2	D/9/3/1/1	D/9/3/1/2
16.50							.1		
21.10	1.6	3.6		.1	2.1		.2		.1
27.00	.0	1.3		1.6	.8	.1	.4		1.4
34.65	2.0	4.2		.0	4.6	.2	2.8		.0
44.60	2.2	3.2		1.4	1.6	.5	2.5		.4
57.40	3.5	10.5	1.8	3.6	6.1	1.8	4.4	1.8	5.1
74.45	11.5	16.7	6.2	11.7	19.0	6.2	12.1	4.9	11.8
98.55	21.8	22.4	11.1	20.7	19.1	10.7	16.2	14.1	24.0
136.55	18.6	13.2	16.6	15.8	13.9	15.5	13.0	16.5	18.5
210.95	21.0	12.7	29.3	25.4	26.0	29.2	32.2	25.4	26.0
412.80	17.8	12.2	35.1	19.7	6.7	35.8	16.2	37.2	12.8

TABLE 5.21

TABLE 5.22

SAUTER MEAN DIAMETERS (MICRONS)

EXPERIMENTAL CODE	PARTICLE SIZER	PHOTOGRAPHIC
D/2/3/2	111.3	112.9
D/2/3/3	81.1	87.7
E/2/3/1	174.8	192.4
E/2/3/2	123.6	128.3
E/2/3/3	91.3	97.7
E/9/3/1	171.7	178.7
E/9/3/2	116.7	111.2
D/9/3/1/1	174.8	173.5
D/9/3/1/2	118.3	120.8

CHAPTER SIX

DISCUSSION

6.1 Droplets residence time distribution

6.2 Droplets trajectories

6.3 Drop size distribution

6.1 DROPLETS RESIDENCE TIME DISTRIBUTION

The graphs of the model and experimental data shown in Figures 5.1 to 5.40 and the variance between the model and experimental response data shown in Tables 5.1 to 5.8 illustrate that there is a very good fit between the model and experimental response data. As shown in Table 5.1 to 5.8, L = 0 and A + B = 1. This indicates that the droplets reside mainly in streams A and B, there being no flow in stream C (which equals to 1-A-B in Figure 3.1). The model results, RESIDENT 1, 2, 3 are for WMF spray nozzle and RESIDENTS 4, 5, 6, 7, 8 are for SDX spray nozzle. Each result is for one water flowrate and five different air flowrates which increase from top to bottom of the table.

For WMF results, parameter A remains constant for the first three air flowrates in each Table (except for the second where there is a decrease), increase in the fourth and then remains constant again in the fifth. This shows that as the air flowrate is increased more flow goes into the flow stream containing more mixing zones; ST11 and ST12 in Figure 3.1. In addition, the sum of the fractions, K, N and (I-J-K-M-N) also increases from the top to the bottom suggesting that the mixing is intensified as the air flowrate increases. In fact the decrease in A for the second air flowrate is made up for by high values of K, N and (I-J-K-M-N) in that row.

The same row (first, second etc) of Tables 5.1 to 5.3 are for the same air flowrate but different water flowrates. The values of A remain constant but the sum of the fractions K, N and (I-J-K-M-N) icreases from Table 5.1 to 5.3 showing that more droplets come into the mixing zones. This is to be expected because with increase in the feed flowrate, the spray cloud becomes denser with droplets which spread outwards into the mixing zone.

The values of A and B also remain virtually constant while the sum of K, N and (I-J-K-M-N) also increases from top to bottom in Tables 5.4 to 5.8. This is in agreement with the above conception that as the flowrate of air is increased, the intensity of mixing also increases. The sum of K, N, (I-J-K-M-N) also increase for the same row of Table 5.4 to 5.8 showing that more droplets come into the mixing zones with increase in the feed flowrates. However, unlike in Table 5.1 to 5.3, the trend in the values of A in Tables 5.4 to 5.8 is erratic. It decreases from the first row to the third, increases in the fourth and decreases in the fifth for each Table. This is accompanied by corresponding increase, decrease and increase in B. Incidentally when B increases, the proportion going into the plug flow zones also increase showing that less drops enter the 'active' mixing zones.

6.2 DROPLETS TRAJECTORIES

Each of the particle trajectories obtained is in agreement with theory that the velocity components in

both the horizontal and vertical directions decrease as the droplet traverses its path. The velocity of the particle decreases more rapidly in the horizontal than in the vertical direction (see PT1, PT2 etc). In all the trajectories the droplet attain a certain free falling velocity. This velocity and the time at which it takes place vary from droplet to droplet, but they increase with increasing size of droplets that start with the same initial velocity (compare PT1 - PT6, PT2 - PT10, etc). For a droplet projected with different initial velocities (PT1 and PT6, PT11, PT17 and PT23 etc), this velocity and time are virtually the same.

For drop size distribution measured for the same experimental condition (slurry flowrates) used in generating the particle trajectories, tables with the same slurry flowrate code (e.g. 5.10 and 5.15; 5.11 and 5.16 etc) show that droplets of smaller sizes were obtained at the second level (1.31 m) which is farther away from the nozzle. In addition the percentage by weight of the larger drops also decreases. This trend immediately raises the question of whether there is a prevalence of break up or fragmentation of some of the droplets on one hand and coalescence or agglomeration of some of the droplets on the other.

For fragmentation phenomenon, Levich (151) postulated that R_e must be greater than 10.0 before break up of the droplets could take place. Further

the critical diameter, d_{cr} above which fragmentation is likely can be developed from his equation given as follows:

$$\frac{K_f' \rho' U^2}{2} > \frac{3\sigma^3}{r_{cr}^3 \rho^2 U^4} \qquad (6.1)$$

$\rho' U'^2$ was said to be of the same order as ρU^2 and K_f' was of the order 0.5 for spherical drops. Using this information in (6.1) gives:

$$r_{cr} \approx \sqrt[3]{6}.\frac{\sigma}{\rho U^2} \qquad (6.2)$$

$$\text{i.e } d_{cr} \approx \frac{3.63\sigma}{U^2 \rho} \qquad (6.3)$$

For the smallest velocity V = 3.656 meter per second, and smallest droplet d = 74.45 microns

$$R_e = \frac{74.45 \times 10^{-6} \times 3.656 \times 1.2}{1.76 \times 10^{-5}} = 18.56$$

(Viscosity and density values from Table 4.7).
Also using V = U = 3.656 and the values of surface tension and density of the slurry from Table 4.7

$$d_{cr} = \frac{3.63 \times 0.0715}{3.656^2 \times 1040.0}$$

$$= 18.7 \times 10^{-6} m$$

$$= 18.7 \text{ microns.}$$

From the values for R_e and d_{cr}, it is possible for

fragmentation of the droplets to have taken place. A further conclusive way to show that fragmentation and coalescence took place would have been to capture the images of the drops over an interval of time on a video film at the two levels. But because of the small sizes of the droplets, this was not feasible at the time the experiments were conducted.

6.3 DROP SIZE DISTRIBUTION

For each pair of results (i.e. results with the same code), the drop size distribution obtained using particle sizer always contain droplets in size ranges lower and higher than those of photographic method. The reason for this is as follow - in trying to focus the big droplets, many smaller droplets are missed and when the emphasis is on the smaller droplets, the images of the larger droplets are often distorted. Therefore, one has to choose a standard depth of field based upon one's skill and judgement. Since this involves a compromise between leaving out some smaller droplets and including some but not all the large droplets, certain sizes are always sure to be missing.

In the case of particle size analyser, the laser beam permeates through the whole spectrum of drop sizes. Besides, one can always know within a short time after processing the results whether the sizes within the spray are well represented in the results because of the in-built estimates of errors within the processing program. When the errors are greater than the reasonable

tolerance allowed by the software, one has the choice either to repeat the experiment or choose a receiver lens of different focal length. Hence the results obtained in this case using the particle sizer are bound to be more reliable than the photographic method.

CHAPTER SEVEN

CONCLUSION

7.1 Droplets residence time distribution

7.2 Droplets trajectories

7.3 Drop size distribution

7.1 DROPLETS RESIDENCE TIME DISTRIBUTION

The results obtained in Chapter 5 show that at high water and air flowrates, more droplets enter the mixing zones. This conclusion was similar to those of AdeJohn and Jeffreys (60) and other workers who have studied the residence time distribution of air or hot gas. In contrast to Esubiyi (152) who used the same model (as used here) to analyse the residence time distribution of air; there is a conspicuous absence of the third stream C.

The results are also significant in that they are determined directly from the injection of the tracer into the feed stream rather than from the indirect inference from the residence time distribution of air or drying gas. The computer program for simulating the model is numeric and can be run in any computer language in an interactive mode. It can also be run on a top-desk mini computer.

7.2 DROPLETS TRAJECTORIES

The values obtained from the model of the particle trajectories of the droplets show that the droplets present initially at the point of ejection from the nozzle never hit the wall in the horizontal direction, but attain a free falling velocity after a time. This velocity and time are directly proportional to the diameter of the droplets. The drop size distribution of the droplets at two different levels differ, that

for the level farther away from the nozzle having droplets of smaller sizes than that nearer the nozzle. This is not supposed to be so as the values are obtained when drying is not actually taking place. There is either fragmentation of the drops, or fragmentation coupled with coalescence. Possibility of fragmentation is confirmed from the application of a formular developed by Levich.

7.3 DROP SIZE DISTRIBUTION

The results obtained using the particle sizer and the photographic method are close enough showing that the use of the particle size analyser in measuring the drop size distribution of droplets in a spray is very reliable. Due to the fact that the photographic method depends much on human judgement and skill which varies from individual to individual, it is difficult to quantify the errors in the drop size distribution of droplets in a spray where the depth of field is a very important factor. On the other hand, there are in-built tests which have to be satified within the various stages of the operation of the particle size analyser. Therefore the results obtained using the latter tend to be much more reliable and accurate than the photographic method.

CHAPTER EIGHT

RECOMMENDATION FOR FURTHER WORK

RECOMMENDATION FOR FURTHER WORK

1. There are few published data on droplets residence time distribution analysis in the literature. The work done here should be extended to residence time analysis of droplets of slurries and other solutions atomised at higher pressures.

2. The program used to simulate the tracer response is a modified form of that used earlier in this department for air residence time analysis. Further improvement can be done to it to reduce the iteration required to obtain the final parameters. In addition it can be modified for desk top computer application thereby making it easily usable in appropriate industries.

3. The experiments to obtain the drop size distribution of droplets when actual drying is taking place was hindered by misting and adherence of spray dust on the sampling windows. Means should be devised to remove this obstacle.

4. The particle size analyser used in the course of this work has been proved to be good in obtaining drop size distribution of sprayed droplets. Therefore provided (3) can be achieved, future work should concentrate on acquiring data during actual drying operations. Such data could then be used in a more rigorous spray design development than hitherto presented.

5. Instantaneous velocities at various levels are needed to confirm these values obtained from the model for particle trajectories. Future work on particle trajectories should embrace getting these velocities.

6. Space is critically needed to carry out the modifications required on the stainless steel spray drier for future experiments.

APPENDIX A

1. Droplets residence time distribution analysis - Code of the air and water flowrates used for response data, Tables FR1 and FR2.
2. Droplets residence time distribution analysis - Pulse data, Tables P1 to P8.
3. Droplets residence time distribution analysis - Experimental and model response data, Tables R1 to R40.

TABLE FR1

EXPERIMENTAL DATA	CODE	
	WATER	AIR
WMF1	W1	
WMF2	W1	A1
WMF3	W1	A2
WMF4	W1	A3
WMF5	W1	A4
WMF6	W1	A5
WMF7	W2	
WMF8	W2	A1
WMF9	W2	A2
WMF10	W2	A3
WMF11	W2	A4
WMF12	W2	A5
WMF13	W3	
WMF14	W3	A1
WMF15	W3	A2
WMF16	W3	A3
WMF17	W3	A4
WMF18	W3	A5
SDX19	W4	
SDX20	W4	A1
SDX21	W4	A2
SDX22	W4	A3
SDX23	W4	A4
SDX24	W4	A5

TABLE FR2

EXPERIMENTAL DATA	CODE	
	WATER	AIR
SDX25	W5	
SDX26	W5	A1
SDX27	W5	A2
SDX28	W5	A3
SDX29	W5	A4
SDX30	W5	A5
SDX31	W6	
SDX32	W6	A1
SDX33	W6	A2
SDX34	W6	A3
SDX35	W6	A4
SDX36	W6	A5
SDX37	W7	
SDX38	W7	A1
SDX39	W7	A2
SDX40	W7	A3
SDX41	W7	A4
SDX42	W7	A5
SDX43	W8	
SDX44	W8	A1
SDX45	W8	A2
SDX46	W8	A3
SDX47	W8	A4
SDX48	W8	A5

TABLE P1 : PULSE DATA (WMF1) FOR WMF2 - WMF6

TIME (S)	DIMENSIONLESS TIME (THETA)	EXIT CONCENTRATION (MICROMHO CM^{-1})
0	.000	.0
10	.108	3.0
20	.216	10.7
30	.324	22.0
40	.432	35.2
50	.539	40.5
60	.647	41.5
70	.755	39.8
80	.863	36.0
90	.971	30.5
100	1.079	27.5
110	1.187	25.0
120	1.295	22.0
130	1.403	18.4
140	1.510	16.5
150	1.618	13.5
160	1.726	13.0
170	1.834	11.8
180	1.942	10.2
190	2.050	8.6
200	2.158	8.2
210	2.266	7.8

TABLE P2 : PULSE DATA (WMF7) FOR WMF8 - WMF12

TIME (S)	DIMENSIONLESS TIME (THETA)	EXIT CONCENTRATION (MICROMHO CM^{-1})
0	.000	.0
10	.133	4.0
20	.266	17.0
30	.400	42.0
40	.533	56.4
50	.666	58.8
60	.799	50.0
70	.932	42.0
80	1.066	34.0
90	1.199	26.4
100	1.332	21.4
110	1.465	17.4
120	1.598	14.4
130	1.731	12.4
140	1.865	10.6
150	1.998	8.6
160	2.131	7.5
170	2.264	6.2
180	2.397	5.0
190	2.531	4.5
200	2.664	3.6
210	2.797	3.2

TABLE P3 : PULSE DATA (WMF13) FOR WMF14 - WMF18

TIME (S)	DIMENSIONLESS TIME (THETA)	EXIT CONCENTRATION (MICROMHO CM^{-1})
0	.000	.0
10	.156	5.0
20	.312	22.0
30	.467	42.0
40	.623	55.0
50	.779	53.0
60	.935	41.5
70	1.091	31.5
80	1.247	23.0
90	1.402	17.4
100	1.558	13.0
110	1.714	9.5
120	1.870	7.5
130	2.026	6.0
140	2.181	5.0
150	2.337	3.8
160	2.493	3.0
170	2.649	2.6
180	2.805	2.3
190	2.960	2.0
200	3.116	1.6
210	3.272	1.5

TABLE P4 : PULSE DATA (SDX19) FOR SDX20 - SDX24

TIME (S)	DIMENSIONLESS TIME (THETA)	EXIT CONCENTRATION (MICROMHO CM^{-1})
0	.000	.0
10	.138	5.0
20	.276	27.0
30	.414	50.0
40	.552	58.6
50	.690	53.0
60	.828	42.4
70	.966	34.0
80	1.104	27.0
90	1.242	21.6
100	1.380	17.0
110	1.518	14.0
120	1.656	11.0
130	1.794	9.4
140	1.932	7.6
150	2.070	6.5
160	2.208	5.8
170	2.346	5.0
180	2.484	4.4
190	2.622	4.0
200	2.760	3.2
210	2.898	3.0
220	3.035	2.6
230	3.173	2.5
240	3.311	2.2

TABLE P5 : PULSE DATA (SDX25) FOR SDX26 - SDX30

TIME (S)	DIMENSIONLESS TIME (THETA)	EXIT CONCENTRATION (MICROMHO CM^{-1})
0	.000	.0
10	.157	12.0
20	.314	50.0
30	.471	68.8
40	.628	59.4
50	.785	46.0
60	.942	35.5
70	1.100	26.5
80	1.257	21.0
90	1.414	16.4
100	1.571	13.0
110	1.728	11.0
120	1.885	9.0
130	2.042	7.5
140	2.199	6.5
150	2.356	5.5
160	2.513	4.6
170	2.670	4.0
180	2.827	3.5
190	2.984	3.2
200	3.142	2.8
210	3.299	2.4
220	3.456	2.2
230	3.613	2.0
240	3.770	1.8

TABLE P6 : PULSE DATA (SDX31) FOR SDX32 - SDX36

TIME (S)	DIMENSIONLESS TIME (THETA)	EXIT CONCENTRATION (MICROMHO CM^{-1})
0	.000	.0
10	.165	10.0
20	.329	47.5
30	.494	70.9
40	.658	57.7
50	.823	40.7
60	.987	30.7
70	1.152	22.5
80	1.316	17.5
90	1.481	14.0
100	1.645	11.5
110	1.810	9.5
120	1.974	8.0
130	2.139	6.5
140	2.303	5.0
150	2.468	4.5
160	2.632	3.7
170	2.797	3.3
180	2.962	2.7
190	3.126	2.5
200	3.291	2.0
210	3.455	1.9
220	3.620	1.5
230	3.784	1.5
240	3.949	1.5

TABLE P7 : PULSE DATA (SDX37) FOR SDX38 - SDX42

TIME (S)	DIMENSIONLESS TIME (THETA)	EXIT CONCENTRATION (MICROMHO CM^{-1})
0	.000	.0
10	.149	3.5
20	.298	19.0
30	.446	50.0
40	.595	59.0
50	.744	47.0
60	.893	35.8
70	1.041	25.0
80	1.190	17.5
90	1.339	16.0
100	1.488	12.0
110	1.637	9.5
120	1.785	7.5
130	1.934	6.5
140	2.083	5.2
150	2.232	4.5
160	2.380	4.0
170	2.529	3.0
180	2.678	2.8
190	2.827	2.4
200	2.976	2.0
210	3.124	2.0
220	3.273	1.8
230	3.422	1.6
240	3.571	1.4

TABLE P8 : PULSE DATA (SDX43) FOR SDX44 - SDX48

TIME (S)	DIMENSIONLESS TIME (THETA)	EXIT CONCENTRATION (MICROMHO CM^{-1})
0	.000	.0
10	.167	10.0
20	.333	34.0
30	.500	53.5
40	.667	48.5
50	.833	37.0
60	1.000	26.0
70	1.167	19.0
80	1.333	15.4
90	1.500	11.0
100	1.667	8.8
110	1.833	7.0
120	2.000	6.0
130	2.167	5.0
140	2.333	4.0
150	2.500	3.3
160	2.667	2.8
170	2.833	2.4
180	3.000	2.0
190	3.167	1.8
200	3.333	1.5
210	3.500	1.4
220	3.667	1.0
230	3.833	1.0
240	4.000	1.0

TABLE R1 : WMF2

TIME (S)	DIMENSIONLESS TIME (THETA)	EXIT CONCENTRATION (MICROMHO CM^{-1})	
		EXPERIMENTAL	MODEL
0	.000	.0	.0
10	.110	2.0	3.0
20	.219	11.5	10.6
30	.329	26.5	21.8
40	.439	37.9	35.0
50	.548	47.0	40.4
60	.658	49.9	41.5
70	.768	48.7	39.8
80	.877	44.5	36.1
90	.987	39.5	30.6
100	1.097	34.5	27.6
110	1.206	29.7	25.0
120	1.316	25.3	22.0
130	1.426	20.7	18.5
140	1.535	17.3	16.5
150	1.645	15.5	13.6
160	1.755	13.5	13.0
170	1.864	12.1	11.8
180	1.974	10.5	10.2
190	2.084	9.5	8.6
200	2.193	7.9	8.2
210	2.303	7.1	11.8

TABLE R2 : WMF3

TIME (S)	DIMENSIONLESS TIME (THETA)	EXIT CONCENTRATION (MICROMHO CM^{-1})	
		EXPERIMENTAL	MODEL
0	.000	.0	.0
10	.099	1.4	1.5
20	.198	6.2	6.1
30	.297	16.0	13.8
40	.396	26.5	24.5
50	.495	34.0	32.5
60	.595	39.0	37.1
70	.694	41.0	38.5
80	.793	40.2	37.7
90	.892	38.2	34.2
100	.991	35.5	30.9
110	1.090	32.0	28.0
120	1.189	28.0	25.0
130	1.288	24.8	21.7
140	1.387	21.5	19.1
150	1.486	19.4	16.4
160	1.586	16.3	14.7
170	1.685	14.0	13.3
180	1.784	12.8	11.8
190	1.883	11.3	10.2
200	1.982	10.0	9.2
210	2.081	9.0	10.2

TABLE R3 : WMF4

TIME (S)	DIMENSIONLESS TIME (THETA)	EXIT CONCENTRATION (MICROMHO CM^{-1})	
		EXPERIMENTAL	MODEL
0	.000	.0	.0
10	.100	1.2	1.6
20	.200	6.0	6.4
30	.300	15.5	14.7
40	.400	28.0	26.0
50	.500	36.2	34.3
60	.600	42.6	38.5
70	.700	44.2	39.5
80	.799	43.0	38.1
90	.899	40.4	34.1
100	.999	36.0	30.4
110	1.099	32.5	27.3
120	1.199	28.5	24.4
130	1.299	24.8	21.1
140	1.399	21.0	18.5
150	1.499	18.5	15.8
160	1.599	16.5	14.2
170	1.699	14.4	12.8
180	1.799	13.2	11.4
190	1.899	11.6	9.9
200	1.999	10.0	8.9
210	2.099	9.0	10.5

TABLE R4 : WMF5

TIME (S)	DIMENSIONLESS TIME (THETA)	EXIT CONCENTRATION (MICROMHO CM^{-1})	
		EXPERIMENTAL	MODEL
0	.000	.0	.0
10	.104	.8	1.9
20	.208	6.8	7.3
30	.312	18.3	16.6
40	.416	33.7	28.5
50	.520	42.1	36.2
60	.624	46.7	39.6
70	.728	47.7	39.8
80	.832	45.8	37.9
90	.936	42.0	33.4
100	1.040	37.3	29.7
110	1.144	31.5	26.8
120	1.248	27.8	23.8
130	1.352	23.7	20.5
140	1.457	19.8	17.9
150	1.561	16.8	15.2
160	1.665	14.5	13.8
170	1.769	12.8	12.5
180	1.873	11.5	11.1
190	1.977	9.9	9.5
200	2.081	9.3	8.7
210	2.185	8.8	12.0

TABLE R5 : WMF6

TIME (S)	DIMENSIONLESS TIME (THETA)	EXIT CONCENTRATION (MICROMHO CM^{-1})	
		EXPERIMENTAL	MODEL
0	.000	.0	.0
10	.099	1.0	1.5
20	.198	6.7	5.9
30	.298	16.2	13.8
40	.397	28.0	24.8
50	.496	36.0	33.1
60	.595	42.7	37.6
70	.694	44.2	39.0
80	.793	43.2	38.0
90	.893	41.0	34.5
100	.992	37.4	30.9
110	1.091	33.3	27.9
120	1.190	30.2	25.0
130	1.289	27.2	21.7
140	1.388	23.2	19.0
150	1.488	20.5	16.3
160	1.587	18.6	14.5
170	1.686	15.3	13.1
180	1.785	13.2	11.7
190	1.884	12.0	10.1
200	1.983	10.0	9.1
210	2.083	8.6	11.5

TABLE R6 : WMF8

TIME (S)	DIMENSIONLESS TIME (THETA)	EXIT CONCENTRATION (MICROMHO CM^{-1})	
		EXPERIMENTAL	MODEL
0	.000	.0	.0
10	.120	2.6	2.2
20	.240	13.4	9.8
30	.360	28.8	27.1
40	.481	45.4	43.8
50	.601	54.0	52.8
60	.721	54.0	52.0
70	.841	48.9	46.8
80	.961	41.9	39.9
90	1.081	33.8	32.3
100	1.201	28.4	26.1
110	1.322	23.0	21.2
120	1.442	19.4	17.4
130	1.562	15.4	14.5
140	1.682	13.2	12.3
150	1.802	11.4	10.2
160	1.922	9.6	8.7
170	2.043	8.2	7.3
180	2.163	7.4	6.0
190	2.283	6.4	5.1
200	2.403	5.4	4.3
210	2.523	4.9	5.1

TABLE R7 : WMF9

TIME (S)	DIMENSIONLESS TIME (THETA)	EXIT CONCENTRATION (MICROMHO CM^{-1})	
		EXPERIMENTAL	MODEL
0	.000	.0	.0
10	.109	2.0	1.8
20	.217	9.5	8.1
30	.326	23.5	22.0
40	.434	35.0	34.2
50	.543	42.0	41.8
60	.651	44.0	42.7
70	.760	43.0	41.0
80	.868	39.5	37.9
90	.977	35.4	33.7
100	1.085	31.7	29.6
110	1.194	27.0	25.6
120	1.302	23.6	21.9
130	1.411	20.8	18.9
140	1.519	17.4	16.2
150	1.628	14.6	13.8
160	1.736	12.5	11.8
170	1.845	11.0	10.0
180	1.953	9.6	8.3
190	2.062	9.2	7.1
200	2.170	7.2	6.0
210	2.279	6.4	6.6

TABLE RB : WMF10

TIME (S)	DIMENSIONLESS TIME (THETA)	EXIT CONCENTRATION (MICROMHO CM^{-1})	
		EXPERIMENTAL	MODEL
0	.000	.0	.0
10	.112	3.5	2.0
20	.224	12.0	8.5
30	.336	23.0	23.4
40	.448	38.0	36.9
50	.561	43.0	45.6
60	.673	43.5	48.8
70	.785	41.0	44.5
80	.897	36.0	40.1
90	1.009	32.4	34.2
100	1.121	28.4	28.7
110	1.233	26.5	24.0
120	1.345	21.0	19.9
130	1.457	17.5	16.8
140	1.570	14.6	14.2
150	1.682	12.4	11.9
160	1.794	11.0	10.0
170	1.906	10.0	8.5
180	2.018	9.0	7.0
190	2.130	7.6	6.0
200	2.242	7.0	5.0
210	2.354	6.0	6.6

TABLE R9 : WMF11

TIME (S)	DIMENSIONLESS TIME (THETA)	EXIT CONCENTRATION (MICROMHO CM^{-1})	
		EXPERIMENTAL	MODEL
0	.000	.0	.0
10	.105	2.0	1.2
20	.210	6.6	5.2
30	.315	22.6	16.3
40	.420	32.0	29.3
50	.525	42.0	39.7
60	.631	45.4	44.5
70	.736	42.8	44.5
80	.841	39.0	42.2
90	.946	35.0	36.9
100	1.051	31.0	31.7
110	1.156	29.0	26.6
120	1.261	25.5	22.4
130	1.366	22.0	19.0
140	1.471	18.6	16.1
150	1.576	16.0	13.6
160	1.682	15.0	11.5
170	1.787	12.6	9.8
180	1.892	11.0	8.2
190	1.997	10.0	7.0
200	2.102	8.5	5.9
210	2.207	7.5	5.7

TABLE R10 : WMF12

TIME (S)	DIMENSIONLESS TIME (THETA)	EXIT CONCENTRATION (MICROMHO CM^{-1})	
		EXPERIMENTAL	MODEL
0	.000	.0	.0
10	.109	1.8	1.7
20	.217	8.0	7.8
30	.326	25.6	21.2
40	.434	38.5	35.7
50	.543	46.5	45.1
60	.652	48.6	47.0
70	.760	46.6	45.4
80	.869	42.5	41.0
90	.977	38.0	35.1
100	1.086	33.0	29.4
110	1.194	28.6	24.5
120	1.303	25.0	20.4
130	1.412	23.0	17.2
140	1.520	18.6	14.8
150	1.629	15.5	12.4
160	1.737	13.6	10.5
170	1.846	11.5	8.8
180	1.955	10.0	7.4
190	2.063	9.4	6.3
200	2.172	8.2	5.3
210	2.280	7.0	5.1

TABLE R11 : WMF14

TIME (S)	DIMENSIONLESS TIME (THETA)	EXIT CONCENTRATION (MICROMHO CM^{-1})	
		EXPERIMENTAL	MODEL
0	.000	.0	.0
10	.121	2.0	1.7
20	.243	10.0	8.6
30	.364	25.0	20.2
40	.485	37.4	33.6
50	.607	44.0	41.9
60	.728	45.0	42.9
70	.850	40.5	39.3
80	.971	35.4	33.8
90	1.092	29.8	27.9
100	1.214	25.0	22.1
110	1.335	20.2	17.2
120	1.456	16.6	13.4
130	1.578	13.6	10.5
140	1.699	10.4	8.3
150	1.821	8.8	6.5
160	1.942	7.5	5.1
170	2.063	6.0	4.1
180	2.185	5.2	3.4
190	2.306	4.4	2.8
200	2.427	4.0	2.4
210	2.549	3.4	2.4

TABLE R12 : WMF15

TIME (S)	DIMENSIONLESS TIME (THETA)	EXIT CONCENTRATION (MICROMHO CM^{-1})	
		EXPERIMENTAL	MODEL
0	.000	.0	.0
10	.131	4.5	3.0
20	.263	14.2	13.4
30	.394	28.0	27.3
40	.525	39.0	38.1
50	.656	42.0	40.5
60	.788	38.5	36.5
70	.919	32.0	31.6
80	1.050	27.8	26.8
90	1.182	23.0	22.7
100	1.313	19.4	19.0
110	1.444	14.5	15.8
120	1.575	10.5	13.3
130	1.707	9.0	11.2
140	1.838	8.4	9.5
150	1.969	7.0	7.9
160	2.101	5.5	6.6
170	2.232	4.6	5.6
180	2.363	4.2	4.8
190	2.494	3.5	4.1
200	2.626	2.6	3.4
210	2.757	2.2	4.6

TABLE R13 : WMF16

TIME (S)	DIMENSIONLESS TIME (THETA)	EXIT CONCENTRATION (MICROMHO CM^{-1})	
		EXPERIMENTAL	MODEL
0	.000	.0	.0
10	.124	2.0	2.3
20	.249	12.0	10.4
30	.373	22.8	23.2
40	.498	37.0	35.2
50	.622	42.6	40.6
60	.747	42.3	39.2
70	.871	37.8	35.3
80	.996	30.4	30.2
90	1.120	25.5	25.3
100	1.245	21.0	20.9
110	1.369	16.4	17.0
120	1.494	13.6	13.8
130	1.618	11.6	11.2
140	1.743	10.0	9.2
150	1.867	8.0	7.4
160	1.992	6.6	5.9
170	2.116	5.8	4.8
180	2.241	4.6	4.0
190	2.365	3.6	3.4
200	2.490	3.5	2.8
210	2.614	2.5	3.4

TABLE R14 : WMF17

TIME (S)	DIMENSIONLESS TIME (THETA)	EXIT CONCENTRATION (MICROMHO CM^{-1})	
		EXPERIMENTAL	MODEL
0	.000	.0	.0
10	.124	2.6	2.0
20	.249	10.5	9.4
30	.373	24.0	22.3
40	.497	37.0	35.0
50	.622	43.4	42.2
60	.746	44.2	42.3
70	.871	40.5	38.1
80	.995	35.0	32.4
90	1.119	28.5	26.5
100	1.244	23.8	21.4
110	1.368	18.2	16.9
120	1.492	15.0	13.2
130	1.617	11.8	10.3
140	1.741	10.0	8.2
150	1.865	8.0	6.6
160	1.990	6.5	5.2
170	2.114	5.0	4.2
180	2.238	4.2	3.5
190	2.363	3.8	2.9
200	2.487	3.2	2.4
210	2.612	3.0	2.8

TABLE R15 : WMF18

TIME (S)	DIMENSIONLESS TIME (THETA)	EXIT CONCENTRATION (MICROMHO CM^{-1})	
		EXPERIMENTAL	MODEL
0	.000	.0	.0
10	.118	.5	1.6
20	.236	5.0	7.0
30	.354	11.5	17.4
40	.472	28.9	30.9
50	.590	39.0	40.1
60	.708	42.5	42.6
70	.826	41.9	39.7
80	.944	36.5	34.3
90	1.062	31.3	28.2
100	1.180	26.0	22.7
110	1.298	21.3	17.8
120	1.416	16.9	13.8
130	1.534	12.5	10.8
140	1.652	10.0	8.5
150	1.770	7.7	6.7
160	1.888	5.9	5.3
170	2.006	4.9	4.2
180	2.124	3.9	3.5
190	2.242	3.3	2.9
200	2.360	2.9	2.4
210	2.478	2.0	2.4

TABLE R16 : SDX20

TIME (S)	DIMENSIONLESS TIME (THETA)	EXIT CONCENTRATION (MICROMHO CM^{-1})	
		EXPERIMENTAL	MODEL
0	.000	.0	.0
10	.124	3.4	3.0
20	.248	18.0	16.6
30	.372	40.0	36.6
40	.496	58.0	50.4
50	.620	63.0	52.6
60	.744	56.5	47.4
70	.868	47.0	39.4
80	.992	38.0	31.8
90	1.116	31.5	25.6
100	1.240	26.0	20.4
110	1.365	21.0	16.5
120	1.489	15.6	13.1
130	1.613	14.0	10.9
140	1.737	11.6	8.9
150	1.861	10.4	7.4
160	1.985	9.0	6.5
170	2.109	7.4	5.8
180	2.233	6.4	4.9
190	2.357	5.5	4.3
200	2.481	4.6	3.7
210	2.605	4.2	3.3
220	2.729	3.6	2.9
230	2.853	3.4	2.6
240	2.977	3.0	.7

TABLE R17 : SDX21

TIME (S)	DIMENSIONLESS TIME (THETA)	EXIT CONCENTRATION (MICROMHO CM^{-1})	
		EXPERIMENTAL	MODEL
0	.000	.0	.0
10	.127	7.4	2.8
20	.254	21.0	15.8
30	.381	38.0	34.8
40	.508	49.5	47.7
50	.635	53.0	50.4
60	.762	49.5	46.2
70	.889	42.0	39.3
80	1.017	35.0	32.6
90	1.144	28.0	26.7
100	1.271	23.0	21.3
110	1.398	18.6	17.4
120	1.525	15.5	14.0
130	1.652	13.0	11.6
140	1.779	10.6	9.5
150	1.906	9.0	7.9
160	2.033	7.6	6.8
170	2.160	6.5	5.9
180	2.287	5.4	5.1
190	2.414	4.5	4.5
200	2.541	4.0	3.8
210	2.668	3.4	3.4
220	2.795	2.8	3.0
230	2.922	2.5	2.7
240	3.050	2.0	1.3

TABLE R18 : SDX22

TIME (S)	DIMENSIONLESS TIME (THETA)	EXIT CONCENTRATION (MICROMHO CM^{-1})	
		EXPERIMENTAL	MODEL
0	.000	.0	.0
10	.121	3.5	2.7
20	.242	17.0	15.0
30	.363	35.4	34.1
40	.484	52.5	48.0
50	.605	57.8	51.6
60	.726	54.0	47.7
70	.847	46.8	40.2
80	.968	38.0	33.0
90	1.089	30.5	26.6
100	1.210	25.0	21.3
110	1.331	20.5	17.2
120	1.452	17.0	13.7
130	1.573	14.5	11.2
140	1.694	12.0	9.2
150	1.815	10.2	7.7
160	1.936	8.6	6.6
170	2.057	7.5	5.7
180	2.178	6.5	5.0
190	2.299	5.5	4.4
200	2.420	5.0	3.8
210	2.541	4.5	3.3
220	2.662	4.0	2.9
230	2.783	3.5	2.7
240	2.904	3.4	4.4

TABLE R19 : SDX23

TIME (S)	DIMENSIONLESS TIME (THETA)	EXIT CONCENTRATION (MICROMHO CM^{-1})	
		EXPERIMENTAL	MODEL
0	.000	.0	.0
10	.123	6.6	2.9
20	.245	21.0	16.5
30	.368	35.0	34.8
40	.491	55.0	48.5
50	.613	58.4	51.3
60	.736	54.5	46.8
70	.859	46.0	39.5
80	.982	38.5	32.4
90	1.104	31.0	26.4
100	1.227	25.0	21.1
110	1.350	21.0	17.1
120	1.472	17.0	13.7
130	1.595	14.2	11.3
140	1.718	12.0	9.2
150	1.840	10.0	7.7
160	1.963	8.5	6.7
170	2.086	7.4	5.7
180	2.208	6.5	5.0
190	2.331	5.8	4.4
200	2.454	5.2	3.8
210	2.576	4.6	3.3
220	2.699	4.0	2.9
230	2.822	3.6	2.7
240	2.945	3.2	1.3

TABLE R20 : SDX24

TIME (S)	DIMENSIONLESS TIME (THETA)	EXIT CONCENTRATION (MICROMHO CM^{-1})	
		EXPERIMENTAL	MODEL
0	.000	.0	.0
10	.124	6.4	3.3
20	.249	22.0	18.0
30	.373	41.0	38.0
40	.498	55.0	51.4
50	.622	58.0	52.6
60	.746	54.0	47.1
70	.871	45.0	38.7
80	.995	37.5	31.4
90	1.120	30.0	25.1
100	1.244	25.0	20.0
110	1.368	21.0	16.1
120	1.493	17.0	12.9
130	1.617	14.0	10.7
140	1.742	11.5	8.7
150	1.866	10.0	7.3
160	1.990	8.5	6.4
170	2.115	7.2	5.5
180	2.239	6.2	4.8
190	2.364	5.5	4.3
200	2.488	4.8	3.6
210	2.612	4.5	3.2
220	2.737	4.0	2.8
230	2.861	3.5	2.6
240	2.986	3.0	1.0

TABLE R21 : SDX26

TIME (S)	DIMENSIONLESS TIME (THETA)	EXIT CONCENTRATION (MICROMHO CM^{-1})	
		EXPERIMENTAL	MODEL
0	.000	.0	.0
10	.140	13.0	7.1
20	.279	34.4	30.8
30	.419	47.4	52.5
40	.559	51.4	56.5
50	.698	48.4	50.2
60	.838	40.4	41.8
70	.977	32.4	32.9
80	1.117	26.8	26.0
90	1.257	21.9	20.6
100	1.396	18.0	16.4
110	1.536	14.6	13.4
120	1.676	11.9	10.9
130	1.815	9.6	9.0
140	1.955	8.4	7.6
150	2.094	7.0	6.5
160	2.234	6.4	5.4
170	2.374	5.4	4.6
180	2.513	4.4	4.0
190	2.653	3.9	3.6
200	2.793	3.4	3.1
210	2.932	2.8	2.7
220	3.072	2.4	2.4
230	3.211	1.9	2.2
240	3.351	1.6	1.8

TABLE R22 : SDX27

TIME (S)	DIMENSIONLESS TIME (THETA)	EXIT CONCENTRATION (MICROMHO CM^{-1})	
		EXPERIMENTAL	MODEL
0	.000	.0	.0
10	.118	2.0	4.7
20	.236	12.2	20.4
30	.354	31.0	38.4
40	.472	49.0	46.6
50	.590	53.5	46.8
60	.708	49.0	43.6
70	.826	42.0	37.6
80	.945	34.6	31.3
90	1.063	28.5	25.8
100	1.181	23.5	21.0
110	1.299	19.6	17.3
120	1.417	16.5	14.3
130	1.535	14.0	11.8
140	1.653	12.0	9.9
150	1.771	10.4	8.3
160	1.889	8.5	7.0
170	2.007	7.5	5.9
180	2.125	6.2	5.1
190	2.243	5.5	4.4
200	2.361	5.0	3.8
210	2.479	4.5	3.3
220	2.597	4.0	2.9
230	2.715	3.5	2.6
240	2.834	3.0	1.9

TABLE R23 : SDX28

TIME (S)	DIMENSIONLESS TIME (THETA)	EXIT CONCENTRATION (MICROMHO CM^{-1})	
		EXPERIMENTAL	MODEL
0	.000	.0	.0
10	.119	2.5	4.6
20	.237	15.0	20.1
30	.356	35.0	37.7
40	.475	50.0	46.2
50	.593	51.6	46.5
60	.712	47.5	43.6
70	.831	41.0	37.6
80	.949	35.0	31.4
90	1.068	29.0	26.0
100	1.187	24.0	21.3
110	1.305	19.5	17.6
120	1.424	16.5	14.5
130	1.543	14.2	12.0
140	1.661	12.2	10.0
150	1.780	10.0	8.4
160	1.899	9.0	7.0
170	2.017	7.8	6.0
180	2.136	6.8	5.1
190	2.255	5.8	4.4
200	2.374	5.0	3.8
210	2.492	4.5	3.3
220	2.611	4.0	2.9
230	2.730	3.6	2.6
240	2.848	3.0	2.0

TABLE R24 : SDX29

TIME (S)	DIMENSIONLESS TIME (THETA)	EXIT CONCENTRATION (MICROMHO CM^{-1})	
		EXPERIMENTAL	MODEL
0	.000	.0	.0
10	.117	4.5	4.3
20	.233	17.0	19.7
30	.350	35.0	36.9
40	.466	47.0	45.3
50	.583	50.2	46.5
60	.699	47.0	43.8
70	.816	41.5	37.8
80	.932	37.0	31.9
90	1.049	32.0	26.6
100	1.165	26.0	21.9
110	1.282	21.0	18.1
120	1.398	17.5	14.9
130	1.515	15.0	12.2
140	1.631	12.6	10.2
150	1.748	11.0	8.6
160	1.864	10.0	7.2
170	1.981	8.4	6.1
180	2.097	7.2	5.2
190	2.214	6.5	4.5
200	2.330	5.8	3.9
210	2.447	5.0	3.4
220	2.563	4.4	3.0
230	2.680	4.0	2.7
240	2.796	3.5	2.1

TABLE R25 : SDX30

TIME (S)	DIMENSIONLESS TIME (THETA)	EXIT CONCENTRATION (MICROMHO CM^{-1})	
		EXPERIMENTAL	MODEL
0	.000	.0	.0
10	.116	4.5	4.3
20	.233	20.0	20.4
30	.349	38.0	37.0
40	.466	47.6	45.2
50	.582	50.2	46.2
60	.698	47.0	43.3
70	.815	43.0	37.9
80	.931	36.0	32.2
90	1.048	30.0	26.8
100	1.164	25.4	22.0
110	1.280	22.4	18.1
120	1.397	19.5	15.0
130	1.513	16.4	12.4
140	1.630	14.0	10.4
150	1.746	11.5	8.7
160	1.862	10.0	7.3
170	1.979	8.5	6.2
180	2.095	7.6	5.3
190	2.212	6.6	4.6
200	2.328	6.0	4.0
210	2.444	5.2	3.4
220	2.561	4.5	3.0
230	2.677	4.0	2.7
240	2.794	4.0	2.0

TABLE R26 : SDX32

TIME (S)	DIMENSIONLESS TIME (THETA)	EXIT CONCENTRATION (MICROMHO CM^{-1})	
		EXPERIMENTAL	MODEL
0	.000	.0	.0
10	.137	7.2	5.0
20	.273	23.0	25.7
30	.410	47.0	47.8
40	.546	58.0	53.2
50	.683	54.4	47.7
60	.820	43.0	39.6
70	.956	34.0	31.3
80	1.093	27.4	24.5
90	1.229	21.0	19.3
100	1.366	17.0	15.4
110	1.503	13.6	12.5
120	1.639	11.5	10.3
130	1.776	9.6	8.5
140	1.912	8.0	6.8
150	2.049	6.6	5.6
160	2.185	6.0	4.7
170	2.322	5.0	4.0
180	2.459	4.5	3.4
190	2.595	3.8	3.0
200	2.732	3.5	2.5
210	2.868	3.0	2.2
220	3.005	2.6	1.9
230	3.142	2.5	1.7
240	3.278	2.4	1.1

TABLE R27 : SDX33

TIME (S)	DIMENSIONLESS TIME (THETA)	EXIT CONCENTRATION (MICROMHO CM^{-1})	
		EXPERIMENTAL	MODEL
0	.000	.0	.0
10	.123	1.4	4.2
20	.246	10.5	19.5
30	.369	30.0	40.6
40	.492	47.0	47.8
50	.615	52.6	46.0
60	.738	49.4	39.9
70	.861	41.0	33.1
80	.984	33.0	26.9
90	1.107	27.0	21.6
100	1.229	21.0	17.5
110	1.352	17.0	14.2
120	1.475	14.0	11.6
130	1.598	11.5	9.5
140	1.721	9.4	7.8
150	1.844	8.0	6.4
160	1.967	6.8	5.3
170	2.090	5.8	4.5
180	2.213	5.0	3.8
190	2.336	4.0	3.2
200	2.459	3.8	2.7
210	2.582	3.5	2.4
220	2.705	3.0	2.0
230	2.828	2.8	1.8
240	2.951	2.6	1.3

TABLE R28 : SDX34

TIME (S)	DIMENSIONLESS TIME (THETA)	EXIT CONCENTRATION (MICROMHO CM^{-1})	
		EXPERIMENTAL	MODEL
0	.000	.0	.0
10	.130	5.0	4.2
20	.259	20.2	21.1
30	.389	43.2	43.2
40	.519	54.8	51.4
50	.648	54.0	48.8
60	.778	47.0	41.6
70	.907	38.0	33.4
80	1.037	31.5	26.2
90	1.167	25.0	20.5
100	1.296	20.0	16.4
110	1.426	17.0	13.2
120	1.556	14.0	10.8
130	1.685	11.6	8.9
140	1.815	9.0	7.2
150	1.945	8.0	6.0
160	2.074	7.0	5.0
170	2.204	6.0	4.2
180	2.333	5.0	3.6
190	2.463	4.2	3.1
200	2.593	4.0	2.6
210	2.722	3.5	2.3
220	2.852	3.0	2.0
230	2.982	2.6	1.7
240	3.111	2.5	1.0

TABLE R29 : SDX35

TIME (S)	DIMENSIONLESS TIME (THETA)	EXIT CONCENTRATION (MICROMHO CM^{-1})	
		EXPERIMENTAL	MODEL
0	.000	.0	.0
10	.140	8.6	4.9
20	.279	30.1	24.9
30	.419	47.1	46.6
40	.559	53.6	52.2
50	.699	49.6	47.3
60	.838	41.6	39.5
70	.978	33.6	31.4
80	1.118	26.6	24.9
90	1.257	21.6	19.9
100	1.397	17.8	16.0
110	1.537	14.4	13.0
120	1.677	11.2	10.7
130	1.816	9.1	8.8
140	1.956	7.6	7.1
150	2.096	6.6	5.9
160	2.235	5.6	4.9
170	2.375	4.6	4.2
180	2.515	4.2	3.5
190	2.655	3.6	3.0
200	2.794	3.1	2.6
210	2.934	2.6	2.3
220	3.074	2.6	1.9
230	3.213	1.9	1.7
240	3.353	1.6	1.0

TABLE R30 : SDX36

TIME (S)	DIMENSIONLESS TIME (THETA)	EXIT CONCENTRATION (MICROMHO CM^{-1})	
		EXPERIMENTAL	MODEL
0	.000	.0	.0
10	.130	6.5	4.4
20	.260	23.5	22.5
30	.390	42.5	42.9
40	.521	47.1	49.4
50	.651	51.0	46.4
60	.781	43.5	40.0
70	.911	36.0	32.7
80	1.041	29.9	26.3
90	1.171	24.6	21.2
100	1.301	21.0	17.2
110	1.432	16.5	14.1
120	1.562	13.1	11.6
130	1.692	11.0	9.5
140	1.822	9.3	7.7
150	1.952	8.0	6.4
160	2.082	6.5	5.3
170	2.213	5.7	4.5
180	2.343	5.0	3.7
190	2.473	4.5	3.2
200	2.603	4.0	2.7
210	2.733	3.5	2.4
220	2.863	2.0	2.0
230	2.993	2.5	1.8
240	3.124	2.1	1.4

TABLE R31 : SDX38

TIME (S)	DIMENSIONLESS TIME (THETA)	EXIT CONCENTRATION (MICROMHO CM^{-1})	
		EXPERIMENTAL	MODEL
0	.000	.0	.0
10	.127	1.6	1.6
20	.253	11.0	8.3
30	.380	31.0	27.0
40	.507	45.0	41.7
50	.633	48.0	44.5
60	.760	41.0	41.2
70	.887	34.0	34.1
80	1.013	27.0	26.7
90	1.140	21.5	21.8
100	1.267	17.4	17.4
110	1.393	14.0	13.9
120	1.520	11.0	11.1
130	1.647	8.8	9.0
140	1.773	7.6	7.3
150	1.900	6.5	6.1
160	2.027	5.5	5.1
170	2.153	5.0	4.2
180	2.280	4.4	3.6
190	2.407	4.0	3.1
200	2.533	3.2	2.6
210	2.660	3.0	2.3
220	2.787	2.6	2.1
230	2.913	2.3	1.9
240	3.040	2.0	1.2

TABLE R32 : SDX39

TIME (S)	DIMENSIONLESS TIME (THETA)	EXIT CONCENTRATION (MICROMHO CM^{-1})	
		EXPERIMENTAL	MODEL
0	.000	.0	.0
10	.141	8.3	2.2
20	.282	23.8	12.6
30	.423	40.1	35.7
40	.564	47.2	49.0
50	.705	44.8	46.9
60	.846	36.8	39.8
70	.986	28.8	31.2
80	1.127	23.8	23.2
90	1.268	19.2	19.2
100	1.409	14.8	15.1
110	1.550	11.6	11.9
120	1.691	9.3	9.5
130	1.832	7.8	7.8
140	1.973	6.3	6.3
150	2.114	5.4	5.3
160	2.255	4.8	4.6
170	2.396	4.0	3.7
180	2.537	3.4	3.2
190	2.678	3.0	2.8
200	2.818	2.3	2.3
210	2.959	2.0	2.1
220	3.100	1.8	1.9
230	3.241	1.8	1.7
240	3.382	1.6	2.4

TABLE R33 : SDX40

TIME (S)	DIMENSIONLESS TIME (THETA)	EXIT CONCENTRATION (MICROMHO CM^{-1})	
		EXPERIMENTAL	MODEL
0	.000	.0	.0
10	.127	5.6	1.5
20	.254	17.0	7.7
30	.381	31.5	25.4
40	.508	40.5	39.4
50	.635	41.6	43.0
60	.762	39.4	40.0
70	.889	34.2	34.3
80	1.016	27.5	27.4
90	1.143	22.4	22.7
100	1.270	18.2	18.3
110	1.397	14.8	14.?
120	1.524	12.0	11.8
130	1.651	10.0	9.6
140	1.778	8.5	7.9
150	1.904	7.0	6.5
160	2.031	5.6	5.5
170	2.158	5.0	4.5
180	2.285	4.2	3.8
190	2.412	3.8	3.2
200	2.539	3.2	2.7
210	2.666	3.0	2.4
220	2.793	2.5	2.2
230	2.920	2.3	2.0
240	3.047	2.0	1.5

TABLE R34 : SDX41

TIME (S)	DIMENSIONLESS TIME (THETA)	EXIT CONCENTRATION (MICROMHO CM^{-1})	
		EXPERIMENTAL	MODEL
0	.000	.0	.0
10	.126	4.2	1.7
20	.252	20.3	9.7
30	.378	34.2	28.3
40	.505	39.5	42.6
50	.631	41.6	44.7
60	.757	37.6	40.4
70	.883	32.2	33.5
80	1.009	27.0	26.1
90	1.135	22.6	21.4
100	1.261	18.6	17.0
110	1.388	15.2	13.6
120	1.514	12.8	10.8
130	1.640	10.5	8.9
140	1.766	8.4	7.2
150	1.892	7.2	6.0
160	2.018	6.2	5.1
170	2.144	5.2	4.2
180	2.270	4.6	3.6
190	2.397	4.0	3.1
200	2.523	3.5	2.6
210	2.649	3.0	2.3
220	2.775	2.8	2.1
230	2.901	2.5	1.9
240	3.027	2.0	1.2

TABLE R35 : SDX42

TIME (S)	DIMENSIONLESS TIME (THETA)	EXIT CONCENTRATION (MICROMHO CM^{-1})	
		EXPERIMENTAL	MODEL
0	.000	.0	.0
10	.120	2.5	1.5
20	.240	13.0	8.4
30	.360	27.5	25.1
40	.480	39.3	38.7
50	.600	43.0	42.2
60	.720	39.6	39.6
70	.840	33.8	34.2
80	.961	28.2	27.7
90	1.081	22.8	23.1
100	1.201	19.5	18.7
110	1.321	15.8	15.1
120	1.441	13.0	12.2
130	1.561	11.0	10.0
140	1.681	9.0	8.2
150	1.801	8.0	6.8
160	1.921	6.6	5.7
170	2.041	6.0	4.7
180	2.161	5.0	4.0
190	2.281	4.4	3.4
200	2.401	4.0	2.9
210	2.521	3.5	2.5
220	2.641	3.0	2.3
230	2.761	3.0	2.0
240	2.882	2.5	1.5

TABLE R36 : SDX44

TIME (S)	DIMENSIONLESS TIME (THETA)	EXIT CONCENTRATION (MICROMHO CM^{-1})	
		EXPERIMENTAL	MODEL
0	.000	.0	.0
10	.135	5.7	4.7
20	.271	16.0	17.8
30	.406	30.6	34.9
40	.542	42.4	42.1
50	.677	44.2	40.4
60	.813	38.8	34.4
70	.948	32.4	27.1
80	1.084	25.0	21.4
90	1.219	19.0	16.5
100	1.354	15.0	12.8
110	1.490	11.5	9.9
120	1.625	9.0	8.0
130	1.761	7.5	6.6
140	1.896	6.2	5.4
150	2.032	5.2	4.4
160	2.167	4.4	3.6
170	2.303	3.8	3.0
180	2.438	3.0	2.6
190	2.573	2.6	2.2
200	2.709	2.2	1.9
210	2.844	2.0	1.6
220	2.980	2.0	1.4
230	3.115	2.0	1.2
240	3.251	1.7	.7

TABLE R37 : SDX45

TIME (S)	DIMENSIONLESS TIME (THETA)	EXIT CONCENTRATION (MICROMHO CM^{-1})	
		EXPERIMENTAL	MODEL
0	.000	.0	.0
10	.126	2.0	4.5
20	.252	11.5	16.0
30	.378	27.5	31.7
40	.504	39.2	38.9
50	.630	42.8	37.9
60	.756	39.2	35.3
70	.882	33.0	28.2
80	1.008	26.6	22.8
90	1.134	21.2	17.9
100	1.260	15.6	14.0
110	1.386	13.2	11.0
120	1.512	11.0	8.9
130	1.638	9.0	7.3
140	1.764	7.5	5.9
150	1.890	6.2	4.8
160	2.016	5.4	4.0
170	2.142	4.5	3.3
180	2.268	4.0	2.8
190	2.394	3.4	2.4
200	2.520	3.0	2.0
210	2.646	2.6	1.8
220	2.772	2.4	1.4
230	2.898	2.0	1.2
240	3.024	2.0	.9

TABLE R38 : SDX46

TIME (S)	DIMENSIONLESS TIME (THETA)	EXIT CONCENTRATION (MICROMHO CM^{-1})	
		EXPERIMENTAL	MODEL
0	.000	.0	.0
10	.140	7.0	4.5
20	.280	13.6	17.0
30	.421	38.6	33.7
40	.561	43.6	41.4
50	.701	41.0	40.7
60	.841	35.2	34.6
70	.981	29.0	27.6
80	1.122	23.1	21.8
90	1.262	17.8	16.9
100	1.402	13.2	12.9
110	1.542	10.6	10.1
120	1.682	8.6	8.1
130	1.822	7.2	6.6
140	1.963	5.6	5.4
150	2.103	4.8	4.4
160	2.243	4.0	3.6
170	2.383	3.4	3.0
180	2.523	2.6	2.6
190	2.664	2.2	2.2
200	2.804	2.1	1.9
210	2.944	1.8	1.7
220	3.084	1.8	1.4
230	3.224	1.6	1.2
240	3.365	1.2	.6

TABLE R39 : SDX47

TIME (S)	DIMENSIONLESS TIME (THETA)	EXIT CONCENTRATION (MICROMHO CM^{-1})	
		EXPERIMENTAL	MODEL
0	.000	.0	.0
10	.126	3.5	4.4
20	.251	15.0	16.4
30	.377	29.0	32.5
40	.503	38.0	40.8
50	.628	40.0	40.2
60	.754	36.5	34.9
70	.880	31.4	27.6
80	1.006	25.0	21.9
90	1.131	20.0	16.8
100	1.257	16.0	13.1
110	1.383	12.8	10.2
120	1.508	10.2	8.3
130	1.634	9.2	6.8
140	1.760	8.0	5.6
150	1.885	7.0	4.5
160	2.011	5.5	3.7
170	2.137	5.0	3.1
180	2.262	4.0	2.6
190	2.388	3.5	2.2
200	2.514	3.0	1.9
210	2.639	3.0	1.7
220	2.765	2.6	1.4
230	2.891	2.2	1.2
240	3.017	2.2	.7

TABLE R40 : SDX48

TIME (S)	DIMENSIONLESS TIME (THETA)	EXIT CONCENTRATION (MICROMHO CM^{-1})	
		EXPERIMENTAL	MODEL
0	.000	.0	.0
10	.126	5.0	4.5
20	.253	19.0	17.4
30	.379	31.5	32.8
40	.506	38.2	39.6
50	.632	39.8	38.3
60	.759	37.0	34.1
70	.885	32.0	27.7
80	1.012	26.5	22.6
90	1.138	21.0	17.8
100	1.265	16.5	13.9
110	1.391	14.0	11.1
120	1.518	11.5	9.0
130	1.644	9.2	7.4
140	1.771	8.0	6.0
150	1.897	6.6	4.9
160	2.024	5.8	4.0
170	2.150	5.0	3.4
180	2.277	4.2	2.8
190	2.403	3.8	2.4
200	2.530	3.4	2.0
210	2.656	3.2	1.8
220	2.783	2.8	1.5
230	2.909	2.5	1.3
240	3.036	2.2	.9

APPENDIX B

Droplet Trajectories - Tables PT1 - PT28

TABLE PT1

DIAMETER =74.45 MICRONS
SLURRY FLOWRATE=P1
PLOT CODE=1

TIME (S)	VELOCITY (M/S) HORIZONTAL	VERTICAL	RESULTANT	DISTANCE (M) HORIZONTAL	VERTICAL
0.00	1.828	3.166	3.656	0.0000	0.0000
0.01	0.691	1.261	1.438	0.0116	0.0204
0.02	0.311	0.636	0.708	0.0163	0.0294
0.03	0.154	0.386	0.416	0.0185	0.0344
0.04	0.081	0.275	0.286	0.0197	0.0376
0.05	0.043	0.221	0.225	0.0203	0.0400
0.06	0.024	0.193	0.195	0.0206	0.0421
0.07	0.013	0.179	0.180	0.0208	0.0439
0.08	0.007	0.172	0.172	0.0209	0.0457
0.09	0.004	0.169	0.169	0.0209	0.0474
0.10	0.002	0.167	0.167	0.0209	0.0491
0.11	0.001	0.166	0.166	0.0210	0.0507
0.12	0.001	0.165	0.165	0.0210	0.0524
0.13	0.000	0.165	0.165	0.0210	0.0540
0.14	0.000	0.165	0.165	0.0210	0.0557
0.15	0.000	0.165	0.165	0.0210	0.0573
0.16	0.000	0.165	0.165	0.0210	0.0590
0.17	0.000	0.165	0.165	0.0210	0.0606
0.18	0.000	0.165	0.165	0.0210	0.0623
0.19	0.000	0.165	0.165	0.0210	0.0639
0.20	0.000	0.165	0.165	0.0210	0.0656
0.21	0.000	0.165	0.165	0.0210	0.0672
0.22	0.000	0.165	0.165	0.0210	0.0689
0.23	0.000	0.165	0.165	0.0210	0.0705
0.24	0.000	0.165	0.165	0.0210	0.0721
0.25	0.000	0.165	0.165	0.0210	0.0738
0.26	0.000	0.165	0.165	0.0210	0.0754
0.27	0.000	0.165	0.165	0.0210	0.0771
0.28	0.000	0.165	0.165	0.0210	0.0787
0.29	0.000	0.165	0.165	0.0210	0.0804
0.30	0.000	0.165	0.165	0.0210	0.0820
0.31	0.000	0.165	0.165	0.0210	0.0837
0.32	0.000	0.165	0.165	0.0210	0.0853
0.33	0.000	0.165	0.165	0.0210	0.0869
0.34	0.000	0.165	0.165	0.0210	0.0886
0.35	0.000	0.165	0.165	0.0210	0.0902
0.36	0.000	0.165	0.165	0.0210	0.0919
0.37	0.000	0.165	0.165	0.0210	0.0935
0.38	0.000	0.165	0.165	0.0210	0.0952
0.39	0.000	0.165	0.165	0.0210	0.0968
0.40	0.000	0.165	0.165	0.0210	0.0985
0.41	0.000	0.165	0.165	0.0210	0.1001
0.42	0.000	0.165	0.165	0.0210	0.1018

TABLE PT2

DIAMETER =98.55 MICRONS

SLURRY FLOWRATE=P1

PLOT CODE=2

TIME (S)	VELOCITY (M/S) HORIZONTAL	VERTICAL	RESULTANT	DISTANCE (M) HORIZONTAL	VERTICAL
0.00	1.828	3.166	3.656	0.0000	0.0000
0.01	0.971	1.755	2.005	0.0133	0.0235
0.02	0.573	1.111	1.250	0.0210	0.0377
0.03	0.348	0.754	0.830	0.0254	0.0468
0.04	0.222	0.560	0.603	0.0282	0.0533
0.05	0.145	0.446	0.470	0.0300	0.0582
0.06	0.097	0.379	0.391	0.0312	0.0623
0.07	0.066	0.338	0.344	0.0320	0.0659
0.08	0.045	0.312	0.315	0.0326	0.0691
0.09	0.031	0.295	0.297	0.0329	0.0722
0.10	0.021	0.285	0.286	0.0332	0.0751
0.11	0.015	0.278	0.278	0.0334	0.0779
0.12	0.010	0.273	0.274	0.0335	0.0806
0.13	0.007	0.271	0.271	0.0336	0.0834
0.14	0.005	0.269	0.269	0.0336	0.0860
0.15	0.003	0.267	0.267	0.0337	0.0887
0.16	0.002	0.267	0.267	0.0337	0.0914
0.17	0.002	0.266	0.266	0.0337	0.0941
0.18	0.001	0.266	0.266	0.0337	0.0967
0.19	0.001	0.265	0.265	0.0338	0.0994
0.20	0.001	0.265	0.265	0.0338	0.1020
0.21	0.000	0.265	0.265	0.0338	0.1047
0.22	0.000	0.265	0.265	0.0338	0.1073
0.23	0.000	0.265	0.265	0.0338	0.1100
0.24	0.000	0.265	0.265	0.0338	0.1126
0.25	0.000	0.265	0.265	0.0338	0.1153
0.26	0.000	0.265	0.265	0.0338	0.1179
0.27	0.000	0.265	0.265	0.0338	0.1206
0.28	0.000	0.265	0.265	0.0338	0.1232
0.29	0.000	0.265	0.265	0.0338	0.1259
0.30	0.000	0.265	0.265	0.0338	0.1285
0.31	0.000	0.265	0.265	0.0338	0.1312
0.32	0.000	0.265	0.265	0.0338	0.1338
0.33	0.000	0.265	0.265	0.0338	0.1365
0.34	0.000	0.265	0.265	0.0338	0.1391
0.35	0.000	0.265	0.265	0.0338	0.1418
0.36	0.000	0.265	0.265	0.0338	0.1444
0.37	0.000	0.265	0.265	0.0338	0.1471
0.38	0.000	0.265	0.265	0.0338	0.1497
0.39	0.000	0.265	0.265	0.0338	0.1524
0.40	0.000	0.265	0.265	0.0338	0.1550
0.41	0.000	0.265	0.265	0.0338	0.1577
0.42	0.000	0.265	0.265	0.0338	0.1603

TABLE PT3

DIAMETER =136.55 MICRONS
SLURRY FLOWRATE=P1
PLOT CODE=3

TIME (S)	VELOCITY (M/S) HORIZONTAL	VERTICAL	RESULTANT	DISTANCE (M) HORIZONTAL	VERTICAL
0.00	1.828	3.166	3.656	0.0000	0.0000
0.01	1.227	2.206	2.525	0.0150	0.0264
0.02	0.867	1.642	1.856	0.0253	0.0454
0.03	0.640	1.296	1.446	0.0328	0.0600
0.04	0.492	1.083	1.189	0.0384	0.0718
0.05	0.379	0.921	0.996	0.0427	0.0819
0.06	0.280	0.764	0.814	0.0460	0.0902
0.07	0.216	0.676	0.709	0.0485	0.0974
0.08	0.169	0.616	0.639	0.0504	0.1038
0.09	0.133	0.572	0.588	0.0519	0.1097
0.10	0.105	0.539	0.549	0.0531	0.1153
0.11	0.083	0.513	0.520	0.0540	0.1205
0.12	0.066	0.494	0.498	0.0547	0.1256
0.13	0.052	0.479	0.481	0.0553	0.1304
0.14	0.041	0.467	0.469	0.0558	0.1352
0.15	0.033	0.459	0.460	0.0561	0.1398
0.16	0.026	0.452	0.453	0.0564	0.1443
0.17	0.021	0.447	0.447	0.0567	0.1488
0.18	0.016	0.443	0.443	0.0569	0.1533
0.19	0.013	0.440	0.440	0.0570	0.1577
0.20	0.010	0.438	0.438	0.0571	0.1621
0.21	0.008	0.436	0.436	0.0572	0.1665
0.22	0.007	0.435	0.435	0.0573	0.1708
0.23	0.005	0.434	0.434	0.0573	0.1752
0.24	0.004	0.433	0.433	0.0574	0.1795
0.25	0.003	0.433	0.433	0.0574	0.1838
0.26	0.003	0.432	0.432	0.0575	0.1881
0.27	0.002	0.432	0.432	0.0575	0.1925
0.28	0.002	0.432	0.432	0.0575	0.1968
0.29	0.001	0.432	0.432	0.0575	0.2011
0.30	0.001	0.431	0.431	0.0575	0.2054
0.31	0.001	0.431	0.431	0.0575	0.2097
0.32	0.001	0.431	0.431	0.0576	0.2140
0.33	0.001	0.431	0.431	0.0576	0.2184
0.34	0.000	0.431	0.431	0.0576	0.2227
0.35	0.000	0.431	0.431	0.0576	0.2270
0.36	0.000	0.431	0.431	0.0576	0.2313
0.37	0.000	0.431	0.431	0.0576	0.2356
0.38	0.000	0.431	0.431	0.0576	0.2399
0.39	0.000	0.431	0.431	0.0576	0.2442
0.40	0.000	0.431	0.431	0.0576	0.2485
0.41	0.000	0.431	0.431	0.0576	0.2528
0.42	0.000	0.431	0.431	0.0576	0.2572

TABLE PT4

DIAMETER =210.95 MICRONS
SLURRY FLOWRATE=P1
PLOT CODE=4

TIME (S)	VELOCITY (M/S) HORIZONTAL	VERTICAL	RESULTANT	DISTANCE (M) HORIZONTAL	VERTICAL
0.00	1.828	3.166	3.656	0.0000	0.0000
0.01	1.482	2.656	3.042	0.0165	0.0290
0.02	1.221	2.278	2.585	0.0299	0.0536
0.03	1.019	1.990	2.236	0.0411	0.0748
0.04	0.859	1.767	1.964	0.0504	0.0936
0.05	0.729	1.591	1.750	0.0584	0.1103
0.06	0.624	1.451	1.580	0.0651	0.1255
0.07	0.536	1.340	1.443	0.0709	0.1395
0.08	0.464	1.250	1.333	0.0759	0.1524
0.09	0.403	1.177	1.245	0.0802	0.1645
0.10	0.352	1.119	1.173	0.0840	0.1760
0.11	0.308	1.072	1.115	0.0873	0.1869
0.12	0.270	1.033	1.068	0.0902	0.1974
0.13	0.238	1.002	1.030	0.0927	0.2076
0.14	0.210	0.977	0.999	0.0949	0.2175
0.15	0.186	0.957	0.975	0.0969	0.2272
0.16	0.165	0.940	0.954	0.0987	0.2366
0.17	0.146	0.927	0.938	0.1002	0.2460
0.18	0.130	0.916	0.925	0.1016	0.2552
0.19	0.116	0.907	0.915	0.1028	0.2643
0.20	0.103	0.900	0.906	0.1039	0.2733
0.21	0.092	0.894	0.899	0.1049	0.2823
0.22	0.082	0.890	0.893	0.1058	0.2912
0.23	0.073	0.886	0.889	0.1065	0.3001
0.24	0.065	0.883	0.885	0.1072	0.3089
0.25	0.058	0.880	0.882	0.1078	0.3178
0.26	0.052	0.878	0.880	0.1084	0.3266
0.27	0.046	0.877	0.878	0.1089	0.3353
0.28	0.041	0.875	0.876	0.1093	0.3441
0.29	0.037	0.874	0.875	0.1097	0.3528
0.30	0.033	0.873	0.874	0.1101	0.3616
0.31	0.029	0.873	0.873	0.1104	0.3703
0.32	0.026	0.872	0.873	0.1106	0.3790
0.33	0.023	0.872	0.872	0.1109	0.3878
0.34	0.021	0.871	0.872	0.1111	0.3965
0.35	0.019	0.871	0.871	0.1113	0.4052
0.36	0.017	0.871	0.871	0.1115	0.4139
0.37	0.015	0.871	0.871	0.1116	0.4226
0.38	0.013	0.870	0.871	0.1118	0.4313
0.39	0.012	0.870	0.870	0.1119	0.4400
0.40	0.011	0.870	0.870	0.1120	0.4487
0.41	0.010	0.870	0.870	0.1121	0.4574
0.42	0.008	0.870	0.870	0.1122	0.4661

TABLE PT5

DIAMETER =412.80 MICRONS

SLURRY FLOWRATE=P1

PLOT CODE=5

TIME (S)	VELOCITY (M/S) HORIZONTAL	VERTICAL	RESULTANT	DISTANCE (M) HORIZONTAL	VERTICAL
0.00	1.828	3.166	3.656	0.0000	0.0000
0.01	1.688	3.018	3.458	0.0176	0.0309
0.02	1.562	2.887	3.282	0.0338	0.0604
0.03	1.448	2.771	3.127	0.0488	0.0887
0.04	1.345	2.668	2.988	0.0628	0.1159
0.05	1.251	2.577	2.865	0.0758	0.1421
0.06	1.166	2.496	2.755	0.0879	0.1675
0.07	1.088	2.424	2.657	0.0991	0.1921
0.08	1.017	2.359	2.569	0.1096	0.2160
0.09	0.951	2.301	2.490	0.1195	0.2393
0.10	0.890	2.250	2.419	0.1287	0.2620
0.11	0.834	2.203	2.356	0.1373	0.2843
0.12	0.783	2.162	2.299	0.1454	0.3061
0.13	0.735	2.124	2.248	0.1530	0.3275
0.14	0.690	2.090	2.201	0.1601	0.3486
0.15	0.649	2.060	2.160	0.1668	0.3693
0.16	0.610	2.033	2.122	0.1731	0.3898
0.17	0.574	2.008	2.088	0.1790	0.4100
0.18	0.540	1.985	2.058	0.1846	0.4300
0.19	0.509	1.965	2.030	0.1898	0.4497
0.20	0.480	1.947	2.005	0.1947	0.4693
0.21	0.452	1.930	1.982	0.1994	0.4887
0.22	0.426	1.915	1.962	0.2038	0.5079
0.23	0.402	1.901	1.944	0.2079	0.5270
0.24	0.379	1.889	1.927	0.2118	0.5459
0.25	0.358	1.878	1.912	0.2155	0.5647
0.26	0.338	1.868	1.898	0.2190	0.5835
0.27	0.319	1.858	1.886	0.2223	0.6021
0.28	0.301	1.850	1.874	0.2254	0.6206
0.29	0.284	1.842	1.864	0.2283	0.6391
0.30	0.269	1.835	1.855	0.2311	0.6575
0.31	0.254	1.829	1.846	0.2337	0.6758
0.32	0.240	1.823	1.839	0.2361	0.6941
0.33	0.226	1.818	1.832	0.2385	0.7123
0.34	0.214	1.813	1.826	0.2407	0.7304
0.35	0.202	1.809	1.820	0.2428	0.7485
0.36	0.191	1.805	1.815	0.2447	0.7666
0.37	0.181	1.801	1.810	0.2466	0.7846
0.38	0.171	1.798	1.806	0.2483	0.8026
0.39	0.161	1.795	1.802	0.2500	0.8206
0.40	0.153	1.792	1.798	0.2516	0.8385
0.41	0.144	1.789	1.795	0.2530	0.8564
0.42	0.136	1.787	1.792	0.2545	0.8743

0.43	0.129	1.785	1.789	0.2558	0.8921
0.44	0.122	1.783	1.787	0.2570	0.9100
0.45	0.115	1.781	1.785	0.2582	0.9278
0.46	0.109	1.779	1.783	0.2593	0.9456
0.47	0.103	1.778	1.781	0.2604	0.9634
0.48	0.097	1.777	1.779	0.2614	0.9812
0.49	0.092	1.775	1.778	0.2623	0.9989
0.50	0.087	1.774	1.776	0.2632	1.0167
0.51	0.082	1.773	1.775	0.2641	1.0344
0.52	0.078	1.772	1.774	0.2649	1.0521
0.53	0.074	1.771	1.773	0.2656	1.0699
0.54	0.070	1.771	1.772	0.2664	1.0876
0.55	0.066	1.770	1.771	0.2670	1.1053
0.56	0.062	1.769	1.770	0.2677	1.1230
0.57	0.059	1.769	1.770	0.2683	1.1407
0.58	0.056	1.768	1.769	0.2689	1.1583
0.59	0.053	1.768	1.768	0.2694	1.1760
0.60	0.050	1.767	1.768	0.2699	1.1937
0.61	0.047	1.767	1.767	0.2704	1.2114
0.62	0.045	1.766	1.767	0.2709	1.2290
0.63	0.042	1.766	1.766	0.2713	1.2467
0.64	0.040	1.766	1.766	0.2717	1.2643
0.65	0.038	1.765	1.766	0.2721	1.2820
0.66	0.036	1.765	1.765	0.2725	1.2997
0.67	0.034	1.765	1.765	0.2728	1.3173
0.68	0.032	1.765	1.765	0.2731	1.3349
0.69	0.030	1.764	1.765	0.2735	1.3526
0.70	0.029	1.764	1.764	0.2737	1.3702
0.71	0.027	1.764	1.764	0.2740	1.3879
0.72	0.026	1.764	1.764	0.2743	1.4055
0.73	0.024	1.764	1.764	0.2745	1.4231
0.74	0.023	1.763	1.764	0.2748	1.4408
0.75	0.022	1.763	1.763	0.2750	1.4584
0.76	0.020	1.763	1.763	0.2752	1.4760
0.77	0.019	1.763	1.763	0.2754	1.4937

****

****

216-OKY TERMINAL: 50 26 MAY 83 13:31:30

****

****

TABLE PT6

DIAMETER =74.45 MICRONS
SLURRY FLOWRATE=P2
PLOT CODE=1

TIME (S)	VELOCITY (M/S) HORIZONTAL	VERTICAL	RESULTANT	DISTANCE (M) HORIZONTAL	VERTICAL
0.00	2.239	3.878	4.478	0.0000	0.0000
0.01	0.821	1.485	1.697	0.0138	0.0242
0.02	0.355	0.710	0.794	0.0192	0.0345
0.03	0.173	0.417	0.452	0.0217	0.0399
0.04	0.090	0.289	0.303	0.0230	0.0433
0.05	0.048	0.228	0.233	0.0237	0.0459
0.06	0.026	0.197	0.199	0.0240	0.0480
0.07	0.014	0.181	0.182	0.0242	0.0499
0.08	0.008	0.173	0.173	0.0243	0.0516
0.09	0.004	0.169	0.169	0.0244	0.0533
0.10	0.002	0.167	0.167	0.0244	0.0550
0.11	0.001	0.166	0.166	0.0245	0.0567
0.12	0.001	0.165	0.165	0.0245	0.0583
0.13	0.000	0.165	0.165	0.0245	0.0600
0.14	0.000	0.165	0.165	0.0245	0.0616
0.15	0.000	0.165	0.165	0.0245	0.0633
0.16	0.000	0.165	0.165	0.0245	0.0649
0.17	0.000	0.165	0.165	0.0245	0.0666
0.18	0.000	0.165	0.165	0.0245	0.0682
0.19	0.000	0.165	0.165	0.0245	0.0699
0.20	0.000	0.165	0.165	0.0245	0.0715
0.21	0.000	0.165	0.165	0.0245	0.0732
0.22	0.000	0.165	0.165	0.0245	0.0748
0.23	0.000	0.165	0.165	0.0245	0.0764
0.24	0.000	0.165	0.165	0.0245	0.0781
0.25	0.000	0.165	0.165	0.0245	0.0797
0.26	0.000	0.165	0.165	0.0245	0.0814
0.27	0.000	0.165	0.165	0.0245	0.0830
0.28	0.000	0.165	0.165	0.0245	0.0847
0.29	0.000	0.165	0.165	0.0245	0.0863
0.30	0.000	0.165	0.165	0.0245	0.0880
0.31	0.000	0.165	0.165	0.0245	0.0896
0.32	0.000	0.165	0.165	0.0245	0.0913
0.33	0.000	0.165	0.165	0.0245	0.0929
0.34	0.000	0.165	0.165	0.0245	0.0945
0.35	0.000	0.165	0.165	0.0245	0.0962
0.36	0.000	0.165	0.165	0.0245	0.0978
0.37	0.000	0.165	0.165	0.0245	0.0995
0.38	0.000	0.165	0.165	0.0245	0.1011
0.39	0.000	0.165	0.165	0.0245	0.1028
0.40	0.000	0.165	0.165	0.0245	0.1044
0.41	0.000	0.165	0.165	0.0245	0.1061
0.42	0.000	0.165	0.165	0.0245	0.1077

TABLE PT7

DIAMETER =98.55 MICRONS
SLURRY FLOWRATE=P2
PLOT CODE=2

TIME (S)	VELOCITY (M/S) HORIZONTAL	VERTICAL	RESULTANT	DISTANCE (M) HORIZONTAL	VERTICAL
0.00	2.239	3.878	4.478	0.0000	0.0000
0.01	1.129	2.028	2.321	0.0160	0.0280
0.02	0.676	1.292	1.458	0.0247	0.0441
0.03	0.394	0.830	0.919	0.0298	0.0544
0.04	0.250	0.606	0.655	0.0330	0.0615
0.05	0.162	0.473	0.500	0.0350	0.0668
0.06	0.108	0.395	0.409	0.0364	0.0711
0.07	0.073	0.348	0.355	0.0373	0.0748
0.08	0.050	0.318	0.322	0.0379	0.0781
0.09	0.034	0.299	0.301	0.0383	0.0812
0.10	0.023	0.287	0.288	0.0386	0.0841
0.11	0.016	0.280	0.280	0.0387	0.0870
0.12	0.011	0.275	0.275	0.0389	0.0897
0.13	0.008	0.271	0.271	0.0390	0.0925
0.14	0.005	0.269	0.269	0.0390	0.0952
0.15	0.004	0.268	0.268	0.0391	0.0978
0.16	0.003	0.267	0.267	0.0391	0.1005
0.17	0.002	0.266	0.266	0.0391	0.1032
0.18	0.001	0.266	0.266	0.0391	0.1058
0.19	0.001	0.265	0.265	0.0392	0.1085
0.20	0.001	0.265	0.265	0.0392	0.1111
0.21	0.000	0.265	0.265	0.0392	0.1138
0.22	0.000	0.265	0.265	0.0392	0.1165
0.23	0.000	0.265	0.265	0.0392	0.1191
0.24	0.000	0.265	0.265	0.0392	0.1218
0.25	0.000	0.265	0.265	0.0392	0.1244
0.26	0.000	0.265	0.265	0.0392	0.1271
0.27	0.000	0.265	0.265	0.0392	0.1297
0.28	0.000	0.265	0.265	0.0392	0.1324
0.29	0.000	0.265	0.265	0.0392	0.1350
0.30	0.000	0.265	0.265	0.0392	0.1377
0.31	0.000	0.265	0.265	0.0392	0.1403
0.32	0.000	0.265	0.265	0.0392	0.1430
0.33	0.000	0.265	0.265	0.0392	0.1456
0.34	0.000	0.265	0.265	0.0392	0.1483
0.35	0.000	0.265	0.265	0.0392	0.1509
0.36	0.000	0.265	0.265	0.0392	0.1536
0.37	0.000	0.265	0.265	0.0392	0.1562
0.38	0.000	0.265	0.265	0.0392	0.1589
0.39	0.000	0.265	0.265	0.0392	0.1615
0.40	0.000	0.265	0.265	0.0392	0.1642
0.41	0.000	0.265	0.265	0.0392	0.1668
0.42	0.000	0.265	0.265	0.0392	0.1695

TABLE PT8

DIAMETER =136.55 MICRONS
SLURRY FLOWRATE=P2
PLOT CODE=3

TIME (S)	VELOCITY (M/S) HORIZONTAL	VERTICAL	RESULTANT	DISTANCE (M) HORIZONTAL	VERTICAL
0.00	2.239	3.878	4.478	0.0000	0.0000
0.01	1.457	2.604	2.984	0.0181	0.0318
0.02	1.006	1.880	2.132	0.0302	0.0539
0.03	0.728	1.444	1.617	0.0388	0.0703
0.04	0.549	1.175	1.296	0.0451	0.0833
0.05	0.430	1.008	1.096	0.0500	0.0941
0.06	0.318	0.829	0.888	0.0537	0.1033
0.07	0.241	0.714	0.754	0.0565	0.1110
0.08	0.188	0.643	0.670	0.0586	0.1178
0.09	0.148	0.593	0.611	0.0603	0.1239
0.10	0.116	0.554	0.567	0.0616	0.1297
0.11	0.092	0.525	0.533	0.0626	0.1351
0.12	0.073	0.503	0.508	0.0634	0.1402
0.13	0.058	0.486	0.489	0.0641	0.1451
0.14	0.046	0.473	0.475	0.0646	0.1499
0.15	0.036	0.463	0.464	0.0650	0.1546
0.16	0.029	0.455	0.456	0.0653	0.1592
0.17	0.023	0.449	0.450	0.0656	0.1637
0.18	0.018	0.445	0.445	0.0658	0.1682
0.19	0.014	0.442	0.442	0.0659	0.1726
0.20	0.012	0.439	0.439	0.0661	0.1770
0.21	0.009	0.437	0.437	0.0662	0.1814
0.22	0.007	0.436	0.436	0.0663	0.1857
0.23	0.006	0.435	0.435	0.0663	0.1901
0.24	0.005	0.434	0.434	0.0664	0.1944
0.25	0.004	0.433	0.433	0.0664	0.1988
0.26	0.003	0.433	0.433	0.0664	0.2031
0.27	0.002	0.432	0.432	0.0665	0.2074
0.28	0.002	0.432	0.432	0.0665	0.2117
0.29	0.001	0.432	0.432	0.0665	0.2161
0.30	0.001	0.432	0.432	0.0665	0.2204
0.31	0.001	0.431	0.431	0.0665	0.2247
0.32	0.001	0.431	0.431	0.0665	0.2290
0.33	0.001	0.431	0.431	0.0665	0.2333
0.34	0.000	0.431	0.431	0.0666	0.2376
0.35	0.000	0.431	0.431	0.0666	0.2419
0.36	0.000	0.431	0.431	0.0666	0.2463
0.37	0.000	0.431	0.431	0.0666	0.2506
0.38	0.000	0.431	0.431	0.0666	0.2549
0.39	0.000	0.431	0.431	0.0666	0.2592
0.40	0.000	0.431	0.431	0.0666	0.2635
0.41	0.000	0.431	0.431	0.0666	0.2678
0.42	0.000	0.431	0.431	0.0666	0.2721

TABLE PT9

DIAMETER =210.95 MICRONS
SLURRY FLOWRATE=P2
PLOT CODE=4

TIME (S)	VELOCITY (M/S) HORIZONTAL	VERTICAL	RESULTANT	DISTANCE (M) HORIZONTAL	VERTICAL
0.00	2.239	3.878	4.478	0.0000	0.0000
0.01	1.779	3.168	3.633	0.0200	0.0350
0.02	1.443	2.659	3.025	0.0360	0.0640
0.03	1.190	2.281	2.573	0.0491	0.0886
0.04	0.993	1.994	2.227	0.0600	0.1100
0.05	0.837	1.770	1.958	0.0691	0.1287
0.06	0.711	1.594	1.746	0.0768	0.1455
0.07	0.608	1.454	1.576	0.0834	0.1607
0.08	0.523	1.342	1.441	0.0890	0.1747
0.09	0.452	1.252	1.332	0.0939	0.1877
0.10	0.393	1.180	1.243	0.0981	0.1998
0.11	0.343	1.121	1.172	0.1018	0.2113
0.12	0.300	1.073	1.115	0.1050	0.2223
0.13	0.264	1.035	1.068	0.1078	0.2328
0.14	0.232	1.004	1.030	0.1103	0.2430
0.15	0.205	0.978	0.999	0.1125	0.2529
0.16	0.181	0.958	0.975	0.1144	0.2626
0.17	0.161	0.941	0.955	0.1161	0.2720
0.18	0.143	0.928	0.938	0.1176	0.2814
0.19	0.127	0.917	0.925	0.1190	0.2906
0.20	0.113	0.908	0.915	0.1202	0.2997
0.21	0.100	0.901	0.906	0.1212	0.3088
0.22	0.089	0.895	0.899	0.1222	0.3177
0.23	0.080	0.890	0.894	0.1230	0.3267
0.24	0.071	0.886	0.889	0.1238	0.3355
0.25	0.063	0.883	0.885	0.1244	0.3444
0.26	0.057	0.881	0.882	0.1250	0.3532
0.27	0.050	0.879	0.880	0.1256	0.3620
0.28	0.045	0.877	0.878	0.1260	0.3708
0.29	0.040	0.876	0.876	0.1265	0.3795
0.30	0.036	0.874	0.875	0.1269	0.3883
0.31	0.032	0.874	0.874	0.1272	0.3970
0.32	0.029	0.873	0.873	0.1275	0.4058
0.33	0.026	0.872	0.873	0.1278	0.4145
0.34	0.023	0.872	0.872	0.1280	0.4232
0.35	0.020	0.871	0.872	0.1282	0.4319
0.36	0.018	0.871	0.871	0.1284	0.4406
0.37	0.016	0.871	0.871	0.1286	0.4494
0.38	0.015	0.871	0.871	0.1287	0.4581
0.39	0.013	0.870	0.871	0.1289	0.4668
0.40	0.012	0.870	0.870	0.1290	0.4755
0.41	0.010	0.870	0.870	0.1291	0.4842
0.42	0.009	0.870	0.870	0.1292	0.4929

TABLE PT10

DIAMETER =412.80 MICRONS
SLURRY FLOWRATE=P2
PLOT CODE=5

TIME (S)	VELOCITY (M/S) HORIZONTAL	VERTICAL	RESULTANT	DISTANCE (M) HORIZONTAL	VERTICAL
0.00	2.239	3.878	4.478	0.0000	0.0000
0.01	2.051	3.646	4.183	0.0214	0.0376
0.02	1.884	3.443	3.924	0.0411	0.0730
0.03	1.735	3.264	3.697	0.0592	0.1065
0.04	1.601	3.107	3.495	0.0758	0.1384
0.05	1.481	2.968	3.317	0.0912	0.1687
0.06	1.372	2.845	3.159	0.1055	0.1978
0.07	1.274	2.736	3.019	0.1187	0.2257
0.08	1.185	2.640	2.893	0.1310	0.2526
0.09	1.104	2.553	2.782	0.1424	0.2785
0.10	1.030	2.476	2.682	0.1531	0.3037
0.11	0.962	2.407	2.592	0.1630	0.3281
0.12	0.899	2.346	2.512	0.1723	0.3518
0.13	0.842	2.291	2.440	0.1810	0.3750
0.14	0.788	2.241	2.376	0.1892	0.3977
0.15	0.739	2.196	2.318	0.1968	0.4198
0.16	0.694	2.156	2.265	0.2040	0.4416
0.17	0.652	2.120	2.218	0.2107	0.4630
0.18	0.612	2.087	2.175	0.2170	0.4840
0.19	0.576	2.058	2.137	0.2230	0.5047
0.20	0.542	2.031	2.102	0.2286	0.5252
0.21	0.510	2.007	2.071	0.2338	0.5454
0.22	0.480	1.985	2.042	0.2388	0.5653
0.23	0.452	1.965	2.017	0.2434	0.5851
0.24	0.426	1.947	1.993	0.2478	0.6046
0.25	0.402	1.931	1.972	0.2520	0.6240
0.26	0.379	1.916	1.953	0.2559	0.6433
0.27	0.358	1.903	1.936	0.2595	0.6624
0.28	0.337	1.890	1.920	0.2630	0.6813
0.29	0.318	1.879	1.906	0.2663	0.7002
0.30	0.300	1.869	1.893	0.2694	0.7189
0.31	0.284	1.860	1.881	0.2723	0.7376
0.32	0.268	1.851	1.871	0.2751	0.7561
0.33	0.253	1.844	1.861	0.2777	0.7746
0.34	0.239	1.837	1.852	0.2801	0.7930
0.35	0.226	1.830	1.844	0.2825	0.8113
0.36	0.213	1.825	1.837	0.2846	0.8296
0.37	0.201	1.819	1.830	0.2867	0.8478
0.38	0.190	1.814	1.824	0.2887	0.8660
0.39	0.180	1.810	1.819	0.2905	0.8841
0.40	0.170	1.806	1.814	0.2923	0.9022
0.41	0.161	1.802	1.809	0.2939	0.9202
0.42	0.152	1.799	1.805	0.2955	0.9382

0. 43	0. 144	1. 796	1. 801	0. 2970	0. 9562
0. 44	0. 136	1. 793	1. 798	0. 2984	0. 9741
0. 45	0. 128	1. 790	1. 795	0. 2997	0. 9921
0. 46	0. 121	1. 788	1. 792	0. 3009	1. 0099
0. 47	0. 115	1. 786	1. 789	0. 3021	1. 0278
0. 48	0. 108	1. 784	1. 787	0. 3032	1. 0457
0. 49	0. 103	1. 782	1. 785	0. 3043	1. 0635
0. 50	0. 097	1. 780	1. 783	0. 3053	1. 0813
0. 51	0. 092	1. 779	1. 781	0. 3062	1. 0991
0. 52	0. 087	1. 777	1. 779	0. 3071	1. 1169
0. 53	0. 082	1. 776	1. 778	0. 3080	1. 1346
0. 54	0. 078	1. 775	1. 777	0. 3088	1. 1524
0. 55	0. 073	1. 774	1. 775	0. 3095	1. 1701
0. 56	0. 069	1. 773	1. 774	0. 3102	1. 1879
0. 57	0. 066	1. 772	1. 773	0. 3109	1. 2056
0. 58	0. 062	1. 771	1. 772	0. 3115	1. 2233
0. 59	0. 059	1. 770	1. 771	0. 3121	1. 2410
0. 60	0. 055	1. 770	1. 771	0. 3127	1. 2587
0. 61	0. 052	1. 769	1. 770	0. 3133	1. 2764
0. 62	0. 050	1. 768	1. 769	0. 3138	1. 2941
0. 63	0. 047	1. 768	1. 769	0. 3142	1. 3118
0. 64	0. 044	1. 767	1. 768	0. 3147	1. 3295
0. 65	0. 042	1. 767	1. 767	0. 3151	1. 3471
0. 66	0. 040	1. 767	1. 767	0. 3155	1. 3648
0. 67	0. 038	1. 766	1. 767	0. 3159	1. 3825
0. 68	0. 036	1. 766	1. 766	0. 3163	1. 4001
0. 69	0. 034	1. 765	1. 766	0. 3166	1. 4178
0. 70	0. 032	1. 765	1. 765	0. 3170	1. 4354
0. 71	0. 030	1. 765	1. 765	0. 3173	1. 4531
0. 72	0. 028	1. 765	1. 765	0. 3176	1. 4707

****

****

2216-OKY TERMINAL: 50 26 MAY 83 13:26:11

****

****

TABLE PT11*

DIAMETER =57.40 MICRONS
SLURRY FLOWRATE=P3
PLOT CODE=1

TIME (S)	VELOCITY (M/S) HORIZONTAL	VERTICAL	RESULTANT	DISTANCE (M) HORIZONTAL	VERTICAL
0.00	2.586	4.478	5.171	0.0000	0.0000
0.01	0.549	1.003	1.144	0.0126	0.0221
0.02	0.170	0.369	0.406	0.0158	0.0283
0.03	0.060	0.193	0.202	0.0168	0.0309
0.04	0.023	0.135	0.137	0.0172	0.0325
0.05	0.009	0.115	0.116	0.0173	0.0337
0.06	0.003	0.108	0.108	0.0174	0.0348
0.07	0.001	0.106	0.106	0.0174	0.0359
0.08	0.001	0.105	0.105	0.0174	0.0370
0.09	0.000	0.104	0.104	0.0174	0.0380
0.10	0.000	0.104	0.104	0.0174	0.0390
0.11	0.000	0.104	0.104	0.0174	0.0401
0.12	0.000	0.104	0.104	0.0174	0.0411
0.13	0.000	0.104	0.104	0.0174	0.0422
0.14	0.000	0.104	0.104	0.0174	0.0432
0.15	0.000	0.104	0.104	0.0174	0.0443
0.16	0.000	0.104	0.104	0.0174	0.0453
0.17	0.000	0.104	0.104	0.0174	0.0463
0.18	0.000	0.104	0.104	0.0174	0.0474
0.19	0.000	0.104	0.104	0.0174	0.0484
0.20	0.000	0.104	0.104	0.0174	0.0495
0.21	0.000	0.104	0.104	0.0174	0.0505
0.22	0.000	0.104	0.104	0.0174	0.0516
0.23	0.000	0.104	0.104	0.0174	0.0526
0.24	0.000	0.104	0.104	0.0174	0.0536
0.25	0.000	0.104	0.104	0.0174	0.0547
0.26	0.000	0.104	0.104	0.0174	0.0557
0.27	0.000	0.104	0.104	0.0174	0.0568
0.28	0.000	0.104	0.104	0.0174	0.0578

TABLE PT12

DIAMETER =74.45 MICRONS
SLURRY FLOWRATE=P3
PLOT CODE=2

TIME (S)	VELOCITY (M/S) HORIZONTAL	VERTICAL	RESULTANT	DISTANCE (M) HORIZONTAL	VERTICAL
0.00	2.586	4.478	5.171	0.0000	0.0000
0.01	0.923	1.663	1.902	0.0155	0.0272
0.02	0.386	0.763	0.855	0.0215	0.0384
0.03	0.187	0.439	0.477	0.0242	0.0442
0.04	0.097	0.300	0.315	0.0256	0.0478
0.05	0.052	0.233	0.238	0.0263	0.0504
0.06	0.028	0.199	0.201	0.0267	0.0525
0.07	0.015	0.183	0.183	0.0269	0.0544
0.08	0.008	0.174	0.174	0.0270	0.0562
0.09	0.005	0.169	0.169	0.0271	0.0579
0.10	0.003	0.167	0.167	0.0271	0.0596
0.11	0.001	0.166	0.166	0.0271	0.0613
0.12	0.001	0.165	0.165	0.0271	0.0629
0.13	0.000	0.165	0.165	0.0271	0.0646
0.14	0.000	0.165	0.165	0.0271	0.0662
0.15	0.000	0.165	0.165	0.0272	0.0679
0.16	0.000	0.165	0.165	0.0272	0.0695
0.17	0.000	0.165	0.165	0.0272	0.0712
0.18	0.000	0.165	0.165	0.0272	0.0728
0.19	0.000	0.165	0.165	0.0272	0.0744
0.20	0.000	0.165	0.165	0.0272	0.0761
0.21	0.000	0.165	0.165	0.0272	0.0777
0.22	0.000	0.165	0.165	0.0272	0.0794
0.23	0.000	0.165	0.165	0.0272	0.0810
0.24	0.000	0.165	0.165	0.0272	0.0827
0.25	0.000	0.165	0.165	0.0272	0.0843
0.26	0.000	0.165	0.165	0.0272	0.0860
0.27	0.000	0.165	0.165	0.0272	0.0876
0.28	0.000	0.165	0.165	0.0272	0.0893
0.29	0.000	0.165	0.165	0.0272	0.0909
0.30	0.000	0.165	0.165	0.0272	0.0925
0.31	0.000	0.165	0.165	0.0272	0.0942
0.32	0.000	0.165	0.165	0.0272	0.0958
0.33	0.000	0.165	0.165	0.0272	0.0975
0.34	0.000	0.165	0.165	0.0272	0.0991
0.35	0.000	0.165	0.165	0.0272	0.1008
0.36	0.000	0.165	0.165	0.0272	0.1024
0.37	0.000	0.165	0.165	0.0272	0.1041
0.38	0.000	0.165	0.165	0.0272	0.1057
0.39	0.000	0.165	0.165	0.0272	0.1073
0.40	0.000	0.165	0.165	0.0272	0.1090
0.41	0.000	0.165	0.165	0.0272	0.1106
0.42	0.000	0.165	0.165	0.0272	0.1123

TABLE PT13

DIAMETER =98.55 MICRONS
SLURRY FLOWRATE=P3
PLOT CODE=3

TIME (S)	VELOCITY (M/S) HORIZONTAL	VERTICAL	RESULTANT	DISTANCE (M) HORIZONTAL	VERTICAL
0.00	2.586	4.478	5.171	0.0000	0.0000
0.01	1.257	2.249	2.576	0.0181	0.0318
0.02	0.735	1.392	1.574	0.0277	0.0493
0.03	0.429	0.888	0.986	0.0334	0.0605
0.04	0.271	0.640	0.695	0.0368	0.0680
0.05	0.175	0.493	0.523	0.0390	0.0736
0.06	0.116	0.407	0.423	0.0404	0.0781
0.07	0.078	0.355	0.363	0.0414	0.0819
0.08	0.053	0.323	0.327	0.0420	0.0852
0.09	0.036	0.302	0.304	0.0425	0.0884
0.10	0.025	0.289	0.290	0.0428	0.0913
0.11	0.017	0.281	0.281	0.0430	0.0942
0.12	0.012	0.275	0.276	0.0431	0.0969
0.13	0.008	0.272	0.272	0.0432	0.0997
0.14	0.006	0.269	0.269	0.0433	0.1024
0.15	0.004	0.268	0.268	0.0433	0.1051
0.16	0.003	0.267	0.267	0.0434	0.1077
0.17	0.002	0.266	0.266	0.0434	0.1104
0.18	0.001	0.266	0.266	0.0434	0.1131
0.19	0.001	0.266	0.266	0.0434	0.1157
0.20	0.001	0.265	0.265	0.0434	0.1184
0.21	0.000	0.265	0.265	0.0434	0.1210
0.22	0.000	0.265	0.265	0.0434	0.1237
0.23	0.000	0.265	0.265	0.0434	0.1263
0.24	0.000	0.265	0.265	0.0434	0.1290
0.25	0.000	0.265	0.265	0.0434	0.1316
0.26	0.000	0.265	0.265	0.0434	0.1343
0.27	0.000	0.265	0.265	0.0434	0.1369
0.28	0.000	0.265	0.265	0.0434	0.1396
0.29	0.000	0.265	0.265	0.0434	0.1422
0.30	0.000	0.265	0.265	0.0434	0.1449
0.31	0.000	0.265	0.265	0.0434	0.1475
0.32	0.000	0.265	0.265	0.0434	0.1502
0.33	0.000	0.265	0.265	0.0434	0.1528
0.34	0.000	0.265	0.265	0.0434	0.1555
0.35	0.000	0.265	0.265	0.0434	0.1581
0.36	0.000	0.265	0.265	0.0434	0.1608
0.37	0.000	0.265	0.265	0.0434	0.1634
0.38	0.000	0.265	0.265	0.0434	0.1661
0.39	0.000	0.265	0.265	0.0434	0.1687
0.40	0.000	0.265	0.265	0.0434	0.1714
0.41	0.000	0.265	0.265	0.0434	0.1740
0.42	0.000	0.265	0.265	0.0434	0.1767

TABLE PT14

DIAMETER =136.55 MICRONS
SLURRY FLOWRATE=P3
PLOT CODE=4

TIME (S)	VELOCITY (M/S) HORIZONTAL	VERTICAL	RESULTANT	DISTANCE (M) HORIZONTAL	VERTICAL
0.00	2.586	4.478	5.171	0.0000	0.0000
0.01	1.642	2.923	3.353	0.0206	0.0362
0.02	1.116	2.068	2.350	0.0342	0.0607
0.03	0.796	1.559	1.750	0.0436	0.0787
0.04	0.593	1.246	1.380	0.0505	0.0926
0.05	0.459	1.053	1.149	0.0557	0.1040
0.06	0.348	0.883	0.949	0.0598	0.1137
0.07	0.260	0.744	0.788	0.0628	0.1218
0.08	0.201	0.663	0.693	0.0651	0.1288
0.09	0.158	0.607	0.627	0.0668	0.1351
0.10	0.124	0.565	0.579	0.0682	0.1410
0.11	0.098	0.534	0.543	0.0694	0.1465
0.12	0.078	0.509	0.515	0.0702	0.1517
0.13	0.061	0.491	0.494	0.0709	0.1567
0.14	0.049	0.476	0.479	0.0715	0.1615
0.15	0.039	0.465	0.467	0.0719	0.1662
0.16	0.031	0.457	0.458	0.0722	0.1708
0.17	0.024	0.451	0.452	0.0725	0.1753
0.18	0.019	0.446	0.447	0.0727	0.1798
0.19	0.015	0.442	0.443	0.0729	0.1843
0.20	0.012	0.440	0.440	0.0731	0.1887
0.21	0.010	0.438	0.438	0.0732	0.1931
0.22	0.008	0.436	0.436	0.0733	0.1974
0.23	0.006	0.435	0.435	0.0733	0.2018
0.24	0.005	0.434	0.434	0.0734	0.2061
0.25	0.004	0.433	0.433	0.0734	0.2105
0.26	0.003	0.433	0.433	0.0735	0.2148
0.27	0.002	0.432	0.432	0.0735	0.2191
0.28	0.002	0.432	0.432	0.0735	0.2234
0.29	0.002	0.432	0.432	0.0735	0.2278
0.30	0.001	0.432	0.432	0.0735	0.2321
0.31	0.001	0.431	0.431	0.0735	0.2364
0.32	0.001	0.431	0.431	0.0736	0.2407
0.33	0.001	0.431	0.431	0.0736	0.2450
0.34	0.001	0.431	0.431	0.0736	0.2493
0.35	0.000	0.431	0.431	0.0736	0.2536
0.36	0.000	0.431	0.431	0.0736	0.2580
0.37	0.000	0.431	0.431	0.0736	0.2623
0.38	0.000	0.431	0.431	0.0736	0.2666
0.39	0.000	0.431	0.431	0.0736	0.2709
0.40	0.000	0.431	0.431	0.0736	0.2752
0.41	0.000	0.431	0.431	0.0736	0.2795
0.42	0.000	0.431	0.431	0.0736	0.2838

TABLE PT15

DIAMETER =210.95 MICRONS
SLURRY FLOWRATE=P3
PLOT CODE=5

TIME (S)	VELOCITY (M/S) HORIZONTAL	VERTICAL	RESULTANT	DISTANCE (M) HORIZONTAL	VERTICAL
0.00	2.586	4.478	5.171	0.0000	0.0000
0.01	2.020	3.586	4.116	0.0229	0.0400
0.02	1.619	2.962	3.376	0.0409	0.0726
0.03	1.323	2.509	2.836	0.0556	0.0999
0.04	1.096	2.168	2.429	0.0676	0.1232
0.05	0.918	1.906	2.116	0.0777	0.1435
0.06	0.776	1.702	1.871	0.0861	0.1615
0.07	0.661	1.540	1.676	0.0933	0.1777
0.08	0.567	1.412	1.521	0.0994	0.1924
0.09	0.489	1.308	1.396	0.1047	0.2060
0.10	0.423	1.225	1.296	0.1092	0.2186
0.11	0.369	1.158	1.215	0.1132	0.2305
0.12	0.322	1.103	1.149	0.1166	0.2418
0.13	0.282	1.059	1.096	0.1196	0.2526
0.14	0.248	1.023	1.053	0.1223	0.2630
0.15	0.219	0.994	1.018	0.1246	0.2731
0.16	0.193	0.971	0.990	0.1267	0.2829
0.17	0.171	0.952	0.967	0.1285	0.2925
0.18	0.152	0.936	0.948	0.1301	0.3020
0.19	0.135	0.924	0.933	0.1315	0.3113
0.20	0.120	0.913	0.921	0.1328	0.3204
0.21	0.107	0.905	0.911	0.1339	0.3295
0.22	0.095	0.899	0.904	0.1349	0.3386
0.23	0.085	0.893	0.897	0.1358	0.3475
0.24	0.075	0.889	0.892	0.1366	0.3564
0.25	0.067	0.885	0.888	0.1374	0.3653
0.26	0.060	0.882	0.884	0.1380	0.3741
0.27	0.053	0.880	0.882	0.1386	0.3829
0.28	0.048	0.878	0.879	0.1391	0.3917
0.29	0.043	0.876	0.877	0.1395	0.4005
0.30	0.038	0.875	0.876	0.1399	0.4093
0.31	0.034	0.874	0.875	0.1403	0.4180
0.32	0.030	0.873	0.874	0.1406	0.4267
0.33	0.027	0.873	0.873	0.1409	0.4355
0.34	0.024	0.872	0.872	0.1411	0.4442
0.35	0.022	0.872	0.872	0.1414	0.4529
0.36	0.019	0.871	0.872	0.1416	0.4616
0.37	0.017	0.871	0.871	0.1418	0.4703
0.38	0.015	0.871	0.871	0.1419	0.4790
0.39	0.014	0.871	0.871	0.1421	0.4878
0.40	0.012	0.870	0.870	0.1422	0.4965
0.41	0.011	0.870	0.870	0.1423	0.5052
0.42	0.010	0.870	0.870	0.1424	0.5139

0. 43	0. 009	0. 870	0. 870	0. 1425	0. 5226
0. 44	0. 008	0. 870	0. 870	0. 1426	0. 5313
0. 45	0. 007	0. 870	0. 870	0. 1427	0. 5400
0. 46	0. 006	0. 870	0. 870	0. 1427	0. 5487
0. 47	0. 006	0. 870	0. 870	0. 1428	0. 5574
0. 48	0. 005	0. 870	0. 870	0. 1428	0. 5661
0. 49	0. 004	0. 870	0. 870	0. 1429	0. 5748
0. 50	0. 004	0. 870	0. 870	0. 1429	0. 5835
0. 51	0. 004	0. 870	0. 870	0. 1430	0. 5922
0. 52	0. 003	0. 870	0. 870	0. 1430	0. 6009
0. 53	0. 003	0. 870	0. 870	0. 1430	0. 6096
0. 54	0. 003	0. 870	0. 870	0. 1431	0. 6183
0. 55	0. 002	0. 870	0. 870	0. 1431	0. 6269
0. 56	0. 002	0. 870	0. 870	0. 1431	0. 6356
0. 57	0. 002	0. 870	0. 870	0. 1431	0. 6443
0. 58	0. 002	0. 870	0. 870	0. 1431	0. 6530
0. 59	0. 001	0. 870	0. 870	0. 1432	0. 6617
0. 60	0. 001	0. 870	0. 870	0. 1432	0. 6704
0. 61	0. 001	0. 870	0. 870	0. 1432	0. 6791
0. 62	0. 001	0. 870	0. 870	0. 1432	0. 6878
0. 63	0. 001	0. 870	0. 870	0. 1432	0. 6965
0. 64	0. 001	0. 870	0. 870	0. 1432	0. 7052
0. 65	0. 001	0. 870	0. 870	0. 1432	0. 7139
0. 66	0. 001	0. 870	0. 870	0. 1432	0. 7226
0. 67	0. 001	0. 870	0. 870	0. 1432	0. 7313
0. 68	0. 001	0. 870	0. 870	0. 1432	0. 7400
0. 69	0. 000	0. 870	0. 870	0. 1432	0. 7487
0. 70	0. 000	0. 870	0. 870	0. 1432	0. 7574
0. 71	0. 000	0. 870	0. 870	0. 1433	0. 7661
0. 72	0. 000	0. 870	0. 870	0. 1433	0. 7748
0. 73	0. 000	0. 870	0. 870	0. 1433	0. 7835
0. 74	0. 000	0. 870	0. 870	0. 1433	0. 7922
0. 75	0. 000	0. 870	0. 870	0. 1433	0. 8009
0. 76	0. 000	0. 870	0. 870	0. 1433	0. 8096
0. 77	0. 000	0. 870	0. 870	0. 1433	0. 8183
0. 78	0. 000	0. 870	0. 870	0. 1433	0. 8270
0. 79	0. 000	0. 870	0. 870	0. 1433	0. 8357
0. 80	0. 000	0. 870	0. 870	0. 1433	0. 8444
0. 81	0. 000	0. 870	0. 870	0. 1433	0. 8531
0. 82	0. 000	0. 870	0. 870	0. 1433	0. 8618
0. 83	0. 000	0. 870	0. 870	0. 1433	0. 8705
0. 84	0. 000	0. 870	0. 870	0. 1433	0. 8792
0. 85	0. 000	0. 870	0. 870	0. 1433	0. 8879
0. 86	0. 000	0. 870	0. 870	0. 1433	0. 8966
0. 87	0. 000	0. 870	0. 870	0. 1433	0. 9053
0. 88	0. 000	0. 870	0. 870	0. 1433	0. 9140
0. 89	0. 000	0. 870	0. 870	0. 1433	0. 9227
0. 90	0. 000	0. 870	0. 870	0. 1433	0. 9313
0. 91	0. 000	0. 870	0. 870	0. 1433	0. 9400
0. 92	0. 000	0. 870	0. 870	0. 1433	0. 9487
0. 93	0. 000	0. 870	0. 870	0. 1433	0. 9574
0. 94	0. 000	0. 870	0. 870	0. 1433	0. 9661
0. 95	0. 000	0. 870	0. 870	0. 1433	0. 9748
0. 96	0. 000	0. 870	0. 870	0. 1433	0. 9835
0. 97	0. 000	0. 870	0. 870	0. 1433	0. 9922
0. 98	0. 000	0. 870	0. 870	0. 1433	1. 0009
0. 99	0. 000	0. 870	0. 870	0. 1433	1. 0096
1. 00	0. 000	0. 870	0. 870	0. 1433	1. 0183
1. 01	0. 000	0. 870	0. 870	0. 1433	1. 0270
1. 02	0. 000	0. 870	0. 870	0. 1433	1. 0357

TABLE PT16

DIAMETER =412.80 MICRONS

SLURRY FLOWRATE=P3

PLOT CODE =6

TIME (S)	VELOCITY (M/S) HORIZONTAL	VERTICAL	RESULTANT	DISTANCE (M) HORIZONTAL	VERTICAL
0.00	2.586	4.478	5.171	0.0000	0.0000
0.01	2.354	4.170	4.788	0.0247	0.0432
0.02	2.150	3.903	4.455	0.0472	0.0835
0.03	1.969	3.669	4.164	0.0677	0.1214
0.04	1.809	3.465	3.909	0.0866	0.1570
0.05	1.666	3.285	3.683	0.1040	0.1907
0.06	1.538	3.127	3.484	0.1200	0.2228
0.07	1.423	2.987	3.308	0.1348	0.2533
0.08	1.319	2.863	3.152	0.1485	0.2826
0.09	1.225	2.753	3.013	0.1612	0.3106
0.10	1.139	2.655	2.889	0.1730	0.3377
0.11	1.061	2.568	2.778	0.1840	0.3638
0.12	0.990	2.490	2.679	0.1942	0.3891
0.13	0.924	2.420	2.591	0.2038	0.4136
0.14	0.864	2.358	2.511	0.2128	0.4375
0.15	0.809	2.302	2.440	0.2211	0.4608
0.16	0.758	2.251	2.376	0.2289	0.4835
0.17	0.711	2.206	2.318	0.2363	0.5058
0.18	0.667	2.165	2.266	0.2432	0.5277
0.19	0.626	2.129	2.219	0.2496	0.5491
0.20	0.589	2.095	2.177	0.2557	0.5703
0.21	0.553	2.065	2.138	0.2614	0.5911
0.22	0.521	2.038	2.104	0.2668	0.6116
0.23	0.490	2.014	2.072	0.2718	0.6318
0.24	0.462	1.991	2.044	0.2766	0.6519
0.25	0.435	1.971	2.018	0.2811	0.6717
0.26	0.410	1.953	1.995	0.2853	0.6913
0.27	0.386	1.936	1.974	0.2893	0.7107
0.28	0.364	1.921	1.955	0.2930	0.7300
0.29	0.344	1.907	1.938	0.2966	0.7491
0.30	0.324	1.894	1.922	0.2999	0.7682
0.31	0.306	1.883	1.908	0.3031	0.7870
0.32	0.289	1.873	1.895	0.3060	0.8058
0.33	0.273	1.863	1.883	0.3088	0.8245
0.34	0.257	1.854	1.872	0.3115	0.8431
0.35	0.243	1.847	1.863	0.3140	0.8616
0.36	0.230	1.839	1.854	0.3163	0.8800
0.37	0.217	1.833	1.846	0.3186	0.8984
0.38	0.205	1.827	1.838	0.3207	0.9167
0.39	0.194	1.821	1.832	0.3227	0.9349
0.40	0.183	1.816	1.826	0.3246	0.9531
0.41	0.173	1.812	1.820	0.3263	0.9712
0.42	0.163	1.808	1.815	0.3280	0.9893

0. 43	0. 154	1. 804	1. 810	0. 3296	1. 0074
0. 44	0. 146	1. 800	1. 806	0. 3311	1. 0254
0. 45	0. 138	1. 797	1. 802	0. 3325	1. 0434
0. 46	0. 130	1. 794	1. 799	0. 3339	1. 0614
0. 47	0. 123	1. 791	1. 796	0. 3351	1. 0793
0. 48	0. 117	1. 789	1. 793	0. 3363	1. 0972
0. 49	0. 110	1. 787	1. 790	0. 3375	1. 1151
0. 50	0. 104	1. 785	1. 788	0. 3385	1. 1329
0. 51	0. 099	1. 783	1. 785	0. 3396	1. 1508
0. 52	0. 093	1. 781	1. 783	0. 3405	1. 1686
0. 53	0. 088	1. 779	1. 782	0. 3414	1. 1864
0. 54	0. 083	1. 778	1. 780	0. 3423	1. 2042
0. 55	0. 079	1. 777	1. 778	0. 3431	1. 2219
0. 56	0. 074	1. 775	1. 777	0. 3438	1. 2397
0. 57	0. 070	1. 774	1. 776	0. 3446	1. 2575
0. 58	0. 067	1. 773	1. 775	0. 3453	1. 2752
0. 59	0. 063	1. 772	1. 774	0. 3459	1. 2929
0. 60	0. 060	1. 772	1. 773	0. 3465	1. 3106
0. 61	0. 056	1. 771	1. 772	0. 3471	1. 3283
0. 62	0. 053	1. 770	1. 771	0. 3476	1. 3461
0. 63	0. 050	1. 769	1. 770	0. 3482	1. 3637
0. 64	0. 048	1. 769	1. 769	0. 3487	1. 3814
0. 65	0. 045	1. 768	1. 769	0. 3491	1. 3991
0. 66	0. 043	1. 768	1. 768	0. 3496	1. 4168
0. 67	0. 040	1. 767	1. 768	0. 3500	1. 4345
0. 68	0. 038	1. 767	1. 767	0. 3504	1. 4521
0. 69	0. 036	1. 766	1. 767	0. 3507	1. 4698
0. 70	0. 034	1. 766	1. 766	0. 3511	1. 4875

TABLE PT17

DIAMETER =57.40 MICRONS
SLURRY FLOWRATE=P4
PLOT CODE=1

TIME (S)	VELOCITY (M/S) HORIZONTAL	VERTICAL	RESULTANT	DISTANCE (M) HORIZONTAL	VERTICAL
0.00	2.891	5.006	5.781	0.0000	0.0000
0.01	0.582	1.060	1.209	0.0137	0.0240
0.02	0.178	0.383	0.422	0.0170	0.0305
0.03	0.063	0.197	0.207	0.0181	0.0332
0.04	0.024	0.137	0.139	0.0185	0.0348
0.05	0.009	0.116	0.116	0.0187	0.0360
0.06	0.004	0.109	0.109	0.0188	0.0372
0.07	0.001	0.106	0.106	0.0188	0.0382
0.08	0.001	0.105	0.105	0.0188	0.0393
0.09	0.000	0.104	0.104	0.0188	0.0403
0.10	0.000	0.104	0.104	0.0188	0.0414
0.11	0.000	0.104	0.104	0.0188	0.0424
0.12	0.000	0.104	0.104	0.0188	0.0435
0.13	0.000	0.104	0.104	0.0188	0.0445
0.14	0.000	0.104	0.104	0.0188	0.0455
0.15	0.000	0.104	0.104	0.0188	0.0466
0.16	0.000	0.104	0.104	0.0188	0.0476
0.17	0.000	0.104	0.104	0.0188	0.0487
0.18	0.000	0.104	0.104	0.0188	0.0497
0.19	0.000	0.104	0.104	0.0188	0.0508
0.20	0.000	0.104	0.104	0.0188	0.0518
0.21	0.000	0.104	0.104	0.0188	0.0528
0.22	0.000	0.104	0.104	0.0188	0.0539
0.23	0.000	0.104	0.104	0.0188	0.0549
0.24	0.000	0.104	0.104	0.0188	0.0560
0.25	0.000	0.104	0.104	0.0188	0.0570
0.26	0.000	0.104	0.104	0.0188	0.0581
0.27	0.000	0.104	0.104	0.0188	0.0591
0.28	0.000	0.104	0.104	0.0188	0.0601

TABLE PT18

DIAMETER =74.45 MICRONS
SLURRY FLOWRATE=P4
PLOT CODE=2

TIME (S)	VELOCITY (M/S) HORIZONTAL	VERTICAL	RESULTANT	DISTANCE (M) HORIZONTAL	VERTICAL
0.00	2.891	5.006	5.781	0.0000	0.0000
0.01	0.998	1.792	2.051	0.0170	0.0298
0.02	0.413	0.808	0.908	0.0235	0.0418
0.03	0.198	0.457	0.499	0.0264	0.0478
0.04	0.102	0.308	0.325	0.0278	0.0516
0.05	0.054	0.237	0.243	0.0286	0.0543
0.06	0.029	0.202	0.204	0.0290	0.0564
0.07	0.016	0.184	0.184	0.0292	0.0583
0.08	0.009	0.174	0.175	0.0293	0.0601
0.09	0.005	0.170	0.170	0.0294	0.0618
0.10	0.003	0.167	0.167	0.0294	0.0635
0.11	0.001	0.166	0.166	0.0294	0.0652
0.12	0.001	0.165	0.165	0.0294	0.0668
0.13	0.000	0.165	0.165	0.0294	0.0685
0.14	0.000	0.165	0.165	0.0294	0.0701
0.15	0.000	0.165	0.165	0.0295	0.0718
0.16	0.000	0.165	0.165	0.0295	0.0734
0.17	0.000	0.165	0.165	0.0295	0.0751
0.18	0.000	0.165	0.165	0.0295	0.0767
0.19	0.000	0.165	0.165	0.0295	0.0784
0.20	0.000	0.165	0.165	0.0295	0.0800
0.21	0.000	0.165	0.165	0.0295	0.0817
0.22	0.000	0.165	0.165	0.0295	0.0833
0.23	0.000	0.165	0.165	0.0295	0.0850
0.24	0.000	0.165	0.165	0.0295	0.0866
0.25	0.000	0.165	0.165	0.0295	0.0882
0.26	0.000	0.165	0.165	0.0295	0.0899
0.27	0.000	0.165	0.165	0.0295	0.0915
0.28	0.000	0.165	0.165	0.0295	0.0932
0.29	0.000	0.165	0.165	0.0295	0.0948
0.30	0.000	0.165	0.165	0.0295	0.0965
0.31	0.000	0.165	0.165	0.0295	0.0981
0.32	0.000	0.165	0.165	0.0295	0.0998
0.33	0.000	0.165	0.165	0.0295	0.1014
0.34	0.000	0.165	0.165	0.0295	0.1031
0.35	0.000	0.165	0.165	0.0295	0.1047
0.36	0.000	0.165	0.165	0.0295	0.1063
0.37	0.000	0.165	0.165	0.0295	0.1080
0.38	0.000	0.165	0.165	0.0295	0.1096
0.39	0.000	0.165	0.165	0.0295	0.1113
0.40	0.000	0.165	0.165	0.0295	0.1129
0.41	0.000	0.165	0.165	0.0295	0.1146
0.42	0.000	0.165	0.165	0.0295	0.1162

TABLE PT19

DIAMETER =98.55 MICRONS
SLURRY FLOWRATE=P4
PLOT CODE=3

TIME (S)	VELOCITY (M/S) HORIZONTAL	VERTICAL	RESULTANT	DISTANCE (M) HORIZONTAL	VERTICAL
0.00	2.891	5.006	5.781	0.0000	0.0000
0.01	1.366	2.436	2.792	0.0200	0.0350
0.02	0.780	1.467	1.662	0.0303	0.0538
0.03	0.455	0.932	1.037	0.0363	0.0656
0.04	0.286	0.665	0.724	0.0400	0.0734
0.05	0.184	0.508	0.540	0.0423	0.0792
0.06	0.122	0.415	0.433	0.0438	0.0838
0.07	0.082	0.360	0.369	0.0448	0.0877
0.08	0.056	0.326	0.331	0.0455	0.0911
0.09	0.038	0.304	0.307	0.0459	0.0942
0.10	0.026	0.291	0.292	0.0462	0.0972
0.11	0.018	0.282	0.282	0.0465	0.1001
0.12	0.012	0.276	0.276	0.0466	0.1028
0.13	0.009	0.272	0.272	0.0467	0.1056
0.14	0.006	0.270	0.270	0.0468	0.1083
0.15	0.004	0.268	0.268	0.0468	0.1110
0.16	0.003	0.267	0.267	0.0469	0.1136
0.17	0.002	0.266	0.266	0.0469	0.1163
0.18	0.001	0.266	0.266	0.0469	0.1190
0.19	0.001	0.266	0.266	0.0469	0.1216
0.20	0.001	0.265	0.265	0.0469	0.1243
0.21	0.000	0.265	0.265	0.0469	0.1269
0.22	0.000	0.265	0.265	0.0469	0.1296
0.23	0.000	0.265	0.265	0.0469	0.1322
0.24	0.000	0.265	0.265	0.0469	0.1349
0.25	0.000	0.265	0.265	0.0469	0.1375
0.26	0.000	0.265	0.265	0.0469	0.1402
0.27	0.000	0.265	0.265	0.0469	0.1428
0.28	0.000	0.265	0.265	0.0469	0.1455
0.29	0.000	0.265	0.265	0.0469	0.1481
0.30	0.000	0.265	0.265	0.0469	0.1508
0.31	0.000	0.265	0.265	0.0469	0.1534
0.32	0.000	0.265	0.265	0.0469	0.1561
0.33	0.000	0.265	0.265	0.0469	0.1587
0.34	0.000	0.265	0.265	0.0469	0.1614
0.35	0.000	0.265	0.265	0.0469	0.1640
0.36	0.000	0.265	0.265	0.0469	0.1667
0.37	0.000	0.265	0.265	0.0469	0.1693
0.38	0.000	0.265	0.265	0.0469	0.1720
0.39	0.000	0.265	0.265	0.0469	0.1746
0.40	0.000	0.265	0.265	0.0469	0.1773
0.41	0.000	0.265	0.265	0.0469	0.1799
0.42	0.000	0.265	0.265	0.0469	0.1826

TABLE PT20

DIAMETER =136.55 MICRONS
SLURRY FLOWRATE=P4
PLOT CODE=4

TIME (S)	VELOCITY (M/S) HORIZONTAL	VERTICAL	RESULTANT	DISTANCE (M) HORIZONTAL	VERTICAL
0.00	2.891	5.006	5.781	0.0000	0.0000
0.01	1.798	3.193	3.664	0.0228	0.0400
0.02	1.206	2.223	2.530	0.0376	0.0666
0.03	0.852	1.653	1.860	0.0477	0.0857
0.04	0.629	1.305	1.448	0.0550	0.1004
0.05	0.483	1.089	1.191	0.0606	0.1123
0.06	0.373	0.926	0.998	0.0648	0.1224
0.07	0.275	0.767	0.815	0.0680	0.1308
0.08	0.212	0.678	0.710	0.0705	0.1380
0.09	0.166	0.618	0.640	0.0723	0.1444
0.10	0.131	0.574	0.588	0.0738	0.1504
0.11	0.103	0.540	0.550	0.0750	0.1559
0.12	0.081	0.514	0.520	0.0759	0.1612
0.13	0.064	0.494	0.498	0.0766	0.1662
0.14	0.051	0.479	0.482	0.0772	0.1711
0.15	0.040	0.468	0.469	0.0776	0.1758
0.16	0.032	0.459	0.460	0.0780	0.1805
0.17	0.026	0.452	0.453	0.0783	0.1850
0.18	0.020	0.447	0.448	0.0785	0.1895
0.19	0.016	0.443	0.443	0.0787	0.1940
0.20	0.013	0.440	0.440	0.0788	0.1984
0.21	0.010	0.438	0.438	0.0790	0.2028
0.22	0.008	0.436	0.436	0.0790	0.2071
0.23	0.006	0.435	0.435	0.0791	0.2115
0.24	0.005	0.434	0.434	0.0792	0.2158
0.25	0.004	0.433	0.433	0.0792	0.2202
0.26	0.003	0.433	0.433	0.0793	0.2245
0.27	0.003	0.432	0.432	0.0793	0.2288
0.28	0.002	0.432	0.432	0.0793	0.2331
0.29	0.002	0.432	0.432	0.0793	0.2375
0.30	0.001	0.432	0.432	0.0793	0.2418
0.31	0.001	0.431	0.431	0.0794	0.2461
0.32	0.001	0.431	0.431	0.0794	0.2504
0.33	0.001	0.431	0.431	0.0794	0.2547
0.34	0.001	0.431	0.431	0.0794	0.2590
0.35	0.000	0.431	0.431	0.0794	0.2634
0.36	0.000	0.431	0.431	0.0794	0.2677
0.37	0.000	0.431	0.431	0.0794	0.2720
0.38	0.000	0.431	0.431	0.0794	0.2763
0.39	0.000	0.431	0.431	0.0794	0.2806
0.40	0.000	0.431	0.431	0.0794	0.2849
0.41	0.000	0.431	0.431	0.0794	0.2892
0.42	0.000	0.431	0.431	0.0794	0.2935

TABLE PT21

DIAMETER =210.95 MICRONS
SLURRY FLOWRATE=P4
PLOT CODE=5

TIME (S)	VELOCITY (M/S) HORIZONTAL	VERTICAL	RESULTANT	DISTANCE (M) HORIZONTAL	VERTICAL
0.00	2.891	5.006	5.781	0.0000	0.0000
0.01	2.228	3.945	4.531	0.0254	0.0444
0.02	1.767	3.217	3.671	0.0452	0.0800
0.03	1.433	2.697	3.053	0.0611	0.1094
0.04	1.180	2.311	2.594	0.0741	0.1344
0.05	0.984	2.017	2.244	0.0849	0.1560
0.06	0.829	1.789	1.972	0.0940	0.1749
0.07	0.704	1.609	1.757	0.1016	0.1919
0.08	0.602	1.467	1.586	0.1081	0.2072
0.09	0.518	1.353	1.448	0.1137	0.2213
0.10	0.448	1.261	1.338	0.1185	0.2344
0.11	0.389	1.187	1.249	0.1227	0.2466
0.12	0.339	1.127	1.177	0.1263	0.2582
0.13	0.297	1.078	1.118	0.1295	0.2692
0.14	0.261	1.039	1.071	0.1323	0.2798
0.15	0.230	1.007	1.033	0.1347	0.2900
0.16	0.203	0.981	1.002	0.1369	0.2999
0.17	0.179	0.960	0.977	0.1388	0.3096
0.18	0.159	0.943	0.956	0.1405	0.3191
0.19	0.141	0.929	0.940	0.1420	0.3285
0.20	0.125	0.918	0.927	0.1433	0.3377
0.21	0.111	0.909	0.916	0.1445	0.3468
0.22	0.099	0.902	0.907	0.1455	0.3559
0.23	0.088	0.896	0.900	0.1465	0.3649
0.24	0.079	0.891	0.894	0.1473	0.3738
0.25	0.070	0.887	0.890	0.1481	0.3827
0.26	0.063	0.884	0.886	0.1487	0.3916
0.27	0.056	0.881	0.883	0.1493	0.4004
0.28	0.050	0.879	0.880	0.1498	0.4092
0.29	0.044	0.877	0.878	0.1503	0.4180
0.30	0.040	0.876	0.877	0.1507	0.4267
0.31	0.035	0.875	0.875	0.1511	0.4355
0.32	0.032	0.874	0.874	0.1514	0.4442
0.33	0.028	0.873	0.873	0.1517	0.4529
0.34	0.025	0.872	0.873	0.1520	0.4617
0.35	0.023	0.872	0.872	0.1522	0.4704
0.36	0.020	0.871	0.872	0.1525	0.4791
0.37	0.018	0.871	0.871	0.1527	0.4878
0.38	0.016	0.871	0.871	0.1528	0.4965
0.39	0.014	0.871	0.871	0.1530	0.5052
0.40	0.013	0.870	0.871	0.1531	0.5139
0.41	0.011	0.870	0.870	0.1532	0.5226
0.42	0.010	0.870	0.870	0.1533	0.5314

0. 43	0. 009	0. 870	0. 870
0. 44	0. 008	0. 870	0. 870
0. 45	0. 007	0. 870	0. 870
0. 46	0. 007	0. 870	0. 870
0. 47	0. 006	0. 870	0. 870
0. 48	0. 005	0. 870	0. 870
0. 49	0. 005	0. 870	0. 870
0. 50	0. 004	0. 870	0. 870
0. 51	0. 004	0. 870	0. 870
0. 52	0. 003	0. 870	0. 870
0. 53	0. 003	0. 870	0. 870
0. 54	0. 003	0. 870	0. 870
0. 55	0. 002	0. 870	0. 870
0. 56	0. 002	0. 870	0. 870
0. 57	0. 002	0. 870	0. 870
0. 58	0. 002	0. 870	0. 870
0. 59	0. 002	0. 870	0. 870
0. 60	0. 001	0. 870	0. 870
0. 61	0. 001	0. 870	0. 870
0. 62	0. 001	0. 870	0. 870
0. 63	0. 001	0. 870	0. 870
0. 64	0. 001	0. 870	0. 870
0. 65	0. 001	0. 870	0. 870
0. 66	0. 001	0. 870	0. 870
0. 67	0. 001	0. 870	0. 870
0. 68	0. 001	0. 870	0. 870
0. 69	0. 000	0. 870	0. 870
0. 70	0. 000	0. 870	0. 870
0. 71	0. 000	0. 870	0. 870
0. 72	0. 000	0. 870	0. 870
0. 73	0. 000	0. 870	0. 870
0. 74	0. 000	0. 870	0. 870
0. 75	0. 000	0. 870	0. 870
0. 76	0. 000	0. 870	0. 870
0. 77	0. 000	0. 870	0. 870
0. 78	0. 000	0. 870	0. 870
0. 79	0. 000	0. 870	0. 870
0. 80	0. 000	0. 870	0. 870
0. 81	0. 000	0. 870	0. 870
0. 82	0. 000	0. 870	0. 870
0. 83	0. 000	0. 870	0. 870
0. 84	0. 000	0. 870	0. 870
0. 85	0. 000	0. 870	0. 870
0. 86	0. 000	0. 870	0. 870
0. 87	0. 000	0. 870	0. 870
0. 88	0. 000	0. 870	0. 870
0. 89	0. 000	0. 870	0. 870
0. 90	0. 000	0. 870	0. 870
0. 91	0. 000	0. 870	0. 870
0. 92	0. 000	0. 870	0. 870
0. 93	0. 000	0. 870	0. 870
0. 94	0. 000	0. 870	0. 870
0. 95	0. 000	0. 870	0. 870
0. 96	0. 000	0. 870	0. 870
0. 97	0. 000	0. 870	0. 870
0. 98	0. 000	0. 870	0. 870
0. 99	0. 000	0. 870	0. 870
1. 00	0. 000	0. 870	0. 870
1. 01	0. 000	0. 870	0. 870
1. 02	0. 000	0. 870	0. 870

0. 1534	0. 5401
0. 1535	0. 5488
0. 1536	0. 5575
0. 1537	0. 5662
0. 1537	0. 5749
0. 1538	0. 5836
0. 1538	0. 5922
0. 1539	0. 6009
0. 1539	0. 6096
0. 1540	0. 6183
0. 1540	0. 6270
0. 1540	0. 6357
0. 1540	0. 6444
0. 1541	0. 6531
0. 1541	0. 6618
0. 1541	0. 6705
0. 1541	0. 6792
0. 1541	0. 6879
0. 1541	0. 6966
0. 1542	0. 7053
0. 1542	0. 7140
0. 1542	0. 7227
0. 1542	0. 7314
0. 1542	0. 7401
0. 1542	0. 7488
0. 1542	0. 7575
0. 1542	0. 7662
0. 1542	0. 7749
0. 1542	0. 7836
0. 1542	0. 7923
0. 1542	0. 8010
0. 1542	0. 8097
0. 1542	0. 8184
0. 1542	0. 8271
0. 1542	0. 8358
0. 1542	0. 8445
0. 1542	0. 8532
0. 1542	0. 8619
0. 1542	0. 8706
0. 1542	0. 8793
0. 1542	0. 8880
0. 1542	0. 8967
0. 1542	0. 9054
0. 1542	0. 9140
0. 1542	0. 9227
0. 1542	0. 9314
0. 1542	0. 9401
0. 1542	0. 9488
0. 1542	0. 9575
0. 1542	0. 9662
0. 1542	0. 9749
0. 1542	0. 9836
0. 1542	0. 9923
0. 1542	1. 0010
0. 1542	1. 0097
0. 1542	1. 0184
0. 1542	1. 0271
0. 1542	1. 0358
0. 1542	1. 0445
0. 1542	1. 0532

TABLE PT22

DIAMETER =412.80 MICRONS
SLURRY FLOWRATE=P4
PLOT CODE=6

TIME (S)	VELOCITY (M/S) HORIZONTAL	VERTICAL	RESULTANT	DISTANCE (M) HORIZONTAL	VERTICAL
0.00	2.891	5.006	5.781	0.0000	0.0000
0.01	2.617	4.627	5.316	0.0275	0.0481
0.02	2.379	4.300	4.914	0.0525	0.0927
0.03	2.171	4.017	4.566	0.0752	0.1343
0.04	1.987	3.770	4.261	0.0960	0.1732
0.05	1.824	3.554	3.994	0.1150	0.2098
0.06	1.678	3.364	3.760	0.1325	0.2443
0.07	1.548	3.197	3.552	0.1486	0.2771
0.08	1.431	3.050	3.369	0.1635	0.3083
0.09	1.325	2.919	3.206	0.1773	0.3382
0.10	1.230	2.804	3.061	0.1900	0.3668
0.11	1.143	2.701	2.933	0.2019	0.3943
0.12	1.064	2.609	2.818	0.2129	0.4208
0.13	0.992	2.527	2.715	0.2232	0.4465
0.14	0.926	2.454	2.623	0.2328	0.4714
0.15	0.866	2.388	2.540	0.2417	0.4956
0.16	0.810	2.329	2.466	0.2501	0.5192
0.17	0.759	2.277	2.400	0.2579	0.5422
0.18	0.711	2.229	2.340	0.2653	0.5647
0.19	0.667	2.186	2.286	0.2722	0.5868
0.20	0.626	2.148	2.237	0.2786	0.6085
0.21	0.589	2.113	2.193	0.2847	0.6298
0.22	0.553	2.081	2.153	0.2904	0.6507
0.23	0.520	2.053	2.118	0.2958	0.6714
0.24	0.490	2.027	2.085	0.3008	0.6918
0.25	0.461	2.003	2.056	0.3056	0.7119
0.26	0.434	1.982	2.029	0.3101	0.7319
0.27	0.409	1.963	2.005	0.3143	0.7516
0.28	0.386	1.945	1.983	0.3183	0.7711
0.29	0.364	1.929	1.963	0.3220	0.7905
0.30	0.343	1.915	1.945	0.3255	0.8097
0.31	0.324	1.902	1.929	0.3289	0.8288
0.32	0.305	1.890	1.914	0.3320	0.8478
0.33	0.288	1.879	1.901	0.3350	0.8666
0.34	0.272	1.869	1.888	0.3378	0.8853
0.35	0.257	1.860	1.877	0.3404	0.9040
0.36	0.243	1.851	1.867	0.3429	0.9225
0.37	0.229	1.844	1.858	0.3453	0.9410
0.38	0.216	1.837	1.849	0.3475	0.9594
0.39	0.204	1.830	1.842	0.3496	0.9777
0.40	0.193	1.825	1.835	0.3516	0.9960
0.41	0.182	1.819	1.829	0.3535	1.0142
0.42	0.172	1.815	1.823	0.3552	1.0324

0. 43	0. 163	1. 810	1. 817	0. 3569	1. 0505
0. 44	0. 154	1. 806	1. 813	0. 3585	1. 0686
0. 45	0. 146	1. 802	1. 808	0. 3600	1. 0867
0. 46	0. 138	1. 799	1. 804	0. 3614	1. 1047
0. 47	0. 130	1. 796	1. 801	0. 3628	1. 1226
0. 48	0. 123	1. 793	1. 797	0. 3640	1. 1406
0. 49	0. 116	1. 791	1. 794	0. 3652	1. 1585
0. 50	0. 110	1. 788	1. 792	0. 3663	1. 1764
0. 51	0. 104	1. 786	1. 789	0. 3674	1. 1943
0. 52	0. 098	1. 784	1. 787	0. 3684	1. 2121
0. 53	0. 093	1. 782	1. 785	0. 3694	1. 2299
0. 54	0. 088	1. 781	1. 783	0. 3703	1. 2478
0. 55	0. 083	1. 779	1. 781	0. 3711	1. 2656
0. 56	0. 079	1. 778	1. 779	0. 3719	1. 2833
0. 57	0. 074	1. 776	1. 778	0. 3727	1. 3011
0. 58	0. 070	1. 775	1. 776	0. 3734	1. 3189
0. 59	0. 066	1. 774	1. 775	0. 3741	1. 3366
0. 60	0. 063	1. 773	1. 774	0. 3748	1. 3543
0. 61	0. 059	1. 772	1. 773	0. 3754	1. 3721
0. 62	0. 056	1. 771	1. 772	0. 3759	1. 3898
0. 63	0. 053	1. 771	1. 771	0. 3765	1. 4075
0. 64	0. 050	1. 770	1. 771	0. 3770	1. 4252
0. 65	0. 048	1. 769	1. 770	0. 3775	1. 4429
0. 66	0. 045	1. 769	1. 769	0. 3780	1. 4606
0. 67	0. 043	1. 768	1. 769	0. 3784	1. 4783
0. 68	0. 040	1. 768	1. 768	0. 3788	1. 4959

TABLE PT23

DIAMETER =57.40 MICRONS
SLURRY FLOWRATE=P5
PLOT CODE=1

TIME (S)	VELOCITY (M/S) HORIZONTAL	VERTICAL	RESULTANT	DISTANCE (M) HORIZONTAL	VERTICAL
0.00	3.167	5.485	6.333	0.0000	0.0000
0.01	0.625	1.134	1.295	0.0148	0.0260
0.02	0.188	0.400	0.442	0.0184	0.0328
0.03	0.067	0.203	0.214	0.0195	0.0356
0.04	0.025	0.139	0.141	0.0200	0.0373
0.05	0.010	0.117	0.117	0.0201	0.0385
0.06	0.004	0.109	0.109	0.0202	0.0396
0.07	0.001	0.106	0.106	0.0202	0.0407
0.08	0.001	0.105	0.105	0.0202	0.0418
0.09	0.000	0.104	0.104	0.0202	0.0428
0.10	0.000	0.104	0.104	0.0202	0.0438
0.11	0.000	0.104	0.104	0.0202	0.0449
0.12	0.000	0.104	0.104	0.0202	0.0459
0.13	0.000	0.104	0.104	0.0202	0.0470
0.14	0.000	0.104	0.104	0.0202	0.0480
0.15	0.000	0.104	0.104	0.0202	0.0491
0.16	0.000	0.104	0.104	0.0202	0.0501
0.17	0.000	0.104	0.104	0.0202	0.0511
0.18	0.000	0.104	0.104	0.0202	0.0522
0.19	0.000	0.104	0.104	0.0202	0.0532
0.20	0.000	0.104	0.104	0.0202	0.0543
0.21	0.000	0.104	0.104	0.0202	0.0553
0.22	0.000	0.104	0.104	0.0202	0.0564
0.23	0.000	0.104	0.104	0.0202	0.0574
0.24	0.000	0.104	0.104	0.0202	0.0584
0.25	0.000	0.104	0.104	0.0202	0.0595
0.26	0.000	0.104	0.104	0.0202	0.0605
0.27	0.000	0.104	0.104	0.0202	0.0616
0.28	0.000	0.104	0.104	0.0202	0.0626

TABLE PT24

DIAMETER =74.45 MICRONS
SLURRY FLOWRATE=P5
PLOT CODE=2

TIME	VELOCITY (M/S)			DISTANCE (M)	
(S)	HORIZONTAL	VERTICAL	RESULTANT	HORIZONTAL	VERTICAL
0.00	3.167	5.485	6.333	0.0000	0.0000
0.01	1.051	1.883	2.156	0.0183	0.0320
0.02	0.438	0.851	0.957	0.0252	0.0448
0.03	0.208	0.475	0.518	0.0283	0.0511
0.04	0.107	0.316	0.334	0.0298	0.0550
0.05	0.057	0.241	0.247	0.0306	0.0577
0.06	0.031	0.204	0.206	0.0310	0.0599
0.07	0.017	0.185	0.185	0.0312	0.0619
0.08	0.009	0.175	0.175	0.0314	0.0636
0.09	0.005	0.170	0.170	0.0314	0.0654
0.10	0.003	0.167	0.167	0.0315	0.0671
0.11	0.002	0.166	0.166	0.0315	0.0687
0.12	0.001	0.165	0.165	0.0315	0.0704
0.13	0.000	0.165	0.165	0.0315	0.0720
0.14	0.000	0.165	0.165	0.0315	0.0737
0.15	0.000	0.165	0.165	0.0315	0.0753
0.16	0.000	0.165	0.165	0.0315	0.0770
0.17	0.000	0.165	0.165	0.0315	0.0786
0.18	0.000	0.165	0.165	0.0315	0.0803
0.19	0.000	0.165	0.165	0.0315	0.0819
0.20	0.000	0.165	0.165	0.0315	0.0835
0.21	0.000	0.165	0.165	0.0315	0.0852
0.22	0.000	0.165	0.165	0.0315	0.0868
0.23	0.000	0.165	0.165	0.0315	0.0885
0.24	0.000	0.165	0.165	0.0315	0.0901
0.25	0.000	0.165	0.165	0.0315	0.0918
0.26	0.000	0.165	0.165	0.0315	0.0934
0.27	0.000	0.165	0.165	0.0315	0.0951
0.28	0.000	0.165	0.165	0.0315	0.0967
0.29	0.000	0.165	0.165	0.0315	0.0984
0.30	0.000	0.165	0.165	0.0315	0.1000
0.31	0.000	0.165	0.165	0.0315	0.1016
0.32	0.000	0.165	0.165	0.0315	0.1033
0.33	0.000	0.165	0.165	0.0315	0.1049
0.34	0.000	0.165	0.165	0.0315	0.1066
0.35	0.000	0.165	0.165	0.0315	0.1082
0.36	0.000	0.165	0.165	0.0315	0.1099
0.37	0.000	0.165	0.165	0.0315	0.1115
0.38	0.000	0.165	0.165	0.0315	0.1132
0.39	0.000	0.165	0.165	0.0315	0.1148
0.40	0.000	0.165	0.165	0.0315	0.1165
0.41	0.000	0.165	0.165	0.0315	0.1181
0.42	0.000	0.165	0.165	0.0315	0.1197

TABLE PT25

DIAMETER =98.55 MICRONS
SLURRY FLOWRATE=P5
PLOT CODE =3

TIME (S)	VELOCITY (M/S) HORIZONTAL	VERTICAL	RESULTANT	DISTANCE (M) HORIZONTAL	VERTICAL
0.00	3.167	5.485	6.333	0.0000	0.0000
0.01	1.460	2.598	2.981	0.0216	0.0378
0.02	0.819	1.533	1.738	0.0325	0.0577
0.03	0.479	0.971	1.083	0.0389	0.0701
0.04	0.299	0.686	0.749	0.0427	0.0782
0.05	0.192	0.520	0.555	0.0452	0.0842
0.06	0.127	0.423	0.442	0.0467	0.0888
0.07	0.085	0.365	0.375	0.0478	0.0928
0.08	0.058	0.329	0.334	0.0485	0.0962
0.09	0.039	0.306	0.309	0.0490	0.0994
0.10	0.027	0.292	0.293	0.0493	0.1024
0.11	0.019	0.282	0.283	0.0495	0.1052
0.12	0.013	0.276	0.277	0.0497	0.1080
0.13	0.009	0.272	0.273	0.0498	0.1108
0.14	0.006	0.270	0.270	0.0498	0.1135
0.15	0.004	0.268	0.268	0.0499	0.1162
0.16	0.003	0.267	0.267	0.0499	0.1188
0.17	0.002	0.266	0.266	0.0500	0.1215
0.18	0.001	0.266	0.266	0.0500	0.1242
0.19	0.001	0.266	0.266	0.0500	0.1268
0.20	0.001	0.265	0.265	0.0500	0.1295
0.21	0.000	0.265	0.265	0.0500	0.1321
0.22	0.000	0.265	0.265	0.0500	0.1348
0.23	0.000	0.265	0.265	0.0500	0.1374
0.24	0.000	0.265	0.265	0.0500	0.1401
0.25	0.000	0.265	0.265	0.0500	0.1427
0.26	0.000	0.265	0.265	0.0500	0.1454
0.27	0.000	0.265	0.265	0.0500	0.1480
0.28	0.000	0.265	0.265	0.0500	0.1507
0.29	0.000	0.265	0.265	0.0500	0.1533
0.30	0.000	0.265	0.265	0.0500	0.1560
0.31	0.000	0.265	0.265	0.0500	0.1586
0.32	0.000	0.265	0.265	0.0500	0.1613
0.33	0.000	0.265	0.265	0.0500	0.1639
0.34	0.000	0.265	0.265	0.0500	0.1666
0.35	0.000	0.265	0.265	0.0500	0.1692
0.36	0.000	0.265	0.265	0.0500	0.1719
0.37	0.000	0.265	0.265	0.0500	0.1745
0.38	0.000	0.265	0.265	0.0500	0.1772
0.39	0.000	0.265	0.265	0.0500	0.1798
0.40	0.000	0.265	0.265	0.0500	0.1825
0.41	0.000	0.265	0.265	0.0500	0.1851
0.42	0.000	0.265	0.265	0.0500	0.1878

TABLE PT26

DIAMETER =136.55 MICRONS
SLURRY FLOWRATE=P5
PLOT CODE =4

TIME (S)	VELOCITY (M/S) HORIZONTAL	VERTICAL	RESULTANT	DISTANCE (M) HORIZONTAL	VERTICAL
0.00	3.167	5.485	6.333	0.0000	0.0000
0.01	1.934	3.428	3.936	0.0248	0.0433
0.02	1.284	2.357	2.684	0.0406	0.0717
0.03	0.900	1.734	1.953	0.0513	0.0919
0.04	0.659	1.354	1.506	0.0590	0.1072
0.05	0.503	1.120	1.228	0.0648	0.1195
0.06	0.394	0.964	1.041	0.0692	0.1299
0.07	0.288	0.789	0.840	0.0726	0.1386
0.08	0.221	0.692	0.726	0.0751	0.1460
0.09	0.173	0.628	0.651	0.0771	0.1525
0.10	0.136	0.581	0.597	0.0786	0.1586
0.11	0.107	0.545	0.556	0.0798	0.1642
0.12	0.085	0.518	0.525	0.0808	0.1695
0.13	0.067	0.498	0.502	0.0815	0.1746
0.14	0.053	0.482	0.485	0.0821	0.1795
0.15	0.042	0.469	0.471	0.0826	0.1842
0.16	0.033	0.460	0.461	0.0830	0.1889
0.17	0.027	0.453	0.454	0.0833	0.1934
0.18	0.021	0.448	0.448	0.0835	0.1979
0.19	0.017	0.444	0.444	0.0837	0.2024
0.20	0.013	0.441	0.441	0.0839	0.2068
0.21	0.011	0.438	0.439	0.0840	0.2112
0.22	0.008	0.437	0.437	0.0841	0.2156
0.23	0.007	0.435	0.435	0.0842	0.2199
0.24	0.005	0.434	0.434	0.0842	0.2243
0.25	0.004	0.433	0.433	0.0843	0.2286
0.26	0.003	0.433	0.433	0.0843	0.2330
0.27	0.003	0.432	0.432	0.0843	0.2373
0.28	0.002	0.432	0.432	0.0844	0.2416
0.29	0.002	0.432	0.432	0.0844	0.2459
0.30	0.001	0.432	0.432	0.0844	0.2502
0.31	0.001	0.431	0.431	0.0844	0.2546
0.32	0.001	0.431	0.431	0.0844	0.2589
0.33	0.001	0.431	0.431	0.0844	0.2632
0.34	0.001	0.431	0.431	0.0844	0.2675
0.35	0.000	0.431	0.431	0.0844	0.2718
0.36	0.000	0.431	0.431	0.0844	0.2761
0.37	0.000	0.431	0.431	0.0844	0.2804
0.38	0.000	0.431	0.431	0.0844	0.2847
0.39	0.000	0.431	0.431	0.0844	0.2891
0.40	0.000	0.431	0.431	0.0844	0.2934
0.41	0.000	0.431	0.431	0.0844	0.2977
0.42	0.000	0.431	0.431	0.0844	0.3020

TABLE PT27

DIAMETER =210.95 MICRONS
SLURRY FLOWRATE=P5
PLOT CODE=5

TIME (S)	VELOCITY (M/S) HORIZONTAL	VERTICAL	RESULTANT	DISTANCE (M) HORIZONTAL	VERTICAL
0.00	3.167	5.485	6.333	0.0000	0.0000
0.01	2.412	4.264	4.899	0.0276	0.0483
0.02	1.897	3.440	3.928	0.0490	0.0866
0.03	1.527	2.859	3.241	0.0661	0.1179
0.04	1.252	2.432	2.735	0.0799	0.1443
0.05	1.040	2.110	2.353	0.0913	0.1669
0.06	0.873	1.862	2.057	0.1008	0.1867
0.07	0.740	1.667	1.824	0.1089	0.2043
0.08	0.631	1.513	1.639	0.1157	0.2202
0.09	0.542	1.390	1.492	0.1216	0.2347
0.10	0.468	1.291	1.373	0.1266	0.2481
0.11	0.406	1.211	1.277	0.1310	0.2606
0.12	0.353	1.146	1.200	0.1347	0.2723
0.13	0.309	1.094	1.137	0.1380	0.2835
0.14	0.271	1.052	1.086	0.1409	0.2943
0.15	0.238	1.017	1.045	0.1435	0.3046
0.16	0.210	0.990	1.012	0.1457	0.3146
0.17	0.186	0.967	0.985	0.1477	0.3244
0.18	0.165	0.949	0.963	0.1495	0.3340
0.19	0.146	0.934	0.945	0.1510	0.3434
0.20	0.130	0.922	0.931	0.1524	0.3527
0.21	0.115	0.912	0.919	0.1536	0.3618
0.22	0.103	0.904	0.910	0.1547	0.3709
0.23	0.091	0.898	0.902	0.1557	0.3799
0.24	0.081	0.892	0.896	0.1565	0.3889
0.25	0.073	0.888	0.891	0.1573	0.3978
0.26	0.065	0.885	0.887	0.1580	0.4066
0.27	0.058	0.882	0.884	0.1586	0.4155
0.28	0.052	0.880	0.881	0.1591	0.4243
0.29	0.046	0.878	0.879	0.1596	0.4331
0.30	0.041	0.876	0.877	0.1601	0.4418
0.31	0.037	0.875	0.876	0.1604	0.4506
0.32	0.033	0.874	0.875	0.1608	0.4593
0.33	0.029	0.873	0.874	0.1611	0.4681
0.34	0.026	0.873	0.873	0.1614	0.4768
0.35	0.023	0.872	0.872	0.1616	0.4855
0.36	0.021	0.872	0.872	0.1618	0.4942
0.37	0.019	0.871	0.871	0.1620	0.5030
0.38	0.017	0.871	0.871	0.1622	0.5117
0.39	0.015	0.871	0.871	0.1624	0.5204
0.40	0.013	0.871	0.871	0.1625	0.5291
0.41	0.012	0.870	0.870	0.1626	0.5378
0.42	0.011	0.870	0.870	0.1628	0.5465

TABLE PT28

DIAMETER =412.80 MICRONS
SLURRY FLOWRATE=P5
PLOT CODE=6

TIME (S)	VELOCITY (M/S) HORIZONTAL	VERTICAL	RESULTANT	DISTANCE (M) HORIZONTAL	VERTICAL
0.00	3.167	5.485	6.333	0.0000	0.0000
0.01	2.853	5.035	5.787	0.0301	0.0525
0.02	2.583	4.652	5.321	0.0572	0.1009
0.03	2.349	4.323	4.920	0.0818	0.1458
0.04	2.143	4.038	4.571	0.1043	0.1875
0.05	1.961	3.789	4.266	0.1248	0.2266
0.06	1.800	3.571	3.999	0.1436	0.2634
0.07	1.656	3.380	3.764	0.1608	0.2981
0.08	1.527	3.212	3.556	0.1767	0.3311
0.09	1.412	3.063	3.373	0.1914	0.3624
0.10	1.308	2.931	3.210	0.2050	0.3924
0.11	1.213	2.815	3.065	0.2176	0.4211
0.12	1.128	2.711	2.936	0.2293	0.4487
0.13	1.050	2.618	2.821	0.2402	0.4754
0.14	0.979	2.536	2.718	0.2503	0.5011
0.15	0.914	2.462	2.626	0.2598	0.5261
0.16	0.854	2.396	2.543	0.2686	0.5504
0.17	0.799	2.336	2.469	0.2769	0.5740
0.18	0.748	2.283	2.402	0.2846	0.5971
0.19	0.701	2.235	2.342	0.2918	0.6197
0.20	0.658	2.192	2.288	0.2986	0.6418
0.21	0.618	2.153	2.239	0.3050	0.6636
0.22	0.580	2.117	2.195	0.3110	0.6849
0.23	0.546	2.085	2.156	0.3166	0.7059
0.24	0.513	2.057	2.120	0.3219	0.7266
0.25	0.483	2.030	2.087	0.3269	0.7471
0.26	0.455	2.007	2.058	0.3316	0.7672
0.27	0.428	1.985	2.031	0.3360	0.7872
0.28	0.403	1.966	2.007	0.3402	0.8070
0.29	0.380	1.948	1.985	0.3441	0.8265
0.30	0.359	1.932	1.965	0.3478	0.8459
0.31	0.338	1.917	1.947	0.3513	0.8652
0.32	0.319	1.904	1.930	0.3545	0.8843
0.33	0.301	1.892	1.915	0.3576	0.9032
0.34	0.284	1.880	1.902	0.3606	0.9221
0.35	0.268	1.870	1.889	0.3633	0.9409
0.36	0.253	1.861	1.878	0.3659	0.9595
0.37	0.239	1.853	1.868	0.3684	0.9781
0.38	0.226	1.845	1.859	0.3707	0.9966
0.39	0.213	1.838	1.850	0.3729	1.0150
0.40	0.201	1.832	1.843	0.3750	1.0333
0.41	0.190	1.826	1.836	0.3769	1.0516
0.42	0.180	1.820	1.829	0.3788	1.0698

APPENDIX C

Program listing for Model 1 - Droplet residence time distribution.

```
1 C      PROGRAM NAME IS MODEL1
2        DIMENSION U(100),YR(100)
3        REAL A,B,J,K,L,M,N,YP(100),XE(100),YE(100)
4        REAL K1
5        COMMON/COM1/K1
6        COMMON/COM2/XP(100)
7        COMMON/COM3/TR(100)
8        COMMON/COM4/WR(200)
9        COMMON/COM5/XEND,H,I
10        INTEGER D
11        WRITE(12,5)
12     5 FORMAT(23X,'A',6X,'B',6X,'J',6X,'K',6X,'M',6X,'N',6X,'L')
13        YM=0.
14        L2=0
15        DO 10 J=1,22
16        READ(20,-)XP(J),YP(J)
17        READ(30,-)XE(J),YE(J)
18        IF (YP(J).GT.YM)YM=YP(J)
19        L2=L2+1
20     10 CONTINUE
21        P=XP(2)-XP(1)
22        E=XP(L2)
23     30 MMM=1
24        DO 35 J3=1,L2
25        U(J3)=0.
26        TR(J3)=0.
27        WR(J3)=0.
28        YR(J3)=0.
29     35 CONTINUE
30        WRITE(1,2500)
31   2500 FORMAT(1H1,'INPUT A,B,J,K,M,N,L')
32        READ(1,-)A,B,J,K,M,N,L
33        WRITE(12,37)A,B,J,K,M,N,L
34     37 FORMAT(20X,7F7.3)
35        IF (A.EQ.0.)GO TO 101
36        CALL FUN1(YP,L2,WR)
37        DO 40 J3=1,L2
38        TR(J3)=WR(J3)
39     40 CONTINUE
40        IF(ABS(J+K+M+N+L-1).LT.0.001)GO TO 55
41 C      CSTR1                                                  ST11
42        K1=A/(1-J-K-M-N-L)
43        WRITE(12,7700)K1
44        CALL FUN2(E)
45     55 DO 50 J3=1,L2
46        U(J3)=WR(J3)
47     50 CONTINUE
48        IF (J.EQ.0.)GO TO 80
49        DO 60 J3=1,L2
50        TR(J3)=U(J3)
51     60 CONTINUE
```

```
52          D=J/(A*P)+0.5                                                  PF1
53          WRITE(12,7800)D
54          CALL FUN3(D,L2,TR,WR)
55          DO 70 J3=1,L2
56          U(J3)=WR(J3)
57       70 CONTINUE
58       80 IF (K.EQ.0.)GO TO 101
59  C       CSTR                                                           ST12
60          DO 90 J3=1,L2
61          TR(J3)=U(J3)
62       90 CONTINUE
63          K1=A/K
64          WRITE(12,7700)K1
65          CALL FUN2(E)
66          DO 100 J3=1,L2
67          U(J3)=WR(J3)
68      100 CONTINUE
69      101 IF(B.EQ.0.)GO TO 151
70  C       DELAY                                                          PF2
71          CALL FUN1(YP,L2,WR)
72          DO 110 J3=1,L2
73          YR(J3)=WR(J3)
74          TR(J3)=WR(J3)
75      110 CONTINUE
76          IF(M.EQ.0.)GO TO 131
77          D=M/(B*P)+0.5
78          WRITE(12,7800)D
79          CALL FUN3(D,L2,TR,WR)
80          DO 120 J3=1,L2
81          YR(J3)=WR(J3)
82      120 CONTINUE
83      131 IF(N.EQ.0.)GO TO 151
84  C       CSTR                                                           ST2
85          DO 130 J3=1,L2
86          TR(J3)=YR(J3)
87      130 CONTINUE
88          K1=B/N
89          WRITE(12,7700)K1
90          CALL FUN2(E)
91          DO 140 J3=1,L2
92          YR(J3)=WR(J3)
93      140 CONTINUE
94      151 CALL FUN1(YP,L2,WR)
95          DO 150 J3=1,L2
96          TR(J3)=WR(J3)
97      150 CONTINUE
98          IF (ABS(1.-A-B).LT.0.001)GO TO 157
99  C       DELAY                                                          PF2
100          D=L/(P*(1.-A-B))+0.5
101          WRITE(12,7800)D
102          CALL FUN3(D,L2,TR,WR)
103 C        CALCULATE            RESPONSE
104      157 DO 160 J3=1,L2
105          WR(J3)=A*U(J3)+B*YR(J3)+(1.-A-B)*WR(J3)
106          WRITE(12,7200)XE(J3),YE(J3),WR(J3)
107      160 CONTINUE
108     7200 FORMAT(20X,F10.3,2F10.4)
109     7700 FORMAT(20X,F10.3)
110     7800 FORMAT(20X,I8)
111 C       SUM OF SQUARED ERRORS, VARIANCE AND STANDARD DEVIATION
```

```
      S1=0.
      DO 180 J=1,L2
      S1=S1+(YE(J)-WR(J))**2
  180 CONTINUE
      S2=S1/(L2-1)
      S3=SQRT(S2)
      WRITE(12,8500)S1,S2,S3
 8500 FORMAT(20X,'SUM OF SQUARED ERRORS=',F10.4/20X,
     2'VARIANCE=',F10.4/20X,'STANDARD DEVIATION=',F10.4)
      WRITE(1,200)
  200 FORMAT(1H1,'DO YOU WANT MORE TRIAL?')
      WRITE(1,201)
  201 FORMAT(1H1,'INPUT 1 FOR YES AND 0 FOR NO')
      READ(1,-)MMM
      IF (MMM.EQ.1)GO TO 30
      STOP
      END
      SUBROUTINE FUN1(YP,L2,WR)
      REAL YP(100),WR(200)
      DO 50 J2=1,L2
      WR(J2)=YP(J2)
   50 CONTINUE
      RETURN
      END
      SUBROUTINE FUN2(E)
      REAL H,XEND,TOL,X,W(2,7),Y(2)
      COMMON/COM5/XEND,H,I
      EXTERNAL FCN,OUT
      N=1
      I=1
      IR=1
      TOL=1.0E-6
      X=0.
      XEND=E
      Y(1)=0.
      IFAIL=1
      CALL D02BBF(X,XEND,N,Y,TOL,IR,FCN,OUT,W,IFAIL)
      IF(TOL.LT.0.)WRITE(12,5000)
 5000 FORMAT(5X,'RANGE TOO SHORT FOR TOL')
      IF (IFAIL.GT.0)WRITE(12,6000)IFAIL
 6000 FORMAT(5X,'IFAIL=',I1)
      RETURN
      END
      SUBROUTINE FCN(T,Y,F)
      REAL T,F(2),Y(2),K1
      COMMON/COM1/K1
      COMMON/COM3/TR(100)
      COMMON/COM5/XEND,H,I
      F(1)=K1*(TR(I)-Y(1))
      RETURN
      END
      SUBROUTINE OUT(X,Y)
      REAL X,Y(2),H,XEND
      COMMON/COM4/WR(100)
      COMMON/COM2/XP(100)
      COMMON/COM5/XEND,H,I
      WR(I)=Y(1)
      I=I+1
      X=XP(I)
      RETURN
```

```
172         END
173         SUBROUTINE FUN3(D,L2,TR,WR)
174         REAL TR(100),WR(100)
175         IF (D.LT.1)GOTO 50
176         IF(D.GT.L2)GO TO 60
177         DO 40 J2=1,L2
178         J2=L2+1-J2
179         IF(J2.LE.D)GO TO 70
180         U1=TR(J2-D)
181         GO TO 80
182      70 U1=0.
183      80 WR(J2)=U1
184      40 CONTINUE
185         GO TO 10
186      50 DO 20 J2=1,L2
187         WR(J2)=TR(J2)
188      20 CONTINUE
189         GO TO 10
190      60 DO 30 J2=1,L2
191         WR(J2)=0.
192      30 CONTINUE
193         GO TO 10
194      10 CONTINUE
195         RETURN
196         END
EOF..
```

APPENDIX D

1. Program listing for Model 2 - Droplets trajectories, D1
2. Table for Re against CRe^2 - D2

```
      PROGRAM FOR PARTICLE TRAJECTORY MODEL2
      REAL X(1000),Y(1000),T(1000),M1,D(20)
      REAL V5(5),V6(5),V7(5),V8(5)
      REAL V3(50),V4(50)
      REAL V1(20),V2(20),U2(20)
      REAL A1(20),A2(20),A3(20),A4(20)
      REAL B1(20),B2(20),B3(20),B4(20)
      REAL UR(1000),VH(1000),VV(1000)
      INTEGER N1,N2,N3,J,K,K1,K2,K3,K4,K5
       ANGLE=60.0
       ANGLE=ANGLE*0.0174533
       G=9.81456
       R1=1.2
       M1=0.0000176
       X(1)=0.0
       Y(1)=0.0
       T(1)=0.0
       D(7)=0.000027
       D(8)=0.00003465
       D(9)=0.0000446
       D(10)=0.0000574
       D(11)=0.00007445
       D(12)=0.00009855
       D(13)=0.00013655
       D(14)=0.00021095
       D(15)=0.0004128
       N1=8
       N2=10
       N3=7
       DO 50 I=1,N1
       READ(7,-)B1(I),A1(I),B4(I),A4(I)
   50 CONTINUE
       DO 60 I=1,N2
       READ(7,-)B2(I),A2(I)
   60 CONTINUE
       DO 70 I=1,N3
       READ(7,-)B3(I),A3(I)
   70 CONTINUE
       WRITE(1,72)
   72 FORMAT(5X,'INPUT SLURRY DENSITY AND VELOCITY')
       READ(1,-)R2,UE
       WRITE(1,74)
   74 FORMAT(5X,'INPUT THE START AND END POINT OF DIAMETERS',5X,
     *'TO BE READ IN')
       READ(1,76)JSTART,JSTOP
   76 FORMAT(2I2)
       DO 500 JA=JSTART,JSTOP
       U=UE
       R4=R1*U*D(JA)/M1
       U2(1)=U
       V1(1)=U*SIN(ANGLE/2)
```

```
52        V2(1)=U*COS(ANGLE/2)
53        VH(1)=V1(1)
54        VV(1)=V2(1)
55        UR(1)=U2(1)
56        CALL INTAPO(R4,C,A1,B1,A2,B2,A3,B3,A4,B4,N1,N2,N3)
57        K2=1
58        K3=1
59        K4=10
60        K5=1
61        K=1
62        V3(1)=V1(1)
63        V4(1)=V2(1)
64        U2(1)=U
65        DO 300 J=1,5000
66        K1=1
67        M3=1
68   130  V5(K1)=-(3.*R1*C*V3(K)*U/(4.*R2*D(JA)))*0.001
69        V6(K1)=(G*((R2-R1)/R2)-(3.*R1*C*V4(K)*U/(4.*R2*D(JA))))*0.001
70        IF(K1.LT.2)GOTO 180
71        V7(M3)=(V5(1)+V5(K1))/2
72        V8(M3)=(V6(1)+V6(K1))/2
73        IF (M3.GE.2) GOTO 150
74        K=2
75        V3(K)=V3(1)+V7(M3)
76        V4(K)=V4(1)+V8(M3)
77        U=SQRT((V3(K)**2+V4(K)**2))
78        R4=R1*U*D(JA)/M1
79        CALL INTAPO(R4,C,A1,B1,A2,B2,A3,B3,A4,B4,N1,N2,N3)
80        M3=M3+1
81        GO TO 200
82   150  IF (ABS(V7(1)-V7(2)).LE.0.00001.AND.ABS(V8(1)-V8(2)
83       *).LE.0.00001)GO TO 220
84        K=2
85        V3(K)=V3(1)+V7(M3)
86        V4(K)=V4(1)+V8(M3)
87        U=SQRT((V3(K)**2+V4(K)**2))
88        R4=R1*U*D(JA)/M1
89        CALL INTAPO(R4,C,A1,B1,A2,B2,A3,B3,A4,B4,N1,N2,N3)
90        V7(1)=V7(2)
91        V8(1)=V8(2)
92        M3=2
93        GO TO 200
94   180  K=2
95        V4(K)=V4(K-1)+V6(K1)
96        V3(K)=V3(K-1)+V5(K1)
97        U=SQRT((V3(K)**2+V4(K)**2))
98        R4=R1*U*D(JA)/M1
99        CALL INTAPO(R4,C,A1,B1,A2,B2,A3,B3,A4,B4,N1,N2,N3)
100  200  K1=2
101       GOTO 130
102  220  K2=K2+1
103       V1(K2)=V3(K)
104       V2(K2)=V4(K)
105       U2(K2)=SQRT((V1(K2)**2+V2(K2)**2))
106       K=1
107       V3(K)=V1(K2)
108       V4(K)=V2(K2)
109       IF (K3.EQ.K4)GO TO 250
110       K3=K3+1
111       J=1
```

```
      GO TO 300
  250 K3=1
      K5=K5+1
      CALL INTEGA(V1,V2,K2,H1,H2)
      X(K5)=X(K5-1)+H1
      Y(K5)=Y(K5-1)+H2
      T(K5)=(K5-1)*0.01
      VH(K5)=V1(K2)
      VV(K5)=V2(K2)
      UR(K5)=U2(K2)
      IF (X(K5).EQ.X(K5-1))GO TO 495
      IF (Y(K5).EQ.Y(K5-1))GO TO 495
      IF (X(K5).GT.0.6096.OR.Y(K5).GT.1.5)GO TO 490
      V1(1)=V1(K2)
      V2(1)=V2(K2)
      U2(1)=U2(K2)
      K2=1
      J=1
  300 CONTINUE
  490 K5=K5-1
  495 WRITE(12,4500)
 4500 FORMAT(38X,'PARTICLE  TRAJECTORY'///,20X,'TIME',12X,
     *'VELOCITY  (M/S)',16X,'DISTANCE (M)'/,21X,'(S)',4X,
     *'HORIZONTAL  VERTICAL  RESULTANT',5X,
     *'HORIZONTAL  VERTICAL'/)
      DO 600 JJ=1,K5
      WRITE(12,5000)T(JJ),VH(JJ),VV(JJ),UR(JJ),X(JJ),Y(JJ)
  600 CONTINUE
  500 CONTINUE
 5000 FORMAT(20X,F4.2,3F11.3,F15.4,F11.4)
      STOP
      END
      SUBROUTINE INTAPO(R4,C,A1,B1,A2,B2,A3,B3,A4,B4,N1,N2,N3)
C     INTERPOLATION SECTION
      REAL A1(20),A2(20),A3(20),A4(20)
      REAL B1(20),B2(20),B3(20),B4(20)
      REAL P1(20),P2(20)
      INTEGER N,N1,N2,N3,J1,J2
      REAL P3
      P3=0.0
      IF (R4.LE.0.3)GO TO 500
      IF (R4.LE.10.0)GO TO 510
      IF (R4.LE.1000.0)GO TO 520
      IF (R4.LE.30000.0)GO TO 530
      IF (R4.LE.1000000.0) GO TO 540
  500 C=24.0/R4
  510 N=N1
      DO 515 J1=1,N
      P1(J1)=B1(J1)
      P2(J1)=A1(J1)
  515 CONTINUE
      GO TO 550
  520 N=N2
      DO 525 J1=1,N
      P1(J1)=B2(J1)
      P2(J1)=A2(J1)
  525 CONTINUE
      GO TO 550
  530 N=N3
      DO 535 J1=1,N
```

```
172         P1(J1)=B3(J1)
173         P2(J1)=A3(J1)
174       535 CONTINUE
175         GO TO 550
176       540 N=N1
177         DO 545 J1=1,N
178         P1(J1)=B4(J1)
179         P2(J1)=A4(J1)
180       545 CONTINUE
181       550 DO 570 J1=1,N
182         R3=P2(J1)
183         DO 560 J2=1,N
184         IF (J1.EQ.J2) GO TO 560
185         R3=R3*(R4-P1(J2))/(P1(J1)-P1(J2))
186       560 CONTINUE
187         P3=P3+R3
188       570 CONTINUE
189         C=P3/R4**2
190         RETURN
191         END
192         SUBROUTINE INTEGA(V1,V2,K2,H1,H2)
193         REAL V1(20),V2(20)
194         REAL F1(20),F2(20)
195         INTEGER N4,N5,N6,N7,K6,J6
196         K6=1
197         DO 700 J3=1,K2
198         F1(K6)=V1(J3)
199         F2(K6)=V2(J3)
200         K6=K6+1
201       700 CONTINUE
202         K6=K6-1
203         H=0.001
204         N4=K6-1
205         N5=N4/2
206         H1=0.
207         H2=0.
208         N6=1
209         IF((N4-N5*2).EQ.0)GO TO 800
210         H1=3.*H/8.*(F1(1)+3.*F1(2)+3.*F1(3)+F1(4))
211         H2=3.*H/8.*(F2(1)+3.*F2(2)+3.*F2(3)+F2(4))
212         N6=4
213       800 H1=H1+H/3.*(F1(N6)+4.*F1(N6+1)+F1(K6))
214         H2=H2+H/3.*(F2(N6)+4.*F2(N6+1)+F2(K6))
215         N6=N6+2
216         IF(N6.EQ.K6) GO TO 900
217         N7=K6-2
218         DO 850 J6=N6,N7,2
219         H1=H1+H/3.*(2.*F1(J6)+4.*F1(J6+1))
220         H2=H2+H/3.*(2.*F2(J6)+4.*F2(J6+1))
221       850 CONTINUE
222       900 RETURN
223         END
EOF..
```

D2

TABLE OF Re AGAINST CRe^2

Re	CRe^2
0.1	2.4
0.2	4.8
0.3	7.2
0.5	12.4
0.7	17.9
1.0	26.5
2	57.6
3	93.7
5	173
7	265
10	410
20	1.02×10^3
30	1.80
50	3.75
70	6.23
100	10.7
200	30.8
300	58.5
500	138
700	245
1000	460
2000	1.68×10^6
3000	3.60
5000	9.60
7000	19.1
10000	40.5
20000	180
30000	426
50000	1.23×10^9
70000	2.45
100000	4.8
200000	16.8
300000	18.0
400000	13.4
600000	36.0
1000000	130

NOMENCLATURE

a	radius
A	Area of hemispherical drop
C	constant
C_o, C_1, C_2 etc.	concentrations in Model 1
C_T	crust thickness
d_n	nozzle orifice diameter (m)
D	droplet diameter
D_f	Most frequent diameter
D_{am}	Geometric mean diameter
D_{HM}	Harmonic mean diameter
G	mass flowrate
k	thermal conductivity
K_c	mass transfer coefficient
K_f	constant
L	mean pore length
N	Number of drops
N_A	rate of mass transfer
Nu	Nusset Number ($h_c D/K_d$)
P	pressure
Pr	Prandt Number ($C_p \mu/k$)
q	amplitude
Q_A, Q_B, Q_C	flowrates in Model 1
r	radius
R	swirl chamber radius, radial distance, or Universal gas constant.

R_c	Univeral Gas constant
R_e	Reynolds Number ($dU\rho/\mu$)
S_G	Geometric standard deviation
Sh	Sherwood Number ($K_g D/D_v$)
S_N	Number Standard deviation
t	time
u	vapour velocity
U	velocity
V_j	liquid jet velocity
W	angular velocity (in that equation)
We	Weber Number (dU^2/σ)
Z	factor
Z'	ratio=Weber Number/Reynolds Number

Greek Letters

α	dispersion factor
ϵ	porosity
λ	latent heat or wave length
μ	viscosity
π	constant = 3.1416
ρ	density
σ	surface tension
ψ	constant
θ	dimensionless time or angle of spray

Subscripts

a	air
C_r	critical
h	horizontal
m	maximum
p	particle
s	solid, slurry
v	vertical

REFERENCES

1. Masters K. "Spray Drying Handbook", Third Edition, George Godwin Ltd., London (1976).
2. Keey R. B., "Introduction to Industrial Drying Operations", Pergamon Press.
3. Sloan, C. P., Chem. Eng. 74, (14), 169 - 200, (1967).
4. Nonhebel G. "Chemical Engineering in Practice", Wykeman Publication, London (1973).
5. Rayleigh Lord, Proc. London Math. Soc. 10, (1878).
6. Tyler E., Phil Mag. 16, 504 (1933).
7. Haenlin A., Nat. Adv. Comn., Aeronaut Tech. Mem. 659 (1932).
8. Castleman R. A., Bur. Stand. Journ. Res. 6, No. 281 (1931).
9. Weber C., Z. Angew. Math. Mech. 11, 136 (1931)
10. Ohnesorge G., Z. Angew Math. U. Mech. 16, 355 (1936).
11. Calvert S. Amer. Inst. Chem. Eng. J. 16, No. 3, 392 (1970).
12. Kitamura Y. and Egawa K., J. Chem. Eng. Japan 10, No. 1.1 (1977).
13. Giffen, E. and Muraszew A., Atomization of Liquid Fuels, London: Chapman and Hall, (1953).
14. Vestergaard I. and Masters K., Proc. Biochem., 13, No. 1, (1978).
15. Frazer R. P. et al, Chem. Eng. Sc. 18, 315 (1963).
16. Hinze J. I. & Milborn M. J., App. Mech. 17, No. 2, 145 (1950).

17. Mehrhardt E., Chemic. Eng. Technik, 45, No. 6, 401 (1973).

18. Bauer H. and Kruger R., Verfahrens Technik, 3, No. 3, 107 (1969).

19. Frazer R. P. et al Brit. Chem. Eng. 2, No. 10, 536, (1957).

20. Marshall W. R., Ind. Eng. Chem. 45, No. 1, 47 (1953).

21. Lapple C. E. and Shepherd C. B., Ind. Eng. Chem. 32, No. 5, 605 (1940).

22. Kurabayasi T., Japan Soc. Mech. Eng. Bulletin, 3, No. 11, 352 (1960).

23. Dombrowski N. and Hasson D., Amer. Inst. Chem. Eng. J., 15, No. 4, 604, (1969).

24. Niro Atomizer, British Patent 1.136952 Dec. 18^{1}, (1968) (Wheels).

25. Shell Research Ltd., British Patent 887450 Jan. 17 (1962) (Cup).

26. Masters K. and Straarup O., British Patent 1331, Sep. 26, (1973) (Liquid Distributor).

27. Spray System Company, Illinois, USA.

28. Delavan Manuf. Comp.,"Sray Droplet Technology", Brochure 678A - 1269.

29. Briffa F. E. J. and Dombrowski N., Amer. Inst. Chem. Eng. J. 12, No. 4, 708, (1966).

30. Green H. L. "Flow Properties of Disperse Systems", Chapter 7, North Holland Publ. Co. (1957).

31. Dorman R. G. Brit. J. Appl. Physics 3, 189, (189).

32. Frazer R. D. and Eisenklam P. Trans. Inst. Chem. Eng., 24, 294, (1956).

33. Hargerty & W. and Shea J. F., J. App. Mech. 22, 509, (1955).

34. Dombrowski N. and LLoyd T. L., Chem. Eng. Sc. 8 No. 1, 63, (1974).

35. Niro Atomizer, U.S. Patent 3887133 (3rd June 1975).

36. Gretzinger J. and Marshall W. R. Amer. Inst. Chem. Eng. J. 7, No. 2, 312, (1961).

37. Licht, W., Amer. Inst. Chem. Eng. J. 20, No. 3, 595, (1974).

38. Hukuo K. et al, Proc. Japan Congr. Mater. Res, 19, 244, (1976).

39. Kim K. Y. and Marshall W. R., Amer. Inst. Chem. Eng. J., 17, No. 3, 575, (1971).

40. Nukiyama S. and Tanasawa Y., Trans. Soc. Mech. Eng. Japan, 5, No. 18, 63, (1938).

41. Kaltenbach R. M., Brit. Patent 1202117 (12th Aug. 1970).

42. Popov V. F. et al, Khim. Prom. (Russ), No. 12, 19 - 21 (1964).

43. Litsios J., Inst. Elect. Electron. Eng. Trans. Ultrasonic Eng. No. 9, 91 - 5 (1963).

44. Wilcox R. L. and Tate R. W., Amer. Inst. Chem. Eng. J. 11, No. 1, 69, (1965).

45. Antozevich J. N. Proc. Nat. Electron. Conf. 13, 798 - 807 (1957).

46. Ashley M. J., The Chem Eng. No. 286, 368, (June 1974).

47. Reay D., The Chemical Engineer, 506 (July/Aug.) (1976).

48. Belcher I. W. et al, Chem. Eng. 70, No. 20, 83, Sept. 30, (1963).

49. Masters K., Ind. Eng. Chem. 60, No. 10, 53, (1968).

50. Entwhistle R. E., Food Eng. 38, No. 2, 82, (1966).

51. Chemical Engineering 74, 113, (19th June 1967).

52. Peck, R. E. and Kauh, Y. J., A.I.Ch.E.J. 15, 85, (1969).

53. Gauvin W. H. Int. J. of Multiphase Flow 1, 793 (1975).

54. Katta S. & Gauvin W. H., A.I.Ch.E.J., 21, No. 1, 143, (1975).

55. Stein W. A., Chemie Ing. Technik, 44, No. 22, 1241, (1972).

56. Frazer R. D. et al - Brit. Chem. Eng. 2, No. 9, 196, (1957).

57. Friedman S. J., I. E. C., 38, No. 1, 22 (1946).

58. Higbie R., Trans. Am. Inst. Chem. Eng. 31, 365, (1935).

59. Pham Q. T. & Keey R. B., Can. J. Chem. Eng., 55, 466 (1977).

60. Ade-John A. O. & Jeffreys G. V., Trans. Inst. Chem. Eng. 56, No. 1, 36 (1978).

61. Ranz, W. E. and Marshall W. R., Chem. Eng. Prog. 48, No. 3, 141, (1952).

62. Plate G. et al, Trans. Inst. Chem. Eng. 37, 268 (1959).

63. Sdoli et al, Ind. Eng. Chem. Proc. Dev. 10, No. 2, 157 (1971).

64. Wen C., and Fan T. L., "Models for Flow Systems and Chemical Reactors", Chemical Process and Engineering Series, Vol. 3, Mercel Dekker Inc. New York (1975).

65. Levenspiel I. and Bischoff K. B., Advan. Chem. Eng., 4, 95, (1963).

66. Paris J. R. et al - Ind. Eng. Chem. Proc. Des. Dev. 10, N2, 157, (1971).

67. Chaloud J. H. et al - Chem. Eng. Prog. 53, 593, (1957).

68. Van Meel D. A., Chem. Eng. Sci., 9, 36 - 44 (1958).

69. Nonhebel, G. and Moss A.A.H., "Drying of Solids in the Chemical Industry", P. 71, Butterworths, London (1971).

70. Keey R. B., Chem. Eng. Sc. 23, 1299 - 1308 (1968).

71. Froesling N., Beitr. Geophys. 52, 170, (1938).

72. Maxwell R. W. and Storrow J. A., Chem. Eng. Sci. 6, 204, (1957).

73. Miura K. et al, A.I.Ch.E.J. Symp. series 73, No. 163, (1977).

74. Tsubouchi T. and Sato S. Chem. Eng. Prog. Symp. Series, 56, No. 30, 285 (1960).

75. Marshall W. R., Trans. Amer. Soc. Mech. Eng. 77, No. 11, 1377 (1955).

76. Trommelen, A. M., and Crosby, E. J., A.I.Ch.E.J. 16, No. 5, 857, (1970).

77. Godsave G. AE, Nat. Gas Turbine Est. (England) Rept. R88 (1952).

78. Manning W. P. and Gauvin W. A., A.I.Ch.E.J. 6, No. 2, 184, (1960).

79. Audu T. O. K. and Jeffreys G. V. Trans. Inst. Chem. Eng. 53, No. 3, (1975).

80. Charlesworth D. M. & Marshall W. R. Amer. Inst. Chem. Eng. J. 6, No. 1, 9 (1960).

81. Duffie J. A. and Marshall W. R., Chem. Eng. Prog. 49, 417, 480 (1953).

82. Probert R. P., Phil. Mag. 37, 95 (1946).

83. Fledderman R. G., and Hanson A. R., Univ. Mich. Res. Dept. Report CM 667 (1951).

84. Marshall W. R., Ind. Eng. Chem. 45, No. 1, 47 (1953).

85. Shapiro A. H. and Erikson A. J., J. Amer. Soc. Mech. Eng. 79, 775 (1957).

86. Bose A. K. and Pei D.C.T., Can. J. Chem. Eng. 42, No. 6, 259 (1964).

87. Dickson D. R. and Marshall W. R., A.I.Ch.E.J. 14, No. 4, 541, (1960).

88. Balton L. and Gauvin W. H., Pulp and Paper Research Institute of Canada, Montreal Tech. Report 518, 519 (Aug. 1967).

89. Dloughy J. and Gauvin W. A., A.I.Ch.E.J. 6, No. 1, 29 (1960).

90. Wallman H. and Blyth H. A., Ind. Eng. Chem. 43, 1480, (1951).

91. Stout and Busche, Chem. Eng. Prog. 47, 29 (1951).

92. Celenza, G. J., Chem. Eng. Prog. 66, No. 11, 33 (1970).

93. Chem. Proc. Eng. 55, No. 12, 55 (1969).

94. Klein H., Chemie - Technik 1, 230 (1972).

95. Alonso J. R. F., Chem. Eng. P. 86, (Dec. 13th 1970).

96. Stairmand C. J., The Chem. Eng. No. 254, 375 (Oct. 1971).

97. Rupe, J. 3rd Symposium of Combustion and Flame and Explosion Phenomeno, USA (1949).

98. Tate R. W., A.I.Ch.E.J., 7, 574 (1961).

99. Joyce J. R., J. Inst. Fuel, 22, 150, (1949).

100. Choudhury, A. P. R., Ph.D. Thesis North Western University Esanston 16, (1955).

101. Taylor E. H. and Harmon D. B., Ind. Eng. Chem. 46, 1455 (1954).

102. Clark C. J., and Dombrowski N. J., J. Aerosol Sci., 4, 27 (1973).

103. York J. L. and Stubb H. E. Trans. Am. Soc. Mech. Eng. 74, 1157 (1952).

104. Dombrowski N., Wolfshon D. L., J. Aerosol Sci., 2, 405 (1971).

105. Irani R. R. and Callis C. F. "Particle Size Measurement, Interpretation and Application", New York, Wiley (1963).

106. Davies C., Paper presented at High Speed Photography Conference, (1977).

107. Groves M. J., Kaye B. H. and Scarlett B., Brit. Chem. Eng. 9, (11), 724, (1964).

108. Ranz W. E. and Wong J. B., Ind. Eng. Chem. 44, 1371 (1952).

109. Ranz W. E. and Wong J. B., Ind. Eng. Chem. 49, 288 (1957).

110. Ashton C. J., Ph.D Thesis, University of Aston in Birmingham, England, (1980).

111. Scarlett B., Chem. Proc. Eng. 46, No. 4 (1965).

112. Watson H. H. and Mulford D. F., Bull. Inst. Met. S105 (1954).

113. Rose H. E. and Langmaid R. N., Nature, 179, 774 (1957).

114. Stairmand C. J., Trans. Inst. Chem. Eng. 25, 128 (1947).

115. Colon F. J., Chem. and Ind., P. 263 (Feb.6, 1965).

116. Pruden E. L. and Winstead M. E., Am. J. Med. Technol., (Jan - Feb 1964).

117. Nonhebel F., "Gas Purification Process", Newnes, London (1964).

118. Alder. C. R. and Marshall W. R., Chem. Eng. Prog. 47, 515, 601 (1951).

119. Nelson F. M. and Eggertsen F. T., Anal. Chem., 30, 1387, (1958).

120. Mugele R. A. and Evans H. D., Ind. Eng. Chem. 43, 1317 (1951).

121. Nelson R. A. and Stevens W. F., A.I.Ch.E.J. 7, No. 1, 80 (1961).

122. Galton F. Proc. Roy. Soc. (London), 29, 365, (1879).

123. Tate, R. W., and Marshall W. R., Chem. Eng. Prog. 49, 169 (1953).

124. Rosin, P., and Rammler, E., J. Inst. Fuel, 7, 29, (1933).

125. Nukiyama, S., Tanasawa, Y., Trans. Soc. Mech.Eng. Japan 4, (N14), 86, (1937).

126. Keey, R. B., and Pham, Q. T., Chem. Eng. July/Aug., 516 (1976).

127. Turba J. and Nemeth J., Brit. Chem. Eng. 9, No. 7, 457 (1964).

128. Luikov, A. V., Sushka Raspilenyijen, (Moska: Pischepromizdat) (1955).

129. Longwell J. P. and Weisc A. M., Ind. Eng. Chem. 45, 667 - 776, (1953).

130. Feder A., Chem. Eng. 66, 159 - 162, (1959).

131. Borde I. I., Proc. 2nd All Soviet Union Conference on Heat and Mas transfer 1964, Rand Report R-451-PR, 5, 649.

132. Dolinsky A. A., Proc. 2nd, All Soviet Union Conference on Heat and Mass transfer, Rand Report R-451-PR, 5, 666.

133. Johnstone, H. F., and Eads., D. K. Ind. Eng. Chem. 42, 2293, 1950.

134. Miesse, C. C., Jet Propulsion, 24, 237, (1954).

135. Gluckert F. A., A.I.Ch.E.J. 8, No. 3, 460 (1962).

136. Sjetnitzer F., Chem. Eng. Sc. 1, No. 3, 101 (1952).

137. Greene R. M. et al Chem. Eng. Prog. 44, 591 (1948).

138. Marone, I. Y., "Theoretical Foundation of Chemical Engineering", 5, 546 (1971).

139. Yaron, I. and Gal-or, B., Internat. J. Heat and Mass Transfer 14, 727.

140. Schlunder, E. U., Ph.D. dissertation, Technische Hochshule, Darmstadt, (1962).

141. McIlvried H. G. and Massoth F. E., Ind. Eng. Chem. 14, 727, (1971).

142. Hopkins, M. J., and Eisenklam, P., Proc. Conf. Chemeca '70, Butterworths (Australia), Melbourne/ Sydney (1970).

143. Dloughy, J., and Gauvin, W. H., Can. J. Chem. Eng., 38, 113 (1960).

144. Parti, M., and Palancz, B., Chem. Eng. Sci., 29, 355, (1974).

145. Danckwerts P. V. Chem. Eng. Sci. 9, 78,(1958).

146. Taylor G. I. Proc. Roy. Soc. A223, 446, 1924.

147. Squires R. and Squires W. Jr., Trans. Am. Inst. Chem. Eng. 33, 1 - 12, (1937).

148. Naddell, H., Physics, 2, 457 - 66 (1932).

149. Klein, M. V.,"Optics", Wiley, New York,(1970)

150. Dobbins,R. A. et al, AIAA Journal, Vol.1, pp. 1882-1886, (1963).

151. Levich, V. G., "Physicochemical Hydrodynamics", Prentice Hall, Inc., Englefield Cliffs, N.J.,(1962)

152. Esubiyi,A. O., Ph.D thesis, University of Aston in Birmingham, England, (1980).